



**Università
degli Studi
di Palermo**

AREA QUALITÀ, PROGRAMMAZIONE E SUPPORTO STRATEGICO
SETTORE STRATEGIA PER LA RICERCA
U. O. DOTTORATI

Dottorato Di Ricerca in Scienze Agrarie, Alimentari e Forestali
Settore Scientifico Disciplinare AGR/15 Scienze e Tecnologie Alimentari

**UNDERSTANDING WINE *TERROIR*: METABOLOMIC
APPROACHES TO UNVEIL THE INFLUENCE OF SOIL ON THE
CHEMICAL COMPOSITION OF *NERO D'AVOLA* GRAPES AND
WINES**

**IL DOTTORE
PAOLA BAMBINA**

**IL COORDINATORE
PROF. VINCENZO BAGARELLO**

**IL TUTOR
PROF. ONOFRIO CORONA**

**IL CO-TUTOR
PROF. PELLEGRINO CONTE**

**CICLO XXXV
ANNO CONSEGUIMENTO TITOLO 2023**

Ai miei genitori

The present thesis has been adapted including relevant parts from:

Bambina, P., Spinella, A., Lo Papa, G., Chillura Martino, D. F., Lo Meo, P., Corona, O., ... & Conte, P. (2023). ¹H NMR-Based Metabolomics to Assess the Impact of Soil Type on the Chemical Composition of Nero d'Avola Red Wines. Journal of Agricultural and Food Chemistry, 71(14), 5823-5835.

Bambina, P., Pollon, M., Vitaggio, C., Lo Papa, G., Conte, P., Cinquanta, L., & Corona, O. (2023). Effect Of Soil Type On The Evolution Of Phenolic Compounds During Ripening Of Nero d'Avola Grapes (Note 1). Submitted to American Journal of Enology and Viticulture.

Bambina, P., Pollon, M., Vitaggio, C., Lo Papa, G., Conte, P., Cinquanta, L., & Corona, O. (2023). Effects Of Soil Type On Phenolic And Volatile Composition Of Nero d'Avola Wines (Note 2). Submitted to American Journal of Enology and Viticulture.

Bambina, P., Gancel, A.L., Jourdes, M., & Teissedre, P.L. Influence of soil type on the proanthocyanidins composition of red and white wines obtained from Nero d'Avola and Grillo Vitis vinifera L. cultivars. In prep.

Experiments described in this thesis were conducted at:

Department of Agricultural, Food and Forestry Sciences, University of Palermo

Institute de Sciences de la Vigne et du Vin, University of Bordeaux

INDEX

CHAPTER 1: INTRODUCTION	9
WINE COMPOSITION	10
THE CONCEPT OF <i>TERROIR</i>	15
METABOLOMICS	17
ANALYTICAL TECHNIQUES IN METABOLOMICS	19
METABOLOMICS IN WINE SCIENCE	22
AIM OF THE RESEARCH PROJECT	24
CHAPTER 2: STUDY SITES	25
MATERIALS AND METHODS	26
EXPERIMENTAL AREA	26
SOIL ANALYSES	27
RESULTS	28
SOIL DESCRIPTION AND CLASSIFICATION	28
CLIMATIC CONDITIONS OF 2020 AND 2021 VINTAGES	33
CHAPTER 3: INFLUENCE OF SOIL ON THE CHEMICAL COMPOSITION OF NERO D'AVOLA GRAPES	34
MATERIALS AND METHODS	35
GRAPE BERRIES SAMPLING AND DENSITY SORTING	35
SKINS AND SEEDS EXTRACTS PREPARATION	35
ANALYSIS OF PHENOLIC COMPOUNDS IN GRAPES	36
ANALYSIS OF TOTAL FLAVONOIDS AND TOTAL ANTHOCYANINS	36
ANALYSIS OF MONOMER ANTHOCYANINS, HYDROXYCINNAMOYL TARTARIC ACIDS (HTCAs) AND FLAVONOLS	37
STATISTICAL ANALYSIS	38
RESULTS	40
DENSITY CLASSES DISTRIBUTION	40
GRAPES PHYSICAL-CHEMICAL PARAMETERS	43
PHENOLIC COMPOUNDS IN GRAPES	48
TOTAL FLAVONOIDS AND TOTAL ANTHOCYANINS	48
MONOMER ANTHOCYANINS PROFILES	50
HYDROXYCINNAMOYL TARTARIC ACIDS (HCTAs)	52
FLAVONOLS	54
MODELING OF PHENOLS EVOLUTION DURING RIPENING	56
THE TRANS-CAFFEOYL TARTARIC ACID CASE	56
THE QUERCETIN-3-GLUCOSIDE CASE	59
SOIL EFFECT ON THE CHEMICAL COMPOSITION OF NERO D'AVOLA GRAPES	62
MULTIVARIATE STATISTICAL ANALYSIS	68
CHAPTER 4: INFLUENCE OF SOIL ON THE CHEMICAL COMPOSITION OF NERO D'AVOLA WINES (PART I)	72
MATERIALS AND METHODS	73
VINIFICATION PROCESS	73
MUSTS AND WINES CHEMICAL-PHYSICAL ANALYSES	73
ANALYSIS OF PHENOLIC COMPOUNDS IN WINES	74
GLOBAL CHARACTERIZATION OF POLYPHENOLS	74

ANALYSIS OF MONOMER ANTHOCYANINS, HTCAs AND FLAVONOLS -----	75
PROANTHOCYANIDINS CHARACTERIZATION: ANALYSIS OF MONOMERIC AND OLIGOMERIC FLAVAN-3-OLS -----	75
STRUCTURAL CHARACTERIZATION OF PROANTHOCYANIDINS -----	76
ANALYSIS OF VOLATILE ORGANIC COMPOUNDS (VOCs) -----	77
STATISTICAL ANALYSES -----	78

RESULTS ----- 79

CHEMICAL-PHYSICAL PARAMETERS OF MUSTS AND WINES -----	79
GLOBAL CHARACTERIZATION OF PHENOLS -----	81
MONOMER ANTHOCYANINS PROFILE -----	82
HYDROXYCINNAMOYL TARTARIC ACIDS (HCTAs) -----	85
FLAVONOLS -----	85
PROANTHOCYANIDINS CHARACTERIZATION -----	86
STRUCTURAL CHARACTERISTICS OF PROANTHOCYANIDINS -----	88
VOLATILE ORGANIC COMPOUNDS IN WINES -----	92
SOIL EFFECT ON WINES CHEMICAL COMPOSITION -----	97
SOIL EFFECT ON WINES CHEMICAL-PHYSICAL PARAMETERS -----	97
SOIL EFFECT ON WINES PHENOLS -----	98
SOIL EFFECT ON WINES VOLATILE ORGANIC COMPOUNDS -----	103
MULTIVARIATE STATISTICAL ANALYSES -----	106
PRINCIPAL COMPONENT ANALYSIS 1: PROANTHOCYANIDIN COMPOSITION -----	106
PRINCIPAL COMPONENT ANALYSIS 2: ANTHOCYANINS, HTCAs AND FLAVONOLS -----	107
PRINCIPAL COMPONENT ANALYSIS 3: VOLATILE ORGANIC COMPOUNDS -----	108

CHAPTER 5. INFLUENCE OF SOIL ON THE CHEMICAL COMPOSITION OF NERO D'AVOLA WINES (PART II) ----- 110

MATERIALS AND METHODS ----- 111

¹ H-NMR SPECTROSCOPIC ANALYSIS OF WINES -----	111
TARGETED ANALYSIS (TA): IDENTIFICATION OF COMPOUNDS -----	112
NON-TARGETED ANALYSIS: DATA REDUCTION -----	115
NON-TARGETED ANALYSIS: DATA PREPROCESSING AND MULTIVARIATE STATISTICAL ANALYSIS -----	116

RESULTS ----- 118

¹ H-NMR SPECTRA EVALUATION: TARGETED ANALYSIS -----	118
¹ H-NMR SPECTRA EVALUATION: NON-TARGETED ANALYSIS -----	123
THE H-BOND NETWORK IN WINES AS REVEALED BY THE NON-TARGETED ANALYSIS ----	126
WINE-SOIL RELATIONSHIPS -----	130

Appendix A ----- 135

Appendix B ----- 150

CONCLUDING REMARKS ----- 161

PRIZES AND AWARDS ----- 163

OTHER PUBLICATIONS ----- 164

REFERENCES ----- 166

AKNOWLEDGEMENTS ----- 184

ABSTRACT

The aim of this PhD project was to unveil the soil effect on the chemical composition of grapes and wines from *Vitis vinifera* cv. *Nero d'Avola*. The study focused on six soil chemical-physical parameters, namely texture, pH, total carbonates, cation exchange capacity, electric conductivity, and organic matter. The soil effect on grapes quality was studied through the observation of berries ripening kinetics (e.g., ripeness homogeneity and maturation rate) and of the evolution of phenolic compounds in grapes during the ripening process.

The soil effect on wines quality was considered by studying the phenolic and volatile organic composition of *Nero d'Avola* wines, as determined by chromatography-based metabolomic approaches. Moreover, wines metabolome was investigated through ¹H-NMR-based metabolomic analysis. Two different approaches were applied: the targeted (TA) and the non-targeted one (NTA). The former differentiated the wines by *profiling* (i.e., by identifying and quantifying) a number of different metabolites. The latter provided wine *fingerprinting* by processing the entire spectra with multivariate statistical analysis. NTA also allowed investigation of the hydrogen bond network inside wines, via the analysis of ¹H-NMR chemical shift dispersions.

Results showed that soil had a significant effect on grapes ripening and composition, as well as wines composition. On the one hand, it was observed that cation exchange capacity and soil texture had a remarkable impact on phenolic composition. On the other hand, cation exchange capacity and organic matter affected wines volatile organic composition, particularly the fermentative composition.

Results obtained by ¹H-NMR-based metabolomics showed that the differences among wines were due not only to the concentrations of the various analytes but also to the characteristics of the H-bond network where the different solutes are involved. The H-bond network affects both gustatory and olfactory perceptions by modulating the way how solutes interact with the human sensorial receptors. Moreover, the aforementioned H-bond network is also related to the soil properties from which the grapes were taken.

The importance of our findings lies in the fact that, despite the pivotal role played by soil in grapevine growth, only little information was available about the effect of some soil chemical-physical parameters on grapes and wine chemical composition. Therefore, the present study can be considered as a good attempt to investigate *terroir*, i.e. the relationship between grapes and wine quality and soil characteristics.

CHAPTER 1: INTRODUCTION

WINE COMPOSITION

Wine is a complex mixture of metabolites deriving from the alcoholic fermentation of grape berries. Wine metabolites include a great variety of compounds that are divided into primary and secondary metabolites. Primary metabolites are closely related to plant growth, development, and reproduction. They include sugars, alcohols, organic acids, amino acids, and polysaccharides. Secondary metabolites have important ecological functions, such as defense from predators and resistance to diseases (Ali et al., 2010). Secondary metabolites consist of a wide array of chemicals belonging to different chemical classes, including alkaloids, phenols, and volatile organic compounds. Advances in analytical techniques such as gas chromatography (GC), high performance liquid chromatography (HPLC), mass spectrometry (MS) and nuclear magnetic resonance (NMR) allowed to considerably increase the number of the identified compounds in both grapes and wines. To date, more than 500 compounds, all contributing to determine wine sensory quality, have been identified and quantified in wines. Wine is mainly composed by water ($\approx 85\%$), ethanol ($\approx 12\%$) and glycerol ($\approx 1\%$). Other compounds, such as organic acids, amino acids, phenols, and volatile organic compounds represent about the 2% of the total wine components (Nemzer et al., 2022). However, notwithstanding their low concentration, these compounds are very impactful for wine organoleptic properties.

Organic acids in wines mainly include tartaric, malic, citric, succinic, and acetic acid. While tartaric, malic, and citric acids are directly synthesized in grape berries, succinic and acetic acids derive from yeasts metabolism during alcoholic fermentation (Sirén et al., 2015). The content and the type of organic acids directly influence wine pH. It plays very important roles in wine quality given that it modulates the acidity perception, the sugar/acid balance, the proteic and microbial stability, the color stability, the precipitation of potassium bitartrate, and the occurrence of the malolactic fermentation (Kodur, 2011). Nitrogen compounds are mainly represented by amino acids and proteins. Proline is usually the most present amino acid in wines, given that it is not used for yeast metabolism. Alanine, arginine, leucine, isoleucine, glutamic acid, glutamine, arginine, and γ -aminobutyric acid can also be

found in wines. They all contribute to wine aroma, taste, and appearance (Hernandez-Orte et al., 2003). Wine proteins show molecular weights ranging from 20 to 40 kD, and their solubility depends on temperature, alcohol content, and pH (Lehtonen, 1996).

Phenolics are a large group of secondary metabolites particularly impactful for wine sensory characteristics. Indeed, they are the major responsible for wine color and for bitter and astringent tastes. The major groups of wine phenols are simple phenolics, flavonoids, and stilbenoids. Simple phenolics are derivatives of hydroxycinnamic (HCAs) and hydroxybenzoic acids (HBAs) (Ali et al., 2010). Common hydroxycinnamic acids are *p*-coumaric acid, caffeic acid, sinapic acid, and ferulic acid. In wine, they are almost entirely esterified with tartaric acid, producing hydroxycinnamoyl tartaric acids (HCTAs). Caffeic acid (caffeic acid esterified with tartaric acid) is usually the predominant HCTA. It was observed that HCTAs content in grapes and wines depend on several factors such as grape variety, growing conditions, climate, etc (Monagas et al., 2005). HBAs are mainly composed by gallic acid, gentisic acid, protocatechic acid, and *p*-hydroxybenzoic acid (Pozo-Bayon et al. 2003). In general, the most present HBA is gallic acid, that can be found as both free form and as acyl substituent of flavan-3-ols.

Wine flavonoids derive from the solid parts of grapes (mainly skins and seeds). Therefore, they are released into must/wine during the maceration process. Flavonoids are divided into diverse sub-groups including flavones, flavonols, dihydroflavanols, flavanols, and anthocyanidins. They share the same skeleton, differing from each other for the oxidation state of their central pyran ring. Flavanols comprise (+)-catechin, (-)-epicatechin and their gallate esters (Kennedy, 2008). The polymerization of these latter leads to the production of condensed tannins, also known as proanthocyanidins (as referred to the red colour developing after acidic cleavage). Proanthocyanidins differ into monomer composition and structure, mean degree of polymerization (mDP) and level of galloylation (Versari et al., 2013). The hydroxylation pattern of the flavanol units allows to differentiate proanthocyanidins into two principal classes. On the one hand, *procyanidins* are exclusively composed by (+)-catechin and (-)-epicatechin monomers (Hammerstone et al., 2000). On

the other hand, *prodelphinidins* are composed by (+)-gallocatechin and (-)-epigallocatechin (Vivas et al., 2004). Grape skin tannins contain both procyanidins and prodelphinidins, with high mDP and low level of galloylation. Conversely, grape-seed tannins are composed by procyanidins only, with low mDP and high level of galloylation.

Anthocyanins are water soluble pigments that are responsible for the red color of grapes and wines. Depending on wine pH and on the presence of co-pigmenting agents, they provide different colors that vary from red to purple/blue. They are present as monoglucosides forms, that can be acylated by acetic acid, *p*-coumaric acid, or caffeic acid (Alcalde-Eon et al. 2006). The five major anthocyanins found in wines derived from *Vitis vinifera L.* grapes are malvidin-3-glucoside, delphinidin-3-glucoside, petunidin-3-glucoside, peonidin-3-glucoside, and cyanidin-3-glucoside. These differ from each other for the hydroxylation pattern on the B ring of the molecule. The number and the position of the hydroxyl- and/or methoxyl- groups on the B ring directly affect the chemical reactions in which they are involved, with important implication on their stability. The anthocyanin profile can be used for the chemotaxonomic classification, as the relative proportion among different anthocyanins is mainly a varietal feature (Mattivi et al. 2006). However, it has been observed that grape anthocyanin concentration also depends on different vine growing parameters, such as soil type and climate, together with viticultural practices such as pruning, fertilization, and watering (Gonzalez-Neves et al. 2002).

Flavonols are 3-O-glucoside and 3-O-glucuronide forms of quercetin, myricetin, kaempferol, isorhamnetin, laricitrin, and syringetin (Mattivi et al. 2006). Finally, stilbenes are considered plant phytoalexins, as their formation in grapevines are related to resistance to diseases. They are present in wines in monomeric form, such as resveratrol (3,5,4-trihydroxystilbene), or in oligomeric and polymeric forms, such as ϵ -viniferin, α -viniferin, ampelopsin A and hopeaphenol (Jeandet et al., 2002). These latter are formed by oxidative polymerization of resveratrol through the activity of a peroxidase (Jean-Denis et al. 2006).

Volatile organic compounds (VOCs) determine wine flavour and aroma. Some of the most important VOCs are terpenoids (e.g., monoterpenoids, sesquiterpenoids), together with aromatic aldehydes, esters, and thiols. Volatile compounds in grapes are mainly stored in exocarp cells as nonvolatile, water-soluble glycoside derivatives (e.g., terpenoids), or as amino acid conjugates such as cysteinylated precursors (e.g., aromatic thiols). To be perceived, the hydrolysis and volatilization of compounds stored as conjugates (both glycoside and amino acids derivatives) is mandatory. Therefore, glycosidases and peptidases enzymes (from both grapes and yeasts) play important roles in aromas release. However, in some grape variety aroma compounds are also present in their free forms, coming through alcoholic fermentation unaltered or with minor modifications. The endowment of volatile organic compounds directly deriving from grape berries define the varietal aroma of wines.

Among varietal aroma compounds, terpenes have been extensively studied. More than 40 terpenoids, occurring as hydrocarbons, alcohols, aldehydes, ketones, and esters, have been identified in wines. They are majorly responsible for fruity and floral aromas. Some of the most odoriferous terpenes are alcohols, including linalool, α -terpineol, nerol, geraniol, citronellol and α -trienol.

Norisoprenoids are products of enzymatic and non-enzymatic degradation reactions of carotenoids. These breakdown products are carbonyl compounds with 9, 10, 11 and 13 C-atoms, some of which with powerful aroma properties (Mendes-Pinto, 2009). The C13-norisoprenoids are the most abundant in wines. The qualitative and quantitative profiles of carotenoids and norisoprenoids in grapes are affected by several factors including plant variety, climatic conditions, stage of maturity, soil characteristics and viticultural practices. C13-norisoprenoids are present only at trace levels, but their sensory thresholds are very low. Therefore, they significantly contribute to wine aroma. Grape norisoprenoids are divided into 2 main groups: *megastigmanes* (including β -damascenone, β -ionone, 3-oxo- α -ionol, β -damascone and 3-hydroxy- β -damascone), and *non-megastigmanes* (including 1,1,6-trimethyl-1,2-dihydronaphthalene, or TDN, and (E)-1-(2,3,6-trimethylphenyl)buta-1,3-diene, or TPB).

Methoxypyrazines are nitrogenous heterocyclic structures deriving from amino acid metabolism. They are associated to vegetal notes in wines. The most important methoxypyrazines are 3-isobutyl-2-methoxypyrazine, 2-sec-butyl-3-methoxypyrazine and 3-isopropyl-2-methoxypyrazine.

Among varietal thiols, 4-mercapto-4-methylpentan-2-one, 3-mercaptohexyl acetate, 3-mercaptohexan-1-ol and 3-mercapto-2-methylpropanol have been identified as key molecules contributing to the fruity notes of young wines aroma.

Some authors (Lund & Bohlmann, 2006; van Leeuwen et al., 2004) affirmed that the type and the amount of varietal volatile metabolites are partially determined in vineyard through a complex, and still unwell understood, interplay between the natural environment, agronomic practices, and vine genotypes, including rootstock.

Pre-fermentative aromas are a class of compounds with a C6-moiety produced through enzymatic reactions (e.g., lipoxygenase pathway) occurring when berries are crushed (Kalua et al., 2010). They have grassy and herbaceous odors and are generally considered unpleasant when present at high concentrations (Yang et al., 2009; Ferrandino et al., 2012).

Fermentative aroma compounds are secondary products of yeast metabolism. They mainly include higher alcohols, medium and short chain fatty acids, esters and benzenoids. They are responsible for the vinous and fruity olfactive characteristics of wine. In general, these compounds directly derive from the catabolism of primary metabolites present in musts at the beginning of the alcoholic fermentation. For instance, higher alcohols derive from amino acids catabolism, by means of Ehrlich reaction. Short chain fatty acids are byproducts of the protein metabolism. Linear longer saturated fatty acids with an even number of C atoms are originated from lipid metabolism and from the catabolism of long-chain fatty acids (Pérez Olivero et al. 2011, Lenti et al. 2022). Esters are formed enzymatically during alcoholic fermentation and chemically during wine ageing. Enzymatic ester production during fermentation depends on the rate of ester synthesis and hydrolysis (Sumbly et al., 2010; Fenster et al., 2003), which in turn depends on the activity of the esterase and lipase enzymes produced by yeasts (Kong et al., 2021). Wine esters are divided in acetates of higher alcohols and

ethyl esters of fatty acids. Most esters are present in concentrations around their threshold value. This implies that even modest concentration changes could have a dramatic effect on wine flavor. Finally, volatile benzenoids are formed during the phenylpropanoid synthesis by the phenylalanine ammonia-lyase (PAL) enzyme (Widhalm et al., 2015). This enzyme catalyzes the conversion of phenylalanine to trans-cinnamic acid, which in turn is converted into benzyl alcohol and other derived compounds (Martin et al., 2016).

The composition in primary metabolites of grapes and musts at the beginning of alcoholic fermentation affects not only the kinetics of alcoholic fermentation, but also the production of fermentative aroma compounds (Hernández-Orte et al., 2002).

Due to the great complexity of wine chemical composition, winemaking is worldwide considered as a science-guided art and the production of high-quality wines is increasingly guided by molecular-based knowledge and technologies.

THE CONCEPT OF *TERROIR*

Wine sensorial quality results from a dynamic interaction among several factors, such as grape variety, climate, soil, topography, metabolism of yeasts during alcoholic fermentation and human activities, including viticultural and oenological techniques (Mascellani et al. 2021). This dynamic interaction is referred to as the French concept of *terroir*. The International Organization of Vine and Wine defined *terroir* as “*an area in which the collective knowledge of the interactions between the identifiable physical and biological environment and applied vitivinicultural practices develops, providing distinctive characteristics for the products originating from this area. Terroir includes specific soil, topography, climate, landscape characteristics and biodiversity features*” (OIV 2010). This definition indicates the uniqueness of the oenological products deriving from a specific

production area. As a matter of fact, wines deriving from different production areas have different sensory characteristics, as the environmental conditions affect vine phenology, berries ripening and musts compositions. All the involved factors simultaneously interact with each other, explaining why wine shows an extraordinary diversity through space and time. From a chemical point of view, *terroir* is related to differences in wine composition as affected by different vine growing conditions. In fact, the biosynthesis of the metabolites inside grape berries is strongly influenced by the interactions between vine and its biotic and abiotic surroundings (Cortell et al., 2007). It is largely accepted that the three main components of *terroir* are climate, soil, and cultivar. Among these factors, the impact of climate was found to be predominant with respect to soil and cultivar (van Leeuwen et al. 2004). However, soil plays a pivotal role because it provides the base for grapevine growth. Physical and chemical parameters, such as soil structure, texture, fertility, and soil moisture (de Andrés-De Prado et al., 2007) directly affect vine growth and berry maturation rate. Some studies revealed that soil influences wine composition mainly through the mineral nutrition of the grapevine (Hopfer et al., 2015; Cheng et al., 2014).

The effects of grape variety (Foroni et al. 2007), climate (Cheng et al. 2014, Lee et al. 2009) and production techniques (López-Rituerto et al. 2012, Alves Filho et al. 2022) on wine quality have been evaluated. However, the influence of soil chemistry on wine quality is not fully understood, yet (Blotevogel et al. 2019). Only little information is available about the effect of some soil chemical-physical parameters on wine chemical composition (de Andrés-De Prado et al. 2007).

To date, it has been observed that the effects of soil and climate on berries quality can be due to their effects on vine water status (Hopfer et al. 2015, Cheng et al. 2015, Pérez-Álvarez et al. 2019). Other authors assessed that the soil type, land shape and soil preparation influence vine development and grape composition through their impact on vine water and nitrogen status (de Andrés-De Prado et al. 2007, van Leeuwen et al. 2018). Also, the effects of altitude (Mateus et al. 2001), slope (Mazza et al. 1999) and exposure (Spayd et al. 2002) on vine development have been evaluated. Finally, other

studies focused on the geographical origin, that means the combination of soil, topography, climate, and viticultural practices (Vilanova et al. 2007, Godelmann et al. 2013, Gougeon et al. 2018).

METABOLOMICS

Over the last decades, advances in the “*omics*” sciences (e.g., genomics, transcriptomics, proteomics and metabolomics) significantly improved the understanding of the nature of vine-environment interactions and their effects on wine quality. Omics sciences refer to data-driven approaches that allow to study a biological system in its totality, rather than in limited specific aspects (Fiehn, 2002). Omics sciences make use of large amount of biological data provided by high-throughput technologies that enable to analyse complete sets of biomolecules, including DNA, RNA, proteins, and other metabolites. The study of the ensemble of biomolecules in a biological system provides a comprehensive overview of the molecular processes occurring in a system. While the traditional reductionist approaches focus on specific aspects of the systems, taking the risk of missing significant information, omics sciences employ a holistic view with the aim to identify significant variations in the biological activity of the organisms.

In this context, genomics studies the entire genome, transcriptomics measures the total levels of RNA in a cell (allowing to study the gene expression), proteomics studies the ensemble of proteins (providing an overview of the overall functionality of the system) and metabolomics, the last step in the “omics” cascade, focuses on *metabolome* (Figure 1). The word *metabolome* was firstly introduced by Oliver et al. (1998) to indicate the ensemble of the metabolites contained in a biological sample. Metabolites are intermediates, or end-products, of multiple cellular reactions and include endogenous and exogenous chemical entities such as peptides, amino acids, nucleic acids, carbohydrates, organic acids, vitamins, phenols, alkaloids, minerals and all the other molecules that can be synthesized by a cell. It is the most downstream product of a cell (Pinu, 2018), being the final point of the interactions between genome, transcriptome, proteome, and microbiome, including also environmental effects.

Metabolites produced by cells provide phenotypic information about the response of an organism towards different genetic and/or environmental changes. For this reason, metabolomics represents an optimal tool to study metabolic perturbations in biological systems, providing an integrative overview of the cellular metabolism and phenotypic characteristics of the cells (Pinu, 2018). The term metabolomics (or metabonomics) was, then, introduced as *the quantitative measurement of the dynamic multiparametric metabolic response of living systems to pathophysiological stimuli or genetic modification* (Nicholson et al. 1999). Therefore, it aims at identifying and quantifying the ensemble of the metabolites in a given organism or biological sample at a specific moment and under particular environmental conditions (Wishart et al. 2022). The measure of type and concentration of metabolites provides information about the biochemical activity of an organism, allowing to study whether specific metabolic pathways are affected by environmental stressors. One of the reasons mostly contributing to the rapid growth of metabolomics is its wide range of applications, including plant biology (Leiss et al., 2011), nutrition (Hall et al., 2008), drug discovery (Wishart, 2016), and human diseases (Armitage et al., 2014).

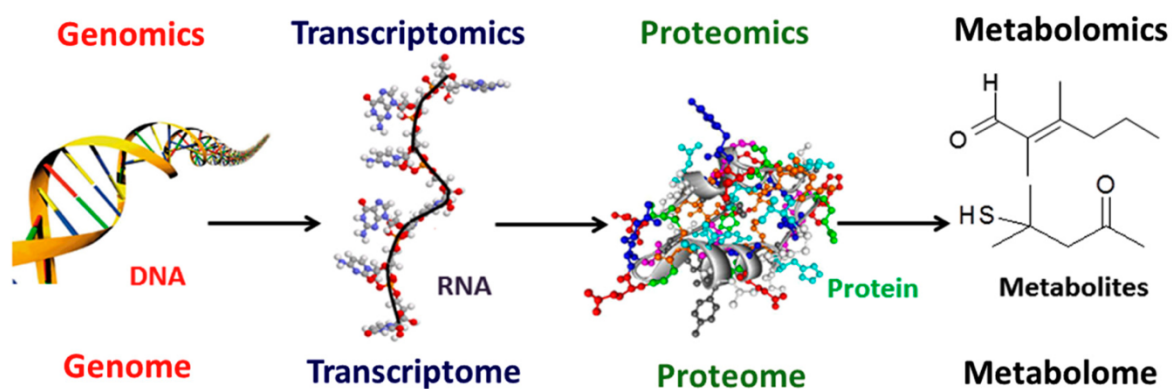


FIGURE 1. HIERARCHY OF "OMICS" SCIENCES (PINU, 2003).

Two different metabolomic approaches have been developed. They are classified as targeted (TA) and non-targeted (NTA) metabolomic analysis. The former, also referred to as *profiling*, aims at accurately identifying and quantifying a pre-defined set of metabolites in biological samples. TA is based on an a-priori knowledge of the bio-matrix. By using TA, known and highly concentrated compounds are usually evaluated, whereas unknown and lowly concentrated compounds, that still

could be significantly informative, are overlooked. Conversely, the NTA approach, also called *fingerprinting*, is a more exploratory technique: it does not necessarily deal with metabolites identification, but rather with the recognition of metabolite patterns by measuring and comparing as many signals as possible (Bingol et al 2018). Therefore, the untargeted metabolic fingerprint contains information about both identified and unknown compounds (Shulaev, 2006). Since NTA produces a large amount of data, multivariate statistical analysis is needed to reduce data complexity and extract the most relevant information (Utpott et al., 2022).

Metabolomic studies generally follow a common protocol, consisting in sample collection, metabolite extraction, identification and quantification, data elaboration and biological interpretation. Sample preparation protocols must avoid the exclusion of any metabolite, in order to provide a complete view of the state of the system. Solid tissues are generally subjected to homogenization and mechanical cell lysis before the extraction phase. On the contrary, a minimal sample preparation is generally required for liquid-state samples (such as wine).

ANALYTICAL TECHNIQUES IN METABOLOMICS

To date, the two principal analytical approaches used for the generation of metabolomic data are Mass Spectrometry (MS) and Nuclear Magnetic Resonance spectroscopy (NMR) (Fuhrer and Zamboni, 2015; Gika et al. 2019). Mass Spectrometry (MS) measures the mass-to-charge ratio (m/z) of ionized compounds. Each ionized (fragmented) compound generates a different peak pattern that represents the fingerprint of the original molecule. The mass-to-charge ratio and the fragmentation patterns are used in MS to identify both known and unknown compounds. A great variety of ionizers are available for MS, including electron impact ionization (EI), electrospray ionization (ESI), matrix assisted desorption ionization (MALDI), thermospray ionization, atmospheric pressure chemical ionization (APCI), fast atom bombardment ionization (FAB), etc. Among these, EI and ESI are the most used

in metabolomics (Dunn et al., 2011). A great variety of mass analyzers are used, such as quadrupole (Q), quadrupole ion-trap (QIT), time of flight (ToF), orbitrap, ion mobility spectrometry (IMS) and Fourier-transform ion cyclotron resonance (FT-ICR).

However, the accurate identification of metabolites by mass-to-charge ratio is quite challenging given that many molecules share the same molecular formula and mass. Therefore, in order to reduce the high complexity of biological samples, and to analyse different kind of molecules at different times, MS is often preceded by a separation phase carried out by means of high-resolution chromatographic techniques. These generally include liquid chromatography (LC) and gas chromatography (GC) (Theodoridis et al., 2011). Chromatographic techniques represent the most versatile tools to analyse a multitude of molecules with different molecular properties. The separation is due to the interaction of different metabolites contained in a mixture with an adsorbent material packed inside the chromatographic column. Metabolites with different chemical properties are differently retained on the adsorbent material, requiring different time to pass through the column. The time needed by each metabolite is called retention time and is used, together with the MS information, to identify the different compounds contained in a mixture with improved accuracy.

Nuclear magnetic resonance spectroscopy (NMR) is a fast and highly reproducible technique used for molecular structure elucidation. It is based on the absorption and re-emission of energy by targeted nuclei due to the application of an external magnetic field (Bothwell and Griffin, 2011). Depending on the type of nucleus being targeted by the applied magnetic field, different types of NMR analysis are conducted, including ^1H -NMR, ^{13}C -NMR, and ^{31}P -NMR. Among the analytical methods mostly used to perform metabolomic analysis, ^1H -NMR spectroscopy plays the major role because it provides structural and quantitative information on almost all organic chemical classes, as based on the abundance of their hydrogen-nuclei. ^1H -NMR spectral data include the chemical shift, the signal multiplicity, and the relative coupling constant, that are used to obtain metabolites' identification and information about chemical structure. Moreover, the area of the spectral peaks is used to quantify

metabolites, given that the area under a peak directly depends on the number of nuclei producing that signal.

One of the main advantages of $^1\text{H-NMR}$ spectroscopy lays in the possibility to investigate a wide range of compounds simultaneously in a non-destructive and highly reproducible way (Wishart et al., 2022). In combination with chemometrics, $^1\text{H-NMR}$ spectroscopy has been extensively used in metabolomic studies of foods and beverages (Tabago et al., 2021; Lee et al., 2009). Samples for NMR experiments generally require minimal preparation. This is often limited to the addition of a deuterated buffer or solvent, and an internal standard.

Once MS or NMR data have been collected, they need to be pre-processed prior to perform multivariate statistical analysis. Data pre-treatment methods aim at correcting several factors that can hinder the biological interpretation of metabolomic data, emphasizing the biological information, and improving their biological interpretability (Van der Berg et al., 2006). Pre-processing steps generally include data filtering, normalization, centring, scaling, and transformation (Spicer et al. 2017). Then, data sets are subjected to statistical elaboration in order to extract the most relevant information. Typical data elaboration focuses on dimensions-reduction methodologies that highlight separation among samples as based on certain sources of variance. The aim is to identify changes in metabolites' concentrations in response to a particular treatment or stressor. Principal component analysis (PCA), partial least squares analysis (PLS), and orthogonal partial least squares analysis (OPLS) are some of most used multivariate statistical approaches in metabolomics. PCA is an unsupervised technique, using unlabelled independent variables to discover hidden patterns in data, as well as clustering and/or associations among samples, as based on chemical similarities or differences. PLS and OPLS are supervised techniques that use a-priori labelled variables for classifying data or predicting outcomes by means of regression.

METABOLOMICS IN WINE SCIENCE

Traditionally, grapes and wines analyses have been carried out by evaluating a limited pre-determined number of compounds. This targeted approach, generally, allowed to investigate only specific groups of metabolites usually present with high concentrations (Pinu, 2018). Thus, the roles played by less concentrated (but still significant) metabolites have been overlooked for long time. Conversely, the comprehensive approach of metabolomics provided capability to analyse a big number of metabolites in a single experiment in both targeted and non-targeted way (Pinu, 2013). Metabolomics is a valuable tool to obtain the chemical *profiling*, by identifying and quantifying key metabolites, and chemical *fingerprinting* by considering the entire molecular spectrum. Metabolomic science has been exponentially improved over the last decades due to advancements of high resolution and sensitive analytical instruments (Dixon et al. 2006; Wishart, 2008). It is currently applied to a great variety of subjects, including agricultural, food and nutrition sciences (Beckner Whitener et al. 2016; Martins et al. 2017; Billet et al. 2018). Foods and beverages are evaluated by analysing their macro- and micro-component composition, with the aim to investigate sensory quality, nutritional content, safety, authenticity, and traceability (Hong et al. 2011, Amargianitaki et al. 2017; Alanon et al. 2015). Indeed, the type and the concentration of metabolites strongly affects food and beverages sensory and nutritional quality. Metabolomic approaches has been used for the characterization of the chemical composition of grape berries (Mulas et al. 2011), wine (Alanon et al. 2015; Arapitsas et al. 2016; Lloyd et al. 2015; Lee et al. 2009), olive oil (Mallamace et al. 2018) and beer (Sanchez-Estebanez et al. 2018). With reference to wine science, metabolomics has been used to address several issues, including the study of *terroir* (Ali et al. 2011). Metabolomics has been applied to classify wines according to grape varieties (Son et al. 2008), to highlight differences due to geographic origin (Gougeon et al., 2019; Godelmann et al., 2013), vintage (Lee et al., 2009) and winemaking techniques (López-Rituerto et al., 2012). Also, studies on metabolites evolution during alcoholic fermentation

(Son et al., 2008; Le Mao et al., 2021) and micro-oxygenation (Conte, 2008) have been carried out. Finally, non-targeted approaches have been developed for the analysis of the ensemble of volatile compounds in wines, often referred to as *volatilome* (Tejero Rioseras et al. 2017).

Although the effects of grape variety (Foroni et al., 2017), climate (Cheng et al., 2014; Lee et al., 2009) and production techniques (Alves Filho et al., 2002; López-Rituerto et al., 2012) on wine quality have been extensively evaluated, the influence of soil chemistry on wine quality is not fully understood (Blotevogel et al. 2019). Only little information is available on the effect of some soil chemical physical parameters (e.g., texture, pH, total carbonates, organic matter, cation exchange capacity and electric conductivity) on wine chemical composition (de Andrés-De Prado et al., 2007).

Moreover, no examples of metabolomic applications in wine science deal with the soil compartment of terroir. As a matter of fact, metabolomic studies already present in literature mainly focused on climate (Lee et al., 2009; López-Rituerto et al., 2012) and winemaking (Le Mao et al., 2021) effects. Other metabolomic applications also aim to classify wines according to geographical origin (Gougeon et al., 2019; Son et al., 2008; Godelmann et al., 2013). The latter encompasses the ensemble of soil, topography, climate, and viticultural practices. Therefore, these studies cannot provide any evaluation of the soil effect in its individuality.

AIM OF THE RESEARCH PROJECT

The French concept of *terroir* involves a complex interplay among grape variety, climate, soil, viticultural and enological practices, influencing the quality of wine. Among these factors, soil plays a fundamental role providing the base for grapevine growth. But despite its importance, only little information is currently available in literature about the influence of the soil chemical and physical parameters on wine composition. Therefore, this study aimed at improving the understanding of the possible role of soil chemistry on wine quality. To attain this goal, four vineyards with different soils located along the southwestern coast of Sicily (Southern Italy) were chosen as study sites. Different soil parameters were analysed, including texture, pH, total carbonates, organic matter, cation exchange capacity, and electric conductivity. Vineyards hosted the same *Vitis vinifera L.* cultivar, namely an autochthonous Sicilian red variety named *Nero d'Avola*. Due to the spatial proximity of the study sites, the variability attributable to macroclimate was reduced. Vines were subjected to the same agronomic management in order to remove the variability associated with viticultural techniques. Then, grapes quality was investigated through the study of the ripening kinetics and through the evolution of phenolic compounds during the ripening process.

Grapes from each vineyard were, then, separately vinified with the same procedure, thus removing the variability associated with the winemaking techniques. Obtained wines were, then, analysed by using both targeted and non-targeted approaches based on chromatographic and ¹H-NMR spectroscopic methods.

The obtained metabolomic data were subjected, together with soil-related data, to correlation analyses in order to point out possible grapes-wines/soil relationships.

Thanks to these arrangements, soil effect in its individuality, without the influence of climate and human activities can be investigated. Thus, the role of soil chemical-physical parameters on wine chemical composition was highlighted.

CHAPTER 2: STUDY SITES

MATERIALS AND METHODS

EXPERIMENTAL AREA

The research was carried out on four different vineyards, located in the hilly landscape nearby Menfi (AG), along the southwestern coast of Sicily (Southern Italy). The vineyards hosted the same *Vitis vinifera L.* cultivar, namely an autochthonous Sicilian red variety called *Nero d'Avola*. Vines were 26 years old and were grafted with 140 Ruggeri rootstock. They were trained by using the same agronomic management: Guyot pruning, 2.50 m x 1.00 m planting density, drip irrigation, and conventional regime. Even the altitude (100 m a.s.l.), slope (5-15%) and sun exposure (south-west/south-east) were consistent among vineyards. The homogeneity in all the aforementioned agronomic factors ensured that the variability associated to viticultural techniques was reduced. Moreover, due to the spatial proximity of the study sites, also the variability associated with climatic factors was reduced. The thermal regime of the area is sub-tropical temperate, with mean annual temperature in the range 15.0-17.5 °C and average annual temperature excursion in the range 15-18 °C. The pluviometric regime is typical Mediterranean, with mean annual rainfall of 648 mm, maximum rainfall between October and January and a dry period of 5-6 months, generally between May and September. The soil udometric regime is xeric, and the thermometric regime is thermic (Soil Survey Staff, 2010). The locations of *Nero d'Avola* vineyards are shown in Figure 2. Vineyard 1 is located at 37°36'17" N 12°55'59" E; Vineyard 2 is located at 37°35'31" N 12°57'04" E; Vineyard 3 is located at 37°38'39" N 12°55'39" E; Vineyard 4 is located at 37°36'13" N 12°52'16" E.

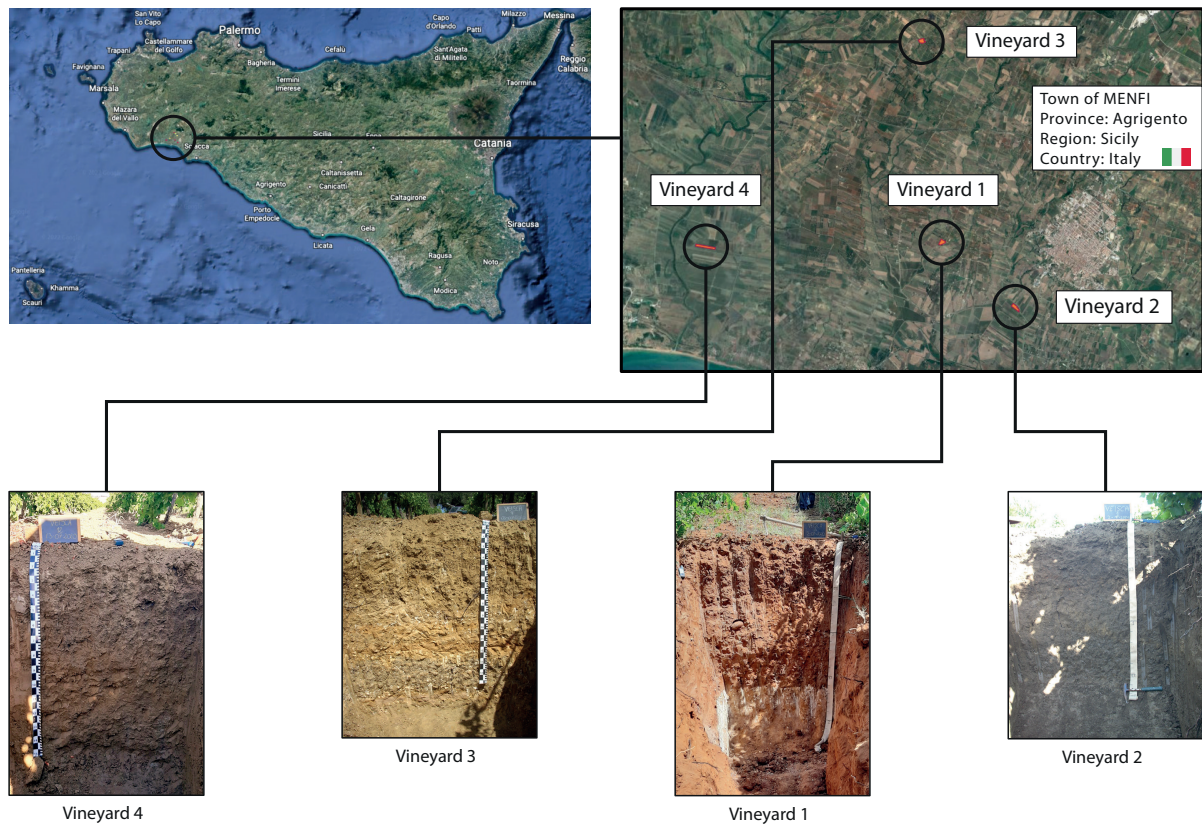


FIGURE 2. LOCATION OF THE STUDY SITES AND SOIL PROFILES. VINEYARDS WERE LOCATED ALONG THE SOUTHWESTERN COAST OF SICILY (SOUTHERN ITALY).

SOIL ANALYSES

A soil survey for each vineyard was carried out and samples from each identified horizon were taken.

The soil samples were first air-dried and then passed through a 2 mm sieve for laboratory analysis.

Six soils' chemical-physical parameters were analyzed, namely texture, pH, total carbonates, organic matter, cation exchange capacity, and electric conductivity.

Particle-size distribution was determined by the pipette method without removal of carbonates. Soil pH was measured in 1:2.5 w v⁻¹ soil-to-water mixtures. Soil electric conductivity was measured in 1:5 w v⁻¹ soil-to-water mixtures. Total carbonate was measured by means of the gas volumetric method after HCl treatment. Cation exchange capacity (CEC) was determined by saturation with BaCl₂ at pH 8.2. Organic carbon was measured using the Walkley and Black (1934) method.

RESULTS

SOIL DESCRIPTION AND CLASSIFICATION

The main morpho-descriptive features of soils are listed in Table 1. The analyzed chemical-physical parameters are reported in Table 2.

Soil 1 (37°36'17" N 12°55'59" E) has 5% slope and south-west sun exposure. It developed on limestone. The solum is 160 cm deep. It is characterized by a plowed surface mineral horizon, referred to as A_p horizon, ranging from 0 to 15 cm of depth. It is followed by a succession of four argillic horizons: B_{t1} (from 15 to 55 cm of depth), B_{t2} (from 55 to 100 cm of depth), B_{t3} (from 100 to 130 cm of depth), and B_{t4} (from 130 to 160 cm of depth). These sub-subsurface horizons are characterized by illuvial accumulation of clay. The latter forms clay-skins on pores and aggregates surfaces. The texture is sandy clay loamy in all horizons, except for B_{t3} horizon, where the texture is sandy loamy. The sand content ranges from 67.9 ± 0.7 % (B_{t1} horizon) to 77.9 ± 0.8 % (B_{t3} horizon). pH ranges between 5.66 ± 0.04 (A_p horizon) and 7.37 ± 0.01 (B_{t4} horizon). Total carbonates reach the maximum content of 1.31 ± 0.01 % in A_p , B_{t2} , and B_{t3} horizons, while in B_{t4} horizon the content is below the detection limits. Organic matter content ranges from 2.60 ± 0.03 g kg⁻¹ of soil (B_{t4} horizon) to 18.5 ± 0.1 g kg⁻¹ of soil (A_p horizon), showing a decreasing content as the soil depth increases. Cation exchange capacity varies between 0.100 ± 0.003 mmol g⁻¹ (B_{t3} horizon) and 0.231 ± 0.005 mmol g⁻¹ (A_p horizon). Electric conductivity ranges from 42.9 ± 0.7 μ S cm⁻¹ (B_{t3} horizon) to 168 ± 5 μ S cm⁻¹ (A_p horizon). The pedon is classified *Haplic Palexeralfs* according to the Soil Taxonomy (Soil Survey Staff, 2010).

Soil 2 (37°35'31" N 12°57'04" E) has 5% slope and south-east sun exposure. The solum is deep (150 cm). It developed on a colluvial and alluvial parent material. It is composed of an A_p surface horizon ranging from 0 to 20 cm of depth. Under the topsoil, a mineral weathered *cambic* horizon, indicated as B_{w1} , ranges from 20 to 80 cm of depth. This is followed by a sub-subsurface *calcic* horizon B_k (from 80 to 115 cm of depth) and a calcic $2B_{kss}$ (from 115 to 150 cm of depth) with vertic properties.

These horizons are characterized by accumulation of secondary calcium carbonate. $2B_{kss}$ horizon also shows convex-concave slip surfaces formed during expansion and contraction of swelling clays, named *slickensides*. The texture is clayey sandy loamy in A_p horizon and loamy-clayey in B_{w1} , B_k , and $2B_{kks}$ horizons. The clay content ranges from $27.5 \pm 0.3 \%$ (A_p horizon) to $38.2 \pm 0.4 \%$ (B_k horizon). pH ranges from 6.25 ± 0.01 (A_p horizon) and 7.19 ± 0.01 (B_{w1} horizon). Total carbonates vary between 8.24 ± 0.07 (A_p and B_{w1} horizons) and $20.2 \pm 0.2 \%$ (B_k horizon). Organic matter content ranges between $11.36 \pm 0.01 \text{ g kg}^{-1}$ of soil ($2B_{kks}$ horizon) and $16.9 \pm 0.1 \text{ g kg}^{-1}$ of soil (A_p horizon). As for soil 1, the organic matter content decreases as the soil depth increases. Cation exchange capacity varies between $0.275 \pm 0.007 \text{ mmol g}^{-1}$ ($2B_{kks}$ horizon) and $0.300 \pm 0.005 \text{ mmol g}^{-1}$ (B_{w1} horizon). Electric conductivity ranges from $129.9 \pm 0.8 \mu\text{S cm}^{-1}$ (B_k horizon) to $243 \pm 6 \mu\text{S cm}^{-1}$ (A_p horizon). According to the Soil Taxonomy, this soil is classified *Vertic Calcixerapt*.

Soil 3 ($37^\circ 38' 39''$ N $12^\circ 55' 39''$ E) shows south-east sun exposure and 15% slope. It formed on sandy marine clays. It is 150 cm deep. It consists of a surface A_p horizon, ranging from 0 to 22 cm of depth, followed by a BA transition horizon, ranging from 22 to 40 cm of depth. This horizon presents dominant characters of B sub-surface horizons together with some features of A surface horizon. Above this latter, B_w cambic horizon (from 40 to 70 cm of depth) and three B_k calcic horizons are also present: B_{k1} (from 70 to 90 cm of depth), B_{kk2} (from 90 to 120 cm of depth), and $2B_k$ (from 120 to 150 cm of depth). The latter horizon ($2B_k$) was formed from a different parent material (in-situ limestone). The texture is clayey sandy loamy in A_p and $2B_k$ horizons, sandy loamy in BA , B_w and B_{k1} horizons, and sandy in B_{kk2} horizon. The sand content ranges from $53.8 \pm 0.6 \%$ (A_p horizon) to $81.5 \pm 0.6 \%$ (B_{kk2} horizon). pH ranges between 7.12 ± 0.01 (B_{k1} horizon) and 7.50 ± 0.01 ($2B_k$ horizon). Total carbonates vary between $12.0 \pm 0.1 \%$ (B_{kk2} horizon) and $26.6 \pm 0.3 \%$ (BA horizon). Organic matter content ranges from $1.95 \pm 0.01 \text{ g kg}^{-1}$ of soil ($2B_k$ horizon) to $8.76 \pm 0.07 \text{ g kg}^{-1}$ of soil (A_p horizon). Cation exchange capacity lies between $0.075 \pm 0.001 \text{ mmol g}^{-1}$ (B_{kk2} horizon) and $0.175 \pm 0.002 \text{ mmol g}^{-1}$ (B_w and B_{k1} horizons). Electric conductivity varies from $94.2 \pm 0.8 \mu\text{S cm}^{-1}$ (B_{kk2}

horizon) and $166 \pm 1 \mu\text{S cm}^{-1}$ ($2B_k$ horizon). This pedon is classified *Typic Calcixerept*, according to the Soil Taxonomy.

Soil 4 ($37^{\circ}36'13''$ N $12^{\circ}52'16''$ E) has a slope of 2% and south-east sun exposure. It developed on a sandy clay substrate. Its depth exceeds 160 cm. The topsoil consists of a A_p *plowed* horizon, ranging from 0 to 20 cm of depth. The subsoil is composed by a B_w *cambic* horizon, ranging from 20 to 65 cm of depth, a typical B_k *calcic* horizon, extending from 65 to 110 cm of depth, and two B_k *calcic* horizons characterized by the presence of slickensides: B_{kss1} (ranging from 110 to 160 cm of depth) and B_{kss2} (extending beyond 160 cm of depth). The texture is clayey in all horizons. The clay content ranges from $41.1 \pm 0.4 \%$ (B_w and B_k horizons) to $49.1 \pm 0.3 \%$ (A_p horizon). pH varies between 7.34 ± 0.04 (A_p horizon) and 7.54 ± 0.03 (B_w horizon). Total carbonates range from $15.0 \pm 0.1 \%$ (B_{kss2} horizon) to $18.4 \pm 0.1 \%$ (B_k horizon). Organic matter lies between $4.80 \pm 0.03 \text{ g kg}^{-1}$ of soil (B_{kss2} horizon) and $11.99 \pm 0.09 \text{ g kg}^{-1}$ of soil (A_p horizon). Cation exchange capacity ranges from $0.163 \pm 0.002 \text{ mmol g}^{-1}$ (B_{kss2} horizon) and $0.275 \pm 0.003 \text{ mmol g}^{-1}$ (A_p horizon). Electric conductivity varies between $267 \pm 1 \mu\text{S cm}^{-1}$ (B_w horizon) and $3325 \pm 49 \mu\text{S cm}^{-1}$ (B_{kss2} horizon). According to the Soil Taxonomy, the pedon is classified *Vertic Calcixerept*.

TABLE 1. MAIN SOIL MORPHO-DESCRIPTIVE PARAMETERS.

	<i>Horizon</i>	<i>Depth</i>	<i>Color</i> ^a	<i>Structure</i> ^b	<i>Consistence</i> ^c	<i>Roots</i> ^d	<i>Boundary</i> ^e
Soil 1	<i>Ap</i>	0-15 cm	7.5YR4/4	sbk - f/m - 2	fi	2, m, co	ab
	<i>Bt1</i>	15-55 cm	7.5YR4/6	abk - m - 2	fi	2, m	cl
	<i>Bt2</i>	55-100 cm	5YR5/8	abk - m/c - 3	ef	2, m, f	cl
	<i>Bt3</i>	100-130 cm	5YR5/8	abk - m - 3	fi	0	cl
	<i>Bt4</i>	130-160 cm	7.5YR5/6	abk - f/m - 2	fi	0	cl
Soil 2	<i>Ap</i>	0-20 cm	2.5Y4/2	gr, sbk - f/m - 3	f	2, m	cl
	<i>Bw1</i>	20-80 cm	5Y4/2	sbk, abk - m/c - 3	f	2, m	cl
	<i>Bk</i>	80-115 cm	5Y3/2	abk - m/c - 3	fi	1, m	cl
	<i>2Bkss</i>	115-150cm	5Y3/2	abk,pr - m - 3	fi	0	cl
Soil 3	<i>Ap</i>	0-22 cm	2.5Y7/6	sbk - f - 2	fi	2, m	ab
	<i>BA</i>	22-40 cm	2.5Y7/6	abk - f/m - 2	ef	2, m	cl
	<i>Bw</i>	40-70 cm	2.5Y7/6	pr/abk - m/f - 2	ef	1, m	cl
	<i>Bk1</i>	70-90 cm	2.5Y7/6	pr/abk - m/f - 2	ef	1, f	ab
	<i>Bkk2</i>	90-120 cm	2.5Y7/6	abk/pr - c/m - 2	ef	1, f	ab
	<i>2Bk</i>	120-150 cm	2.5Y7/4	abk/pr/sg - c/m - 2	ef	1, f	ab
Soil 4	<i>Ap</i>	0-20 cm	5Y5/2	sbk - f/m - 2	fi	2, m	ab
	<i>Bw</i>	20-65 cm	2.5Y5/2	sbk/abk - m - 2	fi	2, m	cl
	<i>Bk</i>	65-110 cm	5Y5/3	sbk/abk - m/c - 3	fi	1, f	gr
	<i>Bssk1</i>	110-160 cm	5Y5/3	pr - m/c - 2	fi	0	gr
	<i>Bkss2</i>	>160 cm	5Y6/2	pr - m/c - 2	fi	0	gr

^a **MUNSELL DRY COLOR.**

^b **STRUCTURE: SBK = SUBANGULAR BLOCKY; ABK = ANGULAR BLOCKY; PR = PRISMATIC; GR = GRANULAR; SG = SINGLE GRAINS; F = FINE; M = MEDIUM; C = COARSE; 1 = WEAK; 2 = MODERATE; 3 = STRONG.**

^c **CONSISTENCE: F = FRIABLE; FI = FIRM; EF = EXTREMELY FIRM.**

^d **ROOTS: 0 = ABSENT; 1 = FEW; 2 = COMMON; F = FINE; M = MEDIUM; CO = COARSE.**

^e **BOUNDARY: AB = ABRUPT; CL = CLEAR; GR = GRADUAL.**

TABLE 2.CHEMICAL-PHYSICAL PARAMETERS ANALYSED FOR EACH SOIL.

Horizon	Depth	Texture			Cation exchange capacity	Total carbonates	Electric conductivity	pH	Organic matter	
		Clay %	Silt %	Sand %	mmol g ⁻¹	%	µS cm ⁻¹		g Kg ⁻¹ of soil	
Soil 1	<i>Ap</i>	0-15 cm	24.3 ± 0.3	6.30 ± 0.07	69.3 ± 0.7	0.231 ± 0.005	1.31 ± 0.01	168 ± 5	5.66 ± 0.04	18.5 ± 0.1
	<i>Bt1</i>	15-55 cm	30.0 ± 0.3	2.05 ± 0.01	67.9 ± 0.7	0.175 ± 0.004	0.88 ± 0.01	48.3 ± 0.3	6.11 ± 0.02	10.38 ± 0.08
	<i>Bt2</i>	55-100 cm	25.6 ± 0.2	1.35 ± 0.01	73.0 ± 0.7	0.188 ± 0.002	1.31 ± 0.01	43.35 ± 0.07	6.65 ± 0.01	3.24 ± 0.02
	<i>Bt3</i>	100-130 cm	19.3 ± 0.2	2.90 ± 0.02	77.9 ± 0.8	0.100 ± 0.003	1.31 ± 0.01	42.9 ± 0.7	6.93 ± 0.01	2.60 ± 0.01
	<i>Bt4</i>	130-160 cm	22.5 ± 0.1	1.30 ± 0.01	76.2 ± 0.6	0.156 ± 0.004	BDL	125 ± 5	7.37 ± 0.01	2.60 ± 0.03
Soil 2	<i>Ap</i>	0-20 cm	27.5 ± 0.3	22.2 ± 0.1	50.3 ± 0.5	0.300 ± 0.001	8.24 ± 0.07	243 ± 6	6.25 ± 0.01	16.9 ± 0.1
	<i>Bw1</i>	20-80 cm	37.1 ± 0.3	19.0 ± 0.1	43.9 ± 0.6	0.300 ± 0.005	8.24 ± 0.06	130 ± 4	7.19 ± 0.01	16.22 ± 0.02
	<i>Bk</i>	80-115 cm	38.2 ± 0.4	23.4 ± 0.1	38.4 ± 0.2	0.281 ± 0.006	20.2 ± 0.2	129.9 ± 0.8	7.11 ± 0.01	13.95 ± 0.01
	<i>2Bkss</i>	115-150 cm	37.7 ± 0.3	31.6 ± 0.2	30.8 ± 0.4	0.275 ± 0.007	18.5 ± 0.2	132.4 ± 0.4	7.03 ± 0.01	11.36 ± 0.01
Soil 3	<i>Ap</i>	0-22 cm	30.1 ± 0.2	16.1 ± 0.2	53.8 ± 0.6	0.125 ± 0.002	20.1 ± 0.2	131.1 ± 0.3	7.36 ± 0.02	8.76 ± 0.07
	<i>BA</i>	22-40 cm	19.5 ± 0.2	15.8 ± 0.1	64.7 ± 0.6	0.138 ± 0.003	26.6 ± 0.3	130 ± 2	7.23 ± 0.01	7.14 ± 0.06
	<i>Bw</i>	40-70 cm	19.2 ± 0.2	14.4 ± 0.1	66.4 ± 0.5	0.175 ± 0.002	24.9 ± 0.3	145 ± 1	7.26 ± 0.02	7.14 ± 0.07
	<i>Bk1</i>	70-90 cm	13.5 ± 0.1	15.85 ± 0.09	70.7 ± 0.7	0.175 ± 0.002	23.1 ± 0.2	99 ± 1	7.12 ± 0.01	6.17 ± 0.05
	<i>Bkk2</i>	90-120 cm	8.10 ± 0.05	10.4 ± 0.1	81.5 ± 0.6	0.075 ± 0.001	12.0 ± 0.1	94.2 ± 0.8	7.46 ± 0.01	5.52 ± 0.03
	<i>2Bk</i>	120-150 cm	22.8 ± 0.1	18.2 ± 0.2	59.0 ± 0.4	0.163 ± 0.001	17.1 ± 0.1	166 ± 1	7.50 ± 0.01	1.95 ± 0.01
Soil 4	<i>Ap</i>	0-20 cm	49.1 ± 0.3	22.5 ± 0.2	28.4 ± 0.3	0.275 ± 0.003	16.3 ± 0.1	295.5 ± 0.7	7.34 ± 0.04	11.99 ± 0.09
	<i>Bw</i>	20-65 cm	41.1 ± 0.4	27.8 ± 0.3	31.1 ± 0.3	0.269 ± 0.003	17.1 ± 0.1	267 ± 1	7.54 ± 0.03	9.25 ± 0.06
	<i>Bk</i>	65-110 cm	41.1 ± 0.4	25.1 ± 0.2	33.7 ± 0.3	0.250 ± 0.002	18.4 ± 0.1	890 ± 10	7.39 ± 0.01	7.88 ± 0.05
	<i>Bssk1</i>	110-160 cm	42.5 ± 0.4	30.4 ± 0.3	27.2 ± 0.3	0.175 ± 0.004	17.6 ± 0.1	1445 ± 137	7.37 ± 0.02	5.14 ± 0.04
	<i>Bkss2</i>	>160 cm	46.1 ± 0.5	30.7 ± 0.3	23.1 ± 0.3	0.163 ± 0.002	15.0 ± 0.1	3325 ± 49	7.43 ± 0.02	4.80 ± 0.03

CLIMATIC CONDITIONS OF 2020 AND 2021 VINTAGES

Meteorological data were recorded by a weather station located at 37°38'47.92" N 12°58'03.48" E. Precipitation showed an inter-annual variability (Table 3). The precipitation (calculated as sum of daily values) during the growing season (May-October) was 166 mm in 2020 and 223 mm in 2021. During the ripening period (August-September) the precipitation was 94 mm in 2020 and 66 mm in 2021. Therefore, in 2020 about 60% of the precipitation of the growing season was concentrated during the ripening period. In 2021, only the 30% of the precipitation was registered during the ripening period.

The relative humidity was about 68% in both vintages. The mean temperatures (calculated as mean of daily values) were 23 °C and 26 °C in growing season and in ripening period, respectively, in both 2020 and 2021 vintages. The maximum temperature was 41-42°C in both vintages. The minimum temperatures were 10 °C in 2020 and 8 °C in 2021 during the growing season, and 13-15 °C during the ripening period (Table 4).

TABLE 3. TEMPERATURE AND PRECIPITATION PARAMETERS FOR THE GROWING SEASON (MAY–OCTOBER) AND THE RIPENING PERIOD (AUGUST–SEPTEMBER) IN THE STUDY SITES OF THE TWO VINTAGES (2020 AND 2021).

	Precipitation (mm)		Relative humidity (%)		Mean temperature (°C)		Maximum temperature (°C)		Minimum temperature (°C)	
	Aug-Sept	May-Oct	Aug-Sept	May-Oct	Aug-Sept	May-Oct	Aug-Sept	May-Oct	Aug-Sept	May-Oct
2020	94	166	69	66	26	23	41	41	13	10
2021	66	223	64	64	26	23	42	42	15	8

CHAPTER 3: INFLUENCE OF SOIL ON THE CHEMICAL COMPOSITION OF NERO D'AVOLA GRAPES¹

¹ This chapter has been adapted including relevant parts from:

Bambina, P., Pollon, M., Vitaggio, C., Lo Papa, G., Conte, P., Cinquanta, L., & Corona, O. (2023). Effect Of Soil Type On The Evolution Of Phenolic Compounds During Ripening Of Nero d'Avola Grapes (Note 1). Submitted to American Journal of Enology and Viticulture.

MATERIALS AND METHODS

GRAPE BERRIES SAMPLING AND DENSITY SORTING

Grape berries of *Nero d'Avola* cultivar (*Vitis vinifera* L.) were collected between August 16th and 18th in 2020 and 2021 vintages, when the sugar content and the titratable acidity were optimal to produce the respective wines (technological maturity).

About 2000 berries were randomly collected from each vineyard (on an area of about 1 hectare), with attached pedicels, from the middle and lower part of clusters exposed and not to the sunlight, representative of the vineyard ripeness level. Then, berries were sorted according to their apparent density by means of flotation in different salt solutions. Six solutions with different concentrations of NaCl, with a gap of 20 mg L⁻¹ between each other, were prepared (from 90 to 190 g L⁻¹ of NaCl). Berries were firstly introduced into the denser solution. The sunken berries have the same density as the solution, whereas the floating berries have lower density. Once sorted, berries belonging to each density class were weighed and counted. The density classes distribution provides a double information. From the one hand, it measures the homogeneity, required to obtain high-quality wines, of berries ripeness at harvest. The knowledge of grapes composition at harvest is a key factor for managing the resulting wine quality. On the other hand, since berry apparent density mainly depends on its reducing sugars content, each density class can be considered as a stage of berry maturation. Therefore, the flotation allows to study the entire ripening curve in only one sampling. This method makes the grapes sampling independent from the natural variability associated with repeated samplings, minimizing both random and systematic errors.

SKINS AND SEEDS EXTRACTS PREPARATION

Three subsamples of 20 berries were used to prepare skins and seeds extracts according to the method described by Squadrito et al., 2007. Briefly, skins and seeds were manually removed from the pulp. Then, they were separately placed in plastic flasks containing 20 ml of pH 3.2 buffer solution (5 g of

tartaric acid, 22.2ml of 1M NaOH, 2g of Na₂S₂O₅, 125 mL of 95% ethanol, brought to the volume of 1 L with deionized water) (Corona et al. 2015). Samples were kept at room temperature for 4 hours, homogenized at 5000 rpm for 1 min with an Ultraturrax T25 high-speed homogenizer (IKA Labortechnik, Staufen, Germany), placed in ultrasonic bath for 3 minutes and centrifuged in a PK 131 centrifuge (ALC International, MI, Italy) at 4,000 rpm. The supernatant was recovered in 50 mL volumetric flask. The resulting pellet was, then, resuspended in 5 mL of pH 3.2 buffer solution and centrifuged for three consecutive times. The combined supernatants were brought to the volume of 50 mL with the buffer solution. The Na₂S₂O₅ contained in the extraction solvent ensures the inactivation of polyphenol oxidase, responsible for the oxidation of phenolic compounds and for the browning of tissues.

The remaining berries, subdivided into three replicates, were manually crushed, centrifuged at 4,000 rpm, and used to determine the main chemical-physical parameters of musts, including reducing sugars content (g L⁻¹), pH, titratable acidity (g L⁻¹), tartaric acid (g L⁻¹), and malic acid (g L⁻¹). The aforementioned parameters were analyzed by using a WinescanTM instrument (FOSS, Hilleroed, Denmark) calibrated by applying the EEC 2676 standard procedure (EEC, 1990).

ANALYSIS OF PHENOLIC COMPOUNDS IN GRAPES

ANALYSIS OF TOTAL FLAVONOIDS AND TOTAL ANTHOCYANINS

Total flavonoids content in skins and seeds and total anthocyanins content in skins were measured by means of UV-Vis Spectrophotometry (Corona et al. 2015), by using a UV-1800 spectrophotometer (Shimadzu Scientific Instruments Inc., Columbia, MD, USA). Total flavonoids content and total anthocyanins content were determined after diluting extracts in hydrochloric ethanol (ethanol:water:hydrochloric acid-37%, 70:30:1 v:v:v) according to the method proposed by Corona

et al. (2015). Analyses were carried out in the wavelengths range of 230 - 700 nm. To quantify total flavonoids in both skins and seeds extracts the corrected absorbance at 280 nm (referred to as E'_{280}) was used. This is the length (in absorbance units) of the segment joining the peak at 280 nm and the intersection point between the perpendicular drawn from the 280 nm peak and the tangent to the spectrum in the UV region. The applied equation for calculating total flavonoids content was:

$$\text{Total flavonoids (mg L}^{-1}\text{)} = 82.4 \times E'_{280} \times d$$

Where:

82.4 = (+)-catechin concentration (mg L⁻¹) / E'_{280} determined on a 10 mg L⁻¹ solution of (+)-catechin;

E'_{280} = corrected absorbance at 280 nm;

d = dilution coefficient.

To measure total anthocyanins content in skins extracts, the absorbance at 540 nm (E_{540}) was measured. The applied equation for calculating total anthocyanins content was:

$$\text{Total anthocyanins (mg L}^{-1}\text{)} = 16.17 \times E_{540} \times d$$

Where:

16.17 = MW/ ϵ of malvidin-3-glucoside in hydrochloric ethanol, calculated from $\epsilon = 33700$ in hydrochloric methanol (Nagel et al., 1979);

E_{540} = absorbance at 540 nm;

d = dilution coefficient.

Total anthocyanins were expressed as mg L⁻¹ of malvidin-3-glucoside, and total flavonoids were expressed as mg L⁻¹ of (+)-catechin.

ANALYSIS OF MONOMER ANTHOCYANINS, HYDROXYCINNAMOYL TARTARIC ACIDS (HTCAs) AND FLAVONOLS

To analyze monomer anthocyanins profile, hydroxycinnamoyl tartaric acids (HCTAs) and flavonols, skins extracts were acidified with 1 M H₃PO₄ (4.5 mL extract + 0.5 mL 1 M H₃PO₄), filtered through a 0.45 μ m nylon membrane filter and placed in a 1.5 mL vial. Analyses were carried out by means of

HPLC (Agilent series 1200 instrument, Milan, Italy), equipped with a Diode Array Detector (Hewlett-Packard 1100 D.A.D), and with a C18 column (Econosphere™ C18, 5 µm, 250 × 4.6 mm i.d., Lokeren, Belgium, part n° 70,066). As reported by Squadrito et al. (2007 and 2010), the injected volume was 20 µL.

Monomer anthocyanins:

The mobile phase was a linear gradient of formic acid in water (10:90 v:v; solvent A) and formic acid and methanol in water (10:40:50 v:v:v; solvent B). The eluent mixture during measurement was as follows: 45% B for 15 min; a linear gradient from 45% to 70% B in 20 min, from 70% to 90% B in 10 min and from 90% to 99% B in 5 min; 99% B for 4 min, a linear gradient from 99% to 45% B in 2 min and, finally 45% B for 5 min. The mobile phase flow rate was 0.48 mL min⁻¹ and the oven temperature was 45°C. Detection was performed at 520 nm. The anthocyanins profile was reported as percentage on the total anthocyanins content.

HCTA and flavonols:

The mobile phase was a mixture of H₃PO₄ 10⁻³ M (solvent A) in HC₃OH (solvent B) changed during analysis as follows: 5% of B for 5 min, a linear gradient from 5% to 10% of B in 5 min, from 10% to 30% of B in 10 min, from 30% to 60% of B in 10 min and from 60% to 100% of B in 10 min; then, a linear gradient from 100% to 5% of B in 5 min. The flow rate was 0.48 mL/min and the oven temperature was 40 °C.

Anthocyanins, HCTAs, and flavonols were identified and quantified by comparison with literature data (Wulf et al., 1978) and with standards isolated in our laboratory. Caffeoyl tartaric acid and *p*-coumaroyl tartaric acid were identified according to Singleton et al. (1978). HCTAs and flavonols are expressed in mg Kg⁻¹ of berries.

STATISTICAL ANALYSIS

To highlight significant differences among grapes from different density classes and different vineyards, the one-way analysis of variance (ANOVA), coupled with the Tukey-b post hoc test was

performed. To determine significant differences between 2020 and 2021 vintages the *Student's t* test was carried out. Differences with p values of less than 5% ($p < 0.05$) were considered statistically significant. These analyses were performed by means of SPSS software (version 25.0; SPSS Inc., Chicago, IL, USA).

The modeling of the evolution of phenolic compounds during ripening was performed by means of non-linear regression analysis, by using Minitab™ statistical software (version 19.0 for Windows, Minitab, LLC, Pennsylvania State University).

To point out possible relationships between soils and grapes physical-chemical parameters, grapes' compositional data were processed together with soil physical-chemical parameters in order to point out possible grape-soil correlations. In the present study, the *Pearson's product-moment correlation coefficient* (*Pearson's r*) was used. The statistics describes the strength and the direction of the linear relationship between two continuous variables. The Pearson's r value tends to -1.0 when the relationship between two variables is negative, that is when a variable decreases as the other variable increases (and vice versa). The *Pearson's r* value tends to +1.0 when the relationship between two variables is positive, namely when two variables increase (or decrease) simultaneously. The *Pearson's r* value is 0 when no relationship exists between the two variables (Goodwin et al., 2006). In this study, correlations with *Pearson's r* values $> |0.95|$ and $p < 0.05$ were considered statistically significant. To better visualize the existing relationships between soil and wine parameters correlation heatmaps were built. Correlation analyses were performed by using of MetaboAnalist 5.0 web-based tool suite (Chong et al., 2018) and SPSS software (version 25.0; SPSS Inc., Chicago, IL, USA).

Finally, to highlight the separation among wine samples due to the soil and climate, the unsupervised principal component analysis (PCA) was performed. The principal component analysis extracts the most important information from a data matrix consisting of several interrelated quantitative dependent variables, retaining as much variation as possible in the data set. To accomplish this purpose, a set of new orthogonal variables, which are linear combinations of the original variables, called principal components, are generated. The principal components are uncorrelated to each other

and represent the directions along which the data show the largest variance. Samples are displayed as points in a map according to similarities or differences among the dependent variables.

Both the correlation analysis and the PCA were performed by using of *MetaboAnalyst 5.0* web-based tool suite.

RESULTS

DENSITY CLASSES DISTRIBUTION

The flotation in solutions with different salt concentrations allowed to determine up to six density classes, referred to the following apparent densities: $I = 1.073 \text{ g cm}^{-3}$, $II = 1.080 \text{ g cm}^{-3}$, $III = 1.087 \text{ g cm}^{-3}$, $IV = 1.094 \text{ g cm}^{-3}$, $V = 1.101 \text{ g cm}^{-3}$, $VI = \geq 1.108 \text{ g cm}^{-3}$.

The distribution of berries among the density classes followed a bell-shaped distribution (Figure 3). The characteristics of the distributions are described by the mode, the skewness, and the kurtosis (Table 4). The mode, that is the value occurring with the highest frequency, represents the most present density class. The skewness, that is the measure of the distortion of a symmetrical distribution, assumes the meaning of maturation rate: high, or right, skewness is related to delayed maturation, and low, or left, skewness is related to anticipated maturation. Finally, the kurtosis, that is the measure of the sharpness of the peak of the distribution, assumes the meaning of ripeness homogeneity: low kurtosis values are typical of flat distributions and are related with uneven ripeness; high kurtosis values are typical of sharp distributions and are related to homogeneous ripeness.

In 2020 vintage, about 80-90% of grape berries from vineyards 2, 3 and 4 were distributed among two density classes and the distributions were characterized by higher values of kurtosis. This means that in these vineyards the ripeness was homogeneous. In 2021 vintage, most of berries were distributed among three or more density classes and the distributions were characterized by lower values of kurtosis. This means that the ripening status in 2021 was quite inhomogeneous. Regarding the ripening rate, vineyards 1 and 2 in 2020 vintage showed a delayed ripening process. In fact, their distributions skewness was higher than in vineyards 3 and 4. This is also confirmed by the mode, that

corresponded to 1087 g cm^{-3} in vineyards 1 and 2 and to 1101 and 1094 g cm^{-3} in vineyards 3 and 4, respectively. In 2021 vintage, in vineyards 2 and 4 the ripening process was delayed with respect to vineyards 1 and 3, given that the most represented density classes were 1.087 and 1.080 g cm^{-3} , respectively. Uneven ripening in *Vitis vinifera L.* has substantial implications in wine composition and quality (Barbagallo et al. 2021, Kontoudakis et al. 2011), since most of sensory attributes of red wines, including color, structure, astringency, and bitterness, are associated with grapes phenolic composition (Canals et al. 2005, Llaudy et al. 2004) depending, in turn, on the phenolic maturity of grapes at harvest. The presence of a certain, non-negligible percentage of unripe berries in vinification causes the appearance of bitter and astringent characters in wine due to the release of low molecular weight proanthocyanidins, especially from seeds (Rolle et al. 2012). For instance, the 1.073 g cm^{-3} density class, that is conceivably responsible for green and bitter notes in wines (Torchio et al. 2010), was not present in 2020 and in 2021 it represented the 11% in vineyard 2, the 3% in vineyard 3 and the 6% in vineyard 4.

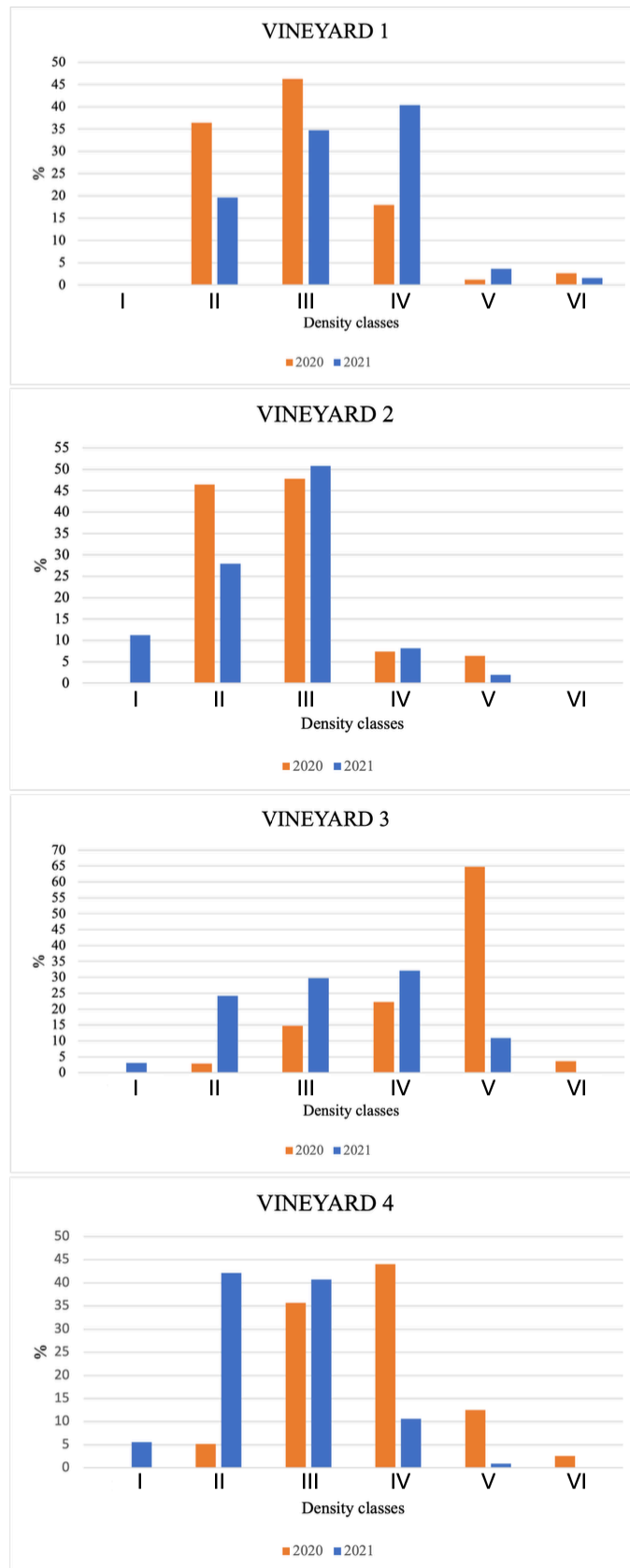


FIGURE 3. DENSITY CLASSES DISTRIBUTIONS OF NERO D'AVOLA GRAPES GROWN ON DIFFERENT SOILS IN 2020 AND 2021 VINTAGES.

TABLE 4. MODE, KURTOSIS, AND SKEWNESS OF DENSITY CLASSES DISTRIBUTIONS. THE MODE REPRESENTS THE MOST PRESENT DENSITY CLASS, THE KURTOSIS REPRESENTS RIPENESS HOMOGENEITY, AND THE SKEWNESS REPRESENTS THE MATURATION RATE.

<i>2020 vintage</i>				
	<i>Vineyard 1</i>	<i>Vineyard 2</i>	<i>Vineyard 3</i>	<i>Vineyard 4</i>
<i>Mode</i>	1.091	1.091	1.109	1.099
<i>Kurtosis</i>	-0.531	-0.184	1.014	0.619
<i>Skewness</i>	0.257	0.635	-1.293	-0.043
<i>2021 vintage</i>				
	<i>Vineyard 1</i>	<i>Vineyard 2</i>	<i>Vineyard 3</i>	<i>Vineyard 4</i>
<i>Mode</i>	1.099	1.091	1.099	1.078
<i>Kurtosis</i>	-0.369	-0.697	-0.920	-1.007
<i>Skewness</i>	-0.348	-0.044	-0.182	0.237

GRAPES PHYSICAL-CHEMICAL PARAMETERS

The main chemical-physical parameters of grape berries, including berry weight and number of seeds per berry, reducing sugars content (g L^{-1}), pH, total acidity (g L^{-1}), tartaric acid content (g L^{-1}) and malic acid content (g L^{-1}), are listed in Table 5.

Berry weight was higher in low-density classes and lower in high-density classes. The number of seeds per berry followed the same trend as berry weight. In fact, the higher the number of seeds per berry the lower the density class. Vineyard 2 had the highest berry weight and number of seeds per berry in both 2020 and 2021 vintages. Reducing sugars content and pH value increased with increasing apparent density. On the contrary, total acidity, tartaric acid and malic acid decreased with maturation. Total acidity and tartaric acid were higher in 2021 than in 2020.

TABLE 5. CHEMICAL-PHYSICAL PARAMETERS DURING RIPENING OF NERO D'AVOLA GRAPES GROWN ON DIFFERENT SOILS IN 2020 AND 2021 VINTAGES.

2020 Vintage

Vineyard 1

<i>Density class</i>	I	II	III	IV	V	VI
<i>% density class</i>	0	36	46	18	3	1
<i>Berry weight (g)</i>	/	1.8 ± 0.1 BC	1.68 ± 0.03 AB	1.40 ± 0.07 A	1.4 ± 0.3	1.3 ± 0.5
<i>n° of seeds/berry</i>	/	1.4 ± 0.1 b	1.2 ± 0.2 ab, α	0.88 ± 0.03 ab, α	0.81 ± 0.02 a, α	0.7 ± 0.04 a, α
<i>Reducing sugars (g L⁻¹)</i>	/	185 ± 9 a	216 ± 10 ab	245 ± 12 bc	273 ± 19 c	284 ± 15 c
<i>pH</i>	/	3.18 ± 0.05	3.21 ± 0.07	3.16 ± 0.05 A	3.16 ± 0.07 A	3.16 ± 0.01 A
<i>Total acidity (g L⁻¹)</i>	/	6.40 ± 0.04	6.06 ± 0.4	6.2 ± 0.5	6.16 ± 0.03	6.2 ± 0.3 B
<i>Tartaric acid (g L⁻¹)</i>	/	7.2 ± 0.6	7.03 ± 0.5	7 ± 3	7.2 ± 0.1	7.6 ± 0.9 C
<i>Malic acid (g L⁻¹)</i>	/	1.3 ± 0.1	0.98 ± 0.09 A	0.94 ± 0.06 A	0.94 ± 0.06	0.88 ± 0.02 A

Vineyard 2

<i>Density class</i>	I	II	III	IV	V	VI
<i>% density class</i>	0	46	48	7	6	0
<i>Berry weight (g)</i>	/	2.1 ± 0.1 C	1.9 ± 0.1 BC	1.8 ± 0.2 AB	1.5 ± 0.1 α	/
<i>n° of seeds/berry</i>	/	1.3 ± 0.2	1.5 ± 0.3	1.0 ± 0.1	0.8 ± 0.2 α	/
<i>Reducing sugars (g L⁻¹)</i>	/	189 ± 10 a	217 ± 14 ab	242 ± 20 ab	268 ± 3 b	/
<i>pH</i>	/	3.31 ± 0.05 a	3.33 ± 0.01 a	3.42 ± 0.05 B, b	3.36 ± 0.02 BC, ab	/
<i>Total acidity (g L⁻¹)</i>	/	5 ± 3 α	5 ± 1 α	4 ± 1 α	4 ± 1 α	/
<i>Tartaric acid (g L⁻¹)</i>	/	5 ± 1 α	4.5 ± 0.8 α	3 ± 1 α	3 ± 1 α	/
<i>Malic acid (g L⁻¹)</i>	/	1.9 ± 0.7	1.6 ± 0.1 B	1.45 ± 0.04 AB	1.41 ± 0.07	/

Vineyard 3

<i>Density class</i>	I	II	III	IV	V	VI
<i>% density class</i>	0	3	15	22	65	4
<i>Berry weight (g)</i>	/	1.51 ± 0.08 a, B	2.13 ± 0.04 C, b, β	2.3 ± 0.1 B, b, β	2.2 ± 0.1 b, β	1.1 ± 0.1 a
<i>n° of seeds/berry</i>	/	1.5 ± 0.3	1.55 ± 0.08	1.6 ± 0.4	0.9 ± 0.1	0.9 ± 0.2
<i>Reducing sugars (g L⁻¹)</i>	/	220 ± 10	236 ± 13	249 ± 40	284 ± 10	290 ± 30
<i>pH</i>	/	3.13 ± 0.09 a, β	3.30 ± 0.07 ab, β	3.44 ± 0.05 B, b, β	3.51 ± 0.04 C, b, β	3.55 ± 0.03 C, b, β
<i>Total acidity (g L⁻¹)</i>	/	6 ± 2 α	5.4 ± 0.3 α	5.8 ± 0.3 α	5.5 ± 0.5 α	5.5 ± 0.8 B, α
<i>Tartaric acid (g L⁻¹)</i>	/	8.4 ± 0.3 α	6.8 ± 0.1 α	6.2 ± 0.9 α	6.5 ± 0.2 α	6.1 ± 0.2 B, α
<i>Malic acid (g L⁻¹)</i>	/	1.0 ± 0.5	1.1 ± 0.1 A	0.8 ± 0.3 A	0.88 ± 0.05	0.8 ± 0.1 A

Vineyard 4

<i>Density class</i>	I	II	III	IV	V	VI
<i>% density class</i>	0	5	36	44	12	3
<i>Berry weight (g)</i>	/	1.13 ± 0.03 a, A, α	1.56 ± 0.03 A, b, α	1.60 ± 0.04 A, b, α	1.7 ± 0.1 b, α	1.26 ± 0.06 a
<i>n° of seeds/berry</i>	/	0.8 ± 0.1 α	1.33 ± 0.08	1.3 ± 0.2	1.4 ± 0.3	1.0 ± 0.2
<i>Reducing sugars (g L⁻¹)</i>	/	180 ± 20	206 ± 28	222 ± 29	250 ± 30	261 ± 28
<i>pH</i>	/	3.28 ± 0.05	3.4 ± 0.1	3.34 ± 0.09 AB	3.31 ± 0.03 AB	3.29 ± 0.02 B
<i>Total acidity (g L⁻¹)</i>	/	5 ± 2 α	5 ± 1 α	4 ± 3 α	4.9 ± 0.3 α	4.8 ± 0.4 A, α
<i>Tartaric acid (g L⁻¹)</i>	/	6 ± 3 α	4 ± 1 α	4 ± 1 α	5 ± 1 α	4.3 ± 0.2 A, α
<i>Malic acid (g L⁻¹)</i>	/	2.4 ± 0.1 c, β	2.4 ± 0.1 C, c, β	2.2 ± 0.2 B, bc	1.8 ± 0.1 ab	1.51 ± 0.06 B, a

2021 vintage

Vineyard 1

Density class	I	II	III	IV	V	VI
% density class	0	20	35	40	4	2
Berry weight (g)	/	1.790 ± 0.006 B, c	1.937 ± 0.002 B, d	1.64 ± 0.01 A, b	1.42 ± 0.03 a	1.37 ± 0.05 a
n° of seeds/berry	/	1.58 ± 0.04 B, bc	1.7 ± 0.1 B, c, β	1.48 ± 0.04 B, b, β	1.3 ± 0.1 a, β	1.1 ± 0.3 a, β
Reducing sugars (g L ⁻¹)	/	169 ± 12	196 ± 14	211 ± 24	245 ± 20	273 ± 8
pH	/	3.17 ± 0.01 B	3.2 ± 0.1 B	3.20 ± 0.03	3.23 ± 0.05	3.22 ± 0.04
Total acidity (g L ⁻¹)	/	6.47 ± 0.05	6.4 ± 0.2	6.6 ± 0.3	6.15 ± 0.01	6.13 ± 0.01
Tartaric acid (g L ⁻¹)	/	8.3 ± 0.7	8.1 ± 0.7	8 ± 1	8.4 ± 0.9	8.4 ± 0.6
Malic acid (g L ⁻¹)	/	1.12 ± 0.09 b	1.06 ± 0.06 b	0.87 ± 0.05 a	0.85 ± 0.04 a	0.83 ± 0.04 a

Vineyard 2

Density class	I	II	III	IV	V	VI
% density class	11	28	51	8	2	0
Berry weight (g)	2.27 ± 0.01 C, b	2.37 ± 0.02 D, c	2.306 ± 0.007 D, b	1.999 ± 0.002 D, a	1.85 ± 0.04 a, β	/
n° of seeds/berry	1.8 ± 0.1 B, d	1.6 ± 0.5 B, c	1.4 ± 0.3 A, b	1.28 ± 0.04 A, a	1.22 ± 0.05 a, β	/
Reducing sugars (g L ⁻¹)	156 ± 4 a	176 ± 9 a	183 ± 24 a	254 ± 9 b	268 ± 1 b	/
pH	3.22 ± 0.01 B	3.27 ± 0.03 B	3.29 ± 0.03 B	3.32 ± 0.07	3.30 ± 0.01	/
Total acidity (g L ⁻¹)	6.9 ± 0.6	7 ± 1 β	6 ± 1 β	7 ± 2 β	7 ± 1 β	/
Tartaric acid (g L ⁻¹)	7 ± 1	8 ± 2 β	8 ± 2 β	7 ± 2 β	7 ± 2 β	/
Malic acid (g L ⁻¹)	2.0 ± 0.2	1.9 ± 0.2	1.6 ± 0.1	1.5 ± 0.2	1.47 ± 0.05	/

Vineyard 3

Density class	I	II	III	IV	V	VI
% density class	3	24	30	32	11	0
Berry weight (g)	1.384 ± 0.005 A, a	1.57 ± 0.01 A, b, α	1.706 ± 0.001 A, c, α	1.72 ± 0.01 B, c, α	1.43 ± 0.03 a	/
n° of seeds/berry	1.33 ± 0.04 A, abc	1.2 ± 0.1 A, ab	1.48 ± 0.04 AB, bc	1.53 ± 0.04 B, c	1.1 ± 0.1 a	/
Reducing sugars (g L ⁻¹)	161 ± 3	193 ± 19	222 ± 10	236 ± 29	240 ± 31	/
pH	2.91 ± 0.06 A	2.99 ± 0.08 A, α	3.1 ± 0.1 A, α	3.1 ± 0.2 α	3.1 ± 0.3 α	/
Total acidity (g L ⁻¹)	9 ± 1	8 ± 1 β	8 ± 2 β	6.1 ± 0.2 β	6.8 ± 0.9 β	/
Tartaric acid (g L ⁻¹)	10.2 ± 0.2	8.9 ± 0.4 β	9 ± 2 β	7.4 ± 0.8 β	7.5 ± 0.7 β	/
Malic acid (g L ⁻¹)	1.2 ± 0.4	1.0 ± 0.2	1.1 ± 0.4	0.8 ± 0.8	0.8 ± 0.4	/

Vineyard 4

Density class	I	II	III	IV	V	VI
% density class	6	42	40	11	1	0
Berry weight (g)	2.08 ± 0.01 B, d	1.87 ± 0.03 C, a	2.021 ± 0.002 C, c	1.962 ± 0.004 C, b	2.03 ± 0.01 b	/
n° of seeds/berry	1.9 ± 0.1 C, c	1.78 ± 0.03 C, c, β	1.55 ± 0.07 AB, b	1.301 ± 0.001 A, a	1.27 ± 0.02 a	/
Reducing sugars (g L ⁻¹)	166 ± 5 a	191 ± 8 ab	222 ± 11 bc	249 ± 19 C, b	260 ± 7 c	/
pH	3.22 ± 0.06 B, a	3.25 ± 0.02 B, ab	3.4 ± 0.1 B, abc	3.40 ± 0.04 bc	3.42 ± 0.06 c	/
Total acidity (g L ⁻¹)	7.8 ± 0.7	7 ± 1 β	7 ± 2 β	7 ± 2 β	6.6 ± 0.8 β	/
Tartaric acid (g L ⁻¹)	9 ± 2	9 ± 2	8 ± 3	8 ± 3	8 ± 2	/
Malic acid (g L ⁻¹)	1.7 ± 0.6	1.5 ± 0.6 α	1.6 ± 0.5 α	1.4 ± 0.6	1.3 ± 0.3	/

PHENOLIC COMPOUNDS IN GRAPES

TOTAL FLAVONOIDS AND TOTAL ANTHOCYANINS

The contents of total flavonoids in skins and seeds and of total anthocyanins in skins were significantly different among vineyards (Table A1 in Appendix A). Total anthocyanins were significantly lower in 2020 with respect to 2021. On the contrary, grape seed tannins were significantly higher in 2020 vintage. Regarding skins flavonoids, their content was significantly lower in 2020, excepting for vineyard 3 that showed an opposite behavior.

Skins total flavonoids and anthocyanins tended to increase during ripening, whereas seeds flavonoids decreased with increasing ripeness (Figure 4). Proanthocyanidins in both skins and seeds are synthesized from early stage of berry development until veraison (González-Manzano et al., 2004; Downey et al., 2003). During ripening the concentration of proanthocyanidins tends to remain constant or to decrease slightly due to oxidative and thermic degradation processes (Geny et al., 2003). Therefore, the increase of skins total flavonoids observed in this study must be attributed to a greater extractability from berry skin cells during ripening caused by histochemical modifications occurring in berry tissues (Peyrot des Gachons et al., 2003). On the contrary, grape seeds undergo to the hardening of their tissues towards ripening, due to a lignification process. Therefore, flavonoids in riper grapes have a lower extractability with respect to insufficiently ripened grapes (Cadot et al., 2006). Moreover, in clusters with uneven ripeness can coexist ripe berries which have already stopped proanthocyanidins biosynthesis at veraison and unripe berries which continue to synthesize proanthocyanidins. The vinification of unripe grapes leads to the production of astringent and bitter wines because of a greater release of proanthocyanidins from seeds.

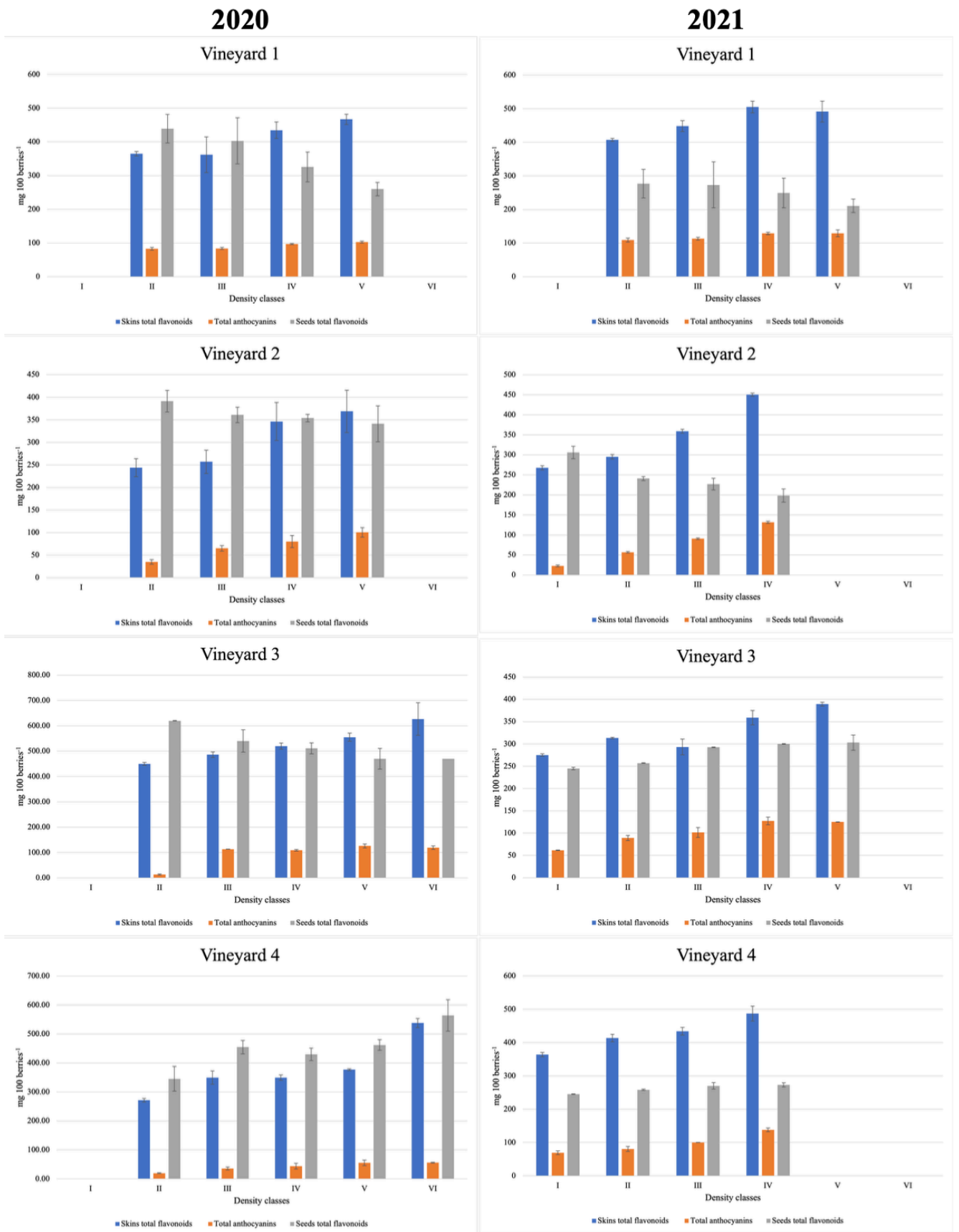


FIGURE 4. SKINS TOTAL FLAVONOIDS, TOTAL ANTHOCYANINS AND SEEDS TOTAL FLAVONOIDS DURING RIPENING OF NERO D'AVOLA GRAPES GROWN ON DIFFERENT SOILS IN 2020 AND 2021 VINTAGES.

MONOMER ANTHOCYANINS PROFILES

In grape skins from all vineyards, tri-oxygenated anthocyanins (malvidin-3-glucoside, petunidin-3-glucoside, and delphinidin-3-glucoside) prevailed over di-oxygenated forms (peonidin-3-glucoside and cyanidin-3-glucoside) (Figure 5 and Table A2 in Appendix A). Among tri-oxygenated forms, malvidin-3-glucoside, namely the anthocyanin mostly involved in wine color stability (Gómez-Míguez et al., 2006), was the most present. Its content increased during the ripening process, reaching about 40% of total monomer anthocyanins at technological maturation, without significant differences among vineyards and vintages. As malvidin-3-glucoside, even the other tri-substituted monomer anthocyanins tended to increase during the ripening process. On the contrary, di-substituted anthocyanins, as well as acetylated anthocyanins showed an irregular trend during ripening, conceivably because of their involvement in coupled oxidation-reduction reactions (Cheynier et al., 1988). *p*-coumaroylated derivatives content was very high in all samples and, in some vineyards and stages of ripening, their content exceeded that of malvidin-3-glucoside itself. Their content tended to decrease during berry ripening. The ratio acetylated/*p*-coumarylated anthocyanins was lower than 1, ranging between 0.3 and 0.7.



FIGURE 5. MONOMER ANTHOCYANINS PROFILES DURING RIPENING OF NERO D'AVOLA GRAPES GROWN ON DIFFERENT SOILS IN 2020 AND 2021 VINTAGES.

HYDROXYCINNAMOYL TARTARIC ACIDS (HCTAs)

Five HCTAs were detected in *Nero d'Avola* wines, namely *cis*-caffeoyl tartaric acid, *trans*-caffeoyl tartaric acid, *cis-p*-coumaroyl tartaric acid, *trans-p*-coumaroyl tartaric acid, and *trans*-feruloyl tartaric acid (Figure 6 and Table A3 in Appendix A). In skins from *Nero d'Avola* grapes the predominant HCTA was *trans*-caffeoyl tartaric acid, whereas the least prevalent was *cis*-caffeoyl tartaric acid. Caffeoyl tartaric acid (in both *trans* and *cis* forms) is very important because it is the substrate of choice for grape polyphenol-oxidase. A similar evolution trend of HCTAs was observed among vineyards and vintages. It was observed that *trans*-caffeoyl tartaric acid decreased from the first (1.073 g cm^{-3}) to the third (1.087 cm^{-3}) stage of ripening, then slightly increased in the last stages of ripening ($1.101 - \geq 1.108 \text{ cm}^{-3}$). The same trend was also observed by Giuffrè (2013). Vineyard 2 showed significantly lower contents of HCTAs and vineyard 3 showed significantly higher contents in both 2020 and 2021 vintages. Some differences were also observed between the two vintages. In fact, *cis*-caffeoyl tartaric acid and the *trans*-feruloyl tartaric acid were significantly higher in 2020, whereas *trans*-caffeoyl tartaric acid, *cis-p*-coumaroyl tartaric acid, and *trans-p*-coumaroyl tartaric acid were significantly higher in 2021.

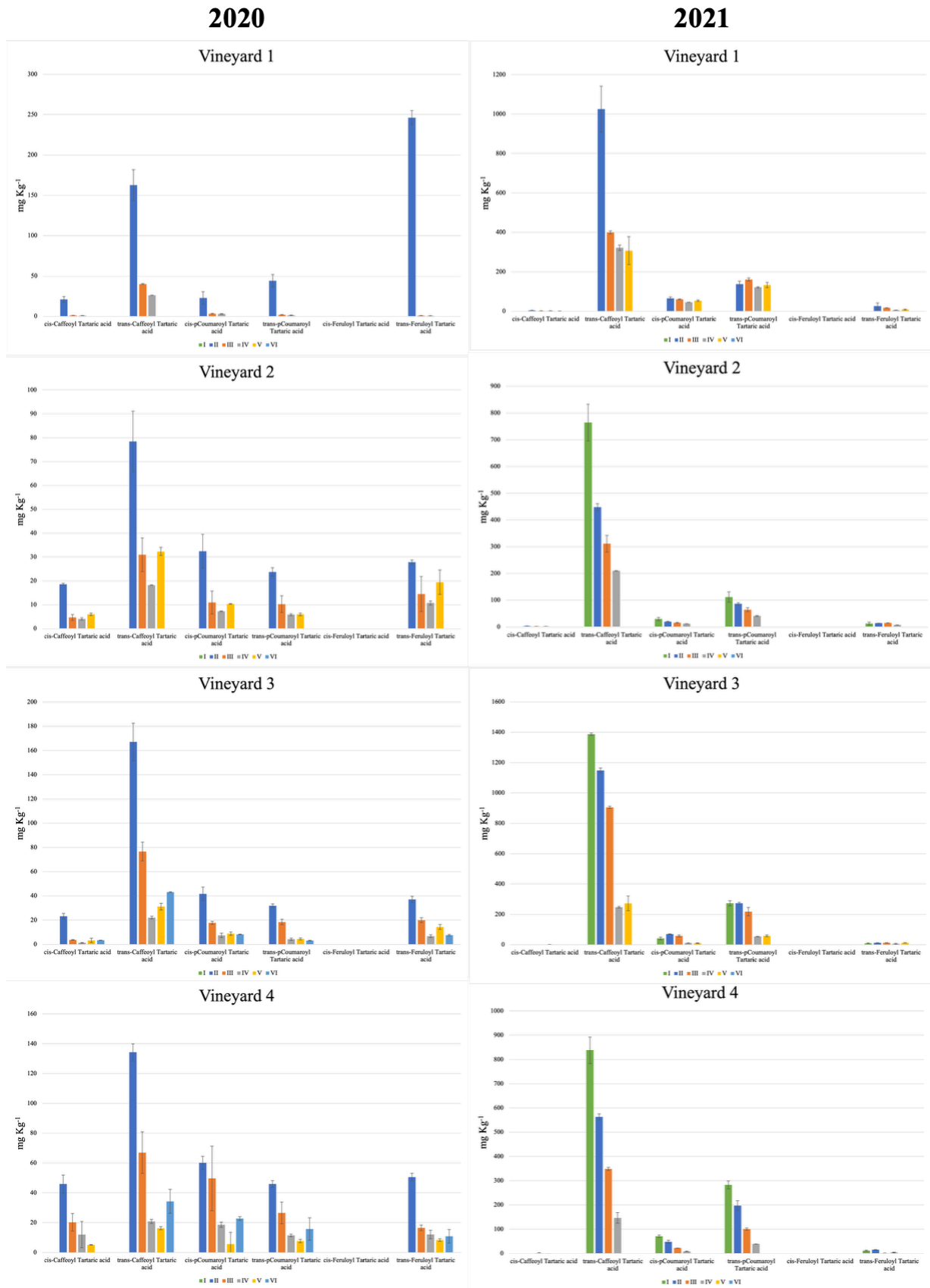


FIGURE 6. HCTAS CONTENT DURING RIPENING OF NERO D'AVOLA GRAPES GROWN ON DIFFERENT SOILS IN 2020 AND 2021 VINTAGES.

FLAVONOLS

Nine flavonols, including myricetin-3-glucuronide, myricetin-3-glucoside, quercetin-3-glucuronide, quercetin-3-glucoside, isorhamnetin-3-glucoside, laricitrin-3-glucoside, kaempferol-3-glucuronide, kaempferol-3-glucoside and syringetin-3-glucoside, were detected in Nero d'Avola wines (Figure 7 and Table A4 in Appendix A). The most abundant flavonol was quercetin-3-glucoside. It was followed by the isorhamnetin-3-glucoside and quercetin-3-glucuronide. Myricetin-3-glucoside was found in 2020, only. Flavonols play important roles, including acting as copigments for anthocyanins (Gambutì et al., 2020). However, precipitate of quercetin can originate from wine upon aging due to the hydrolysis of glycosides (Waterhouse et al., 2016).

The relative ratio among flavonols was almost consistent among the analyzed Nero d'Avola grapes, suggesting that the flavonols pattern is mostly controlled by genotype (Mattivi et al., 2006). However, significant differences in their concentrations were observed among vineyards and between vintages. Their content was significantly higher in 2021 than in 2020.

Flavonols tends to decrease during ripening. An interesting exception was observed in vineyard 2 in 2021, where the quercetin-3-glucoside increased from the first (1.073 g cm^{-3}) to the second (1.080 g cm^{-3}) stage of ripening and then decreased as in other vineyards. This behavior suggested that quercetin-3-glucoside in vineyard 2 was synthesized between the first and second analyzed stages of ripening, while in all other vineyards its biosynthesis was already stopped at the first stage. To date only little information is reported in literature about the evolution of individual flavonols during berry development (Fanzone et al., 2011). Therefore, our findings can open new issues about flavonols evolution during grape maturation.

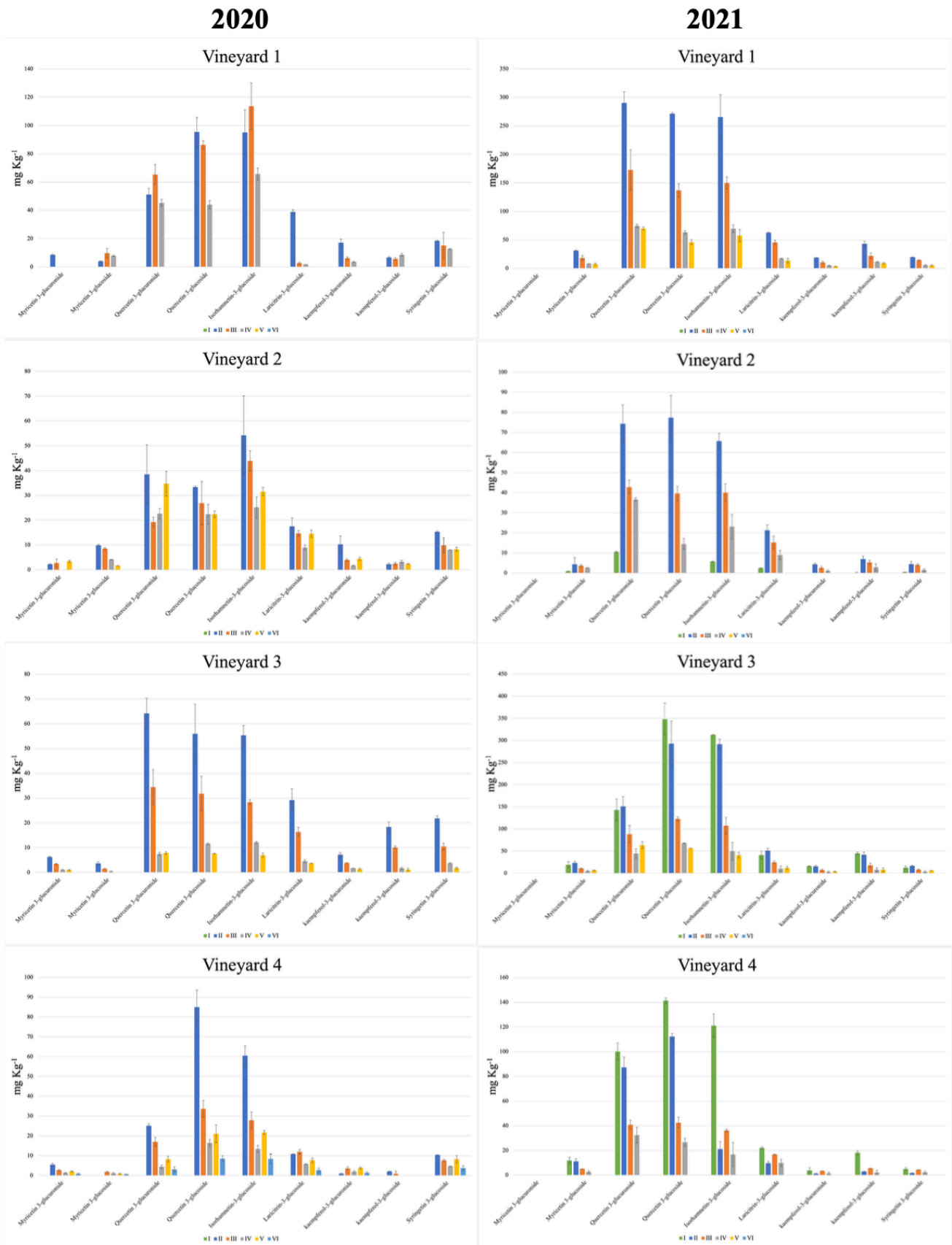


FIGURE 7. FLAVONOLS CONTENT DURING RIPENING OF NERO D'AVOLA GRAPES GROWN ON DIFFERENT SOILS IN 2020 AND 2021 VINTAGES

MODELING OF PHENOLS EVOLUTION DURING RIPENING THE *TRANS*-CAFFEYOYL TARTARIC ACID CASE

The evolution of *trans*-caffeoyl tartaric acid content during grape ripening was modeled by means of the *parabola equation*:

1.
$$y = ax^2 + bx + c$$

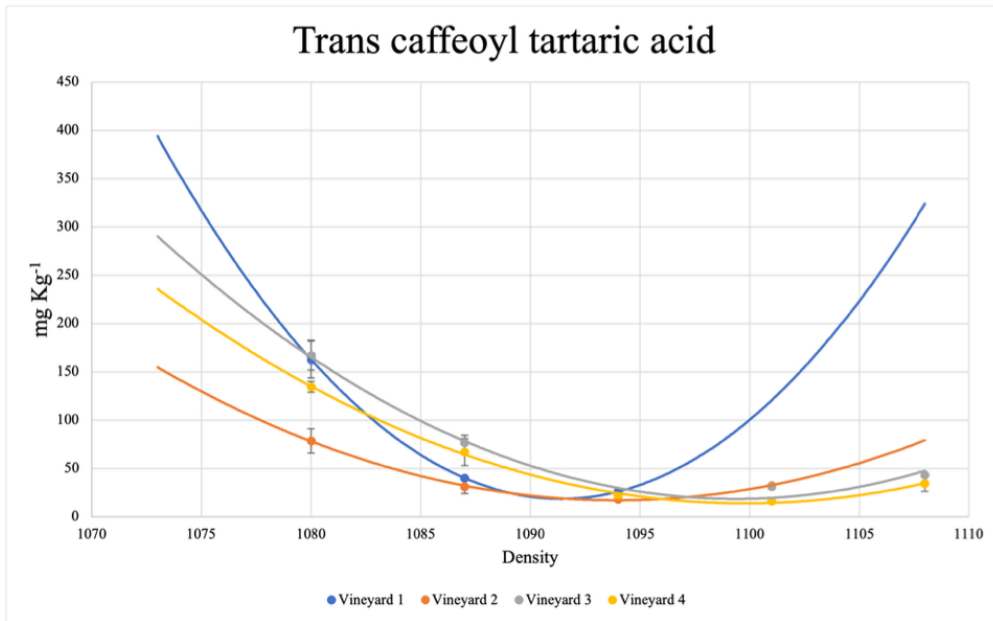
The parameter a represents the concavity and the opening of the parabola. It depends on the decreasing rate of *trans*-caffeoyl tartaric acid during the first stages of ripening and on the slight increase in the last stages of ripening. The parameter b is the position of the symmetry axis with respect to y axis. It depends on the stage of ripening showing the minimum content of *trans*-caffeoyl tartaric acid. Finally, the parameter c is the point of intersection with the y axis. It depends on the content of *trans*-caffeoyl tartaric acid at the first stage of ripening. The graphs reporting the curves fitting the experimental points of *trans*-caffeoyl tartaric acid during grape ripening are shown in Figure 8. The equations describing the evolution of *trans*-caffeoyl tartaric acid together with the R^2 value and the parameters are listed in Table 6. In grapes from vineyard 3, in both 2020 and 2021, the rate of decrease and the initial content were significantly lower than other vineyards. The opposite behavior has observed in vineyard 1.

TABLE 6. MODELLING OF HCTAS DURING RIPENING OF NERO D'AVOLA GRAPES GROWN ON DIFFERENT SOILS IN 2020 AND 2021 VINTAGES: THE TRANS-CAFFEYOYL TARTARIC ACID CASE.

2020		Parameters						
	Equation	R²	a	b	c			
Vineyard 1	$y = 1.1x^2 - 2420x + 1 \cdot 10^6$	$R^2 = 1$	1.1 ± 0.1	b	-2420 ± 30	a	$1 \cdot 10^6 \pm 2.3 \cdot 10^3$	c
Vineyard 2	$y = 0.31x^2 - 680x + 3.74 \cdot 10^5$	$R^2 = 0.9985$	0.31 ± 0.01	a	-680 ± 23	c	$3.74 \cdot 10^5 \pm 210$	a
Vineyard 3	$y = 0.39x^2 - 860x + 4.73 \cdot 10^5$	$R^2 = 0.9841$	0.39 ± 0.01	a	-860 ± 45	b	$4.73 \cdot 10^5 \pm 400$	b
Vineyard 4	$y = 0.31x^2 - 687x + 3.76 \cdot 10^5$	$R^2 = 0.9977$	0.31 ± 0.01	a	-687 ± 22	c	$3.76 \cdot 10^5 \pm 202$	a
2021		Parameters						
	Equation	R²	a	b	c			
Vineyard 1	$y = 3.12x^2 - 6826x + 4 \cdot 10^6$	$R^2 = 0.9669$	3.12 ± 0.01	d	-6826 ± 23	a	$4 \cdot 10^6 \pm 4.03 \cdot 10^3$	d
Vineyard 2	$y = 1.1x^2 - 2401x + 1 \cdot 10^6$	$R^2 = 0.9940$	1.1 ± 0.2	c	-2401 ± 34	b	$1 \cdot 10^6 \pm 3.4 \cdot 10^3$	c
Vineyard 3	$y = 0.17x^2 - 405x + 2.45 \cdot 10^5$	$R^2 = 0.9247$	0.17 ± 0.01	a	-405 ± 9	d	$2.45 \cdot 10^5 \pm 4.2 \cdot 10^3$	a
Vineyard 4	$y = 0.37x^2 - 832x + 4.69 \cdot 10^5$	$R^2 = 0.9996$	0.37 ± 0.02	b	-832 ± 12	c	$4.69 \cdot 10^5 \pm 1.2 \cdot 10^3$	b

DIFFERENT LOWERCASE LETTERS INDICATE SIGNIFICANT DIFFERENCES AMONG DIFFERENT VINEYARDS (P<0.05).

2020



2021

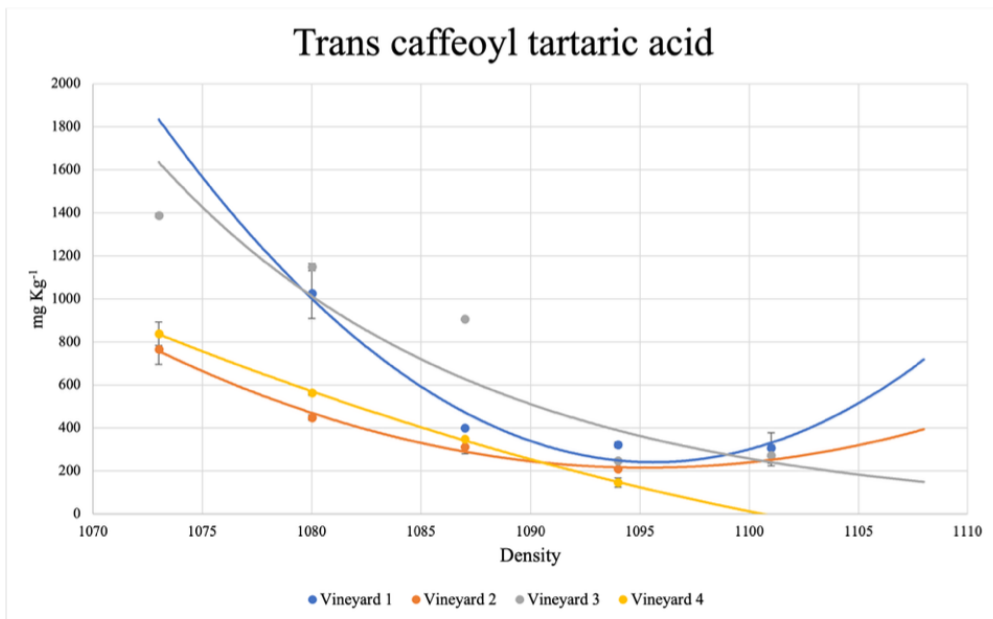


FIGURE 8. MODELING OF HCTAS DURING RIPENING OF NERO D'AVOLA GRAPES GROWN ON DIFFERENT SOILS IN 2020 AND 2021 VINTAGES: THE TRANS-CAFFELOYL TARTARIC ACID CASE

THE QUERCETIN-3-GLUCOSIDE CASE

The evolution of quercetin-3-glucoside content during maturation has been modeled by means of a decreasing *exponential curve*:

$$2. \quad y = ae^{-bx}$$

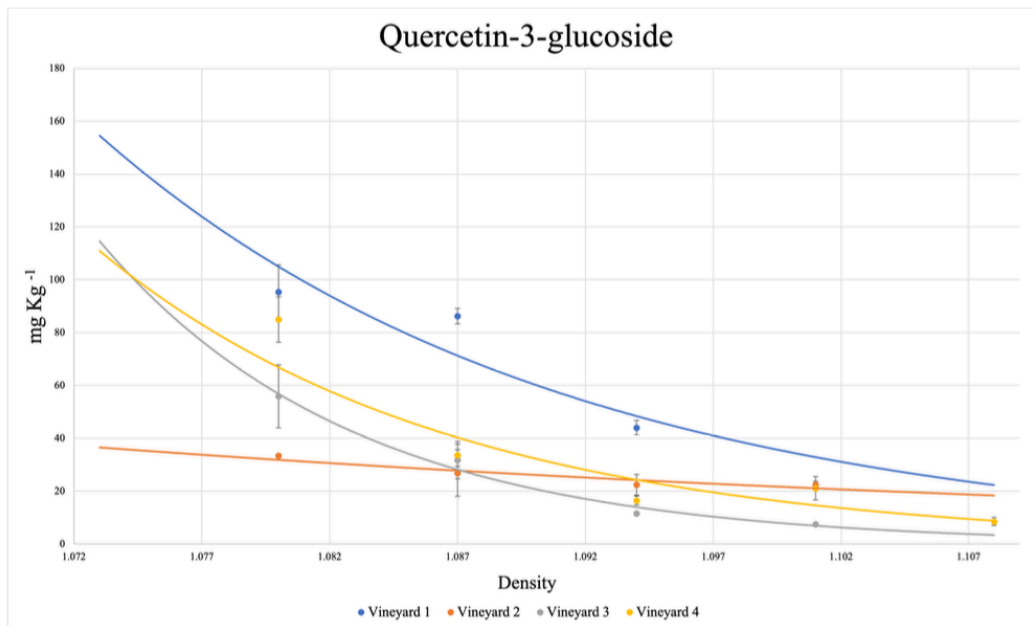
The parameter a depends on the difference between the initial and the final content of quercetin-3-glucoside and the parameter b is the decreasing rate of quercetin-3-glucoside during the maturation process. The graphs reporting the curves fitting the experimental points are shown in Figure 9, while the equations, the R^2 values and the parameters are listed in Table 7. It can be observed that in grapes from vineyard 2 in 2020 the content decreasing was very low with respect to grapes from the other vineyards. No significant differences were observed in the decreasing rate in 2021 vintage.

TABLE 7. MODELLING OF FLAVONOLS DURING RIPENING OF NERO D'AVOLA GRAPES GROWN ON DIFFERENT SOILS IN 2020 AND 2021 VINTAGES: THE QUERCETIN-3-GLUCOSIDE CASE

2020		Parameters				
	Equation	R ²	a	b		
Vineyard 1	$y = 9 \cdot 10^{27} e^{-55x}$	R ² = 0.7977	$9 \cdot 10^{27} \pm 8.70 \cdot 10^3$	b	-55 ± 1	c
Vineyard 2	$y = 5 \cdot 10^{10} e^{-19x}$	R ² = 0.9026	$5 \cdot 10^{10} \pm 2.00 \cdot 10^3$	a	-19 ± 2	d
Vineyard 3	$y = 6 \cdot 10^{48} e^{-100x}$	R ² = 0.9868	$6 \cdot 10^{48} \pm 3.42 \cdot 10^3$	d	-100 ± 4	a
Vineyard 4	$y = 6 \cdot 10^{35} e^{-72x}$	R ² = 0.9133	$6 \cdot 10^{35} \pm 2.00 \cdot 10^2$	c	-72 ± 3	b
2021		Parameters				
	Equation	R ²	a	b		
Vineyard 1	$y = 2 \cdot 10^{43} e^{-87x}$	R ² = 0.9927	$2 \cdot 10^{43} \pm 2.24 \cdot 10^8$	b	-87 ± 13	
Vineyard 2	$y = 1 \cdot 10^{58} e^{-119x}$	R ² = 0.9879	$1 \cdot 10^{58} \pm 3.01 \cdot 10^9$	c	-119 ± 16	
Vineyard 3	$y = 4 \cdot 10^{36} e^{-72x}$	R ² = 0.9229	$4 \cdot 10^{36} \pm 1.09 \cdot 10^7$	a	-72 ± 5	
Vineyard 4	$y = 1 \cdot 10^{42} e^{-85x}$	R ² = 0.9069	$1 \cdot 10^{42} \pm 3.54 \cdot 10^8$	b	-85 ± 8	

DIFFERENT LOWERCASE LETTERS INDICATE SIGNIFICANT DIFFERENCES AMONG DIFFERENT VINEYARDS (P<0.05).

2020



2021

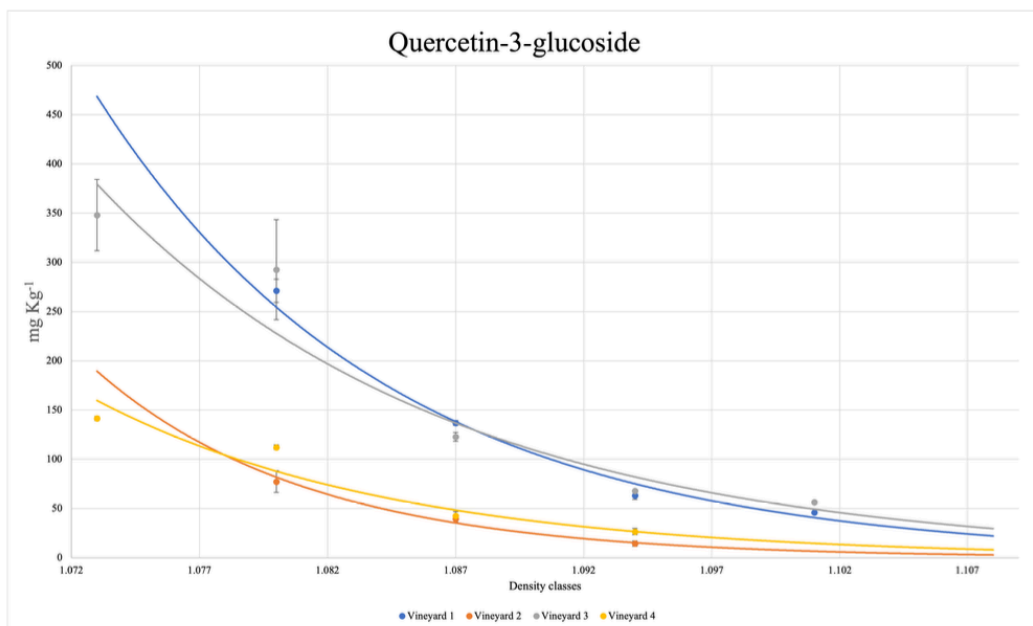


FIGURE 9. MODELING OF FLAVONOLS DURING RIPENING OF NERO D'AVOLA GRAPES GROWN ON DIFFERENT SOILS IN 2020 AND 2021 VINTAGES: THE QUERCETIN-3-GLUCOSIDE CASE.

SOIL EFFECT ON THE CHEMICAL COMPOSITION OF NERO D'AVOLA GRAPES

Compositional data of *Nero d'Avola* grapes were processed together with soil chemical-physical parameters to highlight possible soil-grapes correlations. The correlation heatmaps shown in Figures 10 and 11 report the correlation pattern existing between soils' chemical-physical parameters (Table 3) and grapes' compositional data (Table 5 and Tables A1-A4 in Appendix A) in 2020 and 2021 vintages, respectively. The most outstanding correlations are resumed in Table 8. Although some differences are observable in the correlation patterns of the two studied vintages, some correlations occurred in both 2020 and 2021. These included the positive correlation between soil silt content and organic acids and the negative correlation between silt and flavonols; the positive correlation between organic acids and flavonols with soil sand content; the negative correlation between cation exchange capacity (CEC) and electric conductivity (EC) with reducing sugars and anthocyanins; the negative correlation between soil pH and total carbonates with flavonols.

Soil texture affects several soil features, including nutrient adsorption capacity and water holding capacity. Soil texture affects water and nutrient dynamics primarily through its porosity. In fact, pore size distribution is directly affected by soil particle sizes. Clay-rich soils are mainly characterized by small-sized pores, also referred to as *residual pores*. The latter ($\leq 0.5 \mu\text{m}$) hold water molecules through very efficient $^1\text{H}-^1\text{H}$ dipolar interactions with pores boundaries (Handique et al., 2002). Therefore, the residual water is trapped into the soil system, and it is scarcely available to plant nutrition. Conversely, big-sized pores, or *transmission pores* ($\geq 50 \mu\text{m}$), are characteristic of sandy soils. Unlike *residual pores*, water molecules in transmission pores weakly interact with the pore boundaries. Water in transmission pores is rapidly drained away on behalf of air diffusion. This results in the leakage of dissolved nutrients. Finally, loamy soils are characterized by the presence of intermediate-sized pores, or *storage pores* ($0.5-50 \mu\text{m}$). These can both retain and release water

against gravity making it available for plant nutrition (Conte et al., 20017). Grapevine development, yield, and berries composition are largely affected by water and nutrient dynamics in soil. In particular, high water and nutrient availability determine great vine vigor and canopy development. Great vegetative development and excessive leaves crowding determine low sunlight irradiation in the cluster area causing a low accumulation of several metabolites in grape berries (Cortell et al., 2007). Organic acids, amino acids, flavonoids, and varietal aroma compounds are synthesized directly by berry tissues, in contrast to sugars that are imported into berries through vascular tissues (Mattivi et al., 2006). Therefore, their contents are the results of all the metabolic processes occurring in berries during ripening. Every metabolic perturbation caused by biotic and abiotic factors can modify their composition (Saengnil et al., 2011). For example, flavonoids are known to be highly responsive to changes in solar radiation (Cortell et al., 2007). Therefore, differences in water and nutrient availability due to different soil textures are possible explanation for the observed correlations. The low concentration of organic acids (especially malic acid) observed in soils with high sand content agrees with previous studies that attributed the decrease of malic acid to a malate breakdown due to low vine water status (Esteban et al., 1999; Matthews et al., 1988) and, also, to its respiration due to a thermal effect caused by a reduced vegetative growth (Basile et al., 2011). On the contrary, vines grown on silty soils are generally more vigorous, with a higher canopy development. The canopy architecture, that depends on the leaf crowding, modulates the incoming solar irradiation for grape clusters and their temperature. Low solar irradiation in the cluster region caused by excessive leaf crowding may cause the slowdown of sunlight-dependent metabolic processes, such as flavonols accumulation.

Vine vegetative growth is also affected by the CEC and by the EC, that are two parameters related to soil fertility. On the one hand, CEC is defined as the capacity of a soil to retain cations, such as calcium (Ca^{2+}), magnesium (Mg^{2+}), and potassium (K^+), by electrostatic forces. Indeed, CEC depends on the negative charges carried by soil particles, including clayey minerals, organic matter and sesquioxides (Sumner et al., 2006). Electrostatically retained cations are easily exchangeable with

those present in the soil solution. Therefore, a soil with high CEC has a great capacity to make cations available for plant nutrition. On the other hand, EC is the measure of ions dissolved in the soil solution. Therefore, it provides the concentration of nutrients effectively available for plant nutrition (Neina, 2019).

However, soils with high nutrient availability are known to produce vines with high vigor and excessive canopy development, determining low sunlight irradiation in the cluster region. This could affect the accumulation of sunlight-sensible metabolites in grapes, explaining the negative correlation between CEC and EC with reducing sugars and anthocyanins.

TABLE 8. POSITIVE/NEGATIVE CORRELATIONS BETWEEN SOIL AND WINE CHEMICAL-PHYSICAL PARAMETERS.

	2020	2021
<i>Clay</i>	<p>Positively correlated with: malic acid, <i>cis</i>-caffeoyl tartaric acid and <i>cis</i> p-coumaroyl tartaric acid</p> <p>Negatively correlated with: total acidity, tartaric acid, <i>cis</i>-p-coumaroyl tartaric acid, <i>trans</i>-caffeoyl tartaric acid</p>	<p>Positively correlated with: maturation rate, n° of seeds per berry, trans-Caffeoyl Tartaric acid and quercetin-3-glucoside</p> <p>Negatively correlated with: mode, kurtosis, Isorhamnetin-3-glucoside, and <i>cis</i>-Caffeoyl Tartaric acid</p>
<i>Silt</i>	<p>Positively correlated with: malic acid, <i>cis</i> p-coumaroyl tartaric acid, <i>trans</i>-pCoumaroyl Tartaric acid and <i>trans</i>-Feruloyl Tartaric acid, Myricetin 3-glucuronide</p> <p>Negatively correlated with: total acidity and tartaric acid, trans caffeoyl tartaric acid, Quercetin 3-glucuronide, Quercetin 3-glucoside and kaempferol-3-glucoside</p>	<p>Positively correlated with: skewness, malic acid, trans-Feruloyl Tartaric acid</p> <p>Negatively correlated with: most represented density class, homogeneity of ripeness, total anthocyanins, delphinidin, cyanidin, petunidin and acetylated anthocyanins, Isorhamnetin-3-glucoside, kaempferol-3-glucuronide and kaempferol-3-glucoside</p>
<i>Sand</i>	<p>Positively correlated with: total acidity and tartaric acid, trans-Caffeoyl Tartaric acid and kaempferol-3-glucoside</p> <p>Negatively correlated with: malic acid, <i>cis</i>-Caffeoyl Tartaric acid, <i>cis</i>-pCoumaroyl Tartaric acid, <i>trans</i>-pCoumaroyl Tartaric acid</p>	<p>Positively correlated with: most represented density class, homogeneity of ripeness, total anthocyanins, delphinidin-3-glucoside, malvidin-3-glucoside, Isorhamnetin-3-glucoside, kaempferol-3-glucuronide, kaempferol-3-glucoside and Syringetin 3-glucoside</p> <p>Negatively correlated with: skewness, n° of seeds per berry</p>
<i>CEC</i>	<p>Positively correlated with: maturation rate, n° of seeds per berry</p>	<p>Positively correlated with: grapes pH and malic acid</p>

	Negatively correlated with: with mode, reducing sugars content, skins total flavonoids, seeds total flavonoids and total anthocyanins, monomer anthocyanins	Negatively correlated with: reducing sugars content, and monomer anthocyanins
Soil pH and total carbonates	Positively correlated with: most represented density class, homogeneity of ripeness, grapes pH Negatively correlated with: maturation rate, Myricetin 3-glucoside, Quercetin 3-glucuronide, Quercetin 3-glucoside, Isorhamnetin-3-glucoside, kaempferol-3-glucuronide, kaempferol-3-glucoside and Syringetin 3-glucoside	Negatively correlated with: homogeneity of ripeness, p-coumaroylated anthocyanins, cis-Caffeoyl Tartaric acid, Laricitrin-3-glucoside and Syringetin 3-glucoside
Electric conductivity	Positively correlated with: malic acid, trans-pCoumaroyl Tartaric acid Negatively correlated with: total acidity and tartaric acid, total anthocyanins and seeds total flavonoids, p-coumaroylated anthocyanins	Positively correlated with: skewness, pH and total acidity, trans-Caffeoyl Tartaric acid and <u>trans-Feruloyl Tartaric acid</u> Negatively correlated with: most represented density class, reducing sugars, total anthocyanins, monomer anthocyanins
Organic matter	Positively correlated with: maturation rate Negatively correlated with: most represented density class, homogeneity of ripeness, grapes pH and reducing sugars, Myricetin 3-glucoside, Quercetin 3-glucuronide, Quercetin 3-glucoside, Isorhamnetin-3-glucoside, kaempferol-3-glucuronide, kaempferol-3-glucoside and Syringetin 3-glucoside	Positively correlated with: homogeneity of ripeness, p-coumaroylated anthocyanins, cis-Caffeoyl Tartaric acid, Laricitrin-3-glucoside

Organic matter and soil clay content provided different effects in the two vintages. For instance, in 2020, organic matter positively correlated with maturation rate and negatively correlated with the most present density class and with the homogeneity of ripeness, as well as with pH, reducing sugars and flavonols. In 2021, it positively correlated with homogeneity of ripeness, p-coumaroylated anthocyanins, caffeoyl tartaric acid and laricitrin-3-glucoside (Table 8). Both soil organic matter and soil clay content strongly affect water retention, influencing the available water content for vines (Lal 2020, Rawls et al. 2003). But the impact of organic matter and clay content on soil water retention capacity depends on several factors, including climatic conditions (particularly on the distribution

and the amount of precipitation). Therefore, it appears likely that in a certain vintage, with certain climatic conditions, organic matter and clay in soils produce an effect, and in another vintage, with other climatic conditions, they produce a different effect (Ubalde et al. 2010).

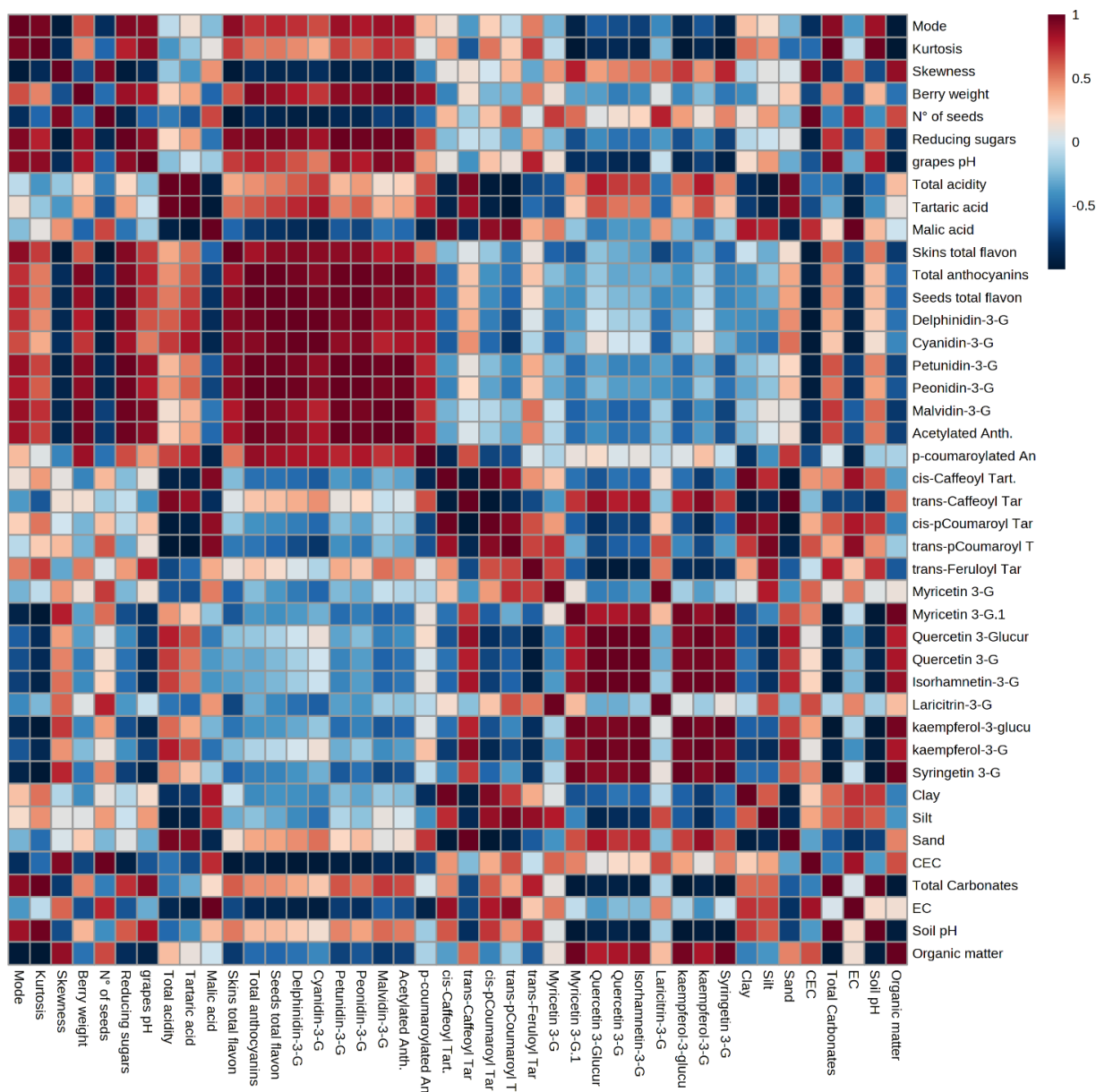


FIGURE 10. CORRELATION HEATMAP TO VISUALIZE THE RELATIONSHIPS EXISTING BETWEEN SOIL AND WINE CHEMICAL-PHYSICAL PARAMETERS IN 2020 VINTAGE. POSITIVE CORRELATIONS ARE INDICATED WITH THE RED COLOR AND NEGATIVE CORRELATIONS ARE INDICATED BY THE BLUE COLOR.

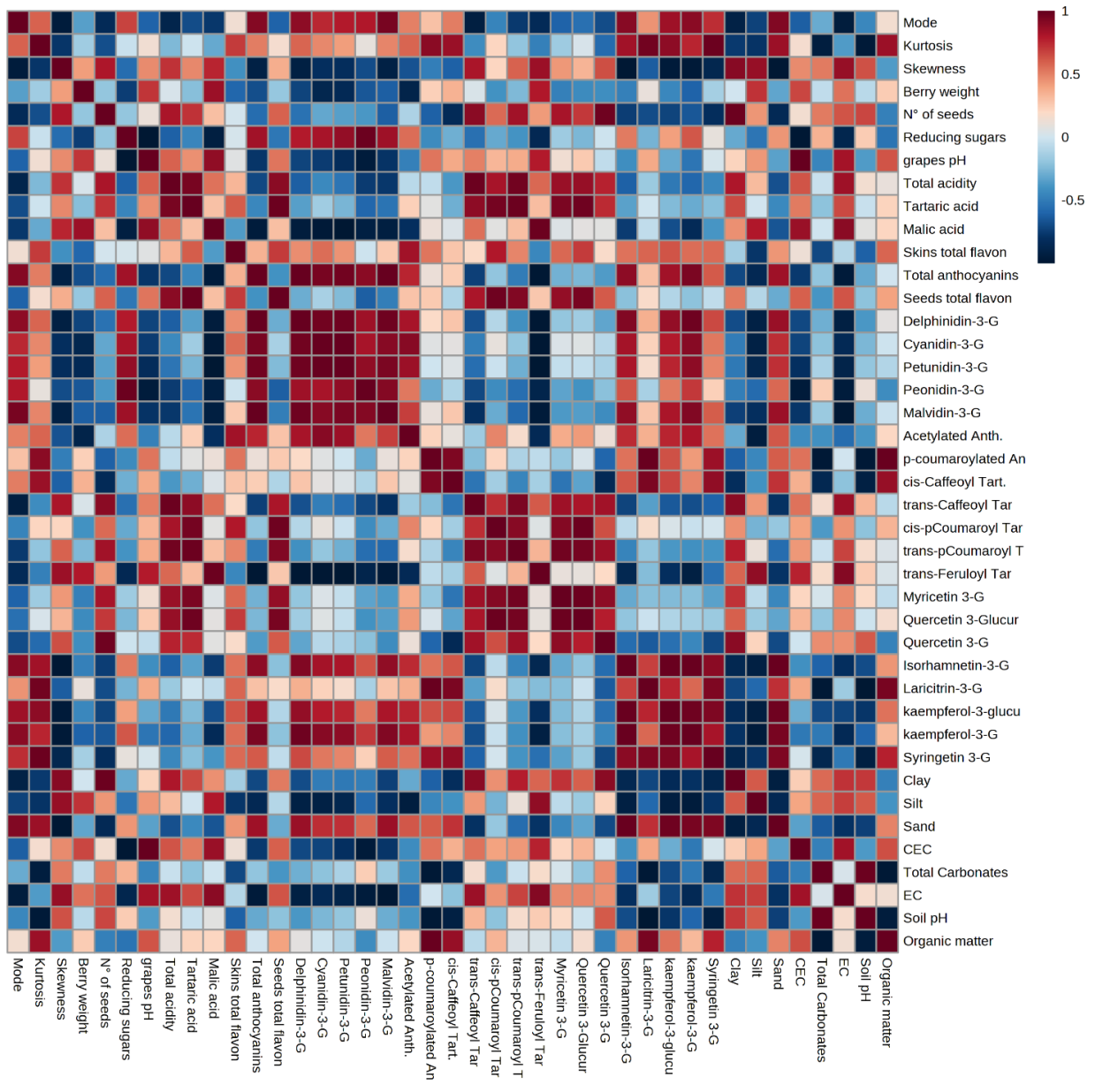


FIGURE 11. CORRELATION HEATMAP TO VISUALIZE THE RELATIONSHIPS EXISTING BETWEEN SOIL AND WINE CHEMICAL-PHYSICAL PARAMETERS IN 2021 VINTAGE. POSITIVE CORRELATIONS ARE INDICATED WITH THE RED COLOR AND NEGATIVE CORRELATIONS ARE INDICATED BY THE BLUE COLOR.

MULTIVARIATE STATISTICAL ANALYSIS

In order to visualize the separation among *Nero d'Avola* grapes from different vineyards, two principal component analysis (PCA) were performed, one for 2020 and one for 2021 vintage (Figure 12). As it can be observed by the 95% confidence regions highlighted with different colors in the two PCA Scores Plots, a clear separation among grapes grown on different soils is obtained in both vintages. In 2020, the first two components accounted for 61% of the total variation in the dataset, while in 2021 the variance explained was 72%. This suggested that the influence of the soil was clear and dominant in both vintages.

Then, to explore whether the soil effect is dominant even considering the inter-annual climatic variability, another PCA was performed considering the two studied vintages, simultaneously.

Figure 13 shows the PCA scores plot performed on *Nero d'Avola* grapes' variables of both 2020 and 2021 vintages. The first two component for this PCA analysis accounted for 70% of the total variation of the dataset. Two different clustering has been proposed: a soil-based clustering (Figure 13 A) and a vintage-based clustering (Figure 13 B). As it can be observed from Figure 13 A, the soil-based clustering did not produce an effective separation among grape samples, given that the 95% confidence regions related to each soil are superimposed to each other. On the contrary, the vintage-based clustering shown in Figure 13 B yielded two clearly distinguishable groups. These analyses suggested that, although the soil effect on grapes physical-chemical parameters is remarkable inside a certain vintage, conceivably through the modulation of water and nutrient dynamics, the vintage effect is still predominant, conceivably due to the inter-annual climatic variability.

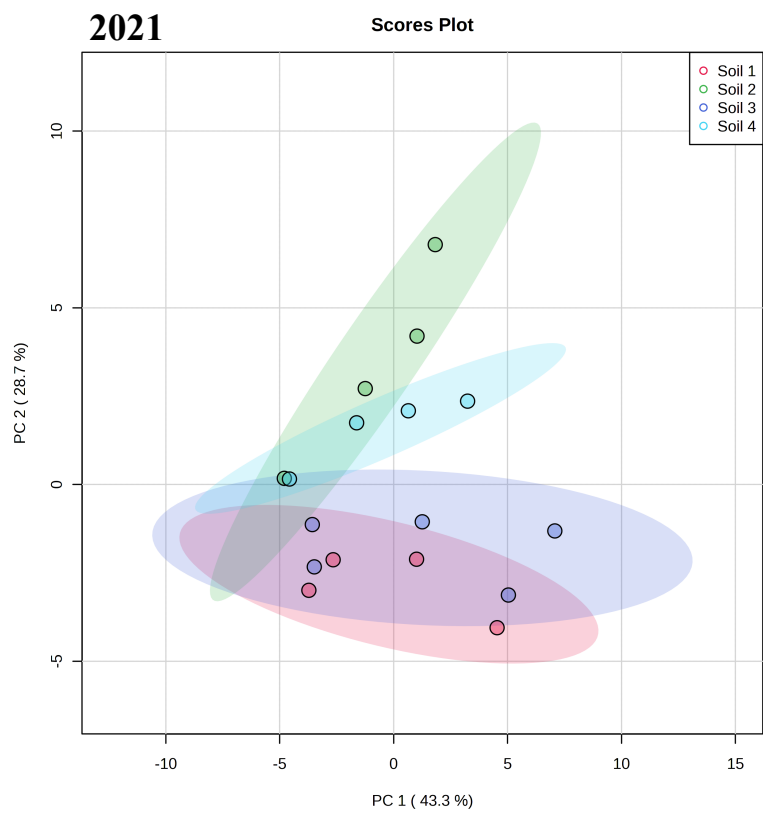
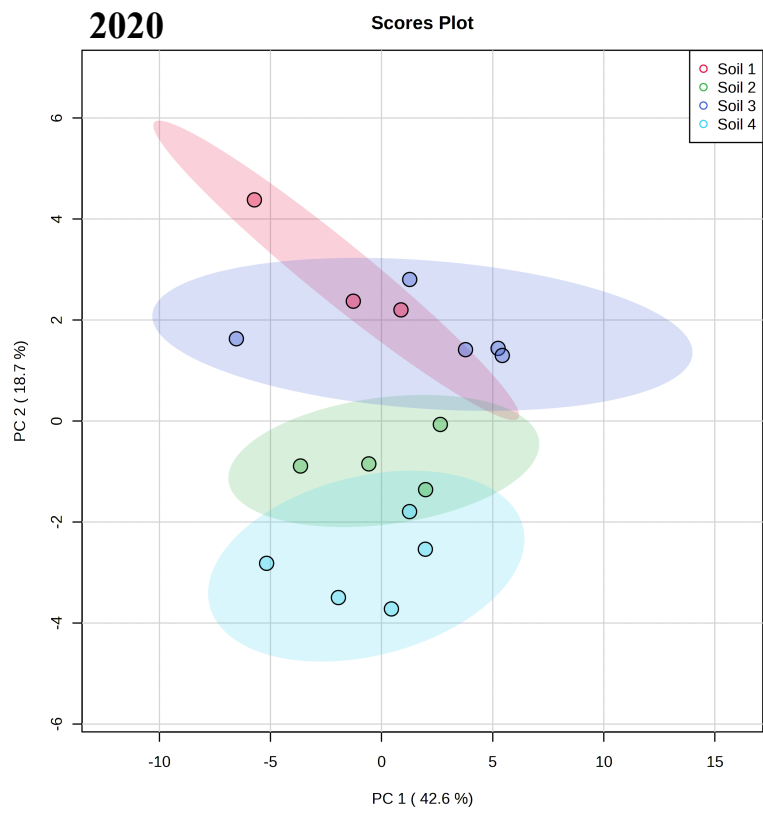


FIGURE 12. 2D PCA BIPLOTS SHOWING THE SEPARATION AMONG NERO D'AVOLA GRAPES GROWN ON DIFFERENT SOILS IN 2020 AND 2021 VINTAGES.

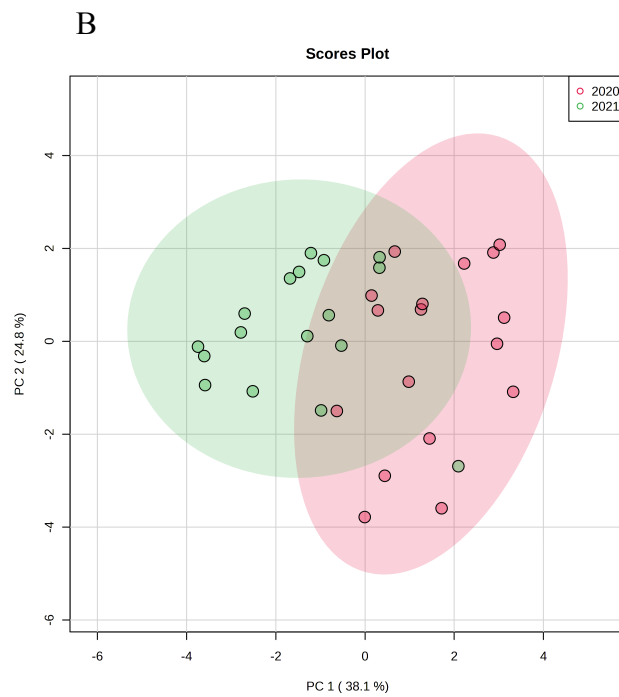
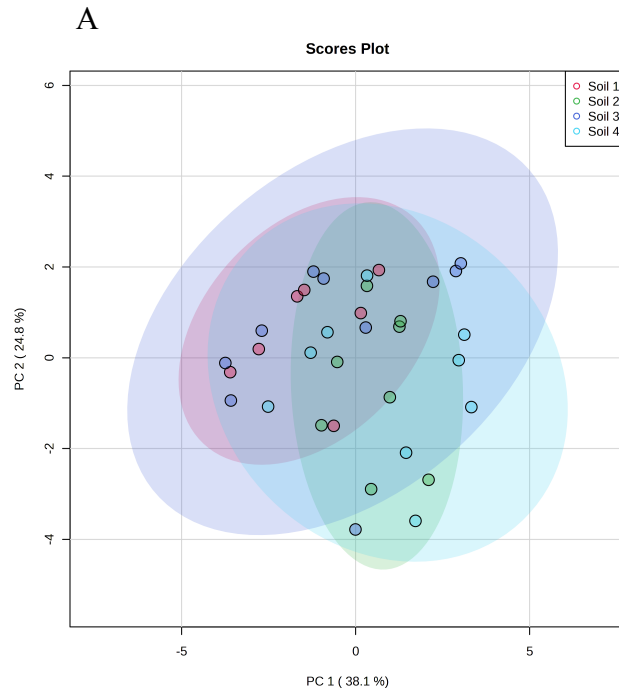


FIGURE 13. 2D PCA BIPLOTS SHOWING THE SEPARATION AMONG NERO D'AVOLA GRAPES GROWN ON DIFFERENT SOILS IN 2020 AND 2021 VINTAGES, SIMULTANEOUSLY. TWO DIFFERENT CLUSTERING ARE SHOWN: A SOIL-BASED CLUSTERING (A) AND A VINTAGE-BASED CLUSTERING (B).

CHAPTER 4: INFLUENCE OF SOIL ON THE CHEMICAL COMPOSITION OF NERO D'AVOLA WINES (PART I)²

² This chapter has been adapted and improved including relevant parts from:

Bambina, P., Pollon, M., Vitaggio, C., Lo Papa, G., Conte, P., Cinquanta, L., & Corona, O. (2023). Effects Of Soil Type On Phenolic And Volatile Composition On Nero d'Avola Wines (Note 2). Submitted to American Journal of Enology and Viticulture.

Bambina, P., Gancel, A.L., Jourdes, M., & Teissedre, P.L. (2023). Influence of soil type on the proanthocyanidins composition of red and white wines obtained from Nero d'Avola and Grillo Vitis vinifera L. cultivars. In prep.

MATERIALS AND METHODS

VINIFICATION PROCESS

Nero d'Avola grape berries from each vineyard were manually harvested at their technological maturation (when about 20° Brix were reached) between September 8th and 9th 2021. Then, the grapes were transported in boxes to the Settesoli winery (Menfi, Sicily, Italy), where they were separately vinified according to the procedure described in Bambina et al. (2023). Briefly, 150 kg of grapes from each vineyard were destemmed, softly crushed, and placed in 100 L stainless steel tanks. Then, they were charged with 5 g hL⁻¹ of K₂S₂O₅. The alcoholic fermentation was carried out by the inoculation of a *pie'd de cuvè* prepared with 20 g hL⁻¹ of Lalvin EC 1118 yeasts and 0.06 g hL⁻¹ of thiamine. Diammonium phosphate (DAP) was added in order to achieve 200 mg L⁻¹ of promptly assimilable nitrogen. The fermentation temperature was 25 ± 1 °C. A punching down per day was carried out till the achievement of 6 % v v⁻¹ of ethanol. Then, two punching down per day were performed until the end of the alcoholic fermentation. Two pump-over were done, the first after 24 hours from the beginning of the alcoholic fermentation and the second when 6 % v v⁻¹ of ethanol was reached. K₂S₂O₅ was added till the achievement of 25 mg L⁻¹ of the free SO₂. The racking was carried out at the end of the alcoholic fermentation. Then, the malolactic fermentation was triggered by inoculation of selected lactic bacteria (Enartis-ML ONE). At the end of malolactic fermentation wines were racked. K₂S₂O₅ was added until wines reached 25 mg L⁻¹ of free SO₂. Then, wines were bottled and stored at 10 °C until the analyses.

MUSTS AND WINES CHEMICAL-PHYSICAL ANALYSES

Musts at the beginning of the alcoholic fermentation and wines at the end of the winemaking process were analyzed by means of FT-IR spectroscopy using a WinescanTM instrument (FOSS, Hilleroed, Denmark) calibrated by applying the EEC 2676 standard procedure (EEC, 1990). The main chemical-

physical parameters were analysed, including reducing sugars content (g L^{-1}) and promptly assimilable nitrogen (mg L^{-1}) in musts; ethanol content ($\% \text{ v v}^{-1}$), total acidity (g L^{-1}), volatile acidity (g L^{-1}), pH, and residual sugars (g L^{-1}) in wines. All the analysis were carried out in triple.

ANALYSIS OF PHENOLIC COMPOUNDS IN WINES

GLOBAL CHARACTERIZATION OF POLYPHENOLS

Different analyses were performed to characterize the polyphenolic fraction of *Nero d'Avola* wines. They included the determination of total polyphenols index (TPI), total polyphenolic content (TPC), total flavonoids (TF), total tannins content (TTC) and total anthocyanins content (TAC). All the aforementioned analyses were performed by means of UV-Vis spectrophotometry.

Total polyphenols index (TPI):

For measuring the TPI, *Nero d'Avola* wines were diluted 100 times with water. Then, the optical density (OD) at 280 nm was measured using a quartz cuvette with 1 cm of path length. TPI was calculated as reported by Jouin et al. (2022):

$$IPT = OD \times \text{dilution factor.}$$

Total polyphenolic content (TPC):

Total polyphenolic content (TPC) was determined by the Folin-Ciocalteu method (Singleton & Rossi, 1965). 20 μL of diluted wine (dilution factor = 20) were added with 100 μL of Folin-Ciocalteu solution and with 80 μL of Na_2CO_3 solution. Absorbance was measured after 30 min at 760 nm on a UV-vis spectrophotometer (BMG FLUOstar Omega). Gallic acid was used as standard and the results were expressed as mg of gallic acid equivalents (GAE).

Total flavonoids (TF):

Total flavonoids in wines were analysed according to the method proposed by (Corona et al. 2015) and previously described in the section *Analysis of phenolic compounds in grapes* of Chapter 3.

Total tannins (TTC):

Total tannins content (TTC) was determined by means of the Bate-Smith reaction (Ribéreau-Gayon et al., 1966). It is based on the transformation of proanthocyanidins in colored anthocyanidins (due to the formation of carbocations partially converted into red cyanidin) by heating at 100°C in acidic conditions. *Nero d'Avola* wines were diluted 50 times prior to perform the reaction. 2 mL of diluted wine, 1 mL of distilled water, and 3 mL of HCl 37% were placed into two different tubes (control and hydrolysis). Control tubes were maintained at room temperature under dark conditions, whereas hydrolysis tubes were capped and heated at 100°C for 30 min. Then, the tubes were cooled in an ice bath for 10 min. 1 mL of EtOH 96% was added to stop the reaction. Absorbance difference between hydrolysis and control tubes was measured at 550 nm.

Tannins concentration was obtained as follows:

$$C \text{ (g L}^{-1}\text{)} = \Delta_{\text{D}0550} \times 50 \times 0.3866$$

Total anthocyanins content (TAC):

Total anthocyanins content was determined according to the method proposed by (Corona et al. 2015) and previously described in the section *Analysis of phenolic compounds in grapes* of Chapter 3.

ANALYSIS OF MONOMER ANTHOCYANINS, HTCAs AND FLAVONOLS

Monomer anthocyanins profiles, HTCAs and flavonols in wines were analysed by means of HPLC-DAD according to the method described in the section *Analysis of monomer anthocyanins, hydroxycinnamoyl tartaric acids (HTCAs) and flavonols* of Chapter 3.

PROANTHOCYANIDINS CHARACTERIZATION: ANALYSIS OF MONOMERIC AND OLIGOMERIC FLAVAN-3-OLS³

Monomer and oligomer proanthocyanidins in *Nero d'Avola* wines were analyzed by means of HPLC-UV-fluo analysis. The HPLC instrument was equipped with a Thermo-Finnigan UV-Vis detector

³ These experiments were conducted at the Institute de Sciences de la Vigne et du Vin, University of Bordeaux.

(Surveyor PDA Plus), a Thermo-Finnigan fluorescence detector (Surveyor FL Plus Detector), a Thermo-Finnigan autosampler (Surveyor autosampler Plus) and a Thermo-Finnigan quaternary pump (Surveyor MS pump Plus). Separation was performed on a reversed-phase LiChrospher 100 RP18 column. The mobile phase was a mixture of 1% (v v⁻¹) aqueous formic acid (solvent A) and 1% (v v⁻¹) formic acid in acetonitrile (solvent B). The composition of elution mixture was as follows: a linear gradient from 0 to 3% of B in 3 min, from 3 to 5% of B in 7 min, 5% of B for 4 min, from 5 to 7% of B in 6 min, from 7 to 10% of B in 2 min, 10% of B for 5 min, from 10 to 12% of B in 5 min, from 12 to 14% of B in 2 min, from 14 to 25% of B in 11 min, from 25 to 100% of B in 1 min, and 100% B for 5 min. Flow rate was 1 mL min⁻¹. UV-Vis detection was performed at the wavelength of 280 nm and fluorescence detection was set at 280 and 320 nm, for excitation and emission wavelengths, respectively. Identification of compounds was performed by comparing their retention times and their UV spectra to pure standards. Quantification of the monomer and oligomer flavan-3-ols was performed by means of fluorimetric detection. Their content was expressed in mg L⁻¹. Calibration curves for the quantification of (+) catechin, (-) epicatechin, B1, B2, B3, and B4 dimers and C1 trimer were established by using external standards.

STRUCTURAL CHARACTERIZATION OF PROANTHOCYANIDINS⁴

Proanthocyanidin structural characteristics mainly include mean degree of polymerization (mDP), percentage of galloylation (%G) and percentage of prodelfinidins (%P). They were determined on monomeric and oligomeric proanthocyanin fractions after acid-catalyzed degradation in presence of phloroglucinol as nucleophilic agent (Drinkine et al., 2007). Briefly, 2.5 mL of wine were evaporated under reduced pressure and then redissolved in 10 mL of distilled water. Then, a fractionation step on a C18 cartridge (12 g) (Supelco) was carried out. Elution was performed with 50 mL of methanol. The methanolic fraction was evaporated to dryness under reduced pressure. Then, it was redissolved in 1 mL of methanol. A reaction mixture composed of 100 µL of concentrated sample and 100 µL of

⁴ These experiments were conducted at the Institute de Sciences de la Vigne et du Vin, University of Bordeaux.

phloroglucinolysis reagent was placed in a HPLC vial. The phloroglucinolysis reagent is a mixture of phloroglucinol (50 g L^{-1}) and ascorbic acid (10 g L^{-1}) dissolved in methanol acidified with HCl 0.1 M . The reaction mixture was heated at 50°C for 20 min. Then, 1 mL of an aqueous solution of sodium acetate (40 mmol L^{-1}) was added to stop the reaction. The reaction products were analyzed by using a HPLC system (Thermo Finnigan Accela system) equipped with a reverse phase Xterra RP18 ($100 \times 4.6 \text{ mm}$, $3.5 \mu\text{m}$) column coupled with a pre-column with the same phase. The flow rate was 1 mL min^{-1} and the injection volume was $20 \mu\text{L}$. The detection was set at 280 nm . The analyses were carried out at room temperature (20°C). The mobile phase was a mixture of water-acetic acid ($99:1$, v v^{-1}) (Solvent A) and methanol (solvent B). The composition of elution mixture was changed during the chromatographic run as follows: 5% of B for 25 min; a linear gradient from 5 to 20% of B in 20 min, from 20 to 32% of B in 15 min, from 32 to 100% of B in 2 min; 100% of B for 5 min; from 100 to 5% of B in 1 min. The identification of compounds was carried out according to their molecular mass. The quantification of the released products allows the calculation of the mean degree of polymerization (mDP), the percentage of galloylation (% G), and the percentage of prodelphinidins (% P) (Lorrain et al., 2011) as well as the quantification (mM L^{-1}) of epigallocatechin, (+) catechin, (-) epicatechin and epicatechin-gallate as both extension and terminal units.

ANALYSIS OF VOLATILE ORGANIC COMPOUNDS (VOCs)

Volatile organic compounds (VOCs) were determined by means of Gas Chromatography (Agilent 6890 Series GC system, Milan, Italy) coupled with Mass Spectrometry (Agilent 5973 NetWork Mass Selective Detector, Milan, Italy). 25 mL of wine was diluted to 75 mL with deionized H_2O and added with 1-heptanol (0.25 mL of 40 mg/L hydroalcoholic solution). Then, the diluted sample was passed through a 1 g C18 cartridge (Isolute, SPE Columns, Uppsala, Sweden, part n° 221-0100-C) formerly activated with 3 mL of methanol and by 4 mL of deionized H_2O . After washing with 30 mL of deionized H_2O , volatiles were eluted with 12 mL of dichloromethane, dehydrated and evaporated to reach the volume of 0.5 mL. The GC instrument was equipped with a DB-WAX column (Agilent

Technologies, 30 m, 0.250 mm i.d., film thickness 0.25 μm , part n° 122–7032). Oven temperatures were: 40 °C for 2 min, from 40 to 60 °C with a rate of 3 °C/min, 60 °C for 2 min, from 60 to 190 °C with a rate of 2 °C/min, 190 °C for 10 min, from 190 to 230 with a rate of 5 °C/min, 230 °C for 15 min. The injection was splitless and the injector temperature was 250 °C. The transfer line temperature was 230 °C. The carrier gas was helium, and the column flow was 1 mL min⁻¹(Corona et al., 2019; Squadrito et al., 2010). VOCs were identified by comparison with the mass spectra and retention times of pure reference compounds and by comparing the mass spectra with those within the NIST/EPA/NIH Mass Spectral Library database (Version 2.0d, build 2015). The analyses of volatile organic compounds (VOCs) were performed in triple.

STATISTICAL ANALYSES

In order to point out significant differences among wines obtained from grapes grown on different soils, the one-way analysis of variance (ANOVA) with Tukey's b post hoc test was carried out. Differences with p values of less than 5% ($p < 0.05$) were considered statistically significant. Wines compositional data were processed together with soil physical-chemical parameters to point out possible correlations. To attain this goal correlation matrixes with *Pearson's r* correlation coefficient were built. Finally, to reduce data complexity and to highlight the separation among wine samples, the unsupervised principal component analysis (PCA) was performed. All data were standardized before running PCA. The ANOVA analysis and the correlation analysis were performed by using SPSS version 13.0 for Windows (SPSS, Inc., Chicago, IL, USA). The principal component analysis was carried out by using MinitabTM statistical software (version 19.0 for Windows, Minitab, LLC, Pennsylvania State University).

RESULTS

CHEMICAL-PHYSICAL PARAMETERS OF MUSTS AND WINES

The knowledge of the chemical-physical parameters of musts and wines is of fundamental importance in modulating a successful winemaking process and in determining the final quality of wines. The chemical-physical parameters analyzed for each Nero d'Avola must and wine are listed in Table 9.

As it can be observed, significant differences were observed in both reducing sugars and promptly assimilable nitrogen (PAN) in musts at the beginning of the alcoholic fermentation, with must 3 showing higher contents of reducing sugars ($229 \pm 6 \text{ g L}^{-1}$) and lower contents of PAN ($125 \pm 3 \text{ mg L}^{-1}$). This latter PAN value was below the minimal concentration of 150 mg L^{-1} that is considered sufficient for a must to launch the alcoholic fermentation (Bell, 2005). Indeed, for a correct outcome of the alcoholic fermentation, diammonium phosphate (DAP) was added until the musts reached 200 mg L^{-1} of PAN. Differences were also observed in the final wines' parameters, with wine 2 showing the lowest alcohol content ($11.1 \pm 0.2 \text{ v v}^{-1}$) and total acidity ($6.8 \pm 0.1 \text{ g L}^{-1}$) and the highest pH (3.30 ± 0.02). Volatile acidity values were those expected in top-quality wines. Volatile acidity was significantly higher in wine 3 (0.36 g L^{-1}) than in wines 1, 2, and 4 (0.30 g L^{-1} , 0.20 g L^{-1} , 0.27 g L^{-1} , respectively).

TABLE 9. CHEMICAL-PHYSICAL PARAMETERS MEASURED FOR EACH MUST AND WINE.

Musts				Wines										
<i>Reducing sugars</i>		<i>Promptly assimilable nitrogen</i>		<i>Alcohol content</i>	<i>Residual sugars</i>		<i>pH</i>	<i>Total acidity</i>		<i>Volatile acidity</i>				
<i>g L⁻¹</i>		<i>g L⁻¹</i>		<i>v v⁻¹</i>	<i>g L⁻¹</i>			<i>g L⁻¹</i>		<i>g L⁻¹</i>				
Wine 1	217 ± 5	bc	156 ± 4	b	12.5 ± 0.4	ab	1.6 ± 0.3	a	2.90 ± 0.02	a	8.8 ± 0.1	b	0.30 ± 0.01	b
Wine 2	187 ± 3	a	169 ± 2	c	11.1 ± 0.2	a	2.4 ± 0.5	a	3.30 ± 0.02	c	6.8 ± 0.1	a	0.20 ± 0.01	a
Wine 3	229 ± 6	c	125 ± 3	a	13.5 ± 0.3	c	2.3 ± 0.3	a	3.00 ± 0.03	b	8.5 ± 0.1	ab	0.36 ± 0.01	c
Wine 4	207 ± 2	b	219 ± 2	d	12.7 ± 0.2	b	1.8 ± 0.1	a	2.90 ± 0.01	a	8.9 ± 0.1	b	0.27 ± 0.01	b

GLOBAL CHARACTERIZATION OF PHENOLS

In order to globally investigate the polyphenolic composition of *Nero d'Avola* wines, different analyses were performed. These included total polyphenols index (TPI), total polyphenolic content (TPC), total flavonoids, total proanthocyanidins content (TP) and total anthocyanins content (TAC). The results of the aforementioned analyses are shown in Table 10. The one-analysis of variance (ANOVA), coupled with the Tukey's b post hoc test, was carried out on the obtained dataset in order to highlight significant differences ($p < 0.05$) among the different *Nero d'Avola* wines, taking into consideration the soil type as factor. As it can be observed, the total polyphenolic index is significantly different among *Nero d'Avola* wines, with wine 3 showing the highest value (57 ± 7). Regarding the total polyphenolic content, wines 2 and 4 were significantly different from wines 1 and 3, showing the values of about 1100 and 1500 mg L⁻¹ of gallic acid equivalent, respectively. Also, total tannins content was significantly different among samples: it was the lowest in wine 2 (1.61 ± 0.08 g L⁻¹) and the highest in wine 3 (2.2 ± 0.1 g L⁻¹).

Total flavonoids were found in significantly higher concentration in wine 3 (1487 ± 28 mg L⁻¹ of (+) catechin), than in other wines (about 950 mg L⁻¹ of (+) catechin).

Finally, significant differences were also observed in total anthocyanins content. It was lower in wine 2 and 4 and higher in wines 1 and 3.

TABLE 10. GLOBAL CHARACTERIZATION OF PHENOLS IN WINES.

	<i>Wine 1</i>		<i>Wine 2</i>		<i>Wine 3</i>		<i>Wine 4</i>	
Total polyphenols index (TPI)	43 ± 6	a	34 ± 2	a	57 ± 7	b	38 ± 2	a
Total polyphenolic content (TPC) (mg L⁻¹ of gallic acid equivalent)	1448 ± 57	b	1186 ± 86	a	1519 ± 89	b	1125 ± 49	a
Total proanthocyanidins content (TTC) (g L⁻¹)	1.9 ± 0.1	ab	1.61 ± 0.08	a	2.2 ± 0.1	b	1.4 ± 0.3	a
Total flavonoids (mg L⁻¹ of (+) catechin)	960 ± 72	a	954 ± 6	a	1487 ± 28	b	984 ± 3	a
Total anthocyanins (mg L⁻¹ of malvidin-3-glucoside)	111 ± 9	b	53.9 ± 0.6	a	122 ± 1	b	43 ± 1	a

MONOMER ANTHOCYANINS PROFILE

The anthocyanins profile was characterized by the prevalence of trisubstituted anthocyanins (malvidin-3-glucoside, petunidin-3-glucoside and delphinidin-3-glucoside) over the disubstituted ones (peonidin-3-glucoside and cyanidin-3-glucoside) in all the analyzed *Nero d'Avola* wines (Figure 16 A and Table 11). Among trisubstituted anthocyanins, malvidin-3-glucoside, that is the compound most involved in the formation of the wine color (Gómez-Míguez et al., 2007), was largely predominant (around 70% of total monomer anthocyanins in all *Nero d'Avola* wines). Although the anthocyanin pattern is maintained almost consistent among wine samples, several differences were observed among their concentrations in the different wines. Acetylated anthocyanins covered the 4-8% of the total anthocyanins content and p-coumaroylated anthocyanins covered 4-9% of the total anthocyanins content. The ratio acetylated/p-coumaroylated anthocyanins ranges between 0.6 (wine 4) and 1.3 (wine 1), although their differences are not statistically significant.

In wines derived from varieties in which tri-oxygenated anthocyanins prevailed over disubstituted ones (such as *Nero d'Avola*), the anthocyanin profile of grapes is substantially retained during alcoholic and malolactic fermentation (Squadrito et al., 2010). However, anthocyanin biosynthesis is also closely related to the *terroir*. In particular, some environmental factors, such as temperature,

sunlight exposure, and water availability in soils were found to influence the biosynthesis of anthocyanin (Castellarin et al., 2007; Ojeda et al., 2002; Tarara et al., 2008). The significant differences in total anthocyanins highlighted in this study suggest that soils chemical-physical parameters affected the anthocyanins content in Nero d'Avola wines conceivably through the modulation of vine vegetative development.

TABLE 11. MONOMER ANTHOCYANINS PROFILES OF EACH NERO D'AVOLA WINE (%)

%	<i>Wine 1</i>	<i>Wine 2</i>	<i>Wine 3</i>	<i>Wine 4</i>
<i>Delphinidin-3-glucoside</i>	3.8 ± 0.6	2.3 ± 0.6	2.6 ± 0.2	3.5 ± 0.1
<i>Cyanidin-3-glucoside</i>	6 ± 1 b	2.8 ± 0.1 a	4.4 ± 0.1 ab	3.9 ± 0.5 ab
<i>Petunidin-3-glucoside</i>	8.2 ± 0.4 c	3.9 ± 0.1 a	7.24 ± 0.02 b	7.34 ± 0.02 b
<i>Peonidin-3-glucoside</i>	3.6 ± 0.1 a	4.1 ± 0.5 a	5.30 ± 0.01 b	4.2 ± 0.1 ab
<i>Malvidin-3-glucoside</i>	69 ± 2	69 ± 2	69.9 ± 0.1	74 ± 1
<i>Acetates anthocyanins</i>	5 ± 1 a	8.9 ± 0.9 b	4.43 ± 0.01 a	4 ± 1 a
<i>Cynnamates anthocyanins</i>	4.0 ± 0.7 a	9.4 ± 0.8 b	6.1 ± 0.1 a	3.6 ± 0.7 a
<i>Acetylated/p-coumarylated</i>	1.3 ± 0.6	0.90 ± 0.01	0.70 ± 0.01	1.1 ± 0.6

DIFFERENT LATIN LETTERS INDICATE SIGNIFICANT DIFFERENCES (P < 0.05) AMONG WINES.

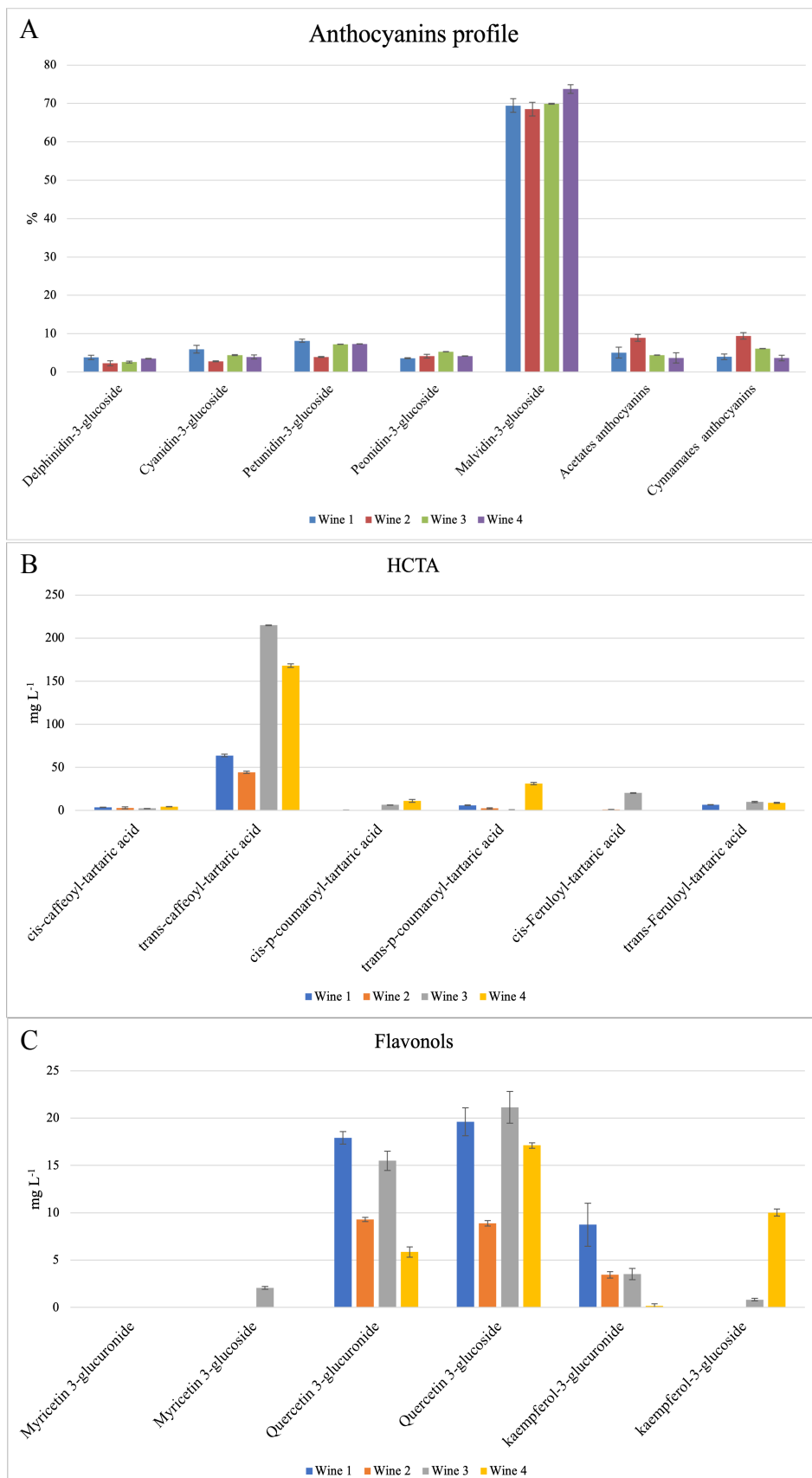


FIGURE 14. TOTAL FLAVONOIDS CONTENTS AND TOTAL ANTHOCYANINS CONTENTS (A), MONOMER ANTHOCYANINS PROFILES (B), HCTA (C) AND FLAVONOIDS (D).

HYDROXYCINNAMOYL TARTARIC ACIDS (HCTAs)

The profiles of hydroxycinnamoyl tartaric acids (HCTAs) of the analyzed *Nero d'Avola* wines are reported in Figure 14 B and Table 12. As it can be observed, the most abundant hydroxycinnamoyl tartaric acid was the *trans*-caffeoyl tartaric acid in all the analyzed *Nero d'Avola* wines. Its content is significantly lower in wine 2 (4 mg L⁻¹) and significantly higher in wine 3 (214.8 mg L⁻¹).

TABLE 12. HCTAS PROFILES OF EACH NERO D'AVOLA WINE (MG L⁻¹).

<i>mg L⁻¹</i>	<i>Wine 1</i>	<i>Wine 2</i>	<i>Wine 3</i>	<i>Wine 4</i>
<i>cis</i> -caffeoyl-tartaric acid	3.61 ± 0.07	3 ± 1	2.34 ± 0.05	4.3 ± 0.2
<i>trans</i> -caffeoyl-tartaric acid	64 ± 2 b	44 ± 1 a	214.8 ± 0.5 d	168 ± 2 c
<i>cis</i> - <i>p</i> -coumaroyl-tartaric acid	0.1 ± 0.2 a	2.3 ± 0.6 a	6.4 ± 0.2 c	11 ± 2 d
<i>trans</i> - <i>p</i> -coumaroyl-tartaric acid	6.0 ± 0.3 b	1.1 ± 0.3 a	0.66 ± 0.06 a	31 ± 1 c
<i>cis</i> -Feruloyl-tartaric acid	BDL	BDL	20.3 ± 0.3	BDL
<i>trans</i> -Feruloyl-tartaric acid	6.58 ± 0.03 b	0.9 ± 0.2 a	9.7 ± 0.7 c	8.9 ± 0.5 c

DIFFERENT LATIN LETTERS INDICATE SIGNIFICANT DIFFERENCES (P < 0.05) AMONG WINES.

FLAVONOLS

The profiles of flavonols of the analyzed *Nero d'Avola* wines are shown in Figure 14 C and in Table 13. The quercetin (3-glucuronide, 3-glucoside and aglycon) was the most abundant flavonol (excepting for wine 2). The concentration of quercetin 3-glucoside was around 20 mg L⁻¹ in wines 1, 3 and 4, whereas it was significantly lower (0.582 mg L⁻¹) in wine 2. This latter wine sample contained the lowest concentration of all the other detected flavonols.

TABLE 13. FLAVONOLS PROFILES OF NERO D'AVOLA WINE (MG L⁻¹).

<i>mg L⁻¹</i>	<i>Wine 1</i>	<i>Wine 2</i>	<i>Wine 3</i>	<i>Wine 4</i>
<i>Myricetin 3-glucuronide</i>	BDL	BDL	BDL	BDL
<i>Myricetin 3-glucoside</i>	BDL	BDL	2.1 ± 0.2	BDL
<i>Quercetin 3-glucuronide</i>	17.9 ± 0.7 d	9.3 ± 0.2 b	15 ± 1 c	5.8 ± 0.5 a
<i>Quercetin 3-glucoside</i>	20 ± 1 b	8.9 ± 0.3 a	21 ± 2 b	17.1 ± 0.3 b
<i>kaempferol-3-glucuronide</i>	9 ± 2 b	3.4 ± 0.3 a	3.5 ± 0.6 a	0.2 ± 0.2 a
<i>kaempferol-3-glucoside</i>	BDL	BDL	0.8 ± 0.1 a	10.0 ± 0.4 b

DIFFERENT LATIN LETTERS INDICATE SIGNIFICANT DIFFERENCES (P < 0.05) AMONG WINES.

PROANTHOCYANIDINS CHARACTERIZATION

In order to investigate the characteristics of proanthocyanidins and to determine the proanthocyanidin profile of Nero d'Avola wines, monomer (e.g., (+) catechin and (-) epicatechin) and oligomer (e.g., B1, B2, B3 and B4 dimers and C1 trimer) proanthocyanidins were analyzed by means of HPLC-UV-fluo analysis. Many studies have been conducted about the proanthocyanidin characterization of different grapes and wines (Chira et al., 2009, Gris et al., 2011), but the proanthocyanidin profile of wines from grapes of *Nero d'Avola L.* cultivar is reported here for the first time (Figure 15). As it can be observed, the most abundant proanthocyanidin is the monomer (+) catechin, representing about the 90% of the total monomers and about 50% of total proanthocyanidins (Table 14). This result agrees with other studies reporting the (+) catechin as the main monomer in grape skins and seeds (Chira et al., 2009; Mattivi et al., 2009). (-) epicatechin represented about 10% of the total monomers and about 6% of total proanthocyanidins. Among oligomer proanthocyanidins, the B3 dimer and the C1 trimer were the most abundant. The former contributed with about 60% of the total dimers and with the 15% of total proanthocyanidins; the latter contributed with about the 18% of total proanthocyanidins. Finally, B1, B2 and B4 dimers separately represented about 11-13% of the total dimers and the 3% of the total proanthocyanidins.

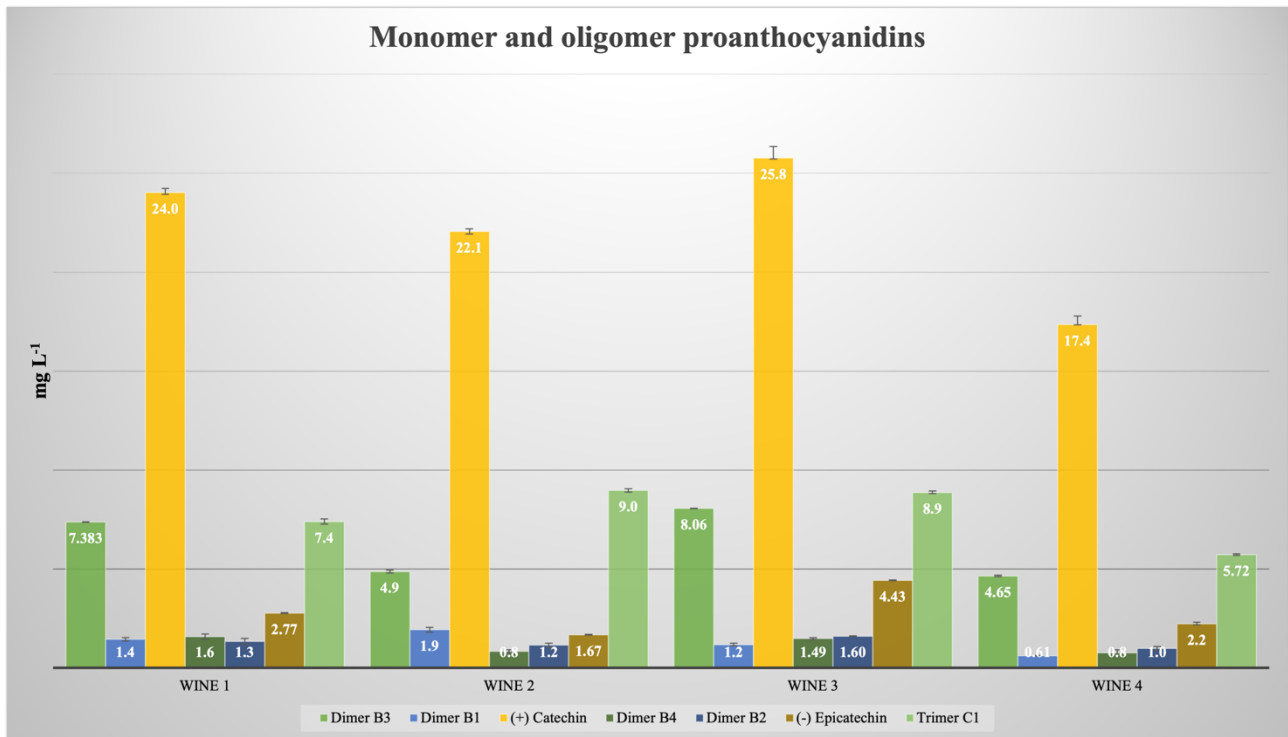


FIGURE 15. PROANTHOCYANIDIN PROFILE OF NERO D'AVOLA WINES DERIVED FROM GRAPES GROWN ON DIFFERENT SOILS.

In general, monomer flavan-3-ols covered about 60% of total tannins, dimer proanthocyanidins covered about 23% of total tannins and trimer proanthocyanidins covered about 18% of total tannins. The fact that the relative ratio among the identified and quantified monomer and oligomer proanthocyanidins is consistent among the different Nero d'Avola wines agrees with what stated by other authors (Rinaldi et al., 2015; Mattivi et al., 2009; Arapitsas et al., 2012), namely that the proanthocyanidin profile is cultivar-specific and genetically controlled. However, significant differences were observed among the concentrations (determined in mg L^{-1}) of each detected proanthocyanidin, suggesting that the rate and intensity of proanthocyanidin accumulation is affected by environmental factors (Chira et al., 2009; Gris et al., 2011; Mattivi et al., 2002), in this case by the soil type. In particular, it was observed that wine 4 showed significantly lower concentrations of all the detected proanthocyanidins, with the sole exception of (-) epicatechin that was lower in wine 2. The highest concentrations of proanthocyanidins were observed in wine 3, with the sole exception of B1 dimer that was higher in wine 2.

TABLE 14. PROANTHOCYANIDIN COMPOSITION IN NERO D'AVOLA WINES.

<i>Proanthocyanidins (mg L⁻¹)</i>	<i>Wine 1</i>		<i>Wine 2</i>		<i>Wine 3</i>		<i>Wine 4</i>	
<i>Dimer B3</i>	7.383 ± 0.003	c	4.9 ± 0.1	b	8.06 ± 0.01	d	4.65 ± 0.04	a
<i>Dimer B1</i>	1.4 ± 0.1	c	1.9 ± 0.1	d	1.2 ± 0.1	b	0.61 ± 0.02	a
<i>(+) Catechin</i>	24.0 ± 0.2	c	22.1 ± 0.1	b	25.8 ± 0.6	d	17.4 ± 0.4	a
<i>Dimer B4</i>	1.6 ± 0.1	b	0.8 ± 0.1	a	1.49 ± 0.05	b	0.8 ± 0.2	a
<i>Dimer B2</i>	1.3 ± 0.1	b	1.2 ± 0.1	ab	1.60 ± 0.02	c	1.0 ± 0.1	a
<i>(-) Epicatechin</i>	2.77 ± 0.02	c	1.67 ± 0.02	a	4.43 ± 0.02	d	2.2 ± 0.1	b
<i>Trimer C1</i>	7.4 ± 0.1	b	8.98 ± 0.08	c	8.87 ± 0.06	c	5.72 ± 0.03	a
<i>Total monomers</i>	26.8 ± 0.2	c	23.7 ± 0.1	b	30.2 ± 0.6	d	19.6 ± 0.4	a
<i>Total dimers</i>	11.8 ± 0.2	c	8.8 ± 0.1	b	12.3 ± 0.1	d	7.0 ± 0.2	a
<i>Total proanthocyanidins</i>	46.0 ± 0.1	c	41.5 ± 0.2	b	51.4 ± 0.6	d	32.3 ± 0.4	a

DIFFERENT LATIN LETTERS INDICATE SIGNIFICANT DIFFERENCES (P < 0.05) AMONG WINES.

STRUCTURAL CHARACTERISTICS OF PROANTHOCYANIDINS

In order to evaluate the structural characteristics of proanthocyanidins, the acid-catalyzed degradation in presence of phloroglucinol as nucleophilic reagent was performed. It allowed to analyze the mean degree of polymerization (mDP), the percentage of galloylation (%G) and the percentage of prodelphinidins (%P), as well as to quantify (mM L⁻¹) the concentrations of epigallocatechin, (+) catechin, (-) epicatechin and epicatechin-gallate as both extension and terminal units.

The data related to the structural characteristics of *Nero d'Avola* wines are listed in Table 15. The table also reports the one-way analysis of variance (ANOVA) with Tukey's b post hoc test.

Wines' proanthocyanidins consist of a mixture of procyanidin and prodelphinidins, both contributing as terminal and extension units of polymer proanthocyanidins. In the analysed *Nero d'Avola* wines, the terminal units were mainly composed by (+) catechin, representing 35-50% of total terminal units. It was followed by the epigallocatechin, that represented the 29-39% of total terminal units. (-) epicatechin covered from 15 to 25% of total terminal units, while epicatechin-gallate represented the

2-5% of total terminal units. Epicatechin-gallate was the only gallate-form found as terminal unit and its concentration in wines is usually very low (Chira et al., 2009; Fernández et al., 2007).

While the concentrations of epigallocatechin and epicatechin-gallate as terminal units were similar among wine samples (around 2 mM L⁻¹ and 0.2 mM L⁻¹, respectively), the concentrations of (+) catechin and (-) epicatechin as terminal units were significantly different among wines. In particular, (+) catechin concentration was lower in wines 3 and 4 (about 2 mM L⁻¹) with respect to wines 1 and 2 (about 3.5 mM L⁻¹) and (-) epicatechin was lower in wine 1 (1.0 ± 0.3 mM L⁻¹) and higher in wine 2 (1.6 ± 0.1 mM L⁻¹). The extension units were mainly represented by (-) epicatechin and epigallocatechin. The former represented from 40 to 50% of the total extension units, while the latter represented from 27 to 38% of total extension units. (+) catechin covered the 15-20% and epicatechin-gallate covered 2.7-4.5% of the total extension units. A similar profile was already observed in other studies (del Rio et al., 2006; Gris et al., 2011). While epigallocatechin as extension unit was present with the same concentration among Nero d'Avola wines (about 2 mM), (+) catechin, (-) epicatechin and epicatechin-gallate were present in different concentrations. They were higher in wine 3 (1.7, 4 and 0.4 mM, respectively) and lower in wine 2 (0.7, 2.6 and 0.2 mM, respectively).

The percentage of prodelphinidins, namely the contribution of epigallocatechin as both terminal and extension units, indicates the contribution to wine tannic structure of skins proanthocyanidins, given that prodelphinidins are not present in grape seeds. It was around 30% in all wines, without significant differences among samples. Percentage of galloylation ranged between 2.2 and 3.9%. It was significantly different among wines, with wines 1 and 2 showing lower values (2.2 and 2.5 %, respectively) than wines 3 and 4 (3.9 % in both samples). In general, the release of galloylated derivatives during maceration is not attributed to grapes skins (Rinaldi et al., 2015), but rather to grape seeds (Mattivi et al., 2009), suggesting that in wines 3 and 4 the contribution from seeds proanthocyanidins was slightly higher than in other wines.

The percentage of procyanidins (namely the contribution of (+) catechin and (-) epicatechin as both terminal and extension units) was about 65% in all Nero d'Avola wines, without significant differences among samples.

Finally, the mean degree of polymerization was very low in all *Nero d'Avola* wines, ranging from 1.6 to 2.6. It was higher in wine 3 (2.6 ± 0.3), due to the higher concentration of extension units, and lower in wine 2 (1.64 ± 0.04).

TABLE 15. STRUCTURAL CHARACTERISTICS OF PROANTHOCYANIDINS IN NERO D'AVOLA WINES. DIFFERENT LATIN LETTERS INDICATE SIGNIFICANT DIFFERENCES (P < 0.05) AMONG NERO D'AVOLA WINES DERIVED FROM GRAPES GROWN ON DIFFERENT SOILS.

	<i>Wine 1</i>			<i>Wine 2</i>			<i>Wine 3</i>			<i>Wine 4</i>		
<i>Extension units (mM L⁻¹)</i>												
<i>epigallocatechin</i>	2.0	±	0.6	1.3	±	0.2	2.7	±	1.0	2.4	±	0.2
<i>catechin</i>	0.9	±	0.5	0.7	±	0.1	1.7	±	0.1	1.1	±	0.1
<i>epicatechin</i>	3.2	±	0.2	2.6	±	0.2	4.0	±	0.5	2.6	±	0.1
<i>epicatechin-gallate</i>	0.2	±	0.1	0.20	±	0.01	0.40	±	0.01	0.20	±	0.01
<i>Terminal units (nM L⁻¹)</i>												
<i>epigallocatechin</i>	2	±	1	2.4	±	0.5	2	±	1	1.6	±	1
<i>catechin</i>	3.5	±	0.6	3.4	±	0.2	2.2	±	0.2	2.3	±	0.2
<i>epicatechin</i>	1.0	±	0.3	1.6	±	0.1	1.2	±	0.1	1.4	±	0.1
<i>epicatechin-gallate</i>	0.1	±	0.1	0.20	±	0.01	0.2	±	0.1	0.30	±	0.01
<i>mDP</i>	1.9	±	0.1	1.64	±	0.04	2.6	±	0.3	2.2	±	0.2
% GALLOYLATION	2.2	±	0.5	2.5	±	0.4	3.9	±	0.7	3.9	±	0.5
% PRODELPHINIDINES	31	±	4	30	±	3	33	±	10	33	±	6
% PROCYANIDINES	67	±	4	68	±	3	63	±	10	63	±	6

VOLATILE ORGANIC COMPOUNDS IN WINES

The analysis of volatile organic compounds (VOCs) in *Nero d'Avola* wines led to the detection and quantification of up to 48 VOCs. These included 11 short and medium chain fatty acids, 10 aging esters, 3 benzenoids, 9 ethyl esters, 5 C13-norisoprenoids, 7 alcohols, 2 terpenes and 1 lactone (Table 16). In Figure 16 it can be observed that the most abundant VOCs were alcohols, followed by benzenoids and aging esters. The most abundant fermentative alcohol in all *Nero d'Avola* wines was isoamyl alcohol (Figure 17 G). Short chain fatty acids are byproducts of the protein metabolism. Linear longer saturated fatty acids with an even number of C atoms are originated from lipid metabolism and from the catabolism of long-chain fatty acids (Lenti et al., 2022; Pérez Olivero et al., 2011). Therefore, their content depends on the composition of primary metabolites (proteins and lipids) in musts at the beginning of the alcoholic fermentation. The total concentration of short and medium chain fatty acids ranged between 3500 $\mu\text{g L}^{-1}$ (wine 3) and 6000 $\mu\text{g L}^{-1}$ (wine 1), with significant differences ($p < 0.05$) among the wine samples. The most abundant volatile fatty acids were hexanoic acid and octanoic acid in all trials (Figure 17 A). In particular, hexanoic acid was present in significant different concentration among wine samples, with the value of 900 $\mu\text{g L}^{-1}$ in wine 3 and 2700 $\mu\text{g L}^{-1}$ in wine 1. Even longer fatty acids, such as dodecanoic, tetradecanoic, hexadecenoic and octadecanoic acids, were present in significant different concentration, with higher values in wine 3 and lower values in wines 1, 2 and 4.

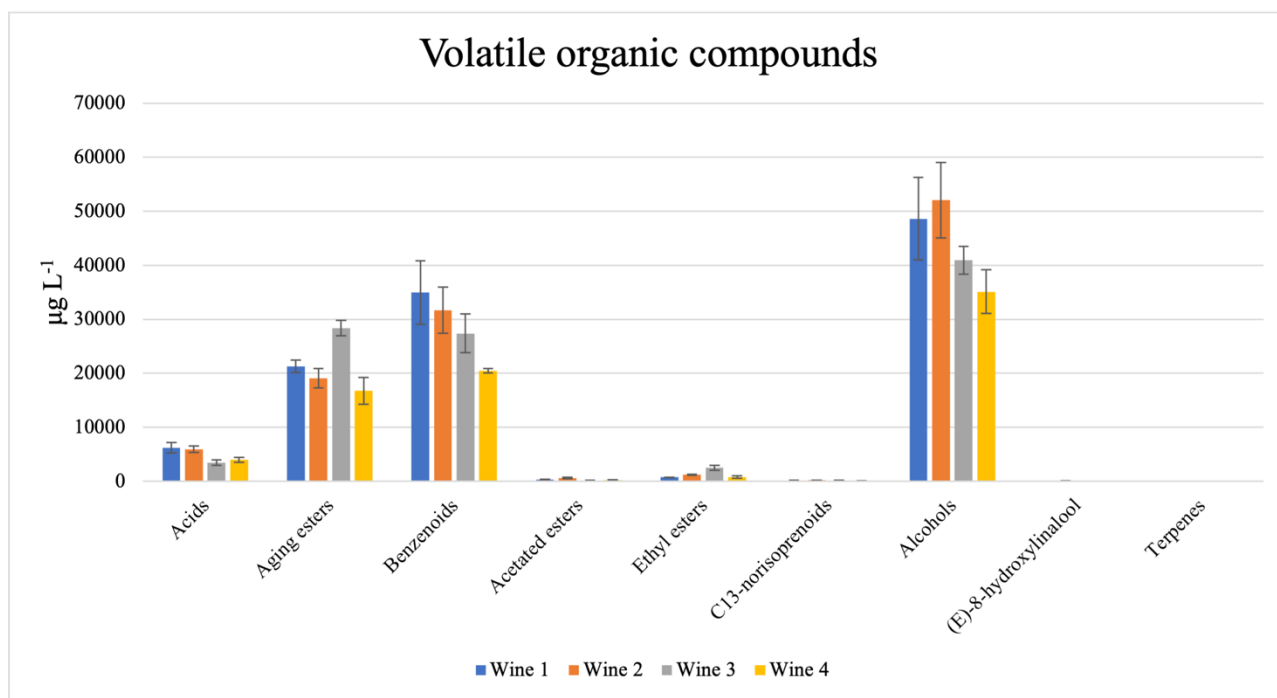


FIGURE 16. VOLATILE ORGANIC COMPOUNDS DETECTED IN NERO D'AVOLA WINES.

Ethyl esters of fatty acids were predominant with respect to acetates of higher alcohols in all trials. The former were present in significantly higher concentration in wine 3 (2500 $\mu\text{g L}^{-1}$) and in lower concentration in wines 1, 2 and 4 (about 1000 $\mu\text{g L}^{-1}$). The latter were present in significantly higher concentration in wine 2 (617 $\mu\text{g L}^{-1}$) and in lower concentration in wines 1, 3 and 4 (about 220 $\mu\text{g L}^{-1}$). Among varietal aroma compounds, C13 norisoprenoids and terpenes were detected. C13 norisoprenoids derive from the degradation of carotenoids. The qualitative and quantitative profile of carotenoids in grapes is affected by several factors including variety, ripening stage, climatic conditions, soil type and viticultural practices (Mendes-Pinto, 2009). The total content of C13 norisoprenoids was about 150 $\mu\text{g L}^{-1}$ in the four wine samples. Significant differences were found in 3-hydroxy- β -damascone content only, with lower values in wine 3 and wine 4 and higher values in wine 2. Finally, terpenes were identified and quantified in wines 1, 2 and 4 only, whereas in wine 3 they were below the detection limit. Among them, free linalool was quantified in wines 2 and 4 only (11 and 2.6 $\mu\text{g L}^{-1}$, respectively), whereas α -terpineol and (E)-8-hydroxylinalool were quantified in wine 1 and 2 only. α -terpineol content was about 20 $\mu\text{g L}^{-1}$ in both wine 1 and wine 2 and (E)-8-

hydroxylinalool content was higher in wine 2 (58 $\mu\text{g L}^{-1}$) and lower in wine 1 (17 $\mu\text{g L}^{-1}$). Finally, γ -butyrolactone content was significantly lower in wine 4 (28 $\mu\text{g L}^{-1}$) and higher in wines 1, 2 and 3 (about 80 $\mu\text{g L}^{-1}$).

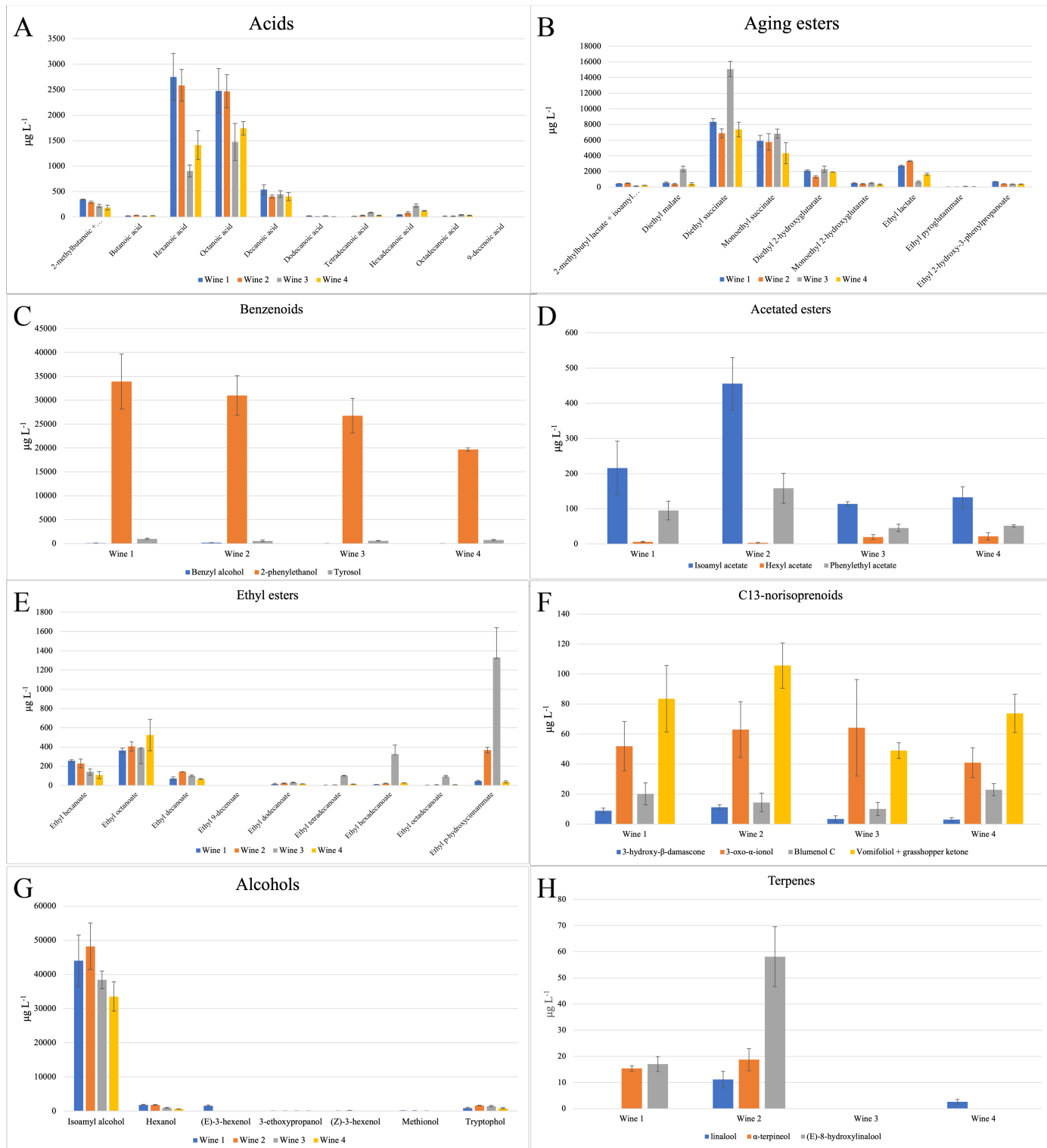


FIGURE 17. VOLATILE ORGANIC COMPOUNDS (VOCs) DIVIDED BY CHEMICAL CLASSES.

TABLE 16. VOLATILE ORGANIC COMPOUNDS (VOCS) OF NERO D'AVOLA WINES (MG L⁻¹).

	Wine 1		Wine 2		Wine 3		Wine 4	
2-methylbutanoic + Isovaleric acid	345 ± 5	b	294 ± 19	ab	218 ± 30	a	187 ± 46	a
Butanoic acid	25 ± 3	a	35 ± 2	b	20 ± 3	a	29 ± 2	ab
Hexanoic acid	2749 ± 460	b	2584 ± 313	b	905 ± 119	a	1413 ± 282	a
Octanoic acid	2478 ± 435		2470 ± 323		1475 ± 364		1743 ± 133	
Decanoic acid	539 ± 94		403 ± 29		452 ± 66		403 ± 80	
Dodecanoic acid	22 ± 5	b	10 ± 1	a	22 ± 2	b	11.2 ± 0.2	a
Tetradecanoic acid	13 ± 3	a	32 ± 6	a	88 ± 7	b	32 ± 7	a
Hexadecanoic acid	43 ± 9	a	82 ± 21	a	226 ± 35	b	123 ± 8	a
Octadecanoic acid	12 ± 8	a	15 ± 7	a	45 ± 7	b	31 ± 6	a
9-decenoic acid	BDL		BDL		BDL		BDL	
Total Acids	6227 ± 1000	b	5925 ± 612	ab	3451 ± 524	a	3972 ± 427	ab
2-methylbutyl lactate + isoamyl lactate	444 ± 8	c	511 ± 38	c	142 ± 24	a	240 ± 11	b
Diethyl malate	549 ± 131	a	384 ± 110	a	2330 ± 365	b	430 ± 146	a
Diethyl succinate	8343 ± 412	a	6880 ± 571	a	15090 ± 988	b	7354 ± 924	a
Monoethyl succinate	5905 ± 696		5781 ± 1047		6829 ± 565		4340 ± 1346	
Diethyl 2-hydroxyglutarate	2087 ± 119	ab	1330 ± 124	a	2296 ± 400	b	1941 ± 10	ab
Monoethyl 2-hydroxyglutarate	498 ± 70		414 ± 78		515 ± 72		348 ± 70	
Ethyl lactate	2722 ± 106	c	3336 ± 60	d	692 ± 107	a	1644 ± 147	b
Ethyl pyroglutammate	31 ± 2	a	28 ± 3	a	96 ± 20	b	54 ± 5	a
Ethyl 2-hydroxy-3-phenylpropanoate	716 ± 18	b	428 ± 8	a	391 ± 27	a	382 ± 26	a
Total aging esters	21294 ± 1157	a	19092 ± 1808	a	28381 ± 1438	b	16734 ± 2493	a
Benzyl alcohol	77 ± 12	a	175 ± 22	b	36 ± 3	a	33 ± 1	a
2-phenylethanol	33896 ± 5753		30979 ± 4128		26769 ± 3614		19677 ± 325	
Tyrosol	984 ± 122		538 ± 171		579 ± 43		767 ± 109	
Total Benzenoids	34957 ± 5862		31693 ± 4277		27384 ± 3575		20476 ± 436	
Isoamyl acetate	216 ± 76	a	456 ± 74	b	114 ± 6	a	133 ± 30	a
Hexyl acetate	6 ± 2		3 ± 2		20 ± 7		22 ± 10	
Phenylethyl acetate	95 ± 27	ab	158 ± 43	b	46 ± 10	a	52 ± 3	a

Total Acetated esters	317 ± 101	a	617 ± 115	b	180 ± 11	a	207 ± 36	a
Ethyl hexanoate	256 ± 11	b	229 ± 46	ab	144 ± 28	ab	108 ± 36	a
Ethyl octanoate	363 ± 24		405 ± 49		388 ± 2		524 ± 163	
Ethyl decanoate	73 ± 14	ab	143 ± 2	c	100 ± 9	b	66 ± 5	a
Ethyl 9-decenoate	BDL		BDL		BDL		BDL	
Ethyl dodecanoate	15 ± 7		22 ± 3		28 ± 6		16.5 ± 0.6	
Ethyl tetradecanoate	3 ± 2	a	5 ± 3	a	101 ± 5	b	13 ± 2	a
Ethyl hexadecanoate	10 ± 2	a	21 ± 2	a	324 ± 97	b	27 ± 1	a
Ethyl octadecanoate	4 ± 1	a	6 ± 2	a	90 ± 15	b	8.5 ± 0.4	a
Ethyl p-hydroxycinnamate	45 ± 8	a	368 ± 29	a	1331 ± 310	b	37 ± 10	a
Total Ethyl esters	769 ± 21	a	1200 ± 72	a	2506 ± 427	b	801 ± 196	a
3-hydroxy-β-damascone	9 ± 2	ab	11 ± 2	b	3 ± 2	a	3 ± 1	a
3-oxo-α-ionol	52 ± 17		63 ± 19		64 ± 32		41 ± 10	
Blumenol C	20 ± 7		14 ± 6		10 ± 4		23 ± 4	
Vomifoliol + grasshopper ketone	84 ± 22		106 ± 15		49 ± 5		74 ± 13	
C13-norisoprenoids	164 ± 33		194 ± 1		127 ± 25		140 ± 5	
Isoamyl alcohol	44025 ± 7488		48199 ± 6789		38407 ± 2571		33542 ± 4264	
Hexanol	1831 ± 132	b	1827 ± 88	b	943 ± 128	a	624 ± 9	a
(E)-3-hexenol	1548 ± 209		BDL		BDL		BDL	
3-ethoxypropanol	99 ± 3		98 ± 4		69 ± 16		66 ± 6	
(Z)-3-hexenol	86 ± 12	b	176 ± 27	c	29 ± 11	a	17 ± 2	a
Methionol	142 ± 11	b	137 ± 25	b	42 ± 16	a	31 ± 9	a
Tryptophol	894 ± 195	a	1631 ± 65	b	1452 ± 178	ab	830 ± 183	a
Total Alcohols	48623 ± 7626		52069 ± 6999		40941 ± 2578		35110 ± 4067	
linalool	BDL		11 ± 3	b	BDL		2.6 ± 0.9	a
α-terpineol	15 ± 1		19 ± 4		BDL	a	BDL	a
(E)-8-hydroxylinalool	17 ± 3	a	58 ± 11	b	BDL		BDL	
Terpenes	32 ± 4	b	88 ± 10	c	BDL		2.6 ± 0.9	a
γ-butyrolactone	78 ± 16	b	92 ± 16	b	76 ± 8	b	28 ± 9	a

DIFFERENT LATIN LETTERS INDICATE SIGNIFICANT DIFFERENCES (P < 0.05) AMONG WINES.

SOIL EFFECT ON WINES CHEMICAL COMPOSITION

SOIL EFFECT ON WINES CHEMICAL-PHYSICAL PARAMETERS

Wines compositional data were processed together with soils' chemical physical parameters in order to point out possible wine-soil relationships. From the correlation heatmap shown in Figure 18, reporting the correlation pattern existing between soils (Table 2) and wines (Table 9) chemical-physical parameters, it can be observed that the soil texture did not affect greatly musts and wines chemical-physical parameters. On the contrary, soil electric conductivity (EC) was positively related with the promptly assimilable nitrogen (APA) in musts. Promptly assimilable nitrogen is a key nutrient for yeasts nutrition and includes NH_4^+ ion and primary amino acids (Hannam et al., 2016). As already discussed in a previous section, EC is the measure of the ions dissolved in the soil solution (Klein et al., 2003). Therefore, it is likely that soils with high EC provide N pool for the production of NH_4^+ ion and primary amino acids in grapes.

	<i>Clay</i>	<i>Silt</i>	<i>Sand</i>	<i>Cation exchange capacity</i>	<i>Total carbonates</i>	<i>Electric conductivity</i>	<i>Soil pH</i>	<i>Organic matter</i>
<i>Reducing sugars</i>	-0.069	-0.568	0.300	-0.906	0.337	-0.716	0.301	-0.533
<i>Promptly assimilable Nitrogen</i>	0.797	0.508	-0.755	0.758	-0.006	0.954*	0.164	0.135
<i>Alcohol content</i>	0.145	-0.002	-0.094	-0.903	0.804	-0.535	0.736	-0.909
<i>Residual sugars</i>	-0.202	0.559	-0.116	-0.206	0.496	-0.156	0.362	-0.405
<i>pH</i>	-0.295	0.575	-0.062	0.213	0.125	0.082	0.015	0.019
<i>Total acidity</i>	0.268	-0.596	0.089	-0.276	-0.096	-0.139	0.005	-0.057
<i>Volatile acidity</i>	0.134	0.056	-0.113	-0.887	0.828	-0.521	0.752	-0.920

FIGURE 18. CORRELATION HEATMAP TO VISUALIZE THE EXISTING RELATIONSHIPS BETWEEN SOIL AND WINE CHEMICAL-PHYSICAL PARAMETERS. POSITIVE CORRELATIONS ARE HIGHLIGHTED WITH DIFFERENT SHADES OF RED AND NEGATIVE CORRELATIONS ARE INDICATED BY DIFFERENT SHADES OF BLUE. SIGNIFICANT CORRELATIONS AT 0.01 LEVEL (TWO-SIDED) ARE INDICATED BY THE DOUBLE ASTERISK (**) WHEREAS SIGNIFICANT CORRELATIONS AT 0.05 LEVEL ARE INDICATED BY AN ASTERISK (*).

SOIL EFFECT ON WINES PHENOLS

Data related to global characterization of polyphenols, proanthocyanidins, monomer anthocyanins profiles, HCTAs, and flavonols (Tables 10-15) were subjected to the correlation analysis together with soils chemical physical-chemical parameters (Table 2), with the aim to highlight the possible existence of significant correlations among soil parameters and wine polyphenolic composition. The obtained correlation heatmap is shown in Figure 19.

	Clay	Silt	Sand	Cation exchange capacity	Electric conductivity	Total carbonates	Soil pH	Organic matter
Total polyphenols index	-0.244	-0.397	0.34	-1.000**	-0.84	0.479	0.371	-0.643
Total polyphenolic content	-0.63	-0.755	0.756	-0.869	-0.985*	-0.015	-0.137	-0.179
Total proanthocyanidins content	-0.571	-0.52	0.61	-0.933	-0.967*	0.225	0.077	-0.387
Total flavonoids	-0.109	-0.045	0.092	-0.930	-0.680	0.713	0.594	-0.813
Total anthocyanins - bleaching method	-0.259	-0.821	0.541	-0.768	-0.751	-0.02	-0.049	-0.196
Total anthocyanins	-0.627	-0.782	0.766	-0.856	-0.978*	-0.044	-0.160	-0.154
Delfinidin-3-Glucoside	-0.548	-0.964*	0.796	-0.621	-0.809	-0.343	-0.394	0.133
Cyanidin-3-Glucoside	-0.579	-0.933	0.802	-0.700	-0.873	-0.265	-0.335	0.053
Petunidin-3-Glucoside	-0.479	-0.856	0.702	-0.812	-0.890	-0.082	-0.155	-0.133
Peonidin-3-Glucoside	-0.468	-0.503	0.535	-0.971*	-0.941	0.304	0.169	-0.471
Malvidin-3-Glucoside	-0.599	-0.779	0.746	-0.867	-0.972*	-0.023	-0.136	-0.177
Acetylated anthocyanins	-0.969*	-0.632	0.924	-0.472	-0.863	-0.376	-0.537	0.265
p-coumaroylated anthocyanins	-0.718	-0.280	0.599	-0.723	-0.863	0.167	-0.019	-0.254
cis-caffeoyl-tartaric acid	0.623	0.071	-0.443	0.650	0.740	-0.285	-0.099	0.332
trans-caffeoyl-tartaric acid	0.507	0.077	-0.369	-0.714	-0.227	0.826	0.836	-0.915
cis-p-coumaroyl-tartaric acid	0.936	0.643	-0.907	-0.057	0.495	0.818	0.911	-0.758
trans-p-coumaroyl-tartaric acid	0.931	0.369	-0.780	0.389	0.753	0.249	0.427	-0.192
cis-Feruloyl-tartaric acid	-0.156	-0.061	0.130	-0.930	-0.705	0.686	0.559	-0.786
trans-Feruloyl-tartaric acid	0.444	-0.222	-0.192	-0.679	-0.275	0.565	0.606	-0.701
Myricetin 3-glucoside	-0.156	-0.061	0.130	-0.930	-0.705	0.686	0.559	-0.786
Quercetin 3-glucuronide	-0.363	-0.873	0.633	-0.748	-0.794	-0.109	-0.149	-0.109
Quercetin 3-glucoside	0.177	-0.550	0.131	-0.703	-0.463	0.263	0.293	-0.447
Isorhamnetin-3-glucoside	-0.398	-0.498	0.487	-0.986*	-0.918	0.344	0.221	-0.516
Laricirin-3-glucoside	-0.115	-0.558	0.327	-0.937	-0.759	0.355	0.302	-0.549
kaempferol-3-glucuronide	-0.632	-0.999**	0.867	-0.379	-0.692	-0.599	-0.635	0.412
kaempferol-3-glucoside	0.988*	0.511	-0.882	0.295	0.737	0.447	0.608	-0.378
Syringetin 3-glucoside	-0.441	-0.013	0.297	-0.773	-0.729	0.491	0.319	-0.551
Quercetin aglicon	0.190	-0.269	-0.004	-0.890	-0.543	0.623	0.597	-0.776
Dimer B3	-0.569	-0.755	0.715	-0.888	-0.969*	0.022	-0.09	-0.222
Dimer B1	-0.843	-0.155	0.625	0.204	-0.285	-0.565	-0.689	0.605
(+) Catechin	-0.848	-0.608	0.833	-0.716	-0.966*	-0.113	-0.281	-0.026
Dimer B4	-0.646	-0.893	0.828	-0.75	-0.933	-0.217	-0.311	0.011
Dimer B2	-0.614	-0.544	0.65	-0.914	-0.978*	0.177	0.026	-0.338
(-) Epicatechin	-0.179	-0.376	0.288	-0.998**	-0.805	0.513	0.416	-0.677
Trimer C1	-0.776	-0.06	0.539	-0.35	-0.61	-0.011	-0.196	0.007
Total monomers	-0.73	-0.588	0.746	-0.839	-0.989*	0.044	-0.116	-0.199
Total dimers	-0.753	-0.765	0.841	-0.793	-0.994**	-0.127	-0.264	-0.054
Total proanthocyanidins	-0.789	-0.578	0.781	-0.782	-0.978*	-0.017	-0.184	-0.127
Epigallocatechin EXT. UNIT	0.39	-0.157	-0.186	-0.773	-0.354	0.671	0.683	-0.802
Catechin EXT. UNIT	0.168	0.008	-0.114	-0.895	-0.518	0.815	0.747	-0.917
Epicatechin EXT. UNIT	-0.395	-0.478	0.476	-0.987*	-0.914	0.359	0.234	-0.529
Epicatechin-gallate EXT. UNIT	-0.009	-0.021	0.015	-0.926	-0.627	0.76	0.658	-0.861
Epigallocatechin TER. UNIT	-0.876	-0.202	0.668	-0.298	-0.643	-0.188	-0.368	0.168
Catechin TER. UNIT	-0.663	-0.405	0.619	0.526	-0.018	-0.952*	-0.971*	0.970*
Epicatechin TER. UNIT	0.179	0.869	-0.51	0.548	0.573	0.212	0.193	-0.005
Epicatechin-gallate TER. UNIT	0.981*	0.648	-0.939	0.089	0.615	0.714	0.832	-0.64
mDP	0.286	-0.082	-0.152	-0.86	-0.451	0.763	0.734	-0.884
% GALLOYLATION	0.712	0.48	-0.685	-0.452	0.102	0.959*	0.986*	-0.958*
% PRODELPHININES	0.621	0.081	-0.446	-0.599	-0.095	0.771	0.816	-0.853
% PROCYANIDINES	-0.667	-0.222	0.54	0.561	0.028	-0.854	-0.894	0.909

FIGURE 19. CORRELATION HEATMAP SHOWING THE CORRELATION PATTERN BETWEEN DATA RELATED TO GLOBAL CHARACTERIZATION OF POLYPHENOLS, MONOMER ANTHOCYANINS PROFILES, HCTAS, FLAVONOLS AND PROANTHOCYANIDINS (TABLES 17-22) WITH SOILS CHEMICAL PHYSICAL-CHEMICAL PARAMETERS (TABLE 3).

Effect on proanthocyanidins:

As it can be observed from Figure 19, the proanthocyanidin composition of Nero d'Avola wines appeared to be strongly affected by cation exchange capacity (CEC) and electric conductivity (EC). The aforementioned soil parameters shared almost the same correlation pattern: they were negatively correlated with total polyphenolic index (TPI), total polyphenolic content (TPC), and total tannins content (TTC). Among monomer and oligomer proanthocyanidins, CEC and EC were negatively correlated with (+) catechin and (-) epicatechin, and with B2, B3 and B4 dimers. Consequently, even total monomer, dimers and total proanthocyanidins showed strong negative correlations. A negative correlation was also found with (-) epicatechin as extension unit. The graphs showing the linear relationships between the aforementioned variables are visible below (Figure 20 (A-F)). CEC and EC are strongly related to each other, explaining the same correlation pattern with proanthocyanidin composition. Dealing with nutrient dynamics in soils, both CEC and EC are two parameters related to soil fertility, that is known to play a fundamental role in modulating vine development and fruits composition. While the relationship between nutrient availability in soil and anthocyanins and flavonols accumulation was previously observed in other studies (Delgado et al., 2004), no examples of relationships between wine tannin composition and soil fertility were reported in literature (Downey et al., 2004). However, Cortell et al. (2005) reported the negative correlation between vine vigor and proanthocyanidin content in grapes. This is in compliance with what observed in the present study, namely that high fertile soils, that are known to enhance vine vigor and vegetative development, produced wines with low contents of proanthocyanidins. Even soil pH plays a fundamental role in the modulation of nutrient availability, affecting the mineralization of organic matter, the dissolution and precipitation of organic matter and metals, the ammonia volatilization, the nitrification and denitrification. In this study, soil pH and total carbonates, that are strongly correlated to each other, were negatively correlated with (+) catechin as terminal unit and positively correlated with the percentage of galloylation (Figure 20 G). Soil pH and total carbonates were also positively

correlated with *trans*-caffeoyl-tartaric acid and *cis*-*p*-coumaroyl-tartaric acid. Finally, organic matter was positively correlated with (+) catechin as extension unit (Figure 20 H) and negatively correlated with the percentage of galloylation. Soil texture did not greatly affect wine proanthocyanidin composition, except for the content of (-) epicatechin-gallate as extension unit. Given that soil texture strongly affects water dynamics in soil, primarily affecting soil porosity, it can be concluded that the water availability does not play a significant role in modulating wine proanthocyanidin composition. The results obtained in this study rather suggested a strong dependence of wine proanthocyanidin composition on those soil physical-chemical parameters related to nutrients' dynamics, namely CEC, EC, pH and organic matter.

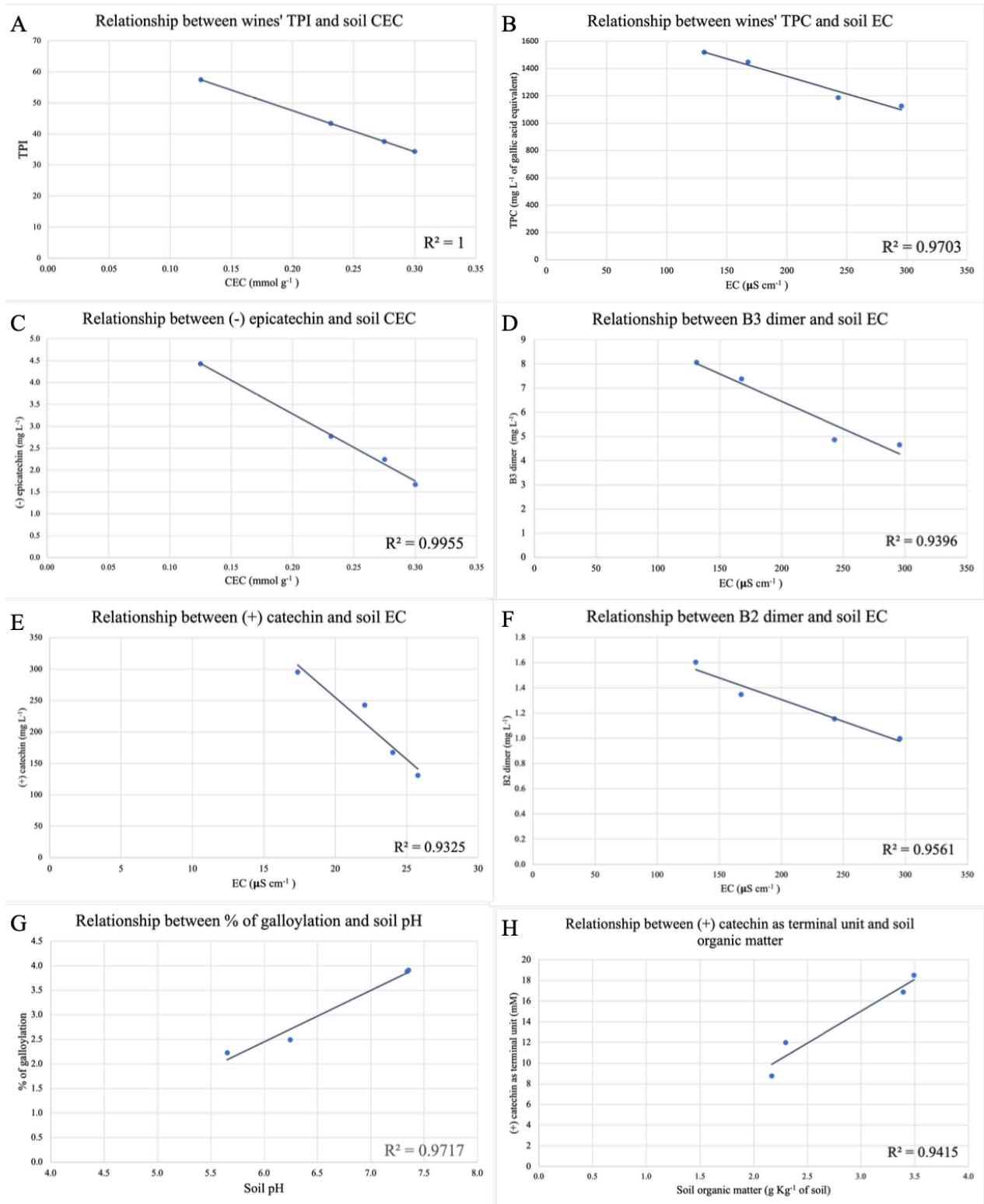


FIGURE 20. LINEAR RELATIONSHIPS EXISTING BETWEEN CATION EXCHANGE CAPACITY (CEC), ELECTRIC CONDUCTIVITY (EC), PH AND ORGANIC MATTER WITH TOTAL POLYPHENOLS INDEX (TPI), TOTAL POLYPHENOLIC CONTENT (TPC), (-) EPICATECHIN, (+) CATECHIN, B2 AND B3 DIMERS, (+) CATECHIN AS TERMINAL UNIT, AND % OF GALLOYLATION.

Effects on anthocyanins, HCTAs and flavonols:

The correlation heatmap shown in Figure 19 revealed that the clay content in soils was negatively correlated with anthocyanins, especially with the acetylated ones. Anthocyanins were also negatively correlated with the silt content. On the contrary, high content of anthocyanins were found to be positively related to the soil sand content. The strong influence of soil texture on anthocyanin concentration can be attributed to the impact of particle size distribution on soil water holding capacity and nutrient adsorption capacity. It has been observed that water deficits (such as those produced by sandy soils) promote high concentrations of anthocyanins in grapes and wines through the greater expression of the genes involved into the anthocyanin biosynthetic pathway, including F3H, DFR, UFGT, LDOX and GST (Castellarin et al. 2007). Among the different anthocyanins, the biosynthesis of tri-hydroxylated anthocyanins is favored because of the up-regulation of F3'5'H gene, that encodes the hydroxylase responsible for the 5' hydroxylation on the B ring of the flavonoid base structure.

Flavonols were not strongly correlated with soil texture, with the exceptions of kaempferol-3-glucoside, that was positively related to the soil clay content, and of kaempferol-3-glucuronide that was negatively related to the silt content. Water deficits caused by high percentage of sand in soil seem to be related to low content of hydroxycinnamoyl tartaric acids in wines, that were positively correlated with the clay content (excepting for *cis*-feruloyl-tartaric acid).

Other standing out relations are the negative correlations between soil CEC (and EC) and anthocyanins (especially the peonidin-3-glucoside), *cis* and *trans* feruloyl tartaric acid, and flavonols (especially isorhamnetin-3-glucoside and laricitrin-3-glucoside). The EC dependence on CEC could explain why EC showed almost the same correlation pattern of CEC. Soil pH and total carbonates, that are related to each other, showed almost the same correlation pattern. They positively correlated with *trans*-caffeoyl-tartaric acid and *cis*-*p*-coumaroyl-tartaric acid. Finally, organic matter showed a negative correlation with *trans*-caffeoyl-tartaric acid.

SOIL EFFECT ON WINES VOLATILE ORGANIC COMPOUNDS

The concentrations of volatile organic compounds (Table 16) and the soils chemical-physical parameters (Table 2) were subjected to the correlation analysis. The correlation heatmap shown in Figure 21 shows that the clay content in soils was negatively correlated with total content of benzenoids, particularly with 2-phenylethanol, and with γ -butyrolactone. On the contrary, it was positively correlated with ethyl octanoate. High silt content in soils was related to low content of decanoic acid. Soil sand content was negatively related to ethyl octanoate. In general, it can be observed that short and medium chain fatty acids, esters, higher alcohols, terpenes and norisoprenoids contents were higher in grapes grown on sandy soils and lower in grapes from clayey and silty soils. Great cation exchange capacity was related to high content of short and medium chain fatty acids (hexanoic acids, octanoic acid, decanoic acid) and low content of longer chain fatty acids (dodecanoic acid, tetradecanoic acid, hexadecanoic acid, octadecanoic acid). The same behavior is observed among longer, medium and short chain fatty acids and soil organic matter. Indeed, organic matter and CEC are related to each other, given that soil organic matter enhances CEC by providing higher charge density per unit surface area and higher surface area for cation adsorption (Liang et al., 2006). The different response of short, medium and longer chain fatty acids can be explained by considering their different origins. As a matter of fact, short chain fatty acids are byproducts of the protein metabolism, whereas linear longer saturated fatty acids are originated from lipid metabolism (Pérez Olivero et al. 2011, Lenti et al. 2022). It can be hypothesized that organic matter, as well as CEC, enhance the concentration of proteins in musts at the beginning of alcoholic fermentation. Organic matter is also positively correlated with higher alcohols and terpenes. Given that fermentative higher alcohols derive from the catabolism of amino acids, the amino acidic composition of must at the beginning of alcoholic fermentation is determinant for the final volatile composition of the resulting wine. Soils with high organic matter content and great CEC provide nutrient sinks for grapevine nutrition and, therefore, nitrogen pools for the production of primary amino acids and proteins in

grapes and musts. This can enhance the production of fermentative higher alcohols by yeasts during alcoholic fermentation. Among terpenes, α -terpineol was detected only in the wines from grapes grown on the two soils richer in organic matter, suggesting the existence of a relation between soil organic matter and terpenes. It appears likely that soil organic matter plays a stimulating role in the transcription of terpenoid synthase genes (VvTPS) (Zhang et al., 2016), through the supply of some key nutrient.

CEC, as well as organic matter and EC, are negatively correlated with ethyl esters formed by the longer chain fatty acids deriving from lipid metabolism. It seems the direct consequence of the lower concentration of longer chain fatty acids in wines from soils with high cation exchange capacity. CEC, organic matter and EC are also negatively correlated with aging esters, such as diethyl malate, diethyl succinate and monoethyl-2-hydroxyglutarate, that derive from the reaction between ethanol and malic acid, succinic acid and glutaric acid, respectively. Finally, soil pH and total carbonates content show the opposite behavior towards medium, short and longer chain fatty acids, higher alcohols and esters. In particular, slightly basic pH values are related with low contents of medium and short chain fatty acids and fermentative higher alcohols, and high content of longer chain fatty acids. In the soils analyzed in the present study, the higher the organic matter content the lower the pH.

	Clay	Silt	Sand	Cation Exchange Capacity	Total Carbonates	Electric Conductivity	Soil pH	Organic Matter
<i>2-methylbutanoic + Isovaleric acid</i>	-0.825	-0.672	0.846	0.214	-0.933	-0.342	-0.982 *	0.879
<i>Butanoic acid</i>	0.165	0.588	-0.373	0.939	-0.317	0.787	-0.261	0.515
<i>Hexanoic acid</i>	-0.536	-0.358	0.514	0.631	-0.964 *	0.118	-0.953 *	0.994 **
<i>Octanoic acid</i>	-0.545	-0.307	0.497	0.646	-0.943	0.131	-0.940	0.986 **
<i>Decanoic acid</i>	-0.596	-0.999 **	0.841	-0.367	-0.598	-0.666	-0.622	0.410
<i>Dodecanoic acid</i>	-0.519	-0.841	0.719	-0.830	-0.072	-0.917	-0.152	-0.140
<i>Tetradecanoic acid</i>	0.008	0.216	-0.101	-0.801	0.825	-0.501	0.713	-0.871
<i>Hexadecanoic acid</i>	0.239	0.309	-0.295	-0.749	0.926	-0.345	0.852	-0.963
<i>Octadecanoic acid</i>	0.412	0.289	-0.401	-0.720	0.947	-0.245	0.912	-0.994
<i>Acids</i>	-0.602	-0.402	0.577	0.572	-0.967 *	0.041	-0.970 *	0.988 *
<i>2-methylbutyl lactate + isoamyl lactate</i>	-0.500	-0.152	0.398	0.712	-0.875	0.217	-0.876	0.950 *
<i>Diethyl malate</i>	-0.184	-0.130	0.181	-0.955 *	0.646	-0.743	0.525	-0.761
<i>Diethyl succinate</i>	-0.206	-0.208	0.230	-0.977 *	0.602	-0.779	0.485	-0.732
<i>Monoethyl succinate</i>	-0.796	-0.439	0.723	-0.730	0.032	-0.926	-0.144	-0.145
<i>Diethyl 2-hydroxyglutarate</i>	0.074	-0.538	0.192	-0.826	0.339	-0.591	0.336	-0.529
<i>Monoethyl 2-hydroxyglutarate</i>	-0.790	-0.753	0.860	-0.768	-0.155	-0.992 **	-0.292	-0.020
<i>Ethyl lactate</i>	-0.395	-0.055	0.285	0.792	-0.837	0.334	-0.822	0.933
<i>Ethyl pyroglutamate</i>	0.200	0.097	-0.174	-0.861	0.857	-0.466	0.791	-0.942
<i>Ethyl 2-hydroxy-3-phenylpropanoate</i>	-0.580	-0.900	0.785	0.043	-0.866	-0.371	-0.856	0.739
<i>Ageing esters</i>	-0.486	-0.375	0.490	-0.947	0.365	-0.915	0.218	-0.507
<i>Benzyl alcohol</i>	-0.510	0.201	0.247	0.594	-0.531	0.183	-0.593	0.659
<i>2-phenylethanol</i>	-0.960 *	-0.658	0.929	-0.019	-0.774	-0.560	-0.876	0.705
<i>Tyrosol</i>	-0.020	-0.730	0.339	0.098	-0.601	-0.045	-0.499	0.480
<i>Benzenoids</i>	-0.953 *	-0.671	0.930	-0.009	-0.789	-0.552	-0.887	0.718
<i>Isoamyl acetate</i>	-0.447	0.250	0.183	0.648	-0.520	0.255	-0.570	0.659
<i>Hexyl acetate</i>	0.755	0.304	-0.635	-0.450	0.848	0.100	0.907	-0.882
<i>Phenylethyl acetate</i>	-0.523	0.108	0.297	0.644	-0.642	0.196	-0.689	0.759
<i>Acetated esters</i>	-0.450	0.238	0.190	0.653	-0.533	0.256	-0.582	0.671
<i>Ethyl hexanoate</i>	-0.849	-0.577	0.819	0.251	-0.905	-0.315	-0.967 *	0.873
<i>Ethyl octanoate</i>	0.980 *	0.697	-0.960 *	0.422	0.470	0.844	0.615	-0.353
<i>Ethyl decanoate</i>	-0.469	0.410	0.127	0.181	-0.024	-0.045	-0.150	0.144
<i>Ethyl dodecanoate</i>	-0.237	0.295	0.026	-0.617	0.644	-0.484	0.493	-0.643
<i>Ethyl tetradecanoate</i>	-0.061	0.008	0.038	-0.913	0.749	-0.638	0.639	-0.842
<i>Ethyl hexadecanoate</i>	-0.121	-0.016	0.088	-0.916	0.715	-0.672	0.596	-0.809
<i>Ethyl octadecanoate</i>	-0.118	-0.022	0.089	-0.919	0.715	-0.673	0.596	-0.810
<i>Ethyl p-hydroxycinnamate</i>	-0.256	0.060	0.144	-0.829	0.650	-0.667	0.503	-0.713
<i>Ethyl esters</i>	-0.233	0.073	0.123	-0.831	0.668	-0.655	0.524	-0.730
<i>3-hydroxy-β-damascone</i>	-0.697	-0.192	0.546	0.520	-0.809	-0.010	-0.863	0.867
<i>3-oxo-α-ionol</i>	-0.743	-0.046	0.513	-0.413	0.060	-0.635	-0.123	-0.071
<i>Blumenol C</i>	0.525	-0.071	-0.316	0.610	-0.382	0.647	-0.205	0.405
<i>Vomifolol + grasshopper ketone</i>	-0.235	0.163	0.082	0.881	-0.704	0.499	-0.677	0.840
<i>C13-norisoprenoids</i>	-0.453	0.072	0.267	0.736	-0.721	0.286	-0.740	0.837
<i>Isoamyl alcohol</i>	-0.832	-0.230	0.653	0.299	-0.696	-0.227	-0.795	0.731
<i>Hexanol</i>	-0.840	-0.451	0.757	0.311	-0.864	-0.254	-0.935	0.861
<i>(E)-3-hexenol</i>	-0.505	-0.921	0.745	-0.013	-0.808	-0.376	-0.787	0.667
<i>3-ethoxypropanol</i>	-0.756	-0.419	0.687	0.431	-0.913	-0.129	-0.959 *	0.925
<i>(Z)-3-hexenol</i>	-0.593	0.084	0.354	0.556	-0.609	0.101	-0.676	0.716
<i>Methionol</i>	-0.763	-0.439	0.700	0.417	-0.918	-0.145	-0.964 *	0.924
<i>Tryptophol</i>	-0.478	0.358	0.157	-0.144	0.209	-0.274	0.053	-0.132
<i>Alcohols</i>	-0.856	-0.308	0.704	0.277	-0.741	-0.264	-0.837	0.761
<i>linalool</i>	-0.087	0.629	-0.224	0.702	-0.176	0.514	-0.201	0.370
<i>α-terpineol</i>	-0.686	-0.263	0.571	0.536	-0.868	-0.004	-0.909	0.915
<i>(E)-8-hydroxylinalool</i>	-0.489	0.219	0.225	0.610	-0.524	0.205	-0.583	0.656
<i>Terpenes</i>	-0.506	0.165	0.261	0.630	-0.585	0.203	-0.638	0.710
<i>γ-butyrolactone</i>	-0.947	-0.327	0.773	-0.148	-0.429	-0.594	-0.586	0.406

FIGURE 21. CORRELATION HEATMAP TO VISUALIZE THE EXISTING RELATIONSHIPS BETWEEN SOIL AND WINE VOLATILE ORGANIC COMPOUNDS (VOCs). POSITIVE CORRELATIONS ARE INDICATED WITH THE RED COLOUR AND NEGATIVE CORRELATIONS ARE INDICATED BY THE BLUE COLOUR. SIGNIFICANT CORRELATIONS AT 0.01 LEVEL (TWO-SIDED) ARE INDICATED BY THE DOUBLE ASTERISK (**) WHEREAS SIGNIFICANT CORRELATIONS AT 0.05 LEVEL ARE INDICATED BY AN ASTERISK (*).

MULTIVARIATE STATISTICAL ANALYSES

PRINCIPAL COMPONENT ANALYSIS 1: PROANTHOCYANIDIN COMPOSITION

In order to visualize the separation among *Nero d'Avola* wines derived from grapes grown on different soils as based on differences on wines' proanthocyanidin composition, the unsupervised principal component analysis (PCA) was carried out. The analysis reduced the number of original variables into 2 components that explained the 90% of the total variance of the dataset. Figure 22 shows the 2D PCA Biplot. It highlighted a great separation among *Nero d'Avola* wines derived from different soils. This separation was mostly driven by: total polyphenols index, total polyphenolic content, total proanthocyanidins content, B3 dimer content and (-)epicatechin as extension unit content, all contributing to the positive side of the PC1; (-) epicatechin and epicatechin-gallate as terminal units, contributing to the negative side of the PC1; % of galloylation and % of prodelphinidins, contributing to the positive side of the PC2; % of procyanidins, (+) catechin as terminal unit and B1 dimer contents, leading the negative side of the PC2. The great separation observed in the PCA analysis suggested that the proanthocyanidin compositional and structural characteristics of Nero d'Avola wines were largely affected by soil chemical-physical parameters.

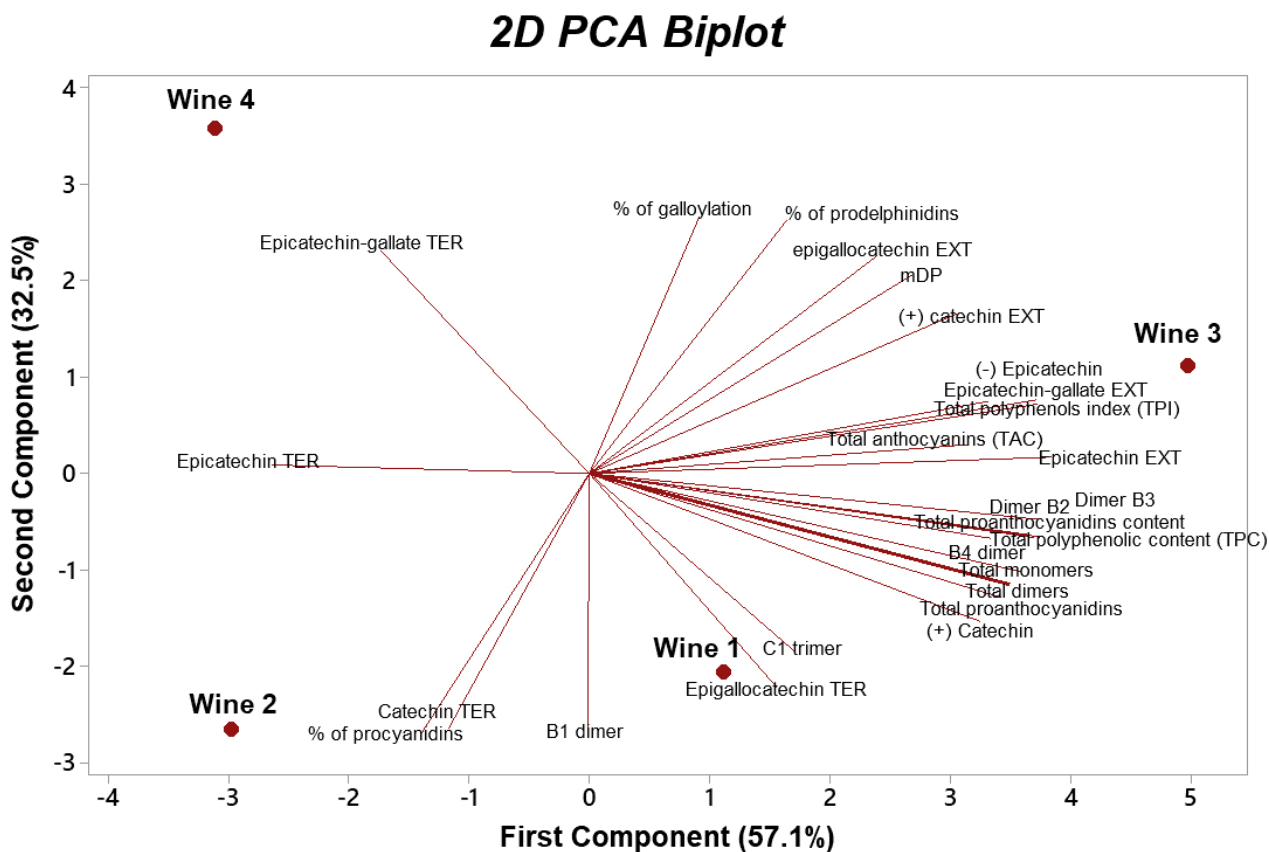


FIGURE 22. 2D PCA BIPLLOT SHOWING THE SEPARATION AMONG NERO D'AVOLA WINES AS BASED ON DIFFERENCES ON PROANTHOCYANIDIN COMPOSITION. THE EXPLAINED VARIANCES ARE SHOWN IN BRACKETS

PRINCIPAL COMPONENT ANALYSIS 2: ANTHOCYANINS, HCTAs AND FLAVONOLS

To visualize the separation among *Nero d'Avola* wines as based on differences in anthocyanins, hydroxycinnamoyl tartaric acids and flavonols composition, another principal component analysis was performed (Figure 23). The obtained PCA reduced the number of original variables into two principal components that accounted for 83.5% of the total variation in the dataset. Individually, PC1 and PC2 explained 59.2% and 24.3% of the total variation. The separation among *Nero d'Avola* wines is mostly driven by the monomer anthocyanins (located on the positive side of PC1), by *cis*-caffeoyl-tartaric acid and *trans*-*p*-coumaroyl-tartaric acid (located on the negative side of PC1) and by *trans*-caffeoyl-tartaric acid, *trans*-feruloyl-tartaric acid, and *cis*-*p*-coumaroyl-tartaric acid (located on the positive side of PC2).

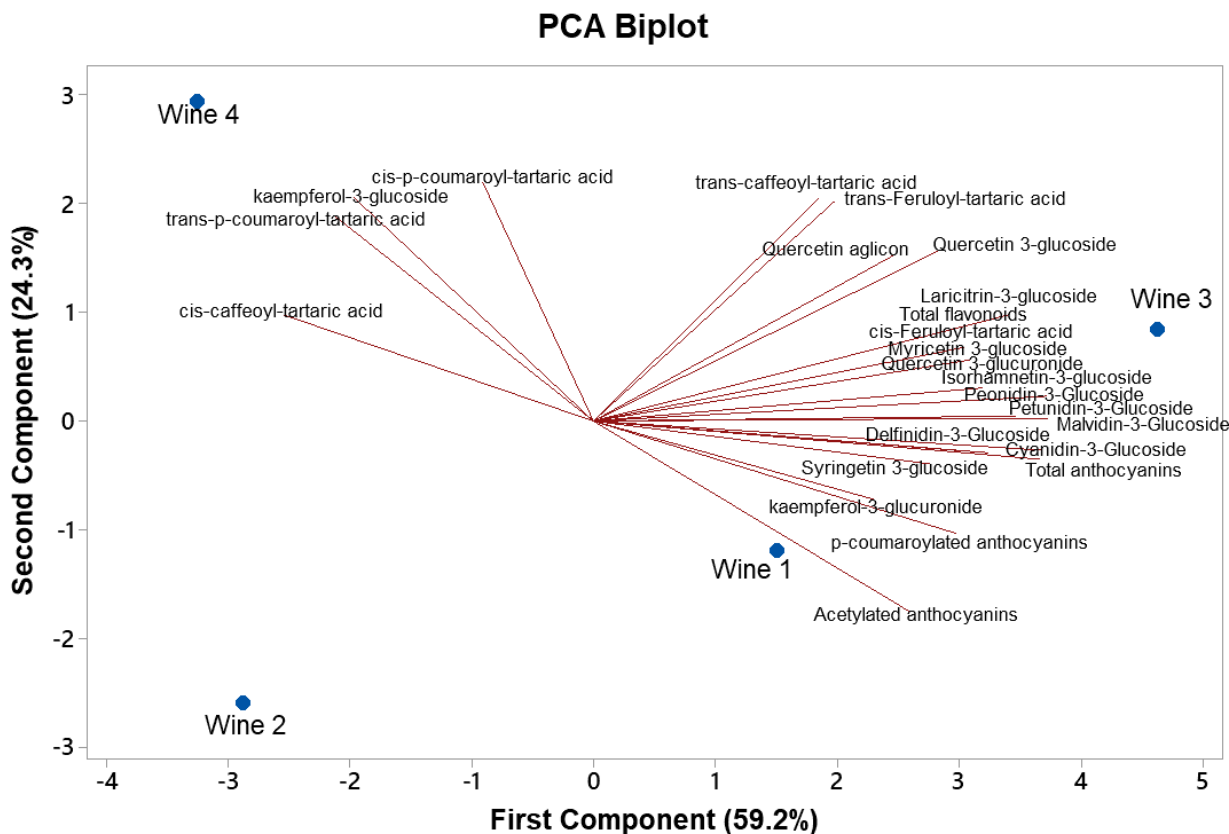


FIGURE 23. 2D PCA BILOT OF POLYPHENOLIC COMPOUNDS SHOWING THE SEPARATION AMONG NERO D'AVOLA WINES. THE EXPLAINED VARIANCES ARE SHOWN IN BRACKETS.

PRINCIPAL COMPONENT ANALYSIS 3: VOLATILE ORGANIC COMPOUNDS

The PCA applied to the dataset containing the concentration of volatile organic compounds (VOCs) reduced the number of original variables into two principal components that accounted for 81% of the total variance in the dataset. Figure 24 shows the 2D PCA Biplot revealing a great separation among *Nero d'Avola* wines. The separation is mostly driven by: hexanoic acid, octanoic acid, acetated esters, aging esters and α -terpineol, that lead the positive side of PC1; by dodecanoic acid, hexadecenoic acid, octadecanoic acid, tetradecanoic acid, and ethyl pyroglutamate, that drive the negative side of PC1; by hexyl acetate, tyrosol, ethyl octanoate and Blumenol C, that lead the positive

side of PC2; monoethyl succinate, isoamyl alcohol, γ -butyrolactone and 3-oxo- α -ionol, that drive the negative side of PC2.

The spatial separation among wines in all the biplots shown above suggested that the soil strongly influences both the polyphenolic and the aromatic composition of the resulting wines.

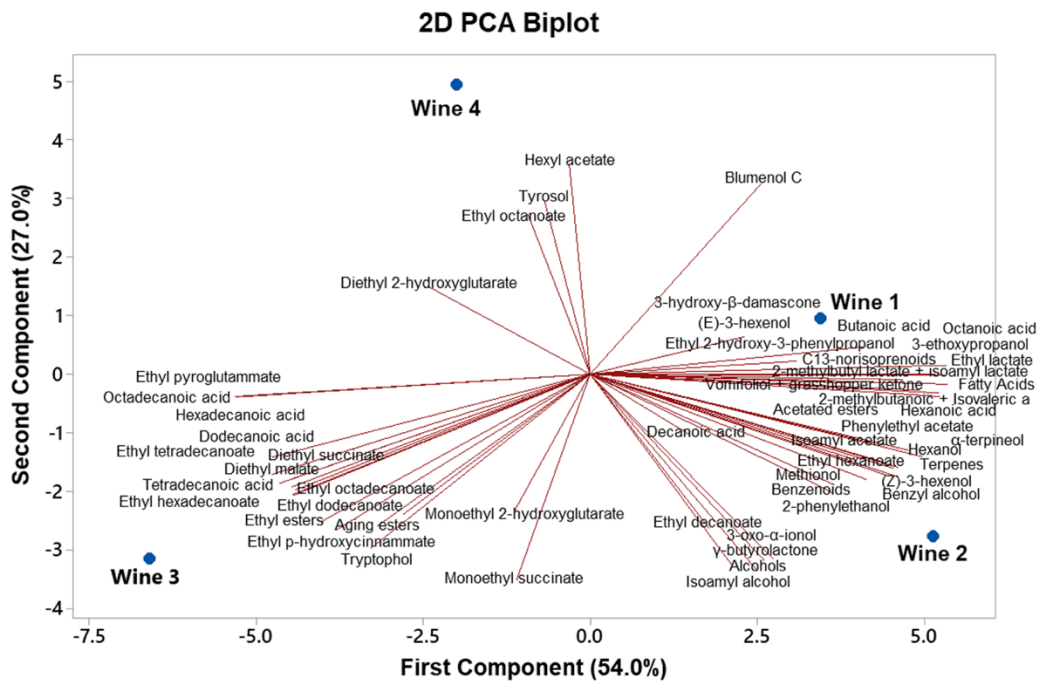


FIGURE 24.2D PCA BILOT OF VOLATILE ORGANIC COMPOUNDS (VOCs) SHOWING THE SEPARATION AMONG NERO D'AVOLA WINES. THE EXPLAINED VARIANCES ARE SHOWN IN BRACKETS.

CHAPTER 5. INFLUENCE OF SOIL ON THE CHEMICAL COMPOSITION OF NERO D'AVOLA WINES (PART II)⁵

⁵ This chapter has been adapted including relevant parts from:

Bambina, P., Spinella, A., Lo Papa, G., Chillura Martino, D. F., Lo Meo, P., Corona, O., ... & Conte, P. (2023). 1H NMR-Based Metabolomics to Assess the Impact of Soil Type on the Chemical Composition of Nero d'Avola Red Wines. Journal of Agricultural and Food Chemistry, 71(14), 5823-5835

MATERIALS AND METHODS

¹H-NMR SPECTROSCOPIC ANALYSIS OF WINES

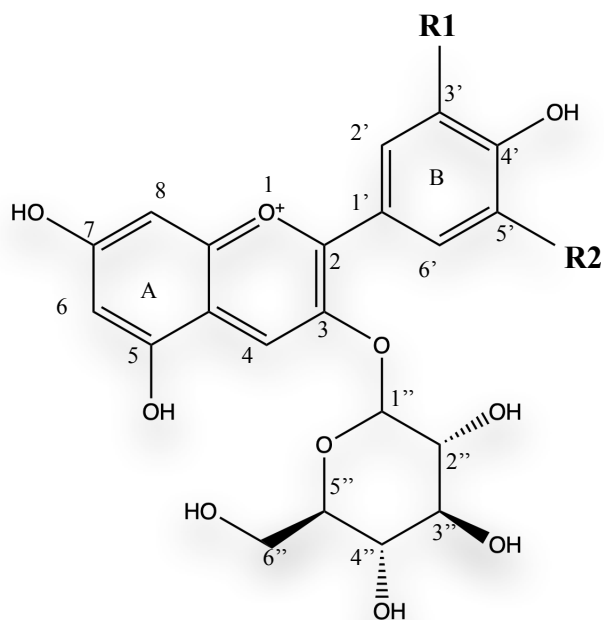
To carry out ¹H-NMR analysis, 0.5 ml of each wine was added with 0.1 ml of D₂O and placed into a 5 mm NMR tube. Wines were analyzed by means of a Bruker Avance II 400 spectrometer operating at a proton Larmor frequency of 400.15 MHz. The ¹H-NMR spectra were acquired at the temperature of 25 °C by applying the NOESYGPPS1D pulse sequence to suppress both water and ethanol signals. In particular, 8 signals were suppressed, namely the singlet produced by water (4.81 ppm), the ethanol methylene quartet (3.60 - 3.68 ppm) and the ethanol methyl triplet (1.15 - 1.20 ppm). The shaped pulse was 0.08 mW. The mixing time was 0.01 s. 4 dummy scans were used. Free induction decays (FIDs) were collected with a 64k time domain, a spectral width of 8012.82 Hz, a relaxation delay of 4 s and an acquisition time of 4 s. 128 scans were applied. An exponential function corresponding to 0.3Hz was applied before Fourier transformation. D₂O was used as an external reference to optimize the field frequency lock. The residual peak of water was used as chemical shift reference. No quantitative internal standard was used. In order to maintain the absolute non-targeted character of the experiment and to avoid any kind of modification of the matrix, no artificial pH adjustment was carried out on wines. In fact, wine pH depends on the relative proportions and strengths of the acids contained therein, thereby reflecting how the protons have been exchanged with cations such as potassium and sodium. The relative proportions of the acids and the potassium and sodium ions concentrations can vary according to cultivar, grape maturity, viticultural practices, and soil type (Coulter et al., 2015). Hence, wine pH can be effectively considered as a parameter influenced by the terroir. ¹H-NMR spectra were manually phased, and the baselines were manually corrected via the Whittaker smoother method by using MNova 14.2.3 software (Mestrelab Research, Santiago de Compostela, Spain). To correct vertical scale errors deriving from the residual water and ethanol signals, quantitative assessment of the spectra was done by normalizing to the total spectral area after

having removed the spectral regions containing water protons signal (4.75 - 4.90 ppm), ethanol methyl protons signal (1.15 - 1.20 ppm), and ^{13}C satellites of ethanol (0.99 -1.05 ppm and 1.30 – 1.36 ppm). The spectral region containing signal of the methylene protons in ethanol (3.60 - 3.68 ppm) was not removed because it also contains signals produced by other metabolites present in wines.

TARGETED ANALYSIS (TA): IDENTIFICATION OF COMPOUNDS

In order to obtain the *Nero d'Avola* wine *profiling* by identifying and quantifying known metabolites, the targeted approach (TA) was applied. Signal assignment in each spectrum was performed by comparison with the pure compounds spectra sourced from Biological Magnetic Resonance Data Bank (*BMRB*) (Ulrich et al., 2008) and Natural Products Magnetic Resonance Database (*NP-MRD*) (Wishart et al., 2022). The reference spectra were collected into a library by means of *Simple Mixture Analysis (SMA)* plug-in of MNova software, that identifies the compounds inside the spectra according to the signal chemical shift, signal multiplicity and relative coupling constants. For compound identification, we used chemical shift ranges (with a centroid tolerance of 0.10 ppm) rather than a single specific value in order to account for the possible chemical shift dispersion deriving from different wines' pH and from different aggregations of molecules inside the samples. The complete list of chemical shift ranges, signal multiplicities and coupling constants used for the identification of all compounds are listed in Table B1 in Appendix B. The identification and quantification of minor compounds, such as anthocyanins, was carried out by applying the global spectral deconvolution method (GSD) to deconvolute overlapping signals in crowded spectral regions. Because all anthocyanins share the same structural scaffold, differing solely for R1 and R2 groups (Figure 25), the discrimination among different anthocyanins was carried out by considering the relevant diagnostic signals reported in Table 17. The table lists the chemical shift ranges and the signal multiplicities used for the discrimination of the different anthocyanins. For their quantification, only the aforementioned diagnostic signals were measured and compared among wines. Possible

discrepancies with anthocyanins chemical shift values reported in literature (Košir et al., 2002; Ferrari et al., 2011) are due to differences in the chemical and physical environment in which the single protons are immersed.



	R1	R2
Malvidin-3-glucoside	- OMe	- OMe
Cyanidin-3-glucoside	-OH	-H
Delphinidin-3-glucoside	-OH	-OH
Peonidin-3-glucoside	-H	- OMe
Petunidin-3-glucoside	-OH	- OMe

FIGURE 25. STRUCTURE OF THE MONOMERIC ANTHOCYANINS PRESENT IN WINE. ALL THE ANTHOCYANINS HAVE THE SAME BASIC STRUCTURE WITH DIFFERENCES IN R1 AND R2, ONLY.

TABLE 17. CHEMICAL SHIFT RANGES AND SIGNAL MULTIPLICITIES USED FOR THE DISCRIMINATION OF THE DIFFERENT ANTHOCYANINS. BECAUSE ALL ANTHOCYANINS SHARE THE SAME STRUCTURAL SCAFFOLD, DIFFERING FOR R1 AND R2 GROUPS ONLY (FIGURE 2), THE DISCRIMINATION AMONG DIFFERENT ANTHOCYANINS, AS WELL AS THEIR QUANTIFICATION, WERE CARRIED OUT BY CONSIDERING THE RELEVANT DIAGNOSTIC SIGNALS LISTED BELOW.

	H2' proton	H3' proton	H5' proton	H6' proton
Peonidin-3-glucoside	6.9-7.1 ppm (d)			
Cyanidin-3-glucoside	7.0-7.1 ppm (d)	8.0 – 8.1 ppm (dd)		
Malvidin-3-glucoside	7.4-7.6 ppm (d)	7.5-7.6 ppm (d)		
Petunidin-3-glucoside	7.6-7.7 ppm (d)	6.8-6.9 ppm (d)		
Delphinidin-3-glucoside	7.6-7.8 ppm (d)			

The absolute integrals of the peaks belonging to the identified compounds were calculated by means of *qNMR* plug-in of MNova software. The relative concentration of the identified metabolites was calculated as percentage of the total spectral area. As already discussed by Palmioli et al. (2020), the quantification of metabolites is relative rather than absolute because the recycle delay used for spectra acquisition was < 25 s, that is the time necessary for all protons inside the wine to relax completely. The recycle time used in this study was long enough to ensure the relaxation of most of the protons present inside the wines, except for some aromatic compounds whose quantification can be underestimated. However, a metabolomic analysis aims at determining the relative variation of the concentration of the identified metabolites among different samples. Therefore, rather than providing the exact metabolite concentration, a metabolomic study must ensure the same percentage error associated to the evaluation of each metabolite, from sample to sample. This is provided by accurately using the same acquisition parameters for recording ¹H NMR spectra, including the receiver gain, the pulse width, and the temperature. Up to 50 different compounds were identified and quantified. The obtained data were organized in a (*m* × 50) matrix, where the *m* rows represented the wine samples, and the 50 columns represented the absolute integrals of each identified compound. The presence of minor compounds identified by means of ¹H-NMR (including anthocyanins, hydroxycinnamoyl tartaric acids, flavonols and aroma compounds) was confirmed by GC-MS and HPLC-DAD analysis.

One-way analysis of variance (ANOVA) with Tukey's HSD post hoc test was applied to the dataset containing the indicative concentration of metabolites identified by means of targeted $^1\text{H-NMR}$. The analysis highlighted the existence of significant differences among wines. Differences with $p < 0.05$ were considered statistically significant. The ANOVA analysis was performed by means of *MetaboAnalyst 5.0* web-based tool suite (Chong et al., 2018). Data obtained by the TA were also subjected to an unsupervised multivariate statistical approach, namely principal component analysis (PCA).

NON-TARGETED ANALYSIS: DATA REDUCTION

In order to obtain the *Nero d'Avola* wine *fingerprinting* and to explore the chemical variability among the investigated wines, the non-targeted approach was applied. The generation of the input variables was done via bucketing (or binning) the spectra by means of MNova software. Through the bucketing operation, each spectrum is divided into segments of constant width (buckets or bins). Each segment is the result of the sum of the integrals of all the points falling inside a bucket, and the sum itself is considered as a new point in the binned spectrum (Bingol et al., 2018). Therefore, the large number of original data points (about sixty-five thousand data points for each spectrum) is reduced into a smaller number of representative buckets, that are used as input variables for subsequent multivariate statistical analysis. Among the bucketing width ranges tested (0.01, 0.02, 0.03, and 0.04 ppm), the width range of 0.01 ppm showed the best balance between the data resolution and the loss of spectral information. The bucketing was performed in the spectral range 0.5-9.5 ppm and divided the spectra into 890 buckets. Therefore, the obtained dataset consisted in a ($m \times 890$) matrix, where the m rows represented the wine samples, and the 890 columns represented the integrals of the spectral buckets. The dataset was imported into *MetaboAnalyst 5.0* web-based tool suite (Chong et al., 2018) to preprocess the data and to run multivariate statistical analysis.

NON-TARGETED ANALYSIS: DATA PREPROCESSING AND MULTIVARIATE STATISTICAL ANALYSIS

Before running multivariate statistical analysis, the data matrix was log transformed, mean-centered and scaled to Pareto variance. The log transformation was applied to correct the heteroscedasticity, to convert multiplicative relations into additive ones, and to turn skewed distributions into more symmetric distributions. The mean-centering is applied to focus the analysis on the differences, despite of the similarities, among the data (van den Berg et al., 2006). The Pareto-scaling uses the standard deviation square root as scaling factor to reduce the relative importance of the large fold changes on small fold changes, keeping data structure partially intact (van den Berg et al., 2006). Figure 26 shows the effects of the preprocessing step. The box plots at the bottom of the figure show the intensity distributions of each spectral bucket. The plots at the top of the figure show the overall concentration distribution based on Kernel density estimation (Xia et al., 2011). To explore the chemical variability and to discriminate wines from grapes grown on different soils an unsupervised multivariate statistical approach, namely principal component analysis (PCA), was performed.

The data obtained from the targeted ¹H-NMR-based metabolomic analysis were processed together with soil physical-chemical parameters to point out possible correlations. To better visualize the existing relationships between soil and wine parameters a correlation heatmap was built. Then, a summary of the information obtained by the correlation analysis was provided by the unsupervised principal component analysis (PCA). Apart from visualizing the separation among samples, PCA allowed also to visualize the correlations among variables, as based on the spatial arrangement of the variables in the Loadings Plot. In particular, adjacent variables are highly positively correlated, while variables arranged according to a 180° angle are highly negatively correlated. Finally, variables arranged according to a 90° angle are uncorrelated. All data were standardized before running PCA. Both the correlation analysis and the principal component analysis were carried out using Minitab™ statistical software.

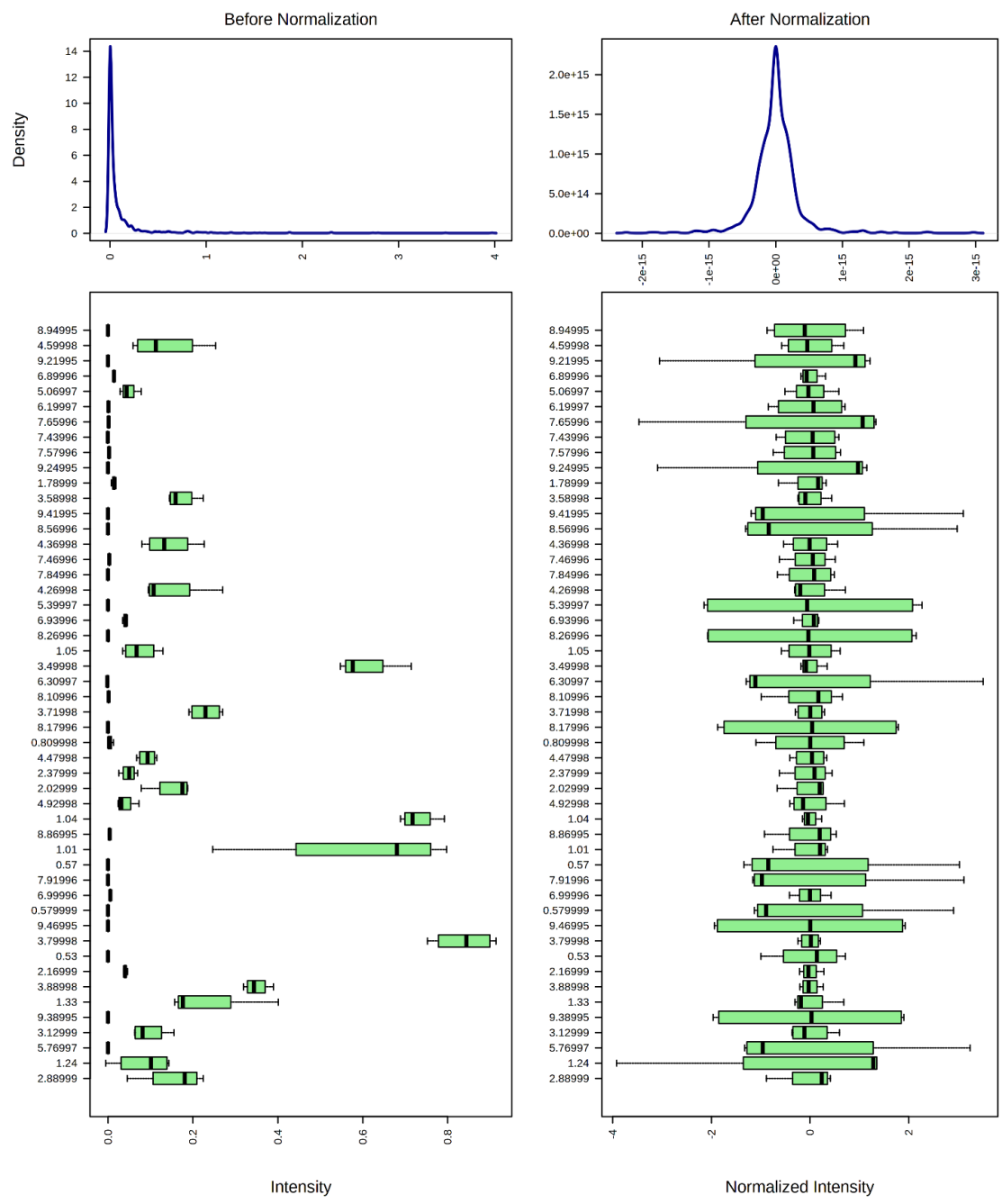


FIGURE 26. EFFECTS OF THE PREPROCESSING STEP ON DATA DISTRIBUTION. THE PREPROCESSING STEP CONSISTED IN MEAN CENTERING, LOG TRANSFORMATION AND PARETO SCALING. THE BOX PLOTS AT THE BOTTOM OF THE FIGURE SHOW THE INTENSITY DISTRIBUTIONS OF EACH SPECTRAL BUCKET. THE PLOTS AT THE TOP OF THE FIGURE SHOW THE OVERALL CONCENTRATION DISTRIBUTION BASED ON KERNEL DENSITY ESTIMATION.

RESULTS

¹H-NMR SPECTRA EVALUATION: TARGETED ANALYSIS

The targeted analysis (TA) led to the *Nero d'Avola* wines *profiling* through the identification and quantification of known metabolites. As described in Materials & Methods, metabolites identification in each spectrum was performed by comparison with pure compounds spectra. The complete list of chemical shift ranges, signal multiplicities and coupling constants used for the identification of all compounds are listed in Table B1 of Appendix B. A representative ¹H-NMR spectrum of one of the analyzed *Nero d'Avola* wines, reporting the signal assignment described above, is reported in Figure 27. As it can be observed, the spectral area between 0.00 and 3.00 ppm is attributed to the aliphatic systems, the area between 3.00 and 5.50 ppm is assigned to the carbinolic region, while the area between 5.50 and 10.00 ppm is typical of protons belonging to polyphenolic compounds.

The targeted analysis allowed the identification and quantification of 48 metabolites, including organic acids, amino acids, polyols, aroma compounds and polyphenolic compounds. Figure 28 reports all the identified compounds together with their indicative quantification (% of the total spectral area). The one-way analysis of variance (ANOVA) applied to the concentration of the identified metabolites highlighted the existence of significant differences ($p < 0.05$) among the investigated wines. Figure 29 shows the results of the ANOVA analysis. Metabolites showing differences with a p -value below the threshold (0.05) are represented by red dots. Metabolites showing differences with a p -value above the threshold are represented by the green dots. In the figure, the green dots represent kaempferol-3-glucoside and *trans*-caffeic acid respectively, that are the only two compounds present in similar concentrations among wines.

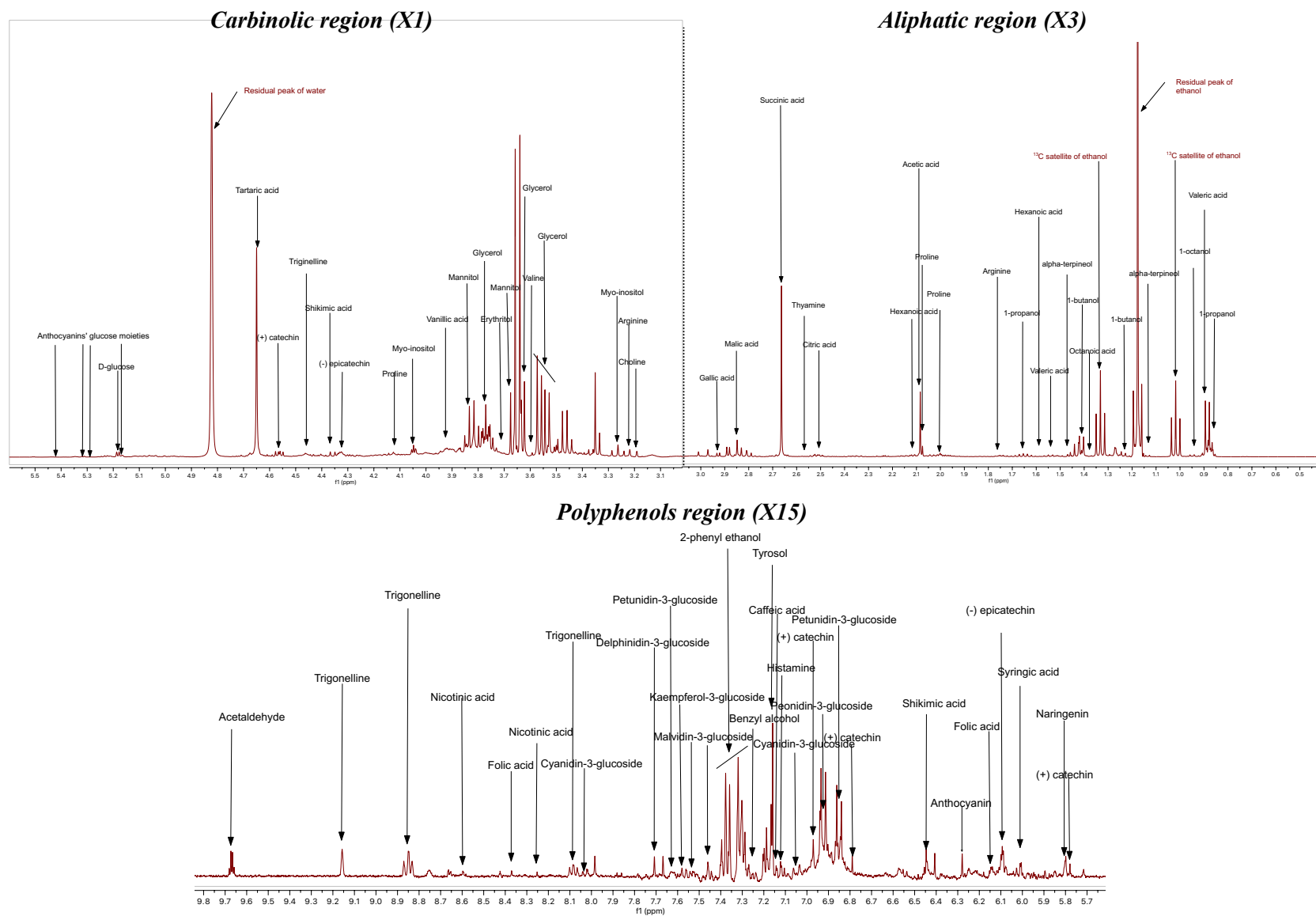


FIGURE 27. A REPRESENTATIVE ¹H-NMR SPECTRUM OF A NERO D'AVOLA WINE WITH SIGNAL ASSIGNMENT. THE SPECTRAL AREA BETWEEN 0.00 AND 3.00 PPM IS THE ALIPHATIC REGION, THE AREA BETWEEN 3.00 AND 5.50 PPM IS THE CARBINOLIC REGION, THE AREA BETWEEN 5.50 AND 10.00 PPM IS THE POLYPHENOLS REGION

NERO D'AVOLA WINES *PROFILING*

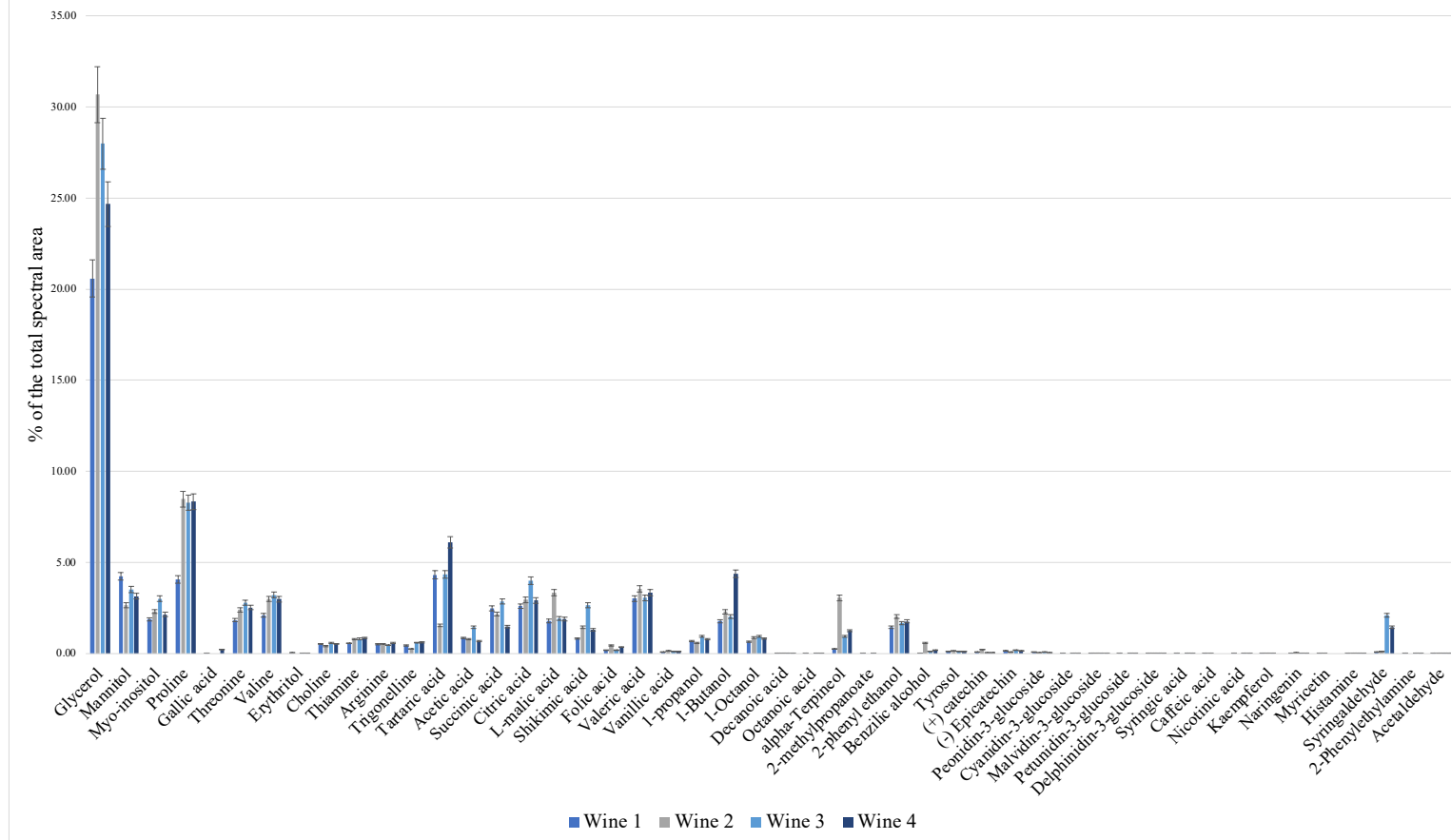
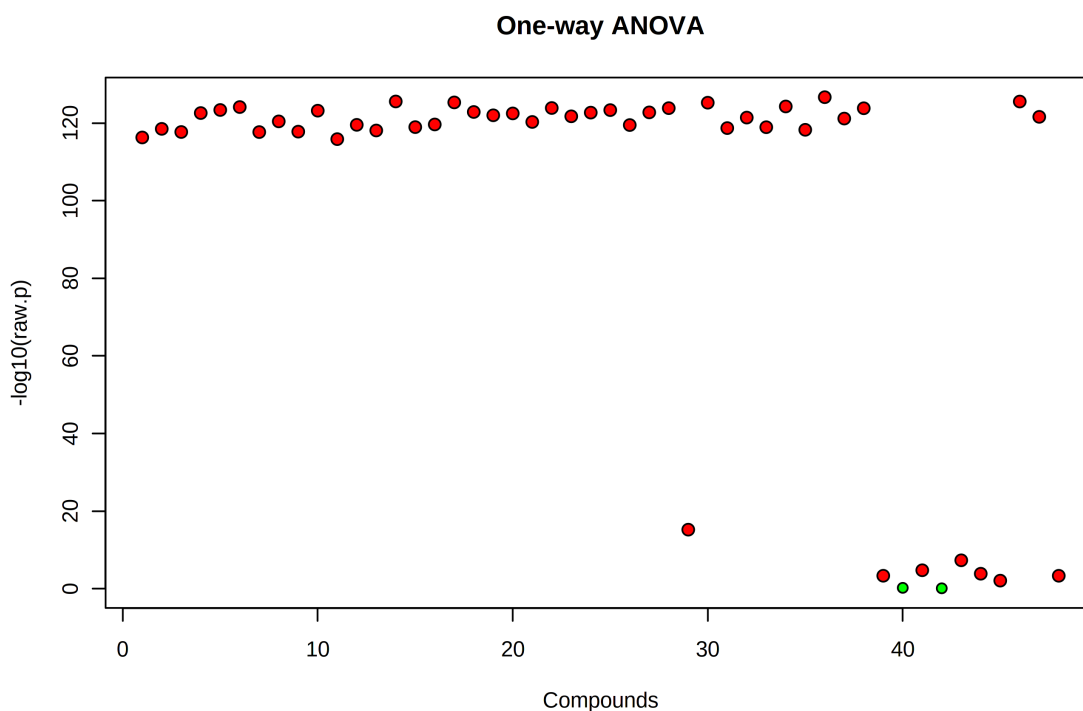


FIGURE 28. LIST OF THE COMPOUNDS IDENTIFIED BY MEANS OF THE TARGET ANALYSIS WITH INDICATIVE CONCENTRATIONS (% ON THE TOTAL SPECTRAL AREA).



1	Glycerol	25	Decanoic acid
2	Mannitol	26	Octanoic acid
3	Myo-inositol	27	alpha-Terpineol
4	Proline	28	2-methylpropanoate
5	Gallic acid	29	2-phenyl ethanol
6	Threonine	30	Benzilic alcohol
7	Valine	31	Tyrosol
8	Erythritol	32	(+) catechin
9	Choline	33	(-) Epicatechin
10	Thiamine	34	Malvidin-3-glucoside
11	Arginine	35	Petunidin-3-glucoside
12	Trigonelline	36	Delphinidin-3-glucoside
13	Tartaric acid	37	Peonidin-3-glucoside
14	Acetic acid	38	Cyanidin-3-glucoside
15	Succinic acid	39	Syringic acid
16	Citric acid	40	Caffeic acid
17	L-malic acid	41	Nicotinic acid
18	Shikimic acid	42	Kaempferol-3-glucoside
19	Folic acid	43	Naringenin
20	Valeric acid	44	Myricetin-3-glucoside
21	Vanillic acid	45	Histamine
22	1-propanol	46	Syringaldehyde
23	1-Butanol	47	2-Phenylethylamine
24	1-Octanol	48	Acetaldehyde

FIGURE 29. ONE-WAY ANALYSIS OF VARIANCE (ANOVA) WITH TUKEY'S HSD POST HOC TEST APPLIED TO THE DATASET CONTAINING THE INDICATIVE CONCENTRATION OF METABOLITES IDENTIFIED BY MEANS OF TARGET ANALYSIS. METABOLITES SHOWING DIFFERENCES WITH A P-VALUE BELOW THE THRESHOLD (0.05) ARE REPRESENTED BY THE RED DOTS. METABOLITES SHOWING DIFFERENCES WITH A P-VALUE ABOVE THE THRESHOLD ARE REPRESENTED BY THE GREEN DOTS. IN THE FIGURE, THE GREEN DOTS REPRESENT KAEMPFEROL-3-GLUCOSIDE AND TRANS-CAFFEIC ACID RESPECTIVELY, THAT ARE THE ONLY TWO COMPOUNDS PRESENT IN NO SIGNIFICANT DIFFERENT CONCENTRATIONS AMONG WINES.

The principal component analysis (PCA) applied to the data matrix obtained by means of the TA reduced the number of original variables (48) into 2 principal components that, combined, accounted for ca. 79% of the total variance of the dataset. Figure 30 shows the 2D PCA Biplot highlighting a clear discrimination among wines derived from grapes grown on different soils. By joining the information obtained by the ANOVA analysis and the PCA, it can be concluded that the most abundant compounds in each wine are those reported in Table 18.

The results obtained by the targeted analysis indicated that the soil strongly influences the chemical composition of the resulting wines. In fact, the ANOVA analysis highlighted the existence of significant differences among the metabolites' concentrations, and the PCA showed a clear separation among the different wines.

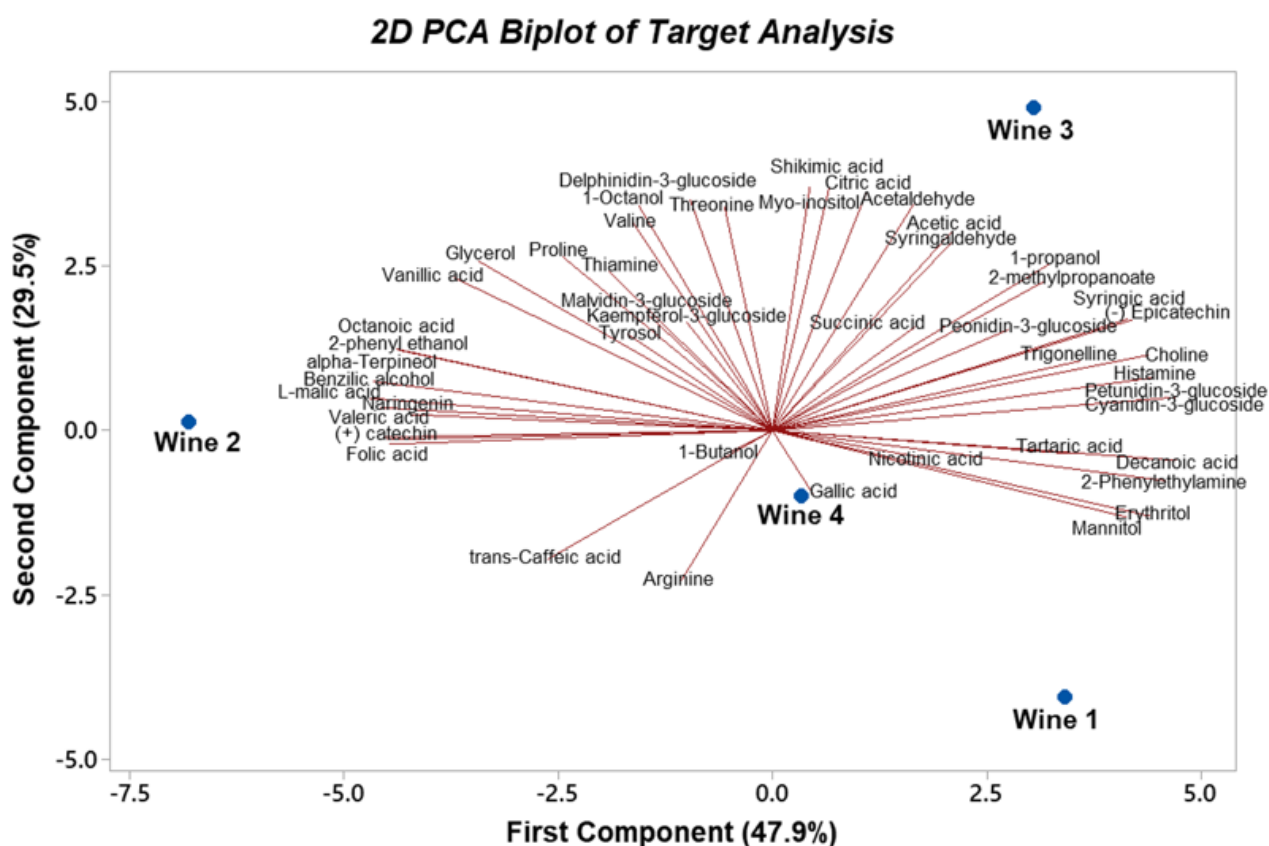


FIGURE 30. 2D PCA BIPLLOT OF DATA DERIVING FROM TARGET ANALYSIS HIGHLIGHTING A CLEAR DISCRIMINATION AMONG WINES DERIVED FROM GRAPES GROWN ON DIFFERENT SOILS.

TABLE 18. MAIN COMPOSITION OF THE FOUR WINES STUDIED IN THE PRESENT PAPER. ALL THE COMPOUNDS ARE THE MOST CONCENTRATED ONES ACCORDING TO ANOVA AND PCA INVESTIGATIONS.

Wine 1	mannitol, erythritol, octanoic acid and 2-phenylethylamine
Wine 2	glycerol, proline, L-malic acid, folic acid, valeric acid, vanillic acid, decanoic acid, α -terpineol, 2-phenyl ethanol, benzylic alcohol, tyrosol, (+) catechin, and naringenin
Wine 3	myo-inositol, threonine, valine, choline, acetic acid, succinic acid, citric acid, shikimic acid, 1-propanol, 1-octanol, 2-methylpropanoate, (-) epicatechin, peonidin-3-glucoside, cyanidin-3-glucoside, petunidin-3-glucoside, delphinidin-3-glucoside, syringic acid, histamine, syringaldehyde and acetaldehyde
Wine 4	gallic acid, arginine, tartaric acid, 1-butanol, nicotinic acid, malvidin-3-glucoside, and succinic acid

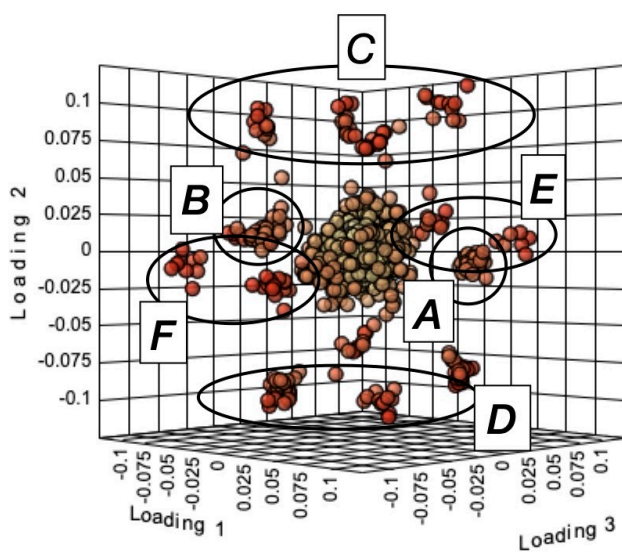
¹H-NMR SPECTRA EVALUATION: NON-TARGETED ANALYSIS

The non-targeted analysis (NTA) led to the *Nero d'Avola* wines *fingerprinting*. In particular, the principal component analysis reduced the number of original variables into three principal components, PC1, PC2 and PC3, that accounted for 100 % of the total variance. The 3D PCA loading plot is shown in Figure 31 (A). Here a differentiation among six groups of ¹H NMR signals (from Group A to Group F) is reported, according to their positive/negative contribution to each principal component. The detailed description of each group is reported in Table 19.

Figure 31 (B) shows the complementary 3D PCA scores plot revealing the separation among wine samples. Wine 2 is described by the highest positive-signed contributions to the PC1, while the negative side of the PC1 characterizes wines 1, 3 and 4. Wine 3 is located in the positive side of PC2,

while the negative side of PC2 describes mainly wine 4. The positive-signed contributions to the PC3 mainly characterizes wine 1, whereas the negative contribution to PC3 describes wines 3 and 4. In order to emphasize the separation among the analyzed wines, two different projections of the selected PCs are displayed in the 2D PCA scores plots shown in Figure 32 (A and B).

A



B

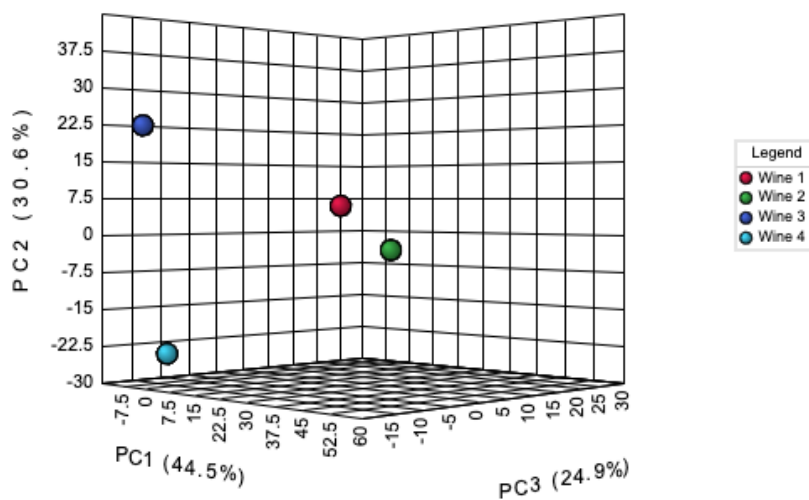


FIGURE 31. (A) 3D PCA LOADINGS PLOT OF NERO D'AVOLA SPECTRAL BUCKETS. (B) 3D PCA SCORES PLOT FOR THE SELECTED PCs. THE EXPLAINED VARIANCES ARE SHOWN IN BRACKETS.

TABLE 19. ASSIGNMENTS OF SPECTRAL REGIONS CONTRIBUTING MOSTLY TO THE NMR SPECTRA OF ALL THE WINES AS OBTAINED BY THE 3D PCA LOADING PLOT REPORTED IN FIGURE 29 (A).

Chemical shift range (in ppm)	Attributions
7.50 – 7.21, and 6.32 – 6.25	Group A. It represents the highest positive-signed contributions to the PC1. It is made by aromatic protons (both benzenic and heterocyclic). In particular, aromatic H of electron-rich systems typically resonate between 6 and 7 ppm. The ¹ H reference chemical shift value of the planar benzene is 7.25 ppm. The spectral section between 6.40 and 6.25 ppm host signals typical of H6 and H8 protons in many anthocyanins (Coletta et al., 2021), whereas the signals related to benzenic protons belonging to 2-phenyl ethanol, benzyl alcohol and vanillic acid (Figure 1) can be found between 7.50 and 7.21 ppm.
5.52 – 5.40, 3.68 – 3.66, and 2.40 – 1.22	Group B. It represents the spectral regions contributing to the negative side of the PC1. In particular, the spectral region 2.40 – 1.22 ppm contains the signals of the pure aliphatic protons belonging to 1-propanol, 1-butanol, 1-octanol, hexanoic acid, octanoic acid, valeric acid, alfa-terpineol, arginine, proline, folic acid, and acetic acid. The region between 3.66 and 3.68 ppm contains the ¹ H signals of glycerol and mannitol. Finally, the spectral region 5.40 – 5.52 ppm contains the ¹ H signals related to anthocyanins glucose moieties. In particular, this region is typical of H1'' proton in anthocyanins (Figure S3 of the Supplementary Materials).
8.30 – 8.25, and 3.63 – 3.61	Group C. It represents the ensemble of signals giving a positive contribution to PC2. The main protons resonating in the two chemical shift intervals belong to systems adjacent to electronegative nuclei (e.g., halogens, nitrogen, oxygen, and anomeric protons of sugars), aromatic moieties in electron-poor environments, glycerol and nicotinic acid.
8.87 – 8.81, 8.75 – 8.71, 8.43 – 8.41, 8.39 – 8.37, and 7.25 – 7.05	Group D. These spectral portions are typical of aromatic protons. In the 7.55-7.05 ppm interval, signals attributed to cyanidin-3-glucoside, histamine, trans-caffeic acid and tyrosol were observed; between 8.39 and 8.37 ppm a signal produced by folic acid is assigned; between 8.87 and 8.81 ppm the signal of trigonelline was found, while the signals in 8.43 – 8.41 ppm and 8.75 – 8.71 ppm intervals remained unidentified.
6.64 – 6.37	Group E. It represents the highest positive-signed contributions to the PC3, and contains the signal of shikimic acid
9.18 – 9.11, 8.78 – 8.67, 8.43 – 8.42, and 8.29 – 8.25	Group F. It represents the negative side of PC3. Trigonelline protons are attributed in the 9.18 – 9.11 ppm range, while nicotinic acid protons are located in the 8.29 – 8.25 ppm interval. The regions 8.78 – 8.67 ppm, and 8.43 – 8.42 ppm remain undefined.

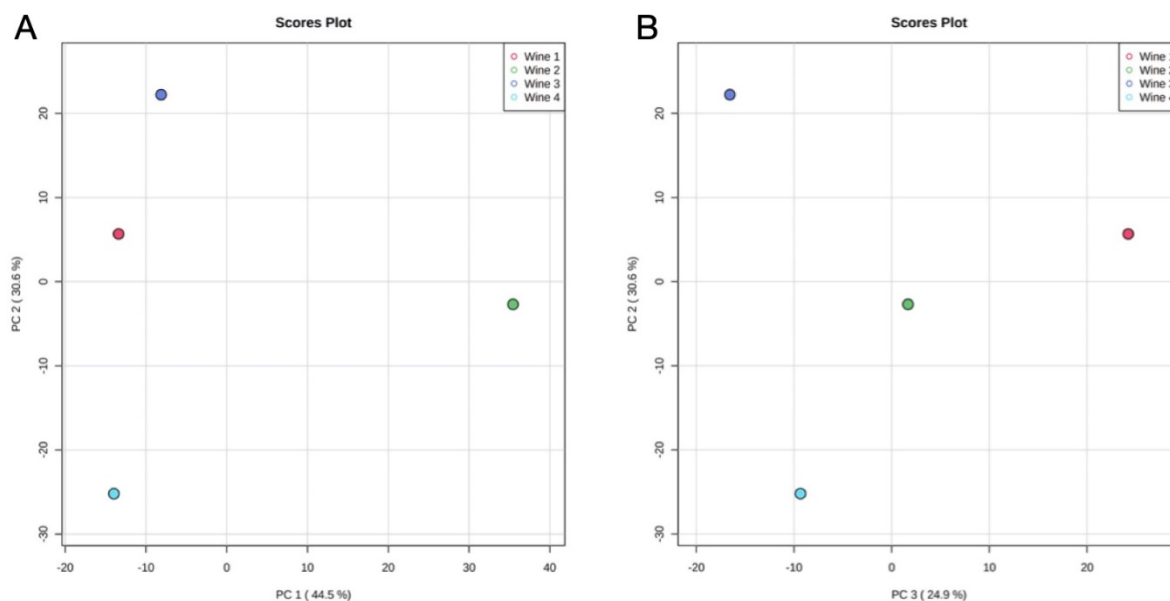


FIGURE 32. 2D PROJECTIONS OF THE SELECTED PCs.

THE H-BOND NETWORK IN WINES AS REVEALED BY THE NON-TARGETED ANALYSIS

Figure 33 reports the stacked $^1\text{H-NMR}$ spectra of the four *Nero d'Avola* wines. From a visual inspection of chemical shift dispersions, it can be observed that spectral signals differ not only in peak intensity but also in their chemical shift values. As a matter of fact, in the spectral portion hosting polyphenols (5.5-9.5 ppm), signals of wines 2 and 3 are misaligned with respect to wines 1 and 4. In particular, the signals in the spectrum of wine 2 are shifted towards higher chemical shift values, while those in the spectrum of wine 3 are shifted towards lower values. Furthermore, in the aliphatic region (0.0-3.5 ppm), signals of wines 1, 3, and 4 are aligned to each other, while signals of wine 2 are shifted towards lower chemical shift values.

Figure 34 shows the aforementioned $^1\text{H-NMR}$ chemical shift dispersion in a representative spectral portion of the aromatic (A) and the aliphatic (B) signals. The region (A) hosts the signals produced by (+) catechin, (-) epicatechin and anthocyanins. Region (B) contains signals belonging to α -

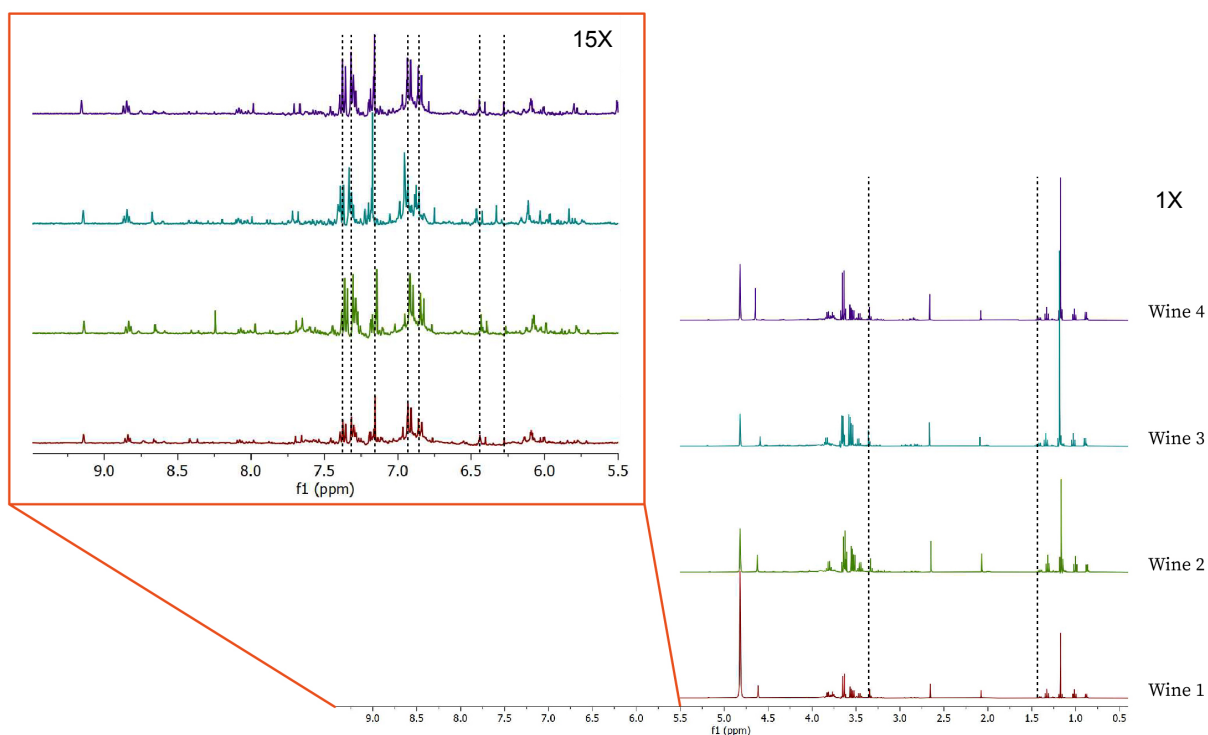


FIGURE 33. STACKED ^1H -NMR SPECTRA. DASHED LINES HIGHLIGHT THE MISALIGNMENT AMONG NERO D'AVOLA SPECTRA.

terpineol, 1-propanol, 1-octanol, hexanoic and octanoic acid. The chemical shift misalignment cannot be explained by the sole difference in wine pH values. Indeed, ^1H -NMR chemical shift is extremely sensitive to intermolecular and intramolecular interactions, such as hydrogen bonds. Some studies (del Bene, 1999, Nose et al., 2004, Charisiadis et al., 2014) highlighted the existence of a correlation between hydrogen bond strength and chemical shift values. In particular, the strengthening of the hydrogen-bonding network corresponds to the enhancement of the chemical shift values (and vice versa). The strength of hydrogen bonds depends, in turn, on the ethanol content and on the nature of dissolved solutes (Nose et al., 2004). In particular, it has been reported that the hydrogen-bonding network is strengthened by small amounts of ethanol, while it is weakened when the amount of ethanol increases (Ickes et al., 2017). Dissolved solutes provide different effects according to their chemical nature. Although the effect of acidic species depends primarily on their $\text{p}K_a$ values, they

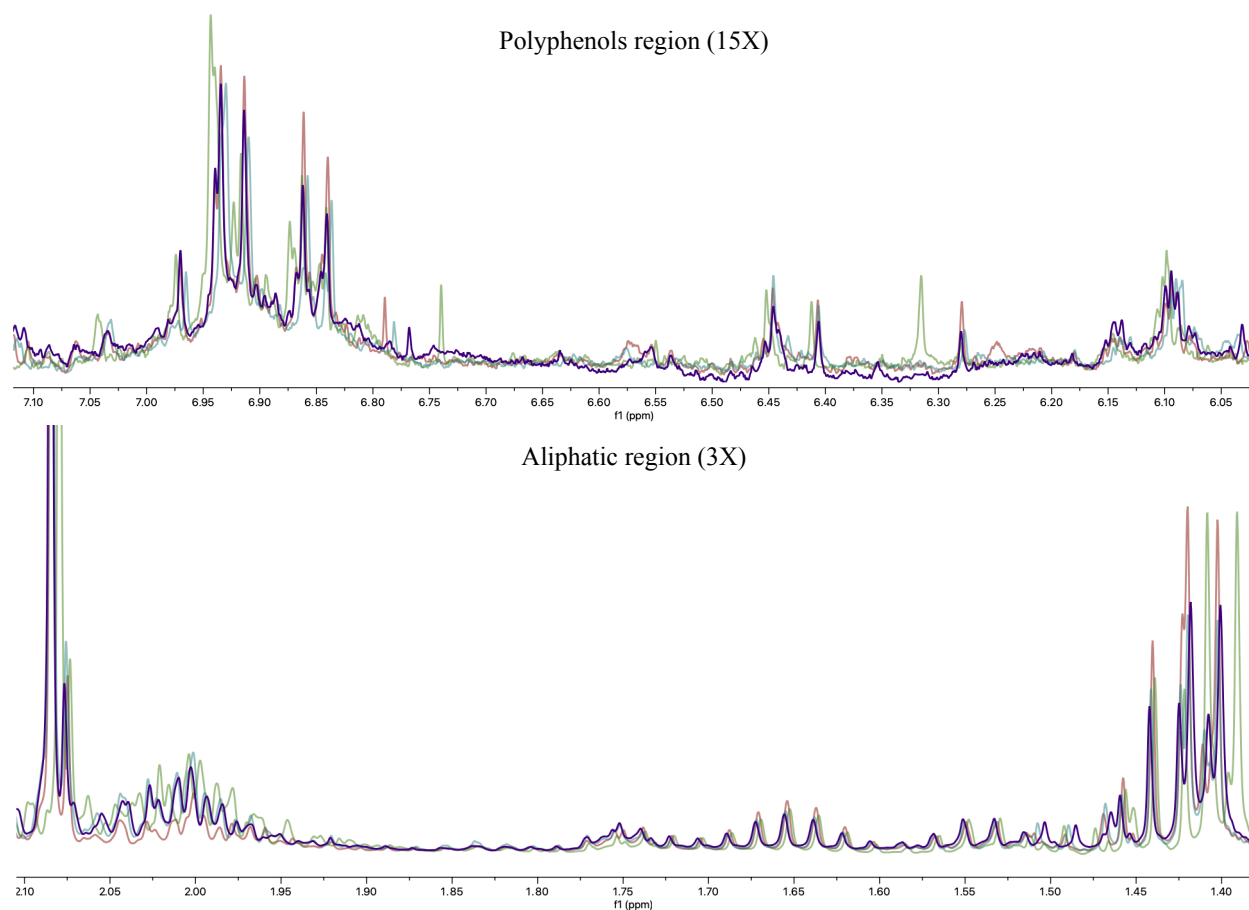


FIGURE 34. ¹H-NMR CHEMICAL SHIFT DISPERSION IN A REPRESENTATIVE SPECTRAL PORTION OF AROMATIC REGION (A) AND OF ALIPHATIC REGION (B). THE (A) REGION HOSTS THE SIGNALS PRODUCED BY (+) CATECHIN, (-) EPICATECHIN AND ANTHOCYANINS. THE (B) REGION CONTAINS SIGNALS BELONGING TO α -TERPINEOL, 1-PROPANOL, 1-OCTANOL, HEXANOIC AND OCTANOIC ACID. THE RED LINE REPRESENTS WINE 1, THE GREEN LINE REPRESENTS WINE 2, THE LIGHT BLUE LINE REPRESENTS WINE 3, AND THE PURPLE LINE REPRESENTS WINE 4.

could strengthen the water-ethanol hydrogen bonds through proton donations. Even polyphenols play a strengthening role inside the wine hydrogen bonding network. This depends on the structure of the polyphenolic compounds, and it is more effective as the -oh substitutions on the aromatic rings increase (Nose et al., 2004). conversely, higher alcohols and esters seem not to exert any measurable effect on the h-bonding structure(Ickes et al., 2017), while some inorganic anions (e.g., Cl⁻, Br⁻, NO₃⁻) are known to weaken the structure of the hydrogen bond network (Nose et al., 2004, Conte et al., 2015).

According to the abovementioned mechanisms, we can hypothesize that wines 1 and 4, with aligned spectral signals, exhibit a very similar hydrogen bonding network. Conversely, wine 2 and wine 3, with misaligned spectral signals in the polyphenolic region, can be supposed to have different

hydrogen bonding networks. In particular, in wine 2, polyphenols are involved in a stronger network of H-bond interactions (kosmotropic effect), while in wine 3 the interactions are weaker (chaotropic effect). Finally, given that in the aliphatic region the behavior of wine 2 signals is reversed, it is conceivable that aroma compounds interact weakly with the matrix, as compared to wines 1, 3, and 4. According to literature (Nose et al., 2004), changes in hydrogen-bonding structure seem to be related to modifications in wine sensorial quality, including gustatory perceptions, such as mouthfeel and taste, and olfactory perceptions (Ickes et al., 2017), that depend on aromas release. For example, oligomers of flavan-3-ols, that are responsible for astringency, can form extensive hydrogen bonds with several substrates, due to the presence of multiple benzenic hydroxyl groups (Handique et al., 2002). The complexation of flavan-3-ols with salivary glycoproteins depends on several factors, including hydrogen bonding. This means that the occurrence of the kosmotropic effect due to the presence of strong H-bonds between flavan-3-ols and other substrates inside the wine could make the benzenic hydroxyl groups less available to bind salivary glycoproteins. Therefore, the type of interactions between solvent and solutes can modulate the way how solutes interact with human sensorial receptors. This means that wines can produce different gustatory and olfactory perceptions due to different hydrogen bonding structures where solutes are involved, even if they are present at the same concentrations. However, this concept has not been fully investigated and deserves a more detailed study (Ickes et al., 2017).

The results obtained by the non-targeted ¹H-NMR-based metabolomic analysis showed that soil can strongly influence the chemical composition of the resulting wines. In fact, the multivariate statistical analysis applied on spectral buckets showed a great separation among wine samples. The differences that affect the separation among wines concern not only the intensity of the signals (which is related to the concentration of the detected analytes), but also the dispersion of the chemical shifts. The latter depends on the strength of the hydrogen bonds network in which a compound is involved. This, in turn, is affected by ethanol content and the nature of the dissolved solute. The NTA gives the opportunity to achieve a holistic characterization of a wine through the study of the chemical shift

dispersion. Investigations on hydrogen bond structure allow to consider how solvents and solutes interact with each other and lead the way for further studies concerning how hydrogen bond structure inside a wine can modulate organoleptic perceptions.

WINE-SOIL RELATIONSHIPS

The concentrations of metabolites obtained by the Targeted Analysis were processed together with the soils physical-chemical parameters, given in Table 2, to evaluate any possible relationships between wine composition and soil features. In the correlation heatmap shown in Figure 35, highly positive correlations are highlighted in red, while highly negative correlations are highlighted in blue. To better visualize the existing relationships between soil and wine, the unsupervised principal component analysis (PCA) was performed. The 2D PCA Biplot is shown in Figure 36. The first two components accounted for ca. 75% of the total variation in the dataset. Individually, PC1 and PC2 explained 43% and 31% of the total variation, respectively. All the soil parameters highly contribute to the selected PCs. In particular, the soil parameters that mostly drive the PC1 are the cation exchange capacity (CEC), the silt content, and the electric conductivity (EC). All of them stay in the positive side of the PC1. Conversely, total carbonates, pH, and clay content lead the negative side of the PC2, whereas organic matter and sand content drive mostly the positive side of PC2. From both the correlation heatmap (Figure 35) and from the spatial arrangement of the variables in the PCA Biplot (Figure 36), several correlations emerge among soil parameters and wine compositional data. They are summarized in Table 20. Even here, it can be observed the strong influence of soil texture (clay, silt, and sand) on wine chemical composition. Differences in water and nutrient availability due to different soil textures are possible explanation for the positive correlations between soil clay and silt contents and organic acids, amino acids, flavonoids and aroma compounds in wines, as well as for the negative correlations between soil sand content and polyols, flavonoids and aroma compounds. Moreover, low water and nutrient availability also determine low berry weight and high skin weight per berry (Cheng et al., 2014). Consequently, metabolites contained in berry tissues undergo to a

concentration effect. Therefore, the correlations observed in this study can be due to a combination of metabolic perturbations and concentration/dilution effects.

	Clay	Silt	Sand	Cation exchange capacity	Total carbonates	Electric conductivity	Soil pH	Organic matter
<i>Glycerol</i>	-0.04	0.74	-0.30	0.05	0.46	0.12	0.36	-0.32
<i>Mannitol</i>	-0.33	-0.94	0.64	-0.49	-0.37	-0.61	-0.36	0.16
<i>Myo-inositol</i>	-0.05	0.28	-0.09	-0.73	0.80	-0.47	0.67	-0.82
<i>Proline</i>	0.49	0.93	-0.74	0.05	0.78	0.39	0.76	-0.64
<i>Gallic acid</i>	0.95*	0.42	-0.82	0.37	0.30	0.76	0.48	-0.24
<i>Threonine</i>	0.42	0.69	-0.59	-0.39	0.96*	0.03	0.90	-0.90
<i>Valine</i>	0.41	0.82	-0.64	-0.19	0.88	0.18	0.83	-0.77
<i>Erythritol</i>	-0.12	-0.85	0.46	-0.47	-0.25	-0.49	-0.21	0.05
<i>Choline</i>	0.26	-0.36	-0.01	-0.79	0.50	-0.45	0.51	-0.66
<i>Thiamine</i>	0.66	0.93	-0.85	0.05	0.83	0.48	0.85	-0.70
<i>Arginine</i>	0.73	0.38	-0.65	0.77	-0.14	0.91	0.04	0.25
<i>Trigonelline</i>	0.62	-0.04	-0.39	-0.55	0.65	-0.08	0.71	-0.75
<i>Tartaric acid</i>	0.69	-0.12	-0.40	-0.26	0.37	0.14	0.50	-0.46
<i>Acetic acid</i>	-0.34	-0.21	0.32	-0.95	0.53	-0.82	0.39	-0.65
<i>Succinic acid</i>	-0.81	-0.58	0.80	-0.76	-0.04	-0.97*	-0.21	-0.10
<i>Citric acid</i>	-0.02	0.19	-0.07	-0.81	0.81	-0.52	0.69	-0.86
<i>L-malic acid</i>	-0.28	0.53	-0.06	0.55	-0.18	0.31	-0.24	0.35
<i>Shikimic acid</i>	-0.01	0.27	-0.12	-0.75	0.82	-0.47	0.70	-0.85
<i>Folic acid</i>	0.30	0.82	-0.57	0.80	0.01	0.79	0.05	0.21
<i>Valeric acid</i>	0.28	0.82	-0.55	0.78	0.02	0.77	0.05	0.20
<i>Vanillic acid</i>	0.03	0.80	-0.38	0.16	0.44	0.23	0.36	-0.28
<i>1-propanol</i>	0.30	-0.03	-0.18	-0.85	0.79	-0.44	0.76	-0.91
<i>1-Butanol</i>	0.98*	0.65	-0.94	0.42	0.43	0.84	0.59	-0.33
<i>1-Octanol</i>	0.25	0.73	-0.50	-0.29	0.85	0.02	0.77	-0.76
<i>Octanoic acid</i>	-0.23	0.62	-0.13	0.38	0.04	0.23	-0.04	0.12
<i>Decanoic acid</i>	0.01	-0.73	0.32	-0.63	0.02	-0.52	0.04	-0.22
<i>alpha-Terpineol</i>	-0.01	0.75	-0.34	0.57	0.05	0.48	0.01	0.15
<i>2-methylpropanoate</i>	-0.39	-0.47	0.47	-0.99*	0.36	-0.91	0.24	-0.53
<i>2-phenyl ethanol</i>	0.17	0.88	-0.51	0.49	0.26	0.54	0.23	-0.06
<i>Benzilic alcohol</i>	-0.05	0.71	-0.28	0.61	-0.03	0.48	-0.07	0.23
<i>Tyrosol</i>	-0.84	-0.12	0.61	-0.25	-0.17	-0.58	-0.34	0.16
<i>(+) catechin</i>	-0.35	0.43	0.04	0.60	-0.32	0.29	-0.38	0.48
<i>(-) Epicatechin</i>	0.23	-0.30	-0.02	-0.86	0.59	-0.51	0.58	-0.75
<i>Peonidin-3-glucoside</i>	0.03	0.75	-0.36	0.63	0.00	0.54	-0.02	0.20
<i>Cyanidin-3-glucoside</i>	-0.62	-0.98*	0.85	-0.20	-0.73	-0.57	-0.75	0.56
<i>Malvidin-3-glucoside</i>	-0.42	0.27	0.16	0.67	-0.52	0.28	-0.56	0.66
<i>Petunidin-3-glucoside</i>	0.15	-0.59	0.17	-0.67	0.20	-0.46	0.24	-0.39
<i>Delphinidin-3-glucoside</i>	0.14	-0.22	0.01	0.75	-0.74	0.54	-0.60	0.77
<i>Syringic acid</i>	-0.09	-0.50	0.28	-0.95*	0.42	-0.75	0.36	-0.61
<i>Caffeic acid</i>	-0.68	-0.24	0.56	0.54	-0.85	0.01	-0.90	0.91
<i>Nicotinic acid</i>	0.93	0.27	-0.73	0.07	0.44	0.53	0.60	-0.44
<i>Kaempferol-3-glucoside</i>	-0.86	-0.22	0.66	-0.39	-0.12	-0.70	-0.30	0.09
<i>Naringenin</i>	-0.48	0.35	0.16	0.46	-0.30	0.13	-0.39	0.44
<i>Histamine</i>	-0.25	-0.72	0.49	-0.88	0.15	-0.81	0.09	-0.36
<i>Syringaldehyde</i>	0.50	0.29	-0.46	-0.68	0.95	-0.18	0.93	-0.99*
<i>2-Phenylethylamine</i>	-0.14	-0.83	0.46	-0.60	-0.13	-0.58	-0.11	-0.08
<i>Acetaldehyde</i>	0.18	0.22	-0.22	-0.81	0.89	-0.43	0.81	-0.95

FIGURE 35. CORRELATION HEATMAP REPORTING THE PEARSON'S R COEFFICIENT FOR EACH ANALYZED VARIABLE. HIGH POSITIVE CORRELATIONS ARE HIGHLIGHTED WITH THE RED COLOR, WHILE HIGH NEGATIVE CORRELATIONS ARE INDICATED BY THE BLUE COLOR. CORRELATIONS WITH PEARSON'S R VALUES $> |\pm 0.95|$ AND $P < 0.05$ WERE CONSIDERED STATISTICALLY SIGNIFICANT AND ARE MARKED WITH *.

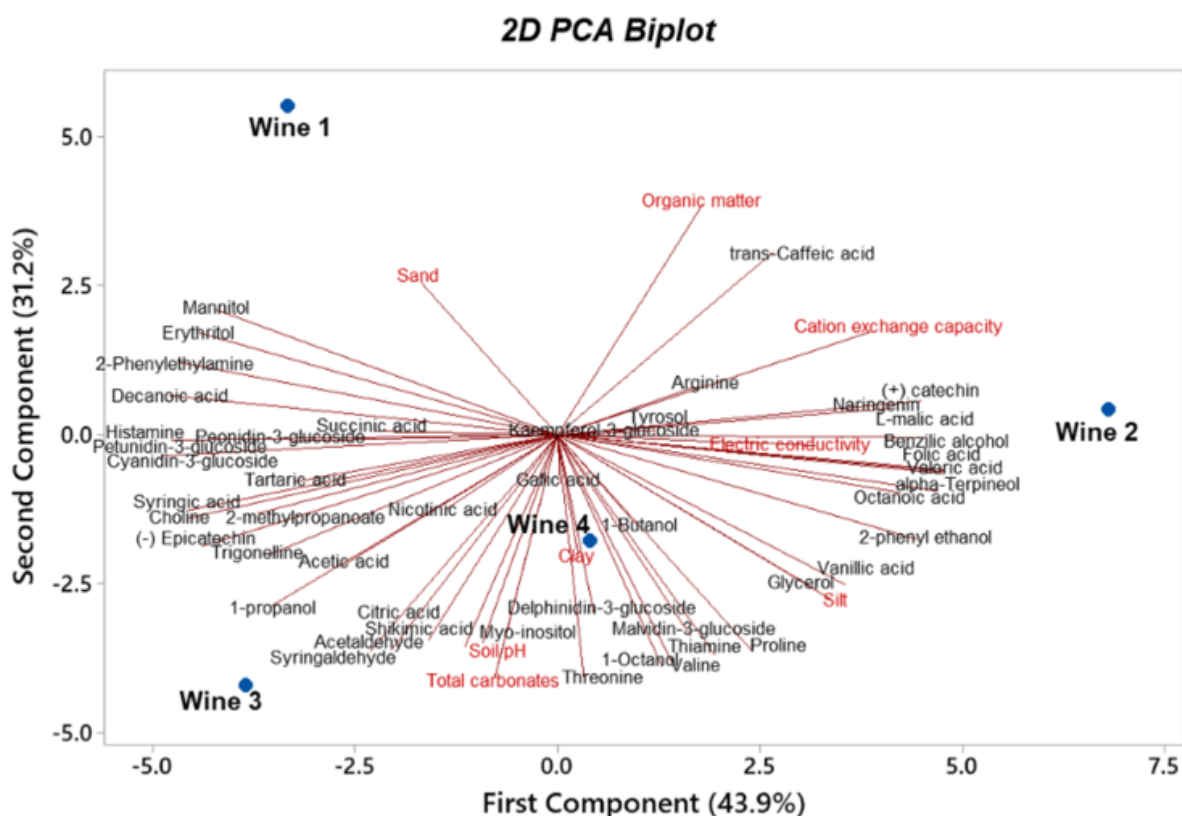


FIGURE 36. 2D PCA BIPLLOT SHOWING THE SEPARATION AMONG SAMPLES AND THE CORRELATIONS AMONG VARIABLES, AS BASED ON THE SPATIAL ARRANGEMENT OF THE VARIABLES. ADJACENT VARIABLES ARE HIGHLY POSITIVELY CORRELATED, VARIABLES ARRANGED ACCORDING TO A 180° ANGLE ARE HIGHLY NEGATIVELY CORRELATED, VARIABLES ARRANGED ACCORDING TO A 90° ANGLE ARE UNCORRELATED.

Organic matter and CEC are indicators of soil quality and productivity. Soils with high nutrient availability are known to produce vines with high vigor and excessive canopy development. The low sunlight irradiation associated with great vine vigor determines the perturbation of sunlight induced metabolic processes (Koundouras et al., 2006). This could explain the reason why organic matter and CEC share almost the same correlation pattern, and why they both negatively correlated with polyols, amino acids, organic acids, aroma compounds and flavonoids.

Electric conductivity is related to salt concentration in saline soils, whereas it depends on soil texture, moisture content, and CEC in non-saline soils (Klein et al., 2003). For this reason, its behavior in relation to wine composition is quite similar to that of CEC and organic matter.

Finally, soil pH and total carbonates, that are strictly related to each other, showed a quite opposite behavior towards wines micro-components as compared to CEC, organic matter and electric conductivity. As a matter of fact, they were positively related to amino acids, organic acids, and aroma compounds. Soil pH plays a pivotal role in soil biogeochemical processes, affecting the modulation of nutrient availability, the mineralization of organic matter, ammonia volatilization, soil enzymes activity, rhizosphere processes, dissolution and precipitation of organic matter and metals, nitrification and denitrification (Neina, 2019). Therefore, it appears likely that that the soil pH plays an important role in determining the composition of grapes and wines through the supply of key nutrients.

TABLE 20. POSITIVE/NEGATIVE CORRELATIONS BETWEEN SOIL CHEMICAL-PHYSICAL PARAMETERS AND WINE COMPONENTS

Soil chemical-physical parameters	Correlation with wine components
Clay	Positively correlated with gallic acid, and 1-butanol
Silt	Positively correlated with glycerol, proline, threonine, valine, thiamine, folic acid, valeric acid, vanillic acid, 2-phenyl ethanol, alpha-terpineol, benzyl alcohol, and petunidin-3-glucoside. Negatively correlated with mannitol, erythritol, cyanidin-3-glucoside and 2-phenylethylamine
Sand	Negatively correlated with proline, valine, arginine, gallic acid, 1-butanol, and thiamine
Cation exchange capacity (CEC)	Negatively correlated with myo-inositol, choline, acetic acid, succinic acid, citric acid, shikimic acid, 1-propanol, 2-methylpropanoate, (-) epicatechin, syringic acid, histamine, and acetaldehyde
Soil organic matter (SOM)	Negatively correlated with myo-inositol, threonine, valine, trigonelline, citric acid, shikimic acid, 1-propanol, 1-octanol, (-) epicatechin, syringaldehyde and acetaldehyde
Total carbonates, and pH	Positively correlated with threonine, valine, thiamine, citric acid, shikimic acid, 1-propanol, 1-octanol, syringaldehyde and acetaldehyde
Electric conductivity (EC)	Positively correlated with arginine and 1-butanol Negatively correlated with succinic acid, 2-methylpropanoate and histamine

APPENDIX A

TABLE A1. TOTAL FLAVONOIDS AND TOTAL ANTHOCYANINS DURING RIPENING OF NERO D'AVOLA GRAPES GROWN ON DIFFERENT SOILS IN 2020 AND 2021 VINTAGES.

2020 vintage										
<i>Vineyard 1</i>										
<i>Density classes</i>	<i>% density class</i>	<i>Skins total flavonoids (mg/100 berries)</i>			<i>Total anthocyanins (mg/100 berries)</i>			<i>Seeds total flavonoids (mg/100 berries)</i>		
<i>I</i>	0	/			/			/		
<i>II</i>	35	365	± 7	B,a,α	56	± 15	B	439	± 43	A,b, β
<i>III</i>	44	362	± 53	AB,a	66	± 19	A, α	403	± 68	AB,ab
<i>IV</i>	17	435	± 24	B,b, α	90	± 13	B,α	326	± 44	A,a
<i>V</i>	1	467	± 15	B	103	± 3	B	260	± 20	A
<i>VI</i>	3	/			/			/		
<i>Vineyard 2</i>										
<i>Density classes</i>	<i>% density class</i>	<i>Skins total flavonoids (mg/100 berries)</i>			<i>Total anthocyanins (mg/100 berries)</i>			<i>Seeds total flavonoids (mg/100 berries)</i>		
<i>I</i>	0	/			/			/		
<i>II</i>	43	244	± 20	A	35	± 5	AB,a	391	± 24	A,β
<i>III</i>	44	257	± 26	A	65	± 6	A,a	361	± 17	A,β
<i>IV</i>	7	346	± 42	A	80	± 13	B,ab,α	354	± 8	A
<i>V</i>	6	369	± 47	A	100	± 10	B,b	341	± 40	B
<i>VI</i>	0	/			/			/		

Vineyard 3

<i>Density classes</i>	<i>% density class</i>	<i>Skins total flavonoids (mg/100 berries)</i>			<i>Total anthocyanins (mg/100 berries)</i>			<i>Seeds total flavonoids (mg/100 berries)</i>			
<i>I</i>	0	/			/			/			
<i>II</i>	3	463	±	69	C,ab, β	13	±	2	A,a, α	623 ± 30	B,β
<i>III</i>	14	470	±	64	B,a, β	113	±	1	B,b	587 ± 1	C,β
<i>IV</i>	21	490	±	51	B,a, β	109	±	3	B,b	578 ± 44	B
<i>V</i>	60	532	±	40	B,ab	126	±	8	B,b	570 ± 22	C,β
<i>VI</i>	2	627	±	64	B,b	119	±	7	B,b	536 ± 41	

Vineyard 4

<i>Density classes</i>	<i>% density class</i>	<i>Skins total flavonoids (mg/100 berries)</i>			<i>Total anthocyanins (mg/100 berries)</i>			<i>Seeds total flavonoids (mg/100 berries)</i>			
<i>I</i>	0	/			/			/			
<i>II</i>	5	271	±	6	A,a, α	20	±	1	A, α	379 ± 16	A,a,β
<i>III</i>	36	350	±	23	AB,b, α	36	±	5	A,α	355 ± 23	BC,b,β
<i>IV</i>	44	349	±	9	A,b, α	44	±	10	A,α	330 ± 22	A,b, β
<i>V</i>	12	377	±	3	A,b	55	±	10	A	262 ± 18	C,b,β
<i>VI</i>	3	538	±	16	A,c	56	±	1	A	231 ± 46	c

2021 vintage

Vineyard 1

<i>Density class</i>	<i>% density class</i>	<i>Skins total flavonoids (mg/100 berries)</i>			<i>Total anthocyanins (mg/100 berries)</i>			<i>Seeds total flavonoids (mg/100 berries)</i>		
<i>I</i>	0	/			/			/		
<i>II</i>	20	407	± 4	B, a, β	109	± 6	C	277	± 17	b,α
<i>III</i>	35	449	± 16	ab	113	± 4	β	273	± 16	AB, b
<i>IV</i>	40	505	± 17	C, b, β	129	± 3	β	249	± 25	AB, ab
<i>V</i>	3	492	± 31	B, b	129	± 10		210.9	± 0.9	A, a
<i>VI</i>	2	/			/			/		

Vineyard 2

<i>Density class</i>	<i>% density class</i>	<i>Skins total flavonoids (mg/100 berries)</i>			<i>Total anthocyanins (mg/100 berries)</i>			<i>Seeds total flavonoids (mg/100 berries)</i>		
<i>I</i>	11	268	± 5	A, a	23	± 2	A, a	306	± 16	b
<i>II</i>	28	295	± 6	A, b	57	± 2	A, b	241	± 5	A, a,α
<i>III</i>	51	359	± 5	B, c	91	± 2	c	227	± 14	A, a,α
<i>IV</i>	8	450	± 4	B, d	132	3	d,β	198	± 16	a
<i>V</i>	2	/			/			/		
<i>VI</i>	0	/			/			/		

Vineyard 3

<i>Density class</i>	<i>% density class</i>	<i>Skins total flavonoids (mg/100 berries)</i>		<i>Total anthocyanins (mg/100 berries)</i>		<i>Seeds total flavonoids (mg/100 berries)</i>	
<i>I</i>	3	275 ± 3	A, a	61.6 ± 0.6	B, a	295 ± 3	a
<i>II</i>	24	313 ± 2	A, a, α	89 ± 6	B, b, β	252 ± 8	a,α
<i>III</i>	30	293 ± 18	A, a, α	101 ± 11	b	242.6 ± 0.9	B, b,α
<i>IV</i>	32	359 ± 16	A, b, α	127 ± 9	c	212.2 ± 0.3	B, b
<i>V</i>	11	389 ± 4	A, b	125.0 ± 0.3	c	221 ± 6	B, a, α
<i>VI</i>	0	/		/		/	

Vineyard 4

<i>Density class</i>	<i>% density class</i>	<i>Skins total flavonoids (mg/100 berries)</i>		<i>Total anthocyanins (mg/100 berries)</i>		<i>Seeds total flavonoids (mg/100 berries)</i>	
<i>I</i>	6	364 ± 6	B, a	69 ± 5	B, a	270 ± 36	
<i>II</i>	42	414 ± 11	B, b, β	81 ± 8	B, a, β	268 ± 31	α
<i>III</i>	40	434 ± 12	C, b, β	100 ± 0	b,β	260 ± 24	AB,α
<i>IV</i>	11	487 ± 23	B, c, β	138 ± 6	c,β	238 ± 1	A,α
<i>V</i>	1	/		/		/	
<i>VI</i>	0	/		/		/	

DIFFERENT LOWERCASE LETTERS INDICATE SIGNIFICANT DIFFERENCES AMONG DIFFERENT DENSITY CLASSES OF THE SAME VINEYARD (P<0.05). DIFFERENT UPPERCASE LETTERS INDICATE SIGNIFICANT DIFFERENCES AMONG SAME DENSITY CLASSES OF DIFFERENT VINEYARDS. DIFFERENT GREEK LETTERS INDICATE SIGNIFICANT DIFFERENCES AMONG VINTAGES.

TABLE A2. MONOMER ANTHOCYANINS PROFILE DURING RIPENING OF NERO D'AVOLA GRAPES GROWN ON DIFFERENT SOILS IN 2020 AND 2021 VINTAGES.

2020 Vintage

Vineyard 1

Density class	I	II	III	IV	V	VI
<i>Delphinidin-3-glucoside</i>	/	4.8 ± 0.1 a, C	5 ± 2 a	7.7 ± 0.1 b, B	/	/
<i>Cyanidin-3-glucoside</i>	/	0.6 ± 0.1 a	1.6 ± 0.1 b, C	2.7 ± 0.3 c, B	/	/
<i>Petunidin-3-glucoside</i>	/	6.5 ± 0.1 a, C	7 ± 1 a, B	9.4 ± 0.2 b	/	/
<i>Peonidin-3-glucoside</i>	/	3.0 ± 0.1 a, B	3.9 ± 0.3 a, B	6.0 ± 0.4 b, B	/	/
<i>Malvidin-3-glucoside</i>	/	43 ± 1 B	45 ± 2	44.5 ± 0.3	/	/
<i>Acetylated</i>	/	13.5 ± 0.2 c	8.7 ± 0.6 b, A	6.9 ± 0.3 a, A	/	/
<i>p-coumaroylated</i>	/	28.3 ± 0.9 A	28 ± 6	22.8 ± 0.5	/	/
<i>Acet./p-coum.</i>	/	0.48 ± 0.01 b	0.3 ± 0.1	0.30 ± 0.02 a, A	/	/

Vineyard 2

Density class	I	II	III	IV	V	VI
<i>Delphinidin-3-glucoside</i>	/	1.4 ± 0.1 a, A	3 ± 1 b	5.05 ± 0.05 c, B	7.3 ± 0.3 d, B	/
<i>Cyanidin-3-glucoside</i>	/	0.3 ± 0.1 a	0.3 ± 0.1 a, A	0.5 ± 0.1 a, A	0.77 ± 0.05 b	/
<i>Petunidin-3-glucoside</i>	/	3.18 ± 0.03 a, A	5 ± 1 b, A	6.55 ± 0.02 b	7.9 ± 0.1 c	/
<i>Peonidin-3-glucoside</i>	/	2.1 ± 0.5 a, A	1.9 ± 0.5 a, A	2.5 ± 0.1 a, A	3.17 ± 0.05 b	/
<i>Malvidin-3-glucoside</i>	/	35.8 ± 0.9 B	40 ± 4	44.4 ± 0.8	44 ± 1	/
<i>Acetylated</i>	/	14.8 ± 0.2	14.1 ± 0.5 B	16.93 ± 0.05 B	15.6 ± 0.2	/
<i>p-coumaroylated</i>	/	42.44 ± 0.03 b, C	36 ± 7 b	24.1 ± 0.6 a	22 ± 1 a	/
<i>Acet./p-coum.</i>	/	0.348 ± 0.004 a	0.4 ± 0.1 a	0.70 ± 0.01 b, C	0.72 ± 0.04 b	/

Vineyard 3											
Density class	I	II	III	IV	V	VI					
<i>Delphinidin-3-glucoside</i>	/	4.7 ± 0.5	a, C	6.2 ± 0.3	b	6.2 ± 0.3	b,B	6.5 ± 0.2	b,B	8.6 ± 0.3	c, B
<i>Cyanidin-3-glucoside</i>	/	0.6 ± 0.1	a	0.88 ± 0.04	ab, B	0.8 ± 0.2	ab, A	0.80 ± 0.02	ab	1.2 ± 0.2	b
<i>Petunidin-3-glucoside</i>	/	6.5 ± 0.8	a, C	7.3 ± 0.3	a, B	7.3 ± 0.3	a	7.7 ± 0.1	a	9.4 ± 0.7	b, B
<i>Peonidin-3-glucoside</i>	/	2.3 ± 0.3	a, A	3.4 ± 0.1	b, B	3.3 ± 0.6	b, A	3.1 ± 0.2	b	4.7 ± 0.7	c
<i>Malvidin-3-glucoside</i>	/	36 ± 3	B	41 ± 2		42.0 ± 0.8		43 ± 1		42 ± 3	
<i>Acetylated</i>	/	14 ± 1		13.7 ± 0.6	B	14.4 ± 0.5	B	14.4 ± 0.1		12 ± 1	
<i>p-coumaroylated</i>	/	36 ± 3	c, B	27 ± 2	b	26 ± 2	b	24.4 ± 0.7	b	18.3 ± 0.7	a
<i>Acet./p-coum.</i>	/	0.38 ± 0.01		0.51 ± 0.01		0.56 ± 0.02	B	0.59 ± 0.02		0.6 ± 0.1	

Vineyard 4											
Density class	I	II	III	IV	V	VI					
<i>Delphinidin-3-glucoside</i>	/	2.4 ± 0.1	a, B	3.2 ± 0.2	b	3.05 ± 0.03	b, A	3.9 ± 0.4	b, A	4.7 ± 0.2	c, A
<i>Cyanidin-3-glucoside</i>	/	0.4 ± 0.1		0.3 ± 0.1	A	0.4 ± 0.1	A	0.8 ± 0.2		0.9 ± 0.1	
<i>Petunidin-3-glucoside</i>	/	4.6 ± 0.1	a, B	5.3 ± 0.1	b, A	5.5 ± 0.1	b	6.9 ± 0.5	c	6.2 ± 0.3	c, A
<i>Peonidin-3-glucoside</i>	/	2.27 ± 0.03	a, A	1.9 ± 0.1	a, A	2.1 ± 0.2	a, A	3.3 ± 0.1	b	3.4 ± 0.3	b
<i>Malvidin-3-glucoside</i>	/	41.4 ± 0.4	B	44.1 ± 0.3		44.7 ± 0.2		44 ± 1		45.2 ± 0.4	
<i>Acetylated</i>	/	15.8 ± 0.9		15.6 ± 0.2	B	16.3 ± 0.4	B	15.35 ± 0.01		16 ± 1	
<i>p-coumaroylated</i>	/	33.3 ± 0.7	c, B	30 ± 1	c	28 ± 1	b	24.9 ± 0.4	a	24 ± 1	a
<i>Acet./p-coum.</i>	/	0.47 ± 0.04		0.53 ± 0.03		0.58 ± 0.04	B	0.62 ± 0.01		0.66 ± 0.04	

2021 Vintage

Vineyard 1

<i>Density class</i>	<i>I</i>	<i>II</i>	<i>III</i>	<i>IV</i>	<i>V</i>	<i>VI</i>
<i>Delphinidin-3-glucoside</i>	/	7.1 ± 0.2 C	8.2 ± 0.4 D	8.0 ± 0.5	10 ± 2	/
<i>Cyanidin-3-glucoside</i>	/	0.4 ± 0.1	0.36 ± 0.08	1.3 ± 0.9	0.9 ± 0.4	/
<i>Petunidin-3-glucoside</i>	/	6 ± 1	7 ± 1 B	7.5 ± 0.4	8.7 ± 0.2	/
<i>Peonidin-3-glucoside</i>	/	2.617 ± 0.005 a	2.80 ± 0.07 AB,ab	2.9 ± 0.4 ab	4.1 ± 0.7 b	/
<i>Malvidin-3-glucoside</i>	/	40 ± 3	38.6 ± 0.2	40 ± 1	36.8 ± 0.8 A	/
<i>Acetylated</i>	/	11 ± 3	12.3 ± 0.6	14 ± 1	15.8 ± 0.4	/
<i>p-coumaroylated</i>	/	32 ± 2 A,b	31 ± 2 A,ab	26 ± 2 ab	24 ± 2 a	/
<i>Acet./p-coum.</i>	/	0.4 ± 0.1 a	0.41 ± 0.05 a	0.53 ± 0.01 ab	0.66 ± 0.08 b	/

Vineyard 2

<i>Density class</i>	<i>I</i>	<i>II</i>	<i>III</i>	<i>IV</i>	<i>V</i>	<i>VI</i>
<i>Delphinidin-3-glucoside</i>	1.2 ± 0.1 A,a	3.00 ± 0.05 A,b	4.5 ± 0.1 A,c	5 ± 1 d	/	/
<i>Cyanidin-3-glucoside</i>	0.12 ± 0.07	0.124 ± 0.004	0.17 ± 0.01	0.6 ± 0.4	/	/
<i>Petunidin-3-glucoside</i>	1.8 ± 0.2 a	3 ± 1 a	3.7 ± 0.2 A,ab	5.4 ± 0.6 b	/	/
<i>Peonidin-3-glucoside</i>	0.97 ± 0.04 A,a	1.69 ± 0.04 b	2.3 ± 0.1 A,c	3.14 ± 0.05 d	/	/
<i>Malvidin-3-glucoside</i>	23 ± 4 A,a	33.3 ± 0.7 b	40 ± 2 b	40 ± 3 b	/	/
<i>Acetylated</i>	29 ± 8 b	13 ± 2 a	13 ± 2 a	15.2 ± 0.1 a	/	/
<i>p-coumaroylated</i>	44 ± 4 B,bc	46 ± 2 B,c	36.06 ± 0.02 B,ab	30 ± 3 a	/	/
<i>Acet./p-coum.</i>	0.7 ± 0.2	0.29 ± 0.06	0.36 ± 0.05	0.50 ± 0.04	/	/

Vineyard 3										
Density class	I		II		III		IV		V	VI
<i>Delphinidin-3-glucoside</i>	4.8 ± 0.8	C,a	5.6 ± 0.3	B,a	6.9 ± 0.2	C,a	7 ± 1	a	11 ± 1	b /
<i>Cyanidin-3-glucoside</i>	0.25 ± 0.07		0.335 ± 0.006		0.6 ± 0.3		1.0 ± 0.2		1.1 ± 0.4	/
<i>Petunidin-3-glucoside</i>	5 ± 2	a	5.0 ± 0.1	ab	6.0 ± 0.8	AB,ab	7.3 ± 0.3	ab	10 ± 1	b /
<i>Peonidin-3-glucoside</i>	3.3 ± 0.8	B	2.6 ± 0.4		3.5 ± 0.4	B	3.4 ± 0.1		4.12 ± 0.07	/
<i>Malvidin-3-glucoside</i>	41 ± 2	B	42 ± 2		43 ± 2		42 ± 1		40.2 ± 0.6	B /
<i>Acetylated</i>	12 ± 4		13 ± 2		11.1 ± 0.7		13 ± 3		12 ± 3	/
<i>p-coumaroylated</i>	33 ± 1	A,b	32 ± 4	A,b	28.9 ± 0.3	A,ab	26 ± 2	ab	22 ± 2	a /
<i>Acet./p-coum.</i>	0.4 ± 0.1		0.40 ± 0.11		0.39 ± 0.02		0.53 ± 0.17		0.54 ± 0.17	/
Vineyard 4										
Density class	I		II		III		IV		V	VI
<i>Delphinidin-3-glucoside</i>	3.3 ± 0.2	B,a	3.7 ± 0.3	A,a	5.69 ± 0.04	B,b	6.2 ± 0.3	b	/	/
<i>Cyanidin-3-glucoside</i>	0.19 ± 0.09		0.485 ± 0.441		0.24 ± 0.01		0.4 ± 0.1		/	/
<i>Petunidin-3-glucoside</i>	2.5 ± 0.3	a	5 ± 1	b	5.1 ± 0.2	AB,b	5.9 ± 0.8	b	/	/
<i>Peonidin-3-glucoside</i>	1.96 ± 0.16	AB	2.37 ± 0.74		2.7 ± 0.4	AB	2.94 ± 0.15		/	/
<i>Malvidin-3-glucoside</i>	35 ± 1	B,a	36.3 ± 3.5	a	40 ± 0.002	ab	42 ± 0.461	b	/	/
<i>Acetylated</i>	12 ± 4		17 ± 3		15 ± 2		14.1 ± 2.0		/	/
<i>p-coumaroylated</i>	45 ± 3	B,b	36 ± 2	A,a	30.94 ± 1.32	A,a	28 ± 2	a	/	/
<i>Acet./p-coum.</i>	0.3 ± 0.1		0.5 ± 0.1		0.5 ± 0.1		0.5 ± 0.1		/	/

DIFFERENT LOWERCASE LETTERS INDICATE SIGNIFICANT DIFFERENCES AMONG DIFFERENT DENSITY CLASSES OF THE SAME VINEYARD (P<0.05). DIFFERENT UPPERCASE LETTERS INDICATE SIGNIFICANT DIFFERENCES AMONG SAME DENSITY CLASSES OF DIFFERENT VINEYARDS. DIFFERENT GREEK LETTERS INDICATE SIGNIFICANT DIFFERENCES AMONG VINTAGES.

TABLE A3. HCTA CONTENT DURING RIPENING OF NERO D'AVOLA GRAPES GROWN ON DIFFERENT SOILS IN 2020 AND 2021 VINTAGES.

2020 vintage

Vineyard 1

Density class	I	II	III	IV	V	VI			
<i>c-CaffeoylTar</i>	/	21 ± 3	b, A, β	1.0 ± 0.1	a, A	0.8 ± 0.2	a	/	/
<i>t-Caffeoyl Tar</i>	/	163 ± 19	c, B, α	40.0 ± 0.6	b, B, α	26.0 ± 0.1	a, C, α	/	/
<i>c-pCumaroyl Tar</i>	/	23 ± 8	b, A, α	3.2 ± 0.5	a, α	2.9 ± 0.4	a, A, α	/	/
<i>t-pCumaroyl Tar</i>	/	44 ± 8	b, C, α	1.9 ± 0.2	a, α	1.2 ± 0.2	a, A, α	/	/
<i>t-Feruloyl Tar</i>	/	5 ± 4	b, A, α	0.7 ± 0.3	a, α	0.6 ± 0.1	a, A, α	/	/

Vineyard 2

Density class	I	II	III	IV	V	VI				
<i>c-CaffeoylTar</i>	/	18.5 ± 0.5	b, A, β	4.6 ± 1	a, A, β	4.0 ± 0.4	a, β	5.9 ± 0.5	a	/
<i>t-Caffeoyl Tar</i>	/	78 ± 13	c, A, α	31 ± 7	b, A, α	18.2 ± 0.1	a, A, α	32 ± 2	b, B	/
<i>c-pCumaroyl Tar</i>	/	32 ± 7	b, A	11 ± 5	a	7.2 ± 0.1	a, B, α	10.3 ± 0.1	a	/
<i>t-pCumaroyl Tar</i>	/	24 ± 2	b, A	10 ± 4	a	5.8 ± 0.4	a, B	5.9 ± 0.6	a, A	/
<i>t-Feruloyl Tar</i>	/	27.8 ± 0.9	b, B, β	14 ± 7	a	10.7 ± 0.9	a, B	19 ± 5	a, B	/

Vineyard 3

Density class	I	II	III	IV	V	VI					
<i>c-CaffeoylTar</i>	/	23 ± 2	b, A, β	3.7 ± 0.2	a, A, β	1.3 ± 0.2	a, β	3 ± 2	a, β	3.4 ± 0.1	a
<i>t-Caffeoyl Tar</i>	/	167 ± 15	e, B, α	77 ± 8	d, C, α	22 ± 1	a, B, α	31 ± 3	b, B, α	43.1 ± 0.3	c
<i>c-pCumaroyl Tar</i>	/	42 ± 6	c, B, α	18 ± 1	b, α	7 ± 2	a, B	9 ± 1	a	8.3 ± 0.2	a
<i>t-pCumaroyl Tar</i>	/	32 ± 2	c, B, α	18 ± 2	b, α	4.3 ± 0.9	a, B, α	4.5 ± 0.8	a, A, α	3.1 ± 0.2	a
<i>t-Feruloyl Tar</i>	/	37 ± 3	d, C, α	20 ± 2	c, α	7 ± 1	a, B	14 ± 2	b, B	7.6 ± 0.6	a

Vineyard 4											
Density class	<i>I</i>	<i>II</i>		<i>III</i>		<i>IV</i>		<i>V</i>		<i>VI</i>	
<i>c-Caffeoyl Tar</i>	/	46 ± 6	c, B, β	20 ± 6	b, B, β	12 ± 9	a, β	5.1 ± 0.1	a, β	BDL	a
<i>t-Caffeoyl Tar</i>	/	134 ± 6	e, C	67 ± 14	d, C	21 ± 1	b, B	16 ± 1	a, A	34 ± 8	c
<i>c-pCumaroyl Tar</i>	/	60 ± 4	c, C	50 ± 22	c, β	19 ± 2	b, C, β	6 ± 8	a	23 ± 1	b
<i>t-pCumaroyl Tar</i>	/	46 ± 2	c, C, α	27 ± 7	b, α	11.5 ± 0.9	a, C, α	8 ± 1	a, B	16 ± 8	b
<i>t-Feruloyl Tar</i>	/	51 ± 3	b, D, β	17 ± 2	a, β	12 ± 3	a, B, β	8.3 ± 0.9	a, A	11 ± 5	a

2021 vintage

Vineyard 1											
Density class	<i>I</i>	<i>II</i>		<i>III</i>		<i>IV</i>		<i>V</i>		<i>VI</i>	
<i>c-Caffeoyl Tar</i>	/		3 ± 2	a, α	2.1 ± 0.4	a	1.8 ± 0.3	a	1.4 ± 0.4	a	/
<i>t-Caffeoyl Tar</i>	/		1025 ± 116	b, B, β	400 ± 8	a, B, β	322 ± 13	a, D, β	307 ± 71	a	/
<i>c-pCumaroyl Tar</i>	/		65 ± 7	c, C, β	61 ± 2	c, C, β	45.2 ± 0.4	a, B, β	54 ± 3	b, B	/
<i>t-pCumaroyl Tar</i>	/		138 ± 15	a, B, β	161 ± 7	b, C, β	121.2 ± 3.3	a, B, β	132 ± 13	a, B	/
<i>t-Feruloyl Tar</i>	/		26 ± 16	b, B, β	16.9 ± 0.6	b, B, β	5 ± 1	a, β	8 ± 2	a	/

Vineyard 2											
Density class	<i>I</i>	<i>II</i>		<i>III</i>		<i>IV</i>		<i>V</i>		<i>VI</i>	
<i>c-Caffeoyl Tar</i>	BDL		2.9 ± 0.2	b, α	1.9 ± 0.2	b, α	2.0 ± 0.3	b, α	/	/	/
<i>t-Caffeoyl Tar</i>	764 ± 68	d, A	448 ± 13	c, A, β	311 ± 31	b, A, β	209.8 ± 0.4	a, B, β	/	/	/
<i>c-pCumaroyl Tar</i>	30 ± 6	d	20 ± 1	c, A	16 ± 1	b, A	11.6463 ± 0.0004	a, A, β	/	/	/
<i>t-pCumaroyl Tar</i>	112 ± 19	d	86 ± 4	c, A, β	64 ± 7	b, A, β	41 ± 2	a, A, β	/	/	/
<i>t-Feruloyl Tar</i>	12 ± 5	b	14.19 ± 0.02	b, A, α	14.8 ± 0.2	b, B	7.2 ± 0.5	a	/	/	/

Vineyard 3

<i>Density class</i>	<i>I</i>		<i>II</i>		<i>III</i>		<i>IV</i>		<i>V</i>		<i>VI</i>
<i>c-Caffeoyl Tar</i>	BDL		BDL		BDL		0.5 ± 0.7		BDL		/
<i>t-Caffeoyl Tar</i>	1387 ± 8	c, B, β	1148 ± 17	bc, B, β	905 ± 7	b, C, β	247 ± 5	a, C, β	273 ± 48	a, β	/
<i>c-pCumaroyl Tar</i>	41 ± 9	b	70 ± 1	c, C, β	58 ± 6	b, C, β	11.6 ± 0.7	a, A	10 ± 1	a, A	/
<i>t-pCumaroyl Tar</i>	273 ± 16	c	273 ± 7	c, C, β	218 ± 28	b, C, β	54 ± 1	a, A, β	59 ± 6	a, A, β	/
<i>t-Feruloyl Tar</i>	9 ± 3		12.9 ± 0.1	A, β	12.7 ± 0.7	B, β	6 ± 3		12.5 ± 0.5		/

Vineyard 4

<i>Density class</i>	<i>I</i>		<i>II</i>		<i>III</i>		<i>IV</i>		<i>V</i>		<i>VI</i>
<i>c-Caffeoyl Tar</i>	BDL		BDL		2.1 ± 0.4	b, α	0.8 ± 0.1	a, α	/		/
<i>t-Caffeoyl Tar</i>	838 ± 55	b, A	563 ± 12	b, A, β	348 ± 7	b, A, β	146 ± 22	a, A, β	/		/
<i>c-pCumaroyl Tar</i>	71 ± 5	d	48.2 ± 6	c, B	22.3 ± 0.2	b, B, α	8.3 ± 0.5	a, A, α	/		/
<i>t-pCumaroyl Tar</i>	282 ± 16	d	197 ± 20	c, B, β	101 ± 5	b, B, β	39.3 ± 0.1	a, A, β	/		/
<i>t-Feruloyl Tar</i>	11 ± 2	b	15.0 ± 0.5	c, A, α	2.0 ± 0.1	a, A, α	4 ± 1	a, α	/		/

DIFFERENT LOWERCASE LETTERS INDICATE SIGNIFICANT DIFFERENCES AMONG DIFFERENT DENSITY CLASSES OF THE SAME VINEYARD (P<0.05). DIFFERENT UPPERCASE LETTERS INDICATE SIGNIFICANT DIFFERENCES AMONG SAME DENSITY CLASSES OF DIFFERENT VINEYARDS. DIFFERENT GREEK LETTERS INDICATE SIGNIFICANT DIFFERENCES AMONG VINTAGES.

TABLE A4. FLAVONOLS CONTENT DURING RIPENING OF NERO D'AVOLA GRAPES GROWN ON DIFFERENT SOILS IN 2020 AND 2021 VINTAGES.

2020 Vintage

Vineyard 1

Density class	I	II	III	IV	V	VI
<i>Myricetin 3-glucuronide</i>	/	8.5 ± 0.5 C	BDL	BDL	/	/
<i>Myricetin 3-glucoside</i>	/	3.9 ± 0.4 A, α	10 ± 3 B, α	7.8 ± 0.2 D	/	/
<i>Quercetin 3-glucuronide</i>	/	51 ± 4 B, α	65 ± 7 C, α	45 ± 2 C, α	/	/
<i>Quercetin 3-glucoside</i>	/	95 ± 10 b, C, α	86 ± 3 b, B, α	44 ± 3 a, D, α	/	/
<i>Isorhamnetin-3-glucoside</i>	/	95 ± 16 b, B, α	114 ± 16 b, C, α	66 ± 4 a, C	/	/
<i>Laricitrin-3-glucoside</i>	/	39 ± 2 b, D, α	2.6 ± 0.5 a, A, α	1.7 ± 0.0 a, A, α	/	/
<i>kaempferol-3-glucuronide</i>	/	17 ± 2 b, C, α	6 ± 1 a	3.6 ± 0.2 a, B	/	/
<i>kaempferol-3-glucoside</i>	/	6.6 ± 0.6 a, B, α	5.6 ± 0.9 a, A, α	9 ± 1 b, B, α	/	/
<i>Syringetin 3-glucoside</i>	/	18.4 ± 0.5 B	15 ± 9	12.7 ± 0.3 C, β	/	/

Vineyard 2

Density class	I	II	III	IV	V	VI
<i>Myricetin 3-glucuronide</i>	/	2.2 ± 0.3 A	3 ± 2	BDL	3.4 ± 0.4 C	/
<i>Myricetin 3-glucoside</i>	/	9.9 ± 0.4 c, B, β	8.5 ± 0.4 c, B	4.11 ± 0.08 b, C	1.675 ± 0.001 a, B	/
<i>Quercetin 3-glucuronide</i>	/	39 ± 12 b, B, α	19 ± 2 a, A, α	23 ± 2 a, B, α	35 ± 5 b, B	/
<i>Quercetin 3-glucoside</i>	/	33.4 ± 0.6 A, α	27 ± 9 A, α	22 ± 4 C	22 ± 1 B	/
<i>Isorhamnetin-3-glucoside</i>	/	54 ± 16 c, A, α	44 ± 4 c, B	25 ± 4 a, B	32 ± 2 b, C	/
<i>Laricitrin-3-glucoside</i>	/	18 ± 3 c, B	15 ± 1 b, B, α	9 ± 1 a, C	15 ± 1 b, C	/
<i>kaempferol-3-glucuronide</i>	/	10 ± 3 c, B, β	4.0 ± 0.4 b	1.7 ± 0.2 a, A	4.4 ± 0.6 b, B	/
<i>kaempferol-3-glucoside</i>	/	2.2 ± 0.4 A, α	2.5 ± 0.5 A	3.2 ± 0.6 A	2.4 ± 0.1	/
<i>Syringetin 3-glucoside</i>	/	15.3 ± 0.3 b, B, β	10 ± 3 a	8.03 ± 0.03 a, B, β	8.3 ± 0.8 a, B	/

Vineyard 3

<i>Density class</i>	<i>I</i>	<i>II</i>	<i>III</i>	<i>IV</i>	<i>V</i>	<i>VI</i>
<i>Myricetin 3-glucuronide</i>	/	6.2 ± 0.3 c, B	3.43 ± 0.05 b	1.0 ± 0.2 a	0.9 ± 0.1 a, A	/
<i>Myricetin 3-glucoside</i>	/	3.6 ± 0.6 c, A, α	1.4 ± 0.1 b, α , A	0.4 ± 0.2 a, A, α	BDL	/
<i>Quercetin 3-glucuronide</i>	/	64 ± 6 c, C, α	34 ± 7 b, B, α	7.4 ± 0.6 a, A, α	7.8 ± 0.5 a, A, α	/
<i>Quercetin 3-glucoside</i>	/	56 ± 12 d, B, α	32 ± 7 A, c, α	11.6 ± 0.2 b, A α	7.56 ± 0.05 a, A, α	/
<i>Isorhamnetin-3-glucoside</i>	/	55 ± 4 d, A, α	28 ± 1 c, A, α	12.1 ± 0.4 b, A, α	7.0 ± 0.9 a, A, α	/
<i>Laricitrin-3-glucoside</i>	/	29 ± 5 c, C, α	16 ± 2 b, B, α	4.5 ± 0.5 a, B	3.65 ± 0.06 a, A, α	/
<i>kaempferol-3-glucuronide</i>	/	7.2 ± 0.8 c, B, α	3.837 ± 0.005 b	1.67 ± 0.01 a, A	1.3 ± 0.3 a, A	/
<i>kaempferol-3-glucoside</i>	/	18 ± 2 c, C, α	10.1 ± 0.5 b, B, α	1.7 ± 0.4 a, A, α	1.1 ± 0.5 a, α	/
<i>Syringetin 3-glucoside</i>	/	22 ± 1 d, C, α	10 ± 1 c	3.7 ± 0.2 b, A	1.7 ± 0.3 a, A, α	/

Vineyard 4

<i>Density class</i>	<i>I</i>	<i>II</i>	<i>III</i>	<i>IV</i>	<i>V</i>	<i>VI</i>
<i>Myricetin 3-glucuronide</i>	/	5.5 ± 0.6 c, B	2.7 ± 0.3 b	1.35 ± 0.05 a	2.1 ± 0.2 b, B	0.8 ± 0.3 a
<i>Myricetin 3-glucoside</i>	/	BDL	1.8 ± 0.3 b, A	1.1 ± 0.4 a, B	0.8 ± 0.1 a, A	0.58 ± 0.05 a
<i>Quercetin 3-glucuronide</i>	/	25 ± 1 d, A, α	17 ± 2 c, A, α	4.5 ± 0.8 a, A, α	8 ± 1 b, A	3 ± 1 a
<i>Quercetin 3-glucoside</i>	/	85 ± 9 d, C, α	34 ± 4 c, A	16 ± 2 b, B, α	21 ± 4 b, B	9 ± 1 a
<i>Isorhamnetin-3-glucoside</i>	/	60 ± 5 d, A, β	28 ± 4 c, A	13 ± 2 a, A	22 ± 1 b, B	8 ± 2 a
<i>Laricitrin-3-glucoside</i>	/	10.8 ± 0.2 c, A, α	12 ± 1 c, B, β	5.8 ± 0.1 a, B	8 ± 1 b, B	3 ± 1 a
<i>kaempferol-3-glucuronide</i>	/	0.9 ± 0.2 a, A	3.6 ± 0.7 b, A	1.9 ± 0.5 a, A	3.8 ± 0.4 b, B	1.3 ± 0.6 a
<i>kaempferol-3-glucoside</i>	/	2.0 ± 0.1 A	1 ± 1 α	BDL	BDL	BDL
<i>Syringetin 3-glucoside</i>	/	10.35 ± 0.03 c, A, β	7.6 ± 0.6 b, β	4.64 ± 0.09 a, A	8 ± 2 b, B	4 ± 1 a

2021 vintage

Vineyard 1

Density class	I	II	III	IV	V	VI
<i>Myricetin 3-glucuronide</i>	/	BDL	BDL	BDL	BDL	/
<i>Myricetin 3-glucoside</i>	/	31.3 ± 0.6 c, D, β	18 ± 4 b, D, β	8.1 ± 0.2 a, C	8 ± 1 a	/
<i>Quercetin 3-glucuronide</i>	/	290 ± 20 c, C, β	173 ± 35 C, β	75 ± 3 a, B, β	70 ± 3 a	/
<i>Quercetin 3-glucoside</i>	/	271 ± 2 d, C, β	137 ± 12 c, B, β	63 ± 3 b, C, β	46 ± 4 a, A	/
<i>Isorhamnetin-3-glucoside</i>	/	265 ± 39 c, C, β	150 ± 11 b, C, β	70 ± 7 a, C	57 ± 10 a	/
<i>Laricitrin-3-glucoside</i>	/	63 ± 1 c, D, β	45 ± 4 b, C, β	17.2 ± 0.8 a, B, β	14 ± 4 a	/
<i>kaempferol-3-glucuronide</i>	/	18.8 ± 0.2 c, C	10 ± 2 b, C	5.0 ± 0.3 a	3.3 ± 0.6 a	/
<i>kaempferol-3-glucoside</i>	/	43 ± 4 c, C, β	22 ± 5 b, B, β	11 ± 1 a, B	9 ± 1 a	/
<i>Syringetin 3-glucoside</i>	/	19.7 ± 0.2 b, D	14.5 ± 0.7 b, C	5.6 ± 0.7 a, α	5.1 ± 0.6 a	/

Vineyard 2

Density class	I	II	III	IV	V	VI
<i>Myricetin 3-glucuronide</i>	BDL	BDL	BDL	BDL	/	/
<i>Myricetin 3-glucoside</i>	0.87 ± 0.06 a, A	4 ± 3 b, A	3.7 ± 0.5 b, A	2.56 ± 0.07 b, A	/	/
<i>Quercetin 3-glucuronide</i>	10.4 ± 0.2 a, A	74 ± 9 d, A, β	43 ± 3 c, A, β	36.6 ± 0.9 b, A, β	/	/
<i>Quercetin 3-glucoside</i>	14 ± 1 a, A	77 ± 11 c, A, β	40 ± 4 b, A, β	14 ± 3 a, A, α	/	/
<i>Isorhamnetin-3-glucoside</i>	5.7 ± 0.2 a, B	66 ± 4 d, B	40 ± 4 c, A	23 ± 6 b, A	/	/
<i>Laricitrin-3-glucoside</i>	2.47 ± 0.02 a, A	21 ± 3 b, B	15 ± 3 b, A	9 ± 2 b, A	/	/
<i>kaempferol-3-glucuronide</i>	BDL	4.3 ± 0.5 c, B	2.6 ± 0.6 b, A	1.0 ± 0.4 a	/	/
<i>kaempferol-3-glucoside</i>	0.1 ± 0.2 a, A	7 ± 1 c, B, β	5 ± 1 b, A	3 ± 2 b, A	/	/
<i>Syringetin 3-glucoside</i>	0.38 ± 0.04 a, A	4 ± 1 c, B, α	4.0 ± 0.6 c, A	1.5 ± 0.5 b, α	/	/

Vineyard 3

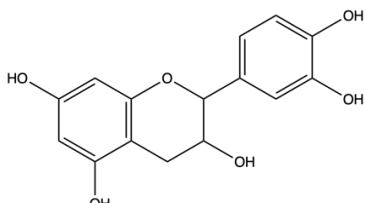
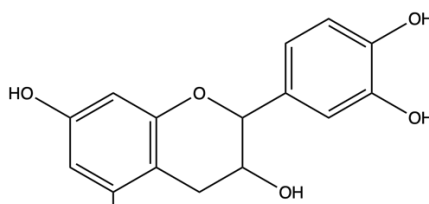
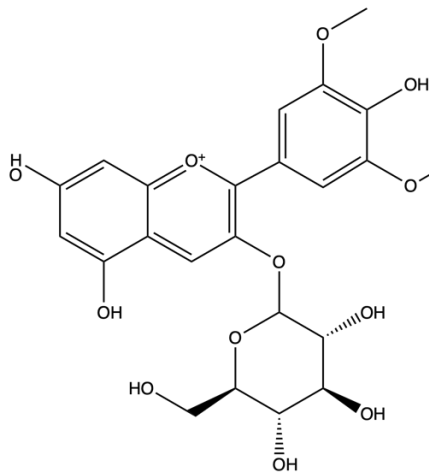
<i>Density class</i>	<i>I</i>		<i>II</i>		<i>III</i>		<i>IV</i>		<i>V</i>		<i>VI</i>
<i>Myricetin 3-glucuronide</i>	BDL		BDL		BDL		BDL		BDL		/
<i>Myricetin 3-glucoside</i>	19 ± 7	c, B	23 ± 4	c, C, β	11 ± 1	b, C, β	5 ± 1	a, B, β	6.5 ± 0.6	a	/
<i>Quercetin 3-glucuronide</i>	143 ± 25	c, C	151 ± 22	c, B, β	88 ± 20	b, B, β	44 ± 11	a, A, β	63 ± 8	b, β	/
<i>Quercetin 3-glucoside</i>	348 ± 36	d, C	293 ± 51	d, C, β	123 ± 4	c, B, β	67.9 ± 0.7	b, C, β	56.4 ± 0.1	a, B, β	/
<i>Isorhamnetin-3-glucoside</i>	312.5 ± 0.2	c, C	292 ± 11	c, C, β	107 ± 19	b, B, β	50 ± 20	a, B, β	41 ± 6	a, β	/
<i>Laricitrin-3-glucoside</i>	41 ± 9	c, C	51 ± 5	c, C, β	25 ± 3	b, B	10 ± 6	a, A	12 ± 3	a, β	/
<i>kaempferol-3-glucuronide</i>	15.9 ± 0.7	c, B	15 ± 2	c, C, β	7 ± 2	b, C	3 ± 2	a	3 ± 1	a	/
<i>kaempferol-3-glucoside</i>	45 ± 3	c, C	42 ± 7	c, C, β	18 ± 5	b, B, β	8 ± 4	a, A, β	8 ± 4	a, β	/
<i>Syringetin 3-glucoside</i>	12 ± 3	c, C	16 ± 1	c, C	8 ± 2	b, B	3 ± 2	a	6.1 ± 0.1	b, β	/

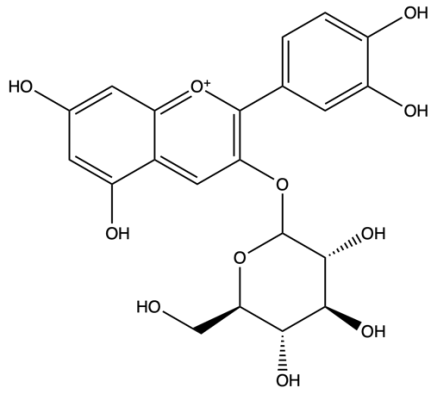
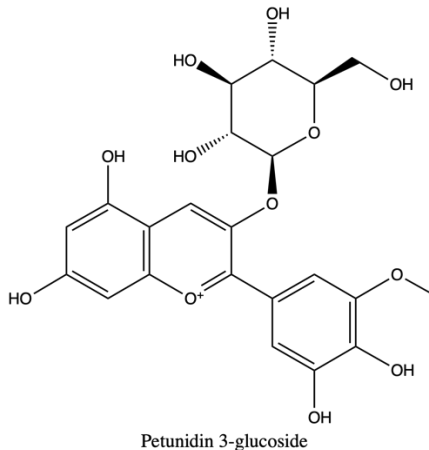
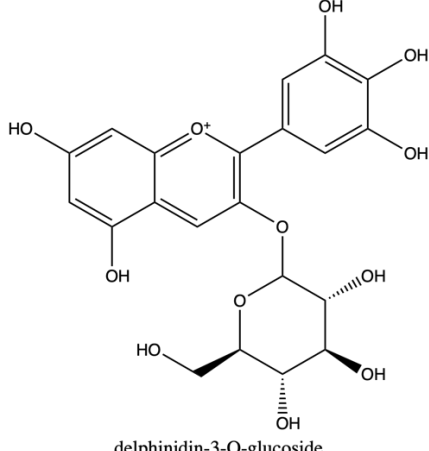
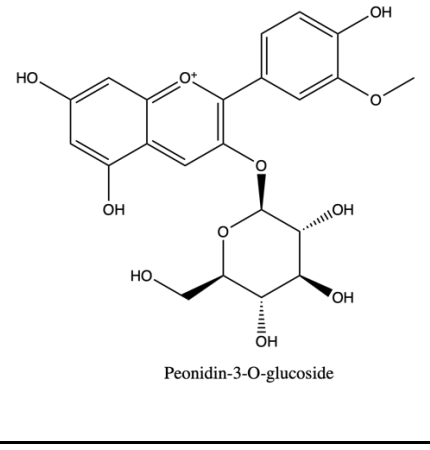
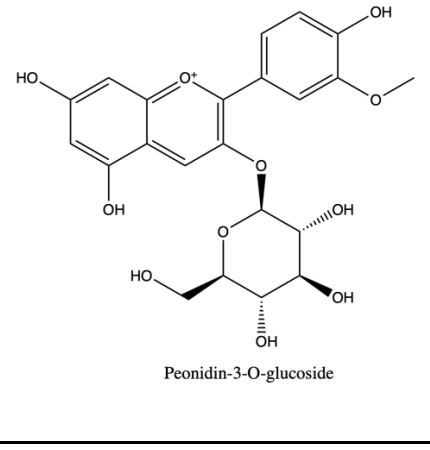
Vineyard 4

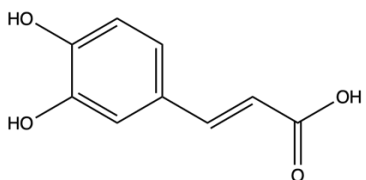
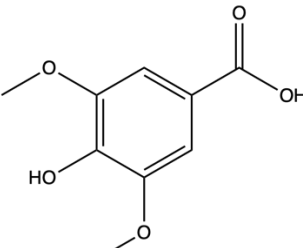
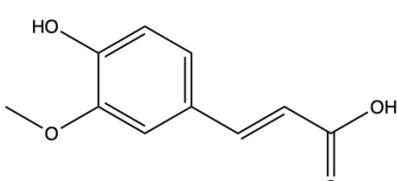
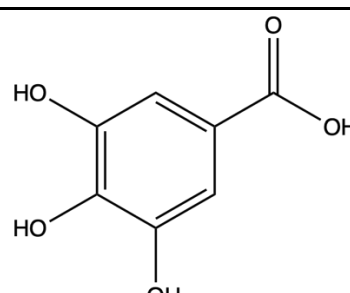
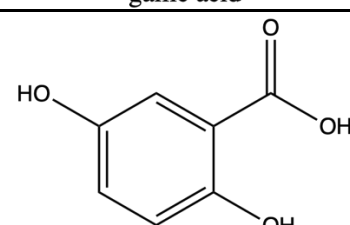
<i>Density class</i>	<i>I</i>		<i>II</i>		<i>III</i>		<i>IV</i>		<i>V</i>	<i>VI</i>
<i>Myricetin 3-glucuronide</i>	BDL		BDL		BDL		BDL		/	/
<i>Myricetin 3-glucoside</i>	12 ± 3	c, B	11 ± 2	c, B, β	5.06 ± 0.01	b, B, β	2.6 ± 0.9	a, A, β	/	/
<i>Quercetin 3-glucuronide</i>	100 ± 7	c, B	87 ± 8	b, A, β	41 ± 3	a, A, β	32 ± 6	a, A, β	/	/
<i>Quercetin 3-glucoside</i>	141 ± 2	d, B	112 ± 3	c, B, β	43 ± 4	b, A	27 ± 3	a, B, β	/	/
<i>Isorhamnetin-3-glucoside</i>	121 ± 9	c, B	21 ± 6	a, A, α	36 ± 1	b, A	17 ± 10	a, A	/	/
<i>Laricitrin-3-glucoside</i>	22.0 ± 0.8	c, B	10 ± 1	a, A	16.7 ± 0.5	b, A	10 ± 3	a, A	/	/
<i>kaempferol-3-glucuronide</i>	4 ± 2	b, A	1.2 ± 0.3	a, A	3.36 ± 0.04	b, B	1 ± 1	a	/	/
<i>kaempferol-3-glucoside</i>	18 ± 2	c, B	2.8 ± 0.4	a, A	5.595 ± 0.005	b, A, β	2 ± 2	a, A	/	/
<i>Syringetin 3-glucoside</i>	5 ± 1	b, B	1.7 ± 0.3	a, A, α	4.31 ± 0.05	b, A, α	2.3 ± 0.9	a	/	/

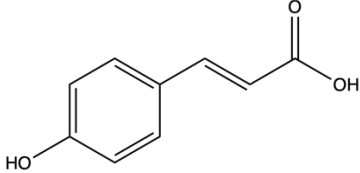
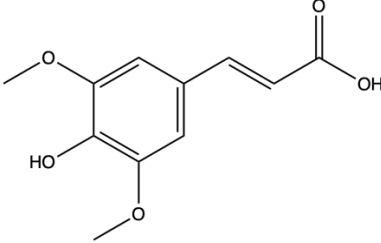
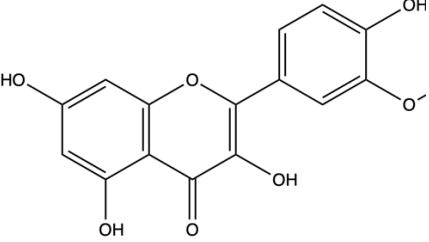
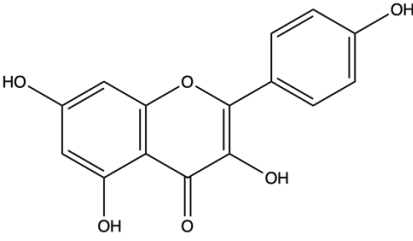
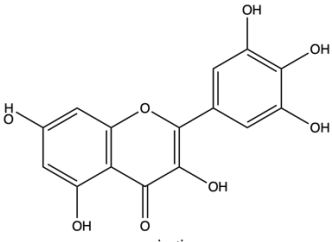
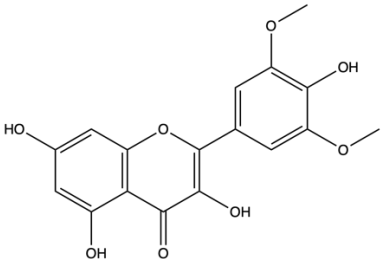
APPENDIX B

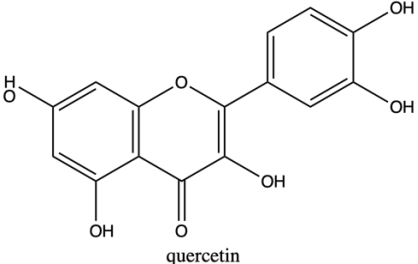
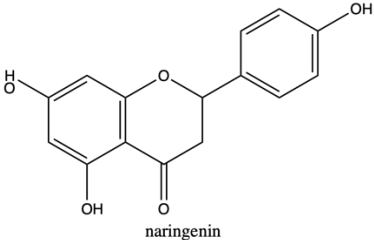
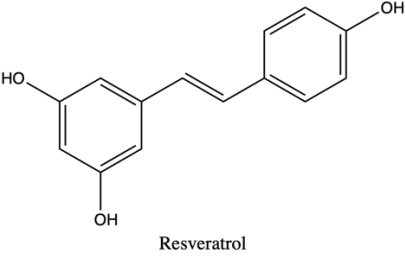
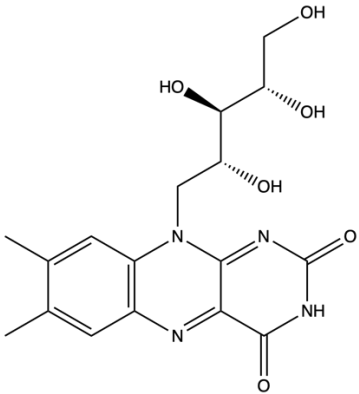
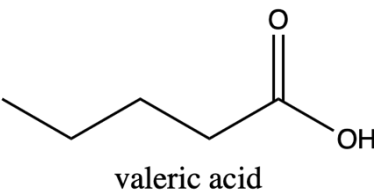
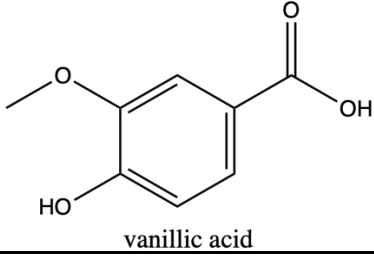
TABLE B1. CHEMICAL SHIFT RANGES, SIGNAL MULTIPLICITIES AND COUPLING CONSTANTS USED FOR THE IDENTIFICATION OF COMPOUNDS.

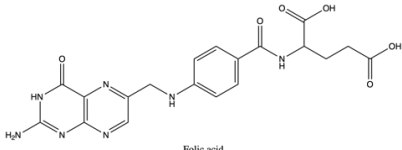
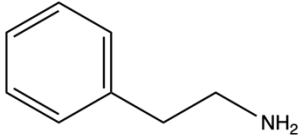
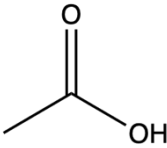
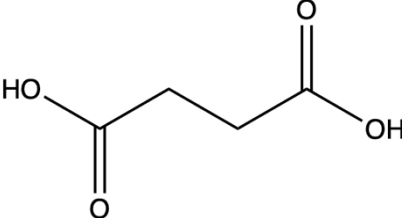
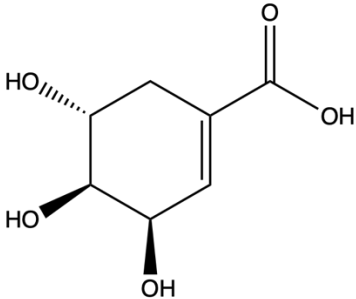
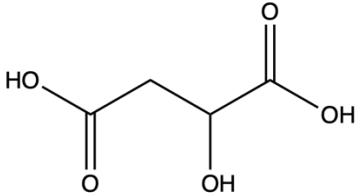
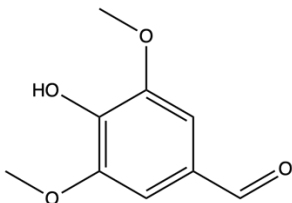
<i>Compound</i>	<i>Chemical shift range (ppm)</i>	<i>Signal multiplicity</i>	<i>J (Hz)</i>
 <p style="text-align: center;">(+)-catechin</p>	from 6.98 to 6.90	doublet	2
	from 6.91 to 6.77	multiplet	
	from 5.95 to 5.91	doublet	2.30
	from 5.87 to 5.83	doublet	2.30
	from 4.59 to 4.54	doublet	7.50
	from 4.01 to 3.94	triple doublet	5.40, 7.90
	from 2.88 to 2.81	double doublet	5.40, 16.10
<hr/>			
 <p style="text-align: center;">(-)-epicatechin</p>	from 7.07 to 7.01	doublet	2
	from 6.99 to 6.86	multiplet	
	from 6.15 to 6.04	double doublet	5.40, 16.10
	from 4.95 to 4.92	singlet	
	from 4.33 to 4.28	double triplet	2.00, 4.00
	from 2.94 to 2.86	multiplet	
	from 2.79 to 2.72	double doublet	2.50, 17.00
<hr/>			
 <p style="text-align: center;">malvidin-3-O-glucoside</p>	from 9.67 to 9.45	singlet	
	from 7.55 to 7.35	doublet	2.00
	from 7.59 to 7.45	doublet	2.00
	from 4.73 to 4.69	singlet	
	from 6.58 to 6.25	doublet	1.50
	from 6.29 to 6.13	singlet	
	from 5.74 to 5.5	doublet	7.00
	from 4.9 to 4.8	singlet	
	from 4.79 to 4.72	singlet	
	from 4.75 to 4.69	singlet	
	from 3.97 to 3.92	singlet	
	from 3.85 to 3.8	singlet	
from 3.72 to 3.68	double doublet	7.00, 7.00	
from 3.6 to 3.55	doublet	7	
<hr/>			
	from 9.15 to 9.11	singlet	
	from 8.37 to 8.31	doublet	2.30
	from 8.07 to 8.03	double doublet	2.30, 8.80
	from 7.09 to 7.04	doublet	10.00
	from 7.04 to 6.99	doublet	8.80

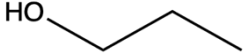
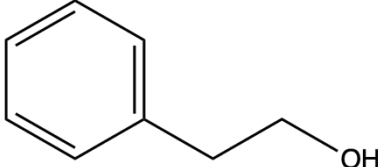
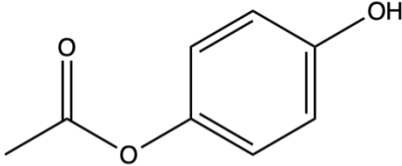
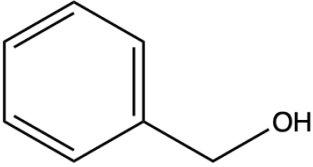
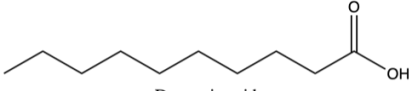
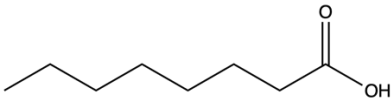
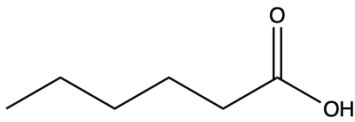
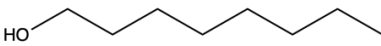
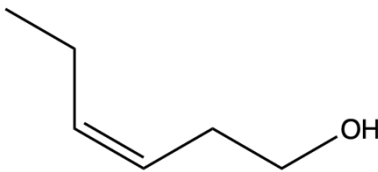
 <p>cyanidin-3-O-glucoside</p>	from 5.32 to 5.26	doublet	8.00
	from 5.17 to 5.13	singlet	
	from 3.98 to 3.92	multiplet	
	from 3.84 to 3.74	multiplet	
	from 3.69 to 3.65	singlet	
	from 3.63 to 3.59	double doublet	1.20, 4.00
	from 3.56 to 3.52	doublet	6.00
 <p>Petunidin 3-glucoside</p>	from 8.96 to 8.88	singlet	
	from 7.90 to 7.81	doublet	2.20
	from 7.76 to 7.66	doublet	2.20
	from 6.87 to 6.75	doublet	1.90
	from 6.68 to 6.60	doublet	2.90
	from 5.34 to 5.30	singlet	
	from 3.97 to 3.93	singlet	
 <p>delphinidin-3-O-glucoside</p>	from 3.95 to 3.89	double doublet	2.20, 12.00
	from 3.77 to 3.73	double doublet	1.00, 3.00
	from 3.71 to 3.64	double doublet	8.00, 9.00
	from 3.62 to 3.55	multiplet	
	from 3.50 to 3.42	triplet	9.50
	from 8.97 to 8.93	singlet	
	from 7.77 to 7.73	doublet	2.20
 <p>Peonidin-3-O-glucoside</p>	from 6.86 to 6.82	singlet	
	from 6.66 to 6.62	singlet	
	from 5.30 to 5.26	singlet	
	from 3.94 to 3.88	double doublet	2.20, 12.00
	from 3.77 to 3.67	double doublet	6.80, 10.50, 15.00
	from 3.57 to 3.53	singlet	
	from 3.50 to 3.42	triplet	9.30
 <p>Peonidin-3-O-glucoside</p>	from 9.57 to 9.52	singlet	
	from 7.53 to 7.49	singlet	
	from 7.46 to 7.42	singlet	
	from 7.12 to 6.88	doublet	1.50
	from 7.01 to 6.97	doublet	7.50
	from 6.69 to 6.65	doublet	1.50
	from 6.22 to 6.18	singlet	
	from 5.62 to 5.58	doublet	7.00
	from 4.90 to 4.86	singlet	
from 4.79 to 4.75	singlet		
from 4.73 to 4.69	singlet		

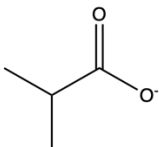
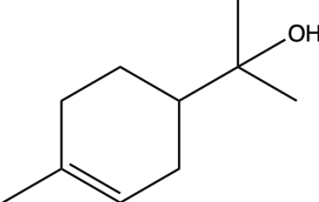
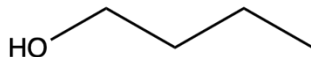
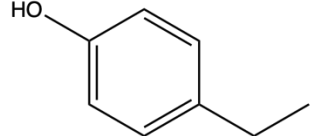
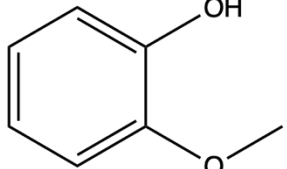
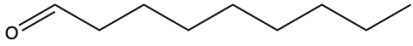
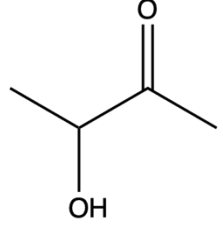
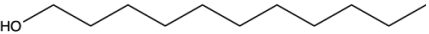
	from 4.02 to 3.98	double doublet	7.00, 7.00
	from 3.96 to 3.92	singlet	
	from 3.85 to 3.81	singlet	
	from 3.72 to 3.68	double doublet	7.00, 7.00
	from 3.58 to 3.52	doublet	7.00
	from 3.62 to 3.58	double doublet	7.00, 7.00
 <p>caffeic acid</p>	from 9.50 to 9.46	singlet	
	from 7.47 to 7.42	doublet	15.10
	from 7.08 to 7.04	doublet	1.50
	from 6.84 to 6.80	doublet	7.50
	from 6.69 to 6.65	double doublet	7.50, 1.50
 <p>Syringic acid</p>	from 8.75 to 8.71	singlet	
	from 7.13 to 7.09	doublet	1.50
	from 3.5 to 3.81	singlet	
 <p>ferulic acid</p>	from 9.57 to 9.52	singlet	
	from 7.47 to 7.43	doublet	15.10
	from 7.13 to 7.10	doublet	1.50
	from 7.02 to 6.97	doublet	7.50
	from 6.81 to 6.77	double doublet	7.50, 1.50
	from 6.29 to 6.25	doublet	15.10
	from 3.85 to 3.81	singlet	
 <p>gallic acid</p>	from 9.50 to 9.46	singlet	
	from 8.75 to 8.71	singlet	
	from 6.93 to 6.89	doublet	1.50
 <p>Genticic acid</p>	from 7.31 to 7.27	doublet	3.13
	from 7.01 to 6.96	double doublet	3.16, 8.78
	from 6.86 to 6.82	doublet	8.77
	from 9.70 to 9.65	singlet	
	from 7.47 to 7.42	double doublet	7.50, 1.51
	from 7.47 to 7.43	doublet	15.10
	from 6.61 to 6.57	double doublet	7.50, 1.50

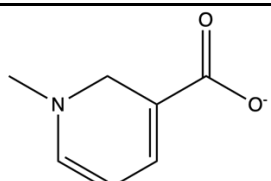
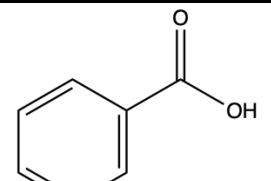
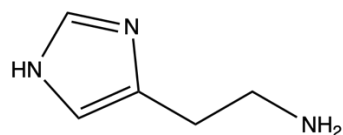
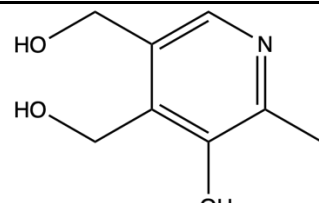
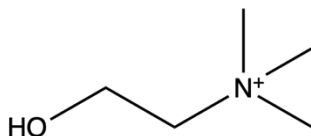
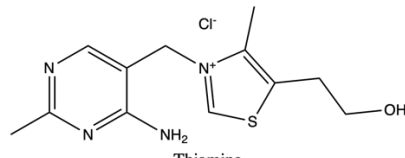
	from 6.30 to 6.25	doublet	15.10
p-coumaric acid			
	from 8.75 to 8.71	singlet	
	from 7.47 to 7.43	doublet	15.10
	from 6.76 to 6.72	doublet	1.50
	from 6.29 to 6.25	doublet	15.10
	from 3.85 to 3.81	singlet	
sinapic acid			
	from 7.77 to 7.73	doublet	2.35
	from 7.70 to 7.66	double doublet	2.40, 8.40
	from 6.96 to 6.92	doublet	8.40
	from 6.49 to 6.45	doublet	2.40
	from 6.21 to 6.17	doublet	2.00
	from 3.82 to 3.79	singlet	
isorhamnetin			
	from 10.79 to 10.74	doublet	1.30
	from 10.12 to 10.07	doublet	1.30
	from 9.40 to 9.35	doublet	2.00
	from 8.09 to 8.00	multiplet	
	from 6.97 to 6.88	multiplet	
	from 6.46 to 6.41	doublet	2.1
	from 6.21 to 6.16	doublet	2.1
kaempferol			
	from 8.28 to 8.25	singlet	
	from 6.84 to 6.56	doublet	18.00
myricetin			
	from 10.70 to 10.66	singlet	
	from 10.20 to 10.16	singlet	
	from 8.75 to 8.71	singlet	
	from 6.04 to 6.00	doublet	1.50
	from 6.37 to 6.33	doublet	1.50
	from 5.97 to 5.93	doublet	1.50
	from 3.85 to 3.87	singlet	
syringetin			
	from 10.82 to 10.79	singlet	
	from 9.64 to 9.60	singlet	
	from 9.42 to 9.38	singlet	
	from 9.36 to 9.32	singlet	
	from 7.71 to 7.67	doublet	2.30

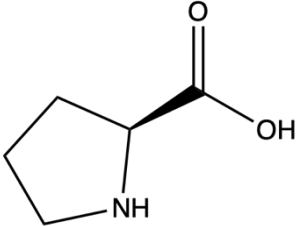
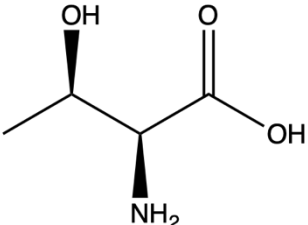
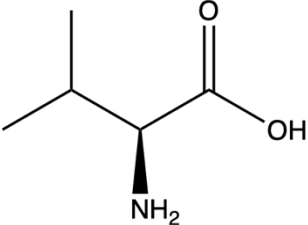
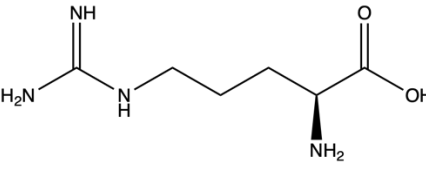
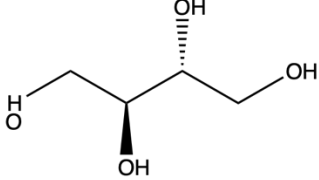
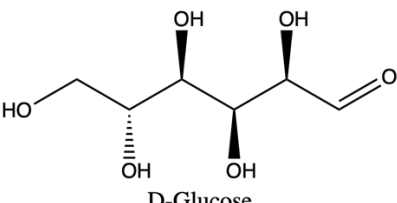
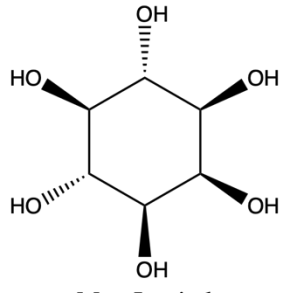
 <p>quercetin</p>	<p>from 7.58 to 7.52 from 6.92 to 6.87 from 6.43 to 6.39 from 6.22 to 6.17</p>	<p>double doublet doublet doublet doublet</p>	<p>2.23,8.46 8.50 2.00 2.00</p>
 <p>naringenin</p>	<p>from 7.34 to 7.28 from 6.82 to 6.76 from 5.90 to 5.86 from 5.47 to 5.41 from 3.30 to 3.20 from 2.72 to 2.64</p>	<p>doublet doublet singlet double doublet multiplet double doublet</p>	<p>8.50 8.50 3.00, 13.00 3.00, 16.50</p>
 <p>Resveratrol</p>	<p>from 9.59 to 9.55 from 9.23 to 9.19 from 7.42 to 7.37 from 6.97 to 6.90 from 6.85 to 6.78 from 6.78 to 6.73 from 6.41 to 6.36 from 6.14 to 6.10</p>	<p>singlet singlet doublet doublet doublet doublet doublet doublet</p>	<p> 8.50 16.00 16.20 8.30 2.15 2.15</p>
 <p>Riboflavin</p>	<p>from 7.34 to 7.33 from 4.27 to 4.21 from 3.98 to 3.90 from 3.90 to 3.79 from 3.75 to 3.68 from 2.34 to 2.30 from 2.24 to 2.18</p>	<p>doublet multiplet triple doublet multiplet double doublet singlet singlet</p>	<p>16.50 2.90, 7.00 6.70, 11.90 </p>
 <p>valeric acid</p>	<p>from 2.24 to 2.21 from 2.21 to 2.16 from 1.56 to 1.48 from 1.35 to 1.25 from 0.91 to 0.86</p>	<p>singlet triplet multiplet sextet triplet</p>	<p> 7.50 7.50 7.50</p>
 <p>vanillic acid</p>	<p>from 7.54 to 7.50 from 7.48 to 7.42 from 6.96 to 6.90 from 3.92 to 3.88 from 8.39 to 8.35 from 7.40 to 7.34</p>	<p>doublet double doublet doublet singlet singlet doublet</p>	<p>2.00 0.62, 2.00, 8.30 8.30 8.2</p>

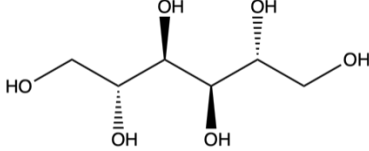
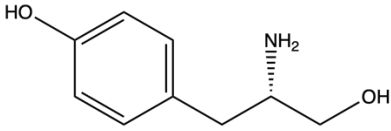
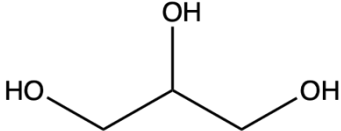
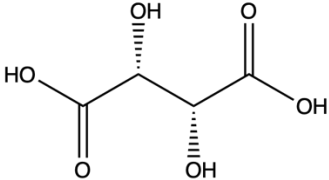
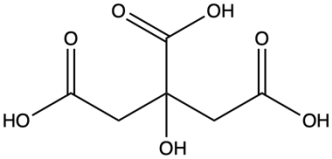
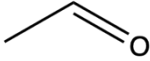
 <p>Folic acid</p>	from 6.20 to 6.13	doublet	8.2
	from 4.31 to 4.24	double doublet	5.00, 8.20
	from 3.96 to 3.92	singlet	
	from 2.42 to 2.25	triplet	8.2
	from 2.20 to 2.11	double doublet	5.30, 13.20
	from 2.11 to 1.98	double quartet	8.00, 15.20
 <p>2-phenylethylamine</p>	from 7.46 to 7.38	double doublet	6.20, 8.50
	from 7.38 to 7.32	multiplet	
	from 3.31 to 3.25	triplet	7.50
	from 3.04 to 2.97	triplet	7.50
 <p>acetic acid</p>	from 2.12 to 2.07	singlet	
 <p>succinic acid</p>	from 2.69 to 2.57	singlet	
 <p>shikimic acid</p>	from 6.98 to 6.94	double doublet	6.2, 1.0
	from 5.79 to 5.75	singlet	
	from 5.20 to 5.16	singlet	
	from 4.39 to 4.35	singlet	
	from 4.08 to 4.04	double doublet	7.00, 6.20
	from 3.77 to 3.73	triplet	7.00
	from 2.25 to 2.21	multiplet	
from 2.00 to 1.96	multiplet		
 <p>malic acid</p>	from 4.32 to 4.25	double doublet	3.05, 10.16
	from 2.92 to 2.85	double doublet	3.06, 15.40
	from 2.85 to 2.75	double doublet	10.17, 15.40
 <p>Syringaldehyde</p>	from 9.80 to 9.76	singlet	
	from 9.62 to 9.59	singlet	
	from 7.23 to 7.19	singlet	
	from 3.86 to 3.83	singlet	
	from 3.85 to 3.82	singlet	
	from 3.36 to 3.33	singlet	
from 3.58 to 3.52	triplet	6.64	
from 1.59 to 1.48	heptet	7.16	

	from 0.91 to 0.85	triplet	7.45
1-propanol			
	from 7.41 to 7.34	triplet	7.64
	from 7.34 to 7.25	multiplet	
	from 4.90 to 4.82	multiplet	
	from 3.86 to 3.80	triplet	6.70
2-phenylethanol	from 2.89 to 2.82	triplet	6.70
	from 7.18 to 7.13	multiplet	
	from 6.88 to 6.82	multiplet	
4-hydroxyphenyl acetate	from 3.45 to 3.42	singlet	
	from 7.34 to 7.30	multiplet	
	from 7.33 to 7.27	multiplet	
	from 7.30 to 7.23	multiplet	
	from 4.55 to 4.51	singlet	
Benzyl alcohol			
	from 2.38 to 2.31	triplet	7.50
	from 1.68 to 1.58	pentet	7.50
	from 1.37 to 1.24	multiplet	
	from 0.91 to 0.85	triplet	7.00
Decanoic acid			
	from 2.39 to 2.31	triplet	7.50
	from 1.69 to 1.58	pentet	7.50
	from 1.38 to 1.23	multiplet	
	from 0.92 to 0.84	multiplet	
Octanoic acid			
	from 2.19 to 2.123	triplet	7.50
	from 1.58 to 1.49	pentet	7.50
	from 1.35 to 1.20	multiplet	
	from 0.91 to 0.83	triplet	7.10
Hexanoic acid			
	from 3.58 to 3.53	triplet	7.00
	from 1.59 to 1.51	multiplet	
	from 1.41 to 1.27	multiplet	
1-octanol	from 0.95 to 0.90	multiplet	
	from 5.64 to 5.54	double triplet triplet	1.50, 7.30, 10.60
	from 5.43 to 5.34	double triplet triplet	1.60, 7.50, 10.50
	from 3.63 to 3.57	triplet	6.50
	from 2.34 to 2.26	multiplet	
	from 2.11 to 2.01	multiplet	
	from 0.98 to 0.90	triplet	6.50
	Cis-3-hexenol	from 2.43 to 2.31	heptet

	from 1.07 to 1.02	doublet	7.00
2-Methylpropanoate	from 5.39 to 5.34	multiplet	
	from 3.21 to 3.14	multiplet	
	from 2.95 to 2.00	multiplet	
	from 2.05 to 2.00	singlet	
α-terpineol	from 2.00 to 1.94	multiplet	
	from 1.97 to 1.87	multiplet	
	from 1.85 to 1.72	multiplet	
	from 1.66 to 1.56	doublet	2.30
	from 1.51 to 1.41	multiplet	
	from 1.29 to 1.15	multiplet	
	from 1.18 to 1.05	doublet	8.20
	from 3.53 to 3.48	triplet	6.7
1-butanol	from 1.46 to 1.38	multiplet	
	from 1.29 to 1.20	multiplet	
	from 0.83 to 0.77	triple doublet	1.00 ,7.50
	from 6.91 to 6.86	doublet	8.05
4-ethylphenol	from 6.55 to 6.49	multiplet	
	from 3.96 to 3.92	singlet	
	from 2.44 to 2.36	quartet	7.5
	from 1.10 to 1.03	triple doublet	1.00 ,7.50
	from 7.08 to 7.02	multiplet	
Guaiacol	from 6.99 to 6.89	multiplet	
	from 3.88 to 3.84	singlet	
	from 2.46 to 2.38	triple doublet	2.00, 7.50
Nonanal	from 1.37 to 1.24	multiplet	
	from 0.91 to 0.85	triplet	6.5
	from 4.45 to 4.38	quartet	7.20
Acetoin	from 2.23 to 2.20	singlet	
	from 2.21 to 2.18	multiplet	
	from 1.39 to 1.31	doublet	7.20
	from 3.77 to 3.65	multiplet	
1-dodecanol	from 3.67 to 3.64	singlet	
	from 3.67 to 3.63	singlet	

	from 3.64 to 3.61	singlet	
	from 3.22 to 3.19	singlet	
	from 1.30 to 1.27	singlet	
	from 1.27 to 1.24	singlet	
	from 9.12 to 9.10	singlet	
	from 8.87 to 8.80	multiplet	
	from 8.12 to 8.04	multiplet	
	from 4.47 to 4.42	singlet	
Trigonellin			
	from 8.95 to 8.90	doublet	2.2
	from 8.62 to 8.56	double doublet	1.70, 4.90
	from 8.27 to 8.20	double triplet	2.00, 8.00
	from 7.54 to 7.47	double doublet	5.00, 8.00
Nicotinic acid			
	from 7.93 to 7.88	doublet	1.2
	from 7.13 to 7.09	quartet	1
	from 3.32 to 3.25	triplet	7
	from 3.04 to 2.97	triple doublet	1.00, 7.00
Histamine			
	from 7.66 to 7.61	singlet	
	from 4.83 to 4.79	singlet	
	from 4.75 to 4.70	singlet	
	from 2.47 to 2.43	singlet	
Pyridoxine			
	from 5.14 to 4.74	multiplet	
	from 4.09 to 4.02	multiplet	
	from 3.67 to 3.49	multiplet	
	from 3.21 to 3.18	singlet	
Choline			
	from 8.70 to 8.67	singlet	
	from 8.06 to 8.03	singlet	
	from 7.50 to 7.46	doublet	1.50
	from 5.45 to 5.46	singlet	
	from 3.91 to 3.85	multiplet	
	from 3.22 to 3.16	triplet	5.80
	from 2.58 to 2.51	doublet	16.00
Thiamine			
	from 4.98 to 4.84	multiplet	
	from 4.15 to 4.08	double doublet	6.50, 9.00
	from 3.45 to 3.36	double triplet	7.00, 12.00
	from 2.39 to 2.28	multiplet	
	from 3.36 to 3.27	double triplet	7.10, 11.60
	from 2.11 to 2.02	double triplet	6.50, 12.00

	from 2.04 to 1.91	double doublet	6.50, 13.50
Proline			
	from 4.28 to 4.21 from 3.59 to 3.54	multiplet doublet	5.00
	from 1.34 to 1.29	doublet	6.50
Threonine			
	from 3.62 to 3.58 from 1.06 to 1.01	doublet doublet	4.5 7.00
	from 1.01 to 0.96	doublet	7.00
Valine			
	from 3.79 to 3.73 from 3.26 to 3.20	triplet triplet	6.00 7.00
	from 1.97 to 1.84	double doublet triplet	3.70, 7.70, 11.00
	from 1.78 to 1.57	multiplet	
Arginine			
	from 3.80 to 3.71 from 3.71 to 3.62	double doublet quartet	2.00, 11.20 4.00
	from 3.66 to 3.56	multiplet	
Erythritol			
	from 5.24 to 5.20 from 4.66 to 4.61	doublet doublet	4.00 8.00
	from 3.92 to 3.67 from 3.55 to 3.35	multiplet multiplet	
	from 3.27 to 3.20	double doublet	8.00, 9.50
D-Glucose			
	from 4.94 to 4.90 from 4.08 to 4.02	singlet triplet	3.00
	from 3.64 to 3.57 from 3.55 to 3.49	triplet double doublet	9.70 2.90, 10.00
	from 3.30 to 3.22	triplet	9.30
Myo-Inositol			
	from 3.88 to 3.82	double doublet	3.00, 12.00

 <p>Mannitol</p>	from 3.80 to 3.71	multiplet	
	from 3.70 to 3.63	double doublet	6.00, 12.00
 <p>Tyrosol</p>	from 7.21 to 7.14	multiplet	
	from 6.90 to 6.82	multiplet	
	from 3.82 to 3.74	triplet	6.70
	from 2.81 to 2.73	triplet	6.70
 <p>Glycerol</p>	from 4.91 to 4.87	singlet	
	from 3.81 to 3.73	triple triplet	4.50, 6.60
	from 3.67 to 3.61	double doublet	4.50, 12.00
	from 3.58 to 3.51	double doublet	6.50, 12.00
 <p>L-tartaric acid</p>	from 4.68 to 4.60	singlet	
 <p>Citric acid</p>	from 2.69 to 2.62	doublet	15.10
	from 2.56 to 2.49	doublet	15.10
 <p>Acetaldehyde</p>	from 9.71 to 9.6	quartet	2.90
	from 2.30 to 2.25	doublet	2.90

CONCLUDING REMARKS

The aim of this study was to achieve a better understanding of the role of soil chemistry on Nero d'Avola grapes and wines quality. To attain this goal, grapes quality was investigated through the study of the ripening kinetics and through the evolution of phenolic compounds during the ripening process. Wines quality was studied by using both targeted and non-targeted metabolomic approaches based on chromatographic and ¹H-NMR spectroscopic methods. The obtained data were subjected, together with soil-related data, to correlation analyses in order to point out possible grapes-wines/soil relationships.

Concerning grapes quality, obtained results highlighted that the soil strongly affects the ripening kinetics, the physical-chemical characteristics, and the phenolic composition of *Nero d'Avola* grapes. The influence of soil can be ascribed to modifications into water and nutrient availability for vines. It also was observed that although the soil effect is remarkable inside a vintage, the vintage effect is still predominant due to the inter-annual climatic variability. As a matter of fact, the impact of some soil parameters depends on climatic conditions, particularly the distribution and the amount of precipitation.

Concerning wines features, results showed that the soil strongly influences the chemical composition of the resulting wines. In particular, it has been pointed out that the phenolic composition of *Nero d'Avola* wines was mainly affected by soil cation exchange capacity and texture, whereas volatile organic composition appeared to be mainly influenced by cation exchange capacity and organic matter content. ¹H-NMR-based metabolomic analysis has been applied here to classify wines according to different soil types for the first time. Our results highlighted that soil exerts a strong influence on wine metabolome. Firstly, the TA unveiled significant differences among the concentrations of compounds detected in wines. Then, the NTA revealed that the differences among wines concerned not only the concentrations of the detected analytes but also the strength of the hydrogen bonds network in which the different compounds were involved. This is very important due

to the effect of H-bonds on both gustatory and olfactory perceptions by modulating the way how solutes interact with the human sensorial receptors. Indeed, understanding how solutes in wines may arrange H-bond network can open new issues in the comprehension of the chemical mechanisms involved in gustatory and olfactory perceptions.

The significance of our findings lies in the fact that, despite the fundamental role played by soil in grapevine growth, only little information was available in literature about the effects of the main soil physical-chemical parameters on grapes and wine quality. Therefore, this study contributed to increase awareness about the mechanisms of *terroir* expression.

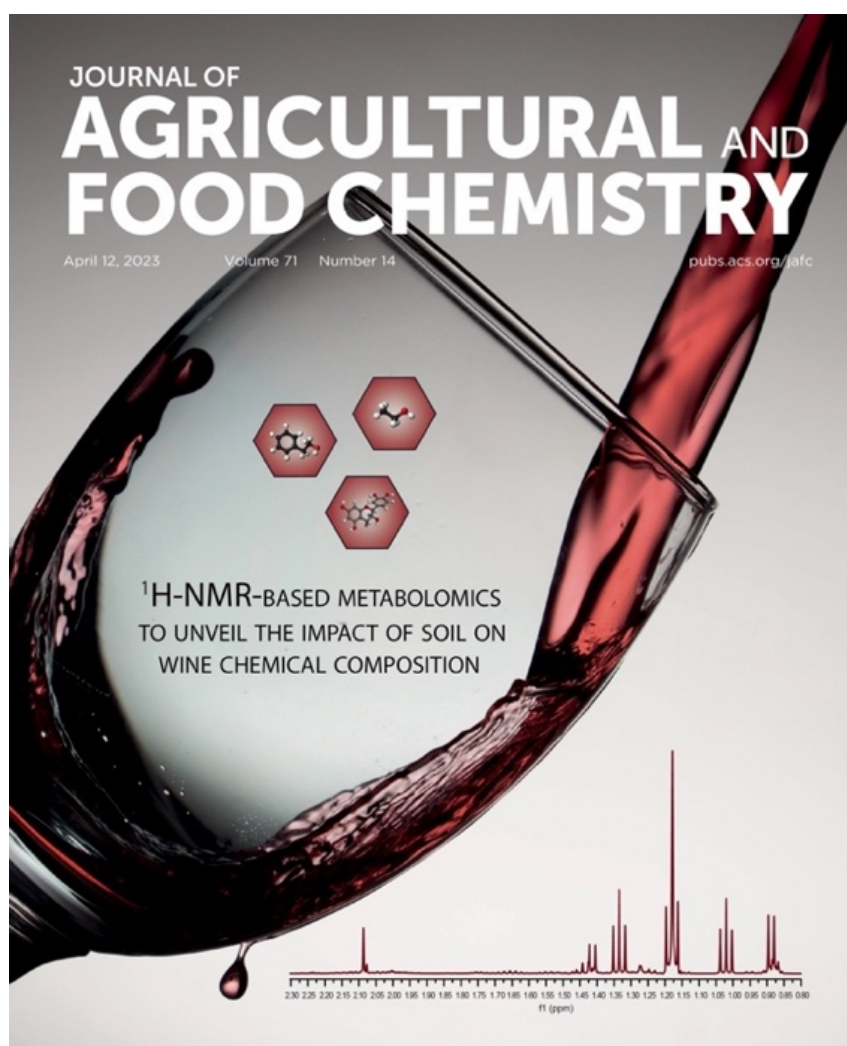
PRIZES AND AWARDS

The PhD candidate Paola Bambina was awarded of 1° place of Enoforum Award 2023 with the research entitled *Effects Of Soil Type On Phenolic And Volatile Composition Of Nero d'Avola Wines*.

Link: <https://www.enoforum.eu/web-2023/a-paola-bambina-delluniversita-di-palermo-il-premio-enoforum-2023>

The cover art associated to the paper: *¹H-NMR-based metabolomics to assess the impact of soil type on the chemical composition of Nero d'Avola red wines* was selected as the main cover of the Volume 71 Issue 14 of *Journal of Agricultural and Food Chemistry*.

MAIN COVER OF VOLUME 71, ISSUE 14 OF JOURNAL OF AGRICULTURAL AND FOOD CHEMISTRY ASSOCIATED TO THE PAPER *¹H-NMR-BASED METABOLOMICS TO ASSESS THE IMPACT OF SOIL TYPE ON THE CHEMICAL COMPOSITION OF NERO D'AVOLA RED WINES BY BAMBINA ET AL. (2023)*.



OTHER PUBLICATIONS

In the following section are listed publications related to collaborations to other research projects occurred during the PhD course:

- *Bambina, P., Malvano, F., Cinquanta, C., Albanese, D., Cirrito, A., Mazza, F., & Corona, O. (2023). Qualitative characteristics of four Sicilian monofloral honeys from *Apis mellifera ssp. sicula*. Italian Journal of Food Science, 35(1), 41-48.*
- *Malvano, F., Corona, O., Pham, P. L., Cinquanta, L., Pollon, M., Bambina, P., ... & Albanese, D. (2022). Effect of alginate-based coating charged with hydroxyapatite and quercetin on colour, firmness, sugars and volatile compounds of fresh cut papaya during cold storage. European Food Research and Technology, 248(11), 2833-2842.*
- *Bambina, P., Pollon M., Squadrito M., Barone S., Cinquanta L., Corona O. Effect of prolonged (150 days) post-fermentative maceration in steel tanks and oak barrels on Cabernet Sauvignon wine quality: mathematical modelization of the phenolic compounds behaviour. Submitted to Journal of Wine Research.*
- *Bambina, P., Pollon M., Vitaggio C., Cinquanta L., Corona O. Fermentation performance of *Saccharomyces cerevisiae* yeast strain with high alcoholigenous power. In prep.*
- *Pollon M., Bambina P., Vitaggio C., De Fillippi D., Amato F., Cinquanta L., Corona O. Automatic fermentation nutrition system compared to traditional one: fermentation performances and composition of white wines. In prep.*
- *Conte, P., Bertani, R., Sgarbossa, P., Bambina, P., Schmidt, H. P., Raga, R., ... & Lo Meo, P. (2021). Recent developments in understanding biochar's physical-chemistry. Agronomy, 11(4), 615.*
- *Corona, O., Planeta, D., Bambina, P., Giacosa, S., Paissoni, M. A., Squadrito, M., ... & Rolle, L. (2020). Influence of different dehydration levels on volatile profiles, phenolic contents and*

skin hardness of alkaline pre-treated grapes cv Muscat of alexandria (Vitis vinifera L.). Foods, 9(5), 666.

- *Corona, O., Bambina, P., De Filippi, D., & Cinquanta, L. (2021). Influence of pre-fermentative addition of aqueous solution tannins extracted from oak wood (Quercus petraea) on the composition of Grillo wines. European Food Research and Technology, 247(7), 1595-1608.*
- *Lo Meo, P., Tavormina, F., Piacenza, E., Bambina, P., Conte, P., Cinquanta, L., & Chillura Martino D. (2021). Indagini spettroscopiche su prodotti lattiero-caseari: un approccio chemiometrico alla tracciabilità.*

REFERENCES

- Alañón, M. E., Pérez-Coello, M. S., & Marina, M. L. (2015). Wine science in the metabolomics era. *TrAC Trends in Analytical Chemistry*, 74, 1-20.
- Alcalde-Eon, C., Escribano-Bailón, M. T., Santos-Buelga, C., & Rivas-Gonzalo, J. C. (2006). Changes in the detailed pigment composition of red wine during maturity and ageing: A comprehensive study. *Analytica Chimica Acta*, 563(1-2), 238-254.
- Ali, K., Maltese, F., Choi, Y. H., & Verpoorte, R. (2010). Metabolic constituents of grapevine and grape-derived products. *Phytochemistry Reviews*, 9, 357-378.
- Alves Filho, E. G., Silva, L. M. A., Lima, T. O., Ribeiro, P. R., Vidal, C. S., Carvalho, E. S., ... & Canuto, K. M. (2022). ¹H NMR and UPLC-HRMS-based metabolomic approach for evaluation of the grape maturity and maceration time of Touriga Nacional wines and their correlation with the chemical stability. *Food Chemistry*, 382, 132359.
- Amargianitaki, M., & Spyros, A. (2017). NMR-based metabolomics in wine quality control and authentication. *Chemical and Biological Technologies in Agriculture*, 4, 1-12.
- Arapitsas, P., Perenzoni, D., Ugliano, M., Slaghenaufi, D., Giacosa, S., Paissoni, M. A., ... & Mattivi, F. (2022). Decoding the proanthocyanins profile of Italian red wines. *Beverages*, 8(4), 76.
- Arapitsas, P., Scholz, M., Vrhovsek, U., Di Blasi, S., Biondi Bartolini, A., Masuero, D., ... & Mattivi, F. (2012). A metabolomic approach to the study of wine micro-oxygenation. *PLoS One*, 7(5), e37783.
- Arapitsas, P., Ugliano, M., Perenzoni, D., Angeli, A., Pangrazzi, P., & Mattivi, F. (2016). Wine metabolomics reveals new sulfonated products in bottled white wines, promoted by small amounts of oxygen. *Journal of Chromatography A*, 1429, 155-165.
- Armitage, E. G., & Barbas, C. (2014). Metabolomics in cancer biomarker discovery: current trends and future perspectives. *Journal of pharmaceutical and biomedical analysis*, 87, 1-11.

- Bambina, P., Spinella, A., Lo Papa, G., Chillura Martino, D. F., Lo Meo, P., Corona, O., ... & Conte, P. (2023). 1H NMR-Based Metabolomics to Assess the Impact of Soil Type on the Chemical Composition of Nero d'Avola Red Wines. *Journal of Agricultural and Food Chemistry*, 71(14), 5823-5835.
- Barbagallo, M. G., Vesco, G., Di Lorenzo, R., Lo Bianco, R., & Pisciotta, A. (2021). Soil and Regulated Deficit Irrigation Affect Growth, Yield and Quality of 'Nero d'Avola' Grapes in a Semi-Arid Environment. *Plants*, 10(4), 641. <https://doi.org/10.3390/plants10040641>
- Basile, B., Marsal, J., Mata, M., Vallverdú, X., Bellvert, J., & Girona, J. (2011). Phenological Sensitivity of Cabernet Sauvignon to Water Stress: Vine Physiology and Berry Composition. *American Journal of Enology and Viticulture*, 62(4), 452–461. <https://doi.org/10.5344/ajev.2011.11003>
- Beckner Whitener, M. E., Stanstrup, J., Panzeri, V., Carlin, S., Divol, B., Du Toit, M., & Vrhovsek, U. (2016). Untangling the wine metabolome by combining untargeted SPME–GCxGC-TOF-MS and sensory analysis to profile Sauvignon blanc co-fermented with seven different yeasts. *Metabolomics*, 12, 1-25.
- Bell, S. J., & Henschke, P. A. (2005). Implications of nitrogen nutrition for grapes, fermentation and wine. *Australian journal of grape and wine research*, 11(3), 242-295.
- Billet, K., Houillé, B., Dugé de Bernonville, T., Besseau, S., Oudin, A., Courdavault, V., ... & Lanoue, A. (2018). Field-based metabolomics of *Vitis vinifera* L. stems provides new insights for genotype discrimination and polyphenol metabolism structuring. *Frontiers in plant science*, 9, 798.
- Bingol, K. (2018). Recent advances in targeted and untargeted metabolomics by NMR and MS/NMR methods. *High-throughput*, 7(2), 9.
- Blotevogel, S., Schreck, E., Laplanche, C., Besson, P., Saurin, N., Audry, S., ... & Oliva, P. (2019). Soil chemistry and meteorological conditions influence the elemental profiles of West European wines. *Food chemistry*, 298, 125033.

- Bothwell, J. H., & Griffin, J. L. (2011). An introduction to biological nuclear magnetic resonance spectroscopy. *Biological Reviews*, 86(2), 493-510.
- Cadot, Y., Miñana-Castelló, M. T., & Chevalier, M. (2006). Anatomical, Histological, and Histochemical Changes in Grape Seeds from *Vitis vinifera* L. cv Cabernet franc during Fruit Development. *Journal of Agricultural and Food Chemistry*, 54(24), 9206–9215. <https://doi.org/10.1021/jf061326f>
- Canals, R., Llaudy, M. C., Valls, J., Canals, J. M., & Zamora, F. (2005). Influence of Ethanol Concentration on the Extraction of Color and Phenolic Compounds from the Skin and Seeds of Tempranillo Grapes at Different Stages of Ripening. *Journal of Agricultural and Food Chemistry*, 53(10), 4019–4025. <https://doi.org/10.1021/jf047872v>
- Castellarin, S. D., Matthews, M. A., Di Gaspero, G., & Gambetta, G. A. (2007). Water deficits accelerate ripening and induce changes in gene expression regulating flavonoid biosynthesis in grape berries. *Planta*, 227, 101-112.
- Charisiadis, P., Kontogianni, V. G., Tsiafoulis, C. G., Tzakos, A. G., Siskos, M., & Gerothanassis, I. P. (2014). ¹H-NMR as a structural and analytical tool of intra- and intermolecular hydrogen bonds of phenol-containing natural products and model compounds. In *Molecules* (Vol. 19, Issue 9, pp. 13643–13682). MDPI AG. doi: 10.3390/molecules190913643
- Cheng, G., He, Y. N., Yue, T. X., Wang, J., & Zhang, Z. W. (2014). Effects of climatic conditions and soil properties on Cabernet Sauvignon berry growth and anthocyanin profiles. *Molecules*, 19(9), 13683-13703.
- Cheyrier, V., Owe, C., & Rigaud, J. (1988). Oxidation of Grape Juice Phenolic Compounds in Model Solutions. *Journal of Food Science*, 53(6), 1729–1732.
- Chira, K., Schmauch, G., Saucier, C., Fabre, S., & Teissedre, P. L. (2009). Grape variety effect on proanthocyanidin composition and sensory perception of skin and seed tannin extracts from Bordeaux wine grapes (Cabernet Sauvignon and Merlot) for two consecutive vintages (2006 and 2007). *Journal of agricultural and food chemistry*, 57(2), 545-553.

- Chong, J., Soufan, O., Li, C., Caraus, I., Li, S., Bourque, G., ... & Xia, J. (2018). MetaboAnalyst 4.0: towards more transparent and integrative metabolomics analysis. *Nucleic acids research*, 46(W1), W486-W494.
- Coletta, A., Toci, A. T., Pati, S., Ferrara, G., Grieco, F., Tufariello, M., & Crupi, P. (2021). Effect of soil management and training system on negroamaro wine aroma. *Foods*, 10(2), 1–15.
- Conte, P., & Nestle, N. (2015). Water dynamics in different biochar fractions. *Magnetic Resonance in Chemistry*, 53(9), 726-734.
- Conte, P. (2008). ¹H NMR spectroscopy with multivariate statistical analysis as a tool for a rapid screening of the molecular changes occurring during micro-oxygenation of an Italian red wine. *Open Magn Reson J*, 1, 77-80.
- Conte, P., & Schmidt, H. P. (2017). Soil-water interactions unveiled by fast field cycling NMR relaxometry. *EMagRes*, 6(4), 453–464. doi: 10.1002/9780470034590.emrstm1535
- Corona, O., Liguori, L., Albanese, D., Di Matteo, M., Cinquanta, L., & Russo, P. (2019). Quality and volatile compounds in red wine at different degrees of dealcoholization by membrane process. *European Food Research and Technology*, 245, 2601-2611.
- Corona, O., Squadrito, M., Vento, G., Tirelli, A., & Di Stefano, R. (2015). Over-evaluation of total flavonoids in grape skin extracts containing sulphur dioxide. *Food Chemistry*, 172, 537-542.
- Cortell, J. M., Halbleib, M., Gallagher, A. V., Righetti, T. L., & Kennedy, J. A. (2007). Influence of vine vigor on grape (*Vitis vinifera* L. cv. Pinot Noir) anthocyanins. 1. Anthocyanin concentration and composition in fruit. *Journal of Agricultural and Food Chemistry*, 55(16), 6575-6584.
- Cortell, J. M., Halbleib, M., Gallagher, A. V., Righetti, T. L., & Kennedy, J. A. (2005). Influence of vine vigor on grape (*Vitis vinifera* L. cv. Pinot noir) and wine proanthocyanidins. *Journal of Agricultural and Food Chemistry*, 53(14), 5798-5808.

- Coulter, A. D., Holdstock, M. G., Cowey, G. D., Simos, C. A., Smith, P. A., & Wilkes, E. N. (2015). Potassium bitartrate crystallisation in wine and its inhibition. *Australian Journal of Grape and Wine Research*, 21, 627-641.
- de Andrés-de Prado, R., Yuste-Rojas, M., Sort, X., Andrés-Lacueva, C., Torres, M., & Lamuela-Raventós, R. M. (2007). Effect of soil type on wines produced from *Vitis vinifera* L. cv. Grenache in commercial vineyards. *Journal of agricultural and food chemistry*, 55(3), 779-786.
- del Bene, J. E. (1999). Hydrogen bond types, binding energies, and ^1H NMR chemical shifts. *Journal of Physical Chemistry A*, 103(40), 8088–8092.
- del Rio, J. L. P., & Kennedy, J. A. (2006). Development of proanthocyanidins in *Vitis vinifera* L. cv. Pinot noir grapes and extraction into wine. *American Journal of Enology and Viticulture*, 57(2), 125-132.
- Delgado, R., Martín, P., Del Álamo, M., & González, M. R. (2004). Changes in the phenolic composition of grape berries during ripening in relation to vineyard nitrogen and potassium fertilisation rates. *Journal of the Science of Food and Agriculture*, 84(7), 623-630.
- Dixon, R. A., Gang, D. R., Charlton, A. J., Fiehn, O., Kuiper, H. A., Reynolds, T. L., ... & Seiber, J. N. (2006). Applications of metabolomics in agriculture. *Journal of agricultural and food chemistry*, 54(24), 8984-8994.
- Downey, M. O., Harvey, J. S., & Robinson, S. P. (2003). Analysis of tannins in seeds and skins of Shiraz grapes throughout berry development. *Australian Journal of Grape and Wine Research*, 9(1), 15–27. <https://doi.org/10.1111/j.1755-0238.2003.tb00228.x>
- Drinkine, J., Lopes, P., Kennedy, J. A., Teissedre, P. L., & Saucier, C. (2007). Analysis of ethylidene-bridged flavan-3-ols in wine. *Journal of agricultural and food chemistry*, 55(4), 1109-1116.
- Dunn, W. B., Broadhurst, D., Begley, P., Zelena, E., Francis-McIntyre, S., Anderson, N., ... & Human Serum Metabolome (HUSERMET) Consortium. (2011). Procedures for large-scale metabolic

profiling of serum and plasma using gas chromatography and liquid chromatography coupled to mass spectrometry. *Nature protocols*, 6(7), 1060-1083.

EEC. 1990. European Communities. Commission Regulation No. 2676/90 on “Community Analysis Methods to Use in Wine Sector”. *Official Journal European Communities* L272/3.10.90.

Esteban, M. A., Villanueva, M. J., & Lissarrague, J. R. (2001). Effect of irrigation on changes in the anthocyanin composition of the skin of cv Tempranillo (*Vitis vinifera* L) grape berries during ripening. *Journal of the Science of Food and Agriculture*, 81(4), 409–420.
[https://doi.org/10.1002/1097-0010\(200103\)81:4<409::AID-JSFA830>3.0.CO;2-H](https://doi.org/10.1002/1097-0010(200103)81:4<409::AID-JSFA830>3.0.CO;2-H)

Fanzone, M., Zamora, F., Jofré, V., Assof, M., & Peña-Neira, Á. (2011). Phenolic Composition of Malbec Grape Skins and Seeds from Valle de Uco (Mendoza, Argentina) during Ripening. Effect of Cluster Thinning. *Journal of Agricultural and Food Chemistry*, 59(11), 6120–6136.
<https://doi.org/10.1021/jf200073k>

Fernández, K., Kennedy, J. A., & Agosin, E. (2007). Characterization of *Vitis vinifera* L. Cv. Carménère grape and wine proanthocyanidins. *Journal of agricultural and food chemistry*, 55(9), 3675-3680.

Ferrandino, A., Carlomagno, A., Baldassarre, S., & Schubert, A. (2012). Varietal and pre-fermentative volatiles during ripening of *Vitis vinifera* cv Nebbiolo berries from three growing areas. *Food chemistry*, 135(4), 2340-2349.

Ferrari, E., Foca, G., Vignali, M., Tassi, L., & Ulrici, A. (2011). Adulteration of the anthocyanin content of red wines: Perspectives for authentication by Fourier Transform-Near InfraRed and ¹H NMR spectroscopies. *Analytica Chimica Acta*, 701(2), 139-151.

Fiehn, O. (2002). Metabolomics—the link between genotypes and phenotypes. *Functional genomics*, 155-171.

Foroni, F., Vignando, M., Aiello, M., Parma, V., Paoletti, M. G., Squartini, A., & Rumiati, R. I. (2017). The smell of terroir! Olfactory discrimination between wines of different grape variety and different terroir. *Food Quality and Preference*, 58, 18-23.

- Fuhrer, T., & Zamboni, N. (2015). High-throughput discovery metabolomics. *Current opinion in biotechnology*, 31, 73-78.
- Gambutì, A., Picariello, L., Rinaldi, A., Forino, M., Blaiotta, G., Moine, V., & Moio, L. (2020). New insights into the formation of precipitates of quercetin in Sangiovese wines. *Journal of Food Science and Technology*, 57(7), 2602–2611. <https://doi.org/10.1007/s13197-020-04296-7>
- Geny, L., Saucier, C., Bracco, S., Daviaud, F., & Glories, Y. (2003). Composition and Cellular Localization of Tannins in Grape Seeds during Maturation. *Journal of Agricultural and Food Chemistry*, 51(27), 8051–8054. <https://doi.org/10.1021/jf030418r>
- Gika, H., Virgiliou, C., Theodoridis, G., Plumb, R. S., & Wilson, I. D. (2019). Untargeted LC/MS-based metabolic phenotyping (metabonomics/metabolomics): The state of the art. *Journal of Chromatography B*, 1117, 136-147.
- Giuffrè, A. M. (2013). HPLC-DAD detection of changes in phenol content of red berry skins during grape ripening. *European Food Research and Technology*, 237(4), 555–564. <https://doi.org/10.1007/s00217-013-2033-7>
- Godelmann, R., Fang, F., Humpfer, E., Schütz, B., Bansbach, M., Schäfer, H., & Spraul, M. (2013). Targeted and nontargeted wine analysis by ¹H NMR spectroscopy combined with multivariate statistical analysis. Differentiation of important parameters: grape variety, geographical origin, year of vintage. *Journal of agricultural and food chemistry*, 61(23), 5610-5619.
- Gómez-Míguez, M. J., Gómez-Míguez, M., Vicario, I. M., & Heredia, F. J. (2007). Assessment of colour and aroma in white wines vinifications: Effects of grape maturity and soil type. *Journal of Food Engineering*, 79(3), 758–764.
- González-Manzano, S., Rivas-Gonzalo, J. C., & Santos-Buelga, C. (2004). Extraction of flavan-3-ols from grape seed and skin into wine using simulated maceration. *Analytica Chimica Acta*, 513(1), 283–289.

- González-Neves, G., Gil, G., & Ferrer, M. (2002). Effect of different vineyard treatments on the phenolic contents in Tannat (*Vitis vinifera* L.) grapes and their respective wines. *Food science and technology international*, 8(5), 315-321.
- Goodwin, L. D., & Leech, N. L. (2006). Understanding correlation: Factors that affect the size of r . *The Journal of Experimental Education*, 74(3), 249-266.
- Gougeon, L., Da Costa, G., Le Mao, I., Ma, W., Teissedre, P. L., Guyon, F., & Richard, T. (2018). Wine analysis and authenticity using $^1\text{H-NMR}$ metabolomics data: Application to Chinese wines. *Food Analytical Methods*, 11, 3425-3434.
- Gris, E. F., Mattivi, F., Ferreira, E. A., Vrhovsek, U., Pedrosa, R. C., & Bordignon-Luiz, M. T. (2011). Proanthocyanidin profile and antioxidant capacity of Brazilian *Vitis vinifera* red wines. *Food Chemistry*, 126(1), 213-220.
- Hall, R. D., Brouwer, I. D., & Fitzgerald, M. A. (2008). Plant metabolomics and its potential application for human nutrition. *Physiologia plantarum*, 132(2), 162-175.
- Hammerstone, J. F., Lazarus, S. A., & Schmitz, H. H. (2000). Procyanidin content and variation in some commonly consumed foods. *The Journal of nutrition*, 130(8), 2086S-2092S.
- Handique, J. G., & Baruah, J. B. (2002). Polyphenolic compounds: an overview. *Reactive and Functional Polymers*, 52(3), 163-188.
- Hannam, K. D., Neilsen, G. H., Neilsen, D., Midwood, A. J., Millard, P., Zhang, Z., ... & Steinke, D. (2016). Amino acid composition of grape (*Vitis vinifera* L.) juice in response to applications of urea to the soil or foliage. *American Journal of Enology and Viticulture*, 67(1), 47-55.
- Hernández-Orte, P., Cacho, J. F., & Ferreira, V. (2002). Relationship between varietal amino acid profile of grapes and wine aromatic composition. Experiments with model solutions and chemometric study. *Journal of agricultural and food chemistry*, 50(10), 2891-2899.
- Hong, Y. S. (2011). NMR-based metabolomics in wine science. *Magnetic Resonance in Chemistry*, 49, S13-S21.

- Hopfer, H., Nelson, J., Collins, T. S., Heymann, H., & Ebeler, S. E. (2015). The combined impact of vineyard origin and processing winery on the elemental profile of red wines. *Food Chemistry*, 172, 486-496.
- Hopfer, H., Nelson, J., Collins, T. S., Heymann, H., & Ebeler, S. E. (2015). The combined impact of vineyard origin and processing winery on the elemental profile of red wines. *Food Chemistry*, 172, 486–496.
- Ickes, C. M., & Cadwallader, K. R. (2017). Effects of Ethanol on Flavor Perception in Alcoholic Beverages. *Chemosensory Perception*, 10(4), 119–134.
- Iqbal, A., Murtaza, A., Hu, W., Ahmad, I., Ahmed, A., & Xu, X. (2019). Activation and inactivation mechanisms of polyphenol oxidase during thermal and non-thermal methods of food processing. *Food and Bioproducts Processing*, 117, 170–182.
- Jean-Denis JB, Pezet R, Tabacchi R (2006) Rapid analysis of stilbenes and derivatives from downy mildew-infected grapevine leaves by liquid chromatography-atmospheric pressure photoionisation mass spectrometry. *J Chroma- togr A* 112:263–268
- Jeandet, P., Douillet-Breuil, A. C., Bessis, R., Debord, S., Sbaghi, M., & Adrian, M. (2002). Phytoalexins from the Vitaceae: biosynthesis, phytoalexin gene expression in transgenic plants, antifungal activity, and metabolism. *Journal of Agricultural and food chemistry*, 50(10), 2731-2741.
- Jouin, A., Zeng, L., Canosa, M. R., Teissedre, P. L., & Jourdes, M. (2022). Evolution of the Crown Procyanidins' Tetramer during Winemaking and Aging of Red Wine. *Foods*, 11(20), 3194.
- Kalua, C. M., & Boss, P. K. (2010). Comparison of major volatile compounds from Riesling and Cabernet Sauvignon grapes (*Vitis vinifera* L.) from fruitset to harvest. *Australian Journal of Grape and Wine Research*, 16(2), 337-348.
- Kennedy, J. A. (2008). Grape and wine phenolics: Observations and recent findings. *Ciencia e investigación agraria*, 35(2), 107-120.

- Klein, K. A., & Santamarina, J. C. (2003). Electrical conductivity in soils: Underlying phenomena. *Journal of Environmental & Engineering Geophysics*, 8(4), 263-273.
- Kodur, S. (2011). Effects of juice pH and potassium on juice and wine quality, and regulation of potassium in grapevines through rootstocks (*Vitis*): A short review. *Vitis: journal of grapevine research*, 50(1), 1-6.
- Kontoudakis, N., González, E., Gil, M., Esteruelas, M., Fort, F., Canals, J. M., & Zamora, F. (2011). Influence of Wine pH on Changes in Color and Polyphenol Composition Induced by Micro-oxygenation. *Journal of Agricultural and Food Chemistry*, 59(5), 1974–1984. <https://doi.org/10.1021/jf103038g>
- Košir, I. J., & Kidrič, J. (2002). Use of modern nuclear magnetic resonance spectroscopy in wine analysis: determination of minor compounds. *Analytica Chimica Acta*, 458(1), 77-84.
- Koundouras, S., Marinos, V., Gkoulioti, A., Kotseridis, Y., & van Leeuwen, C. (2006). Influence of vineyard location and vine water status on fruit maturation of nonirrigated cv. Agiorgitiko (*Vitis vinifera* L.). Effects on wine phenolic and aroma components. *Journal of agricultural and food chemistry*, 54(14), 5077-5086.
- Lal, R. (2020). Soil organic matter and water retention. *Agronomy Journal*, 112(5), 3265–3277. <https://doi.org/10.1002/agj2.20282>
- Le Mao, I., Martin-Pernier, J., Bautista, C., Lacampagne, S., Richard, T., & Da Costa, G. (2021). ¹H-NMR metabolomics as a tool for Winemaking monitoring. *Molecules*, 26(22), 6771.
- Lee, J. E., Hwang, G. S., Van Den Berg, F., Lee, C. H., & Hong, Y. S. (2009). Evidence of vintage effects on grape wines using ¹H NMR-based metabolomic study. *Analytica chimica acta*, 648(1), 71-76.
- Lehtonen, P. (1996). Determination of amines and amino acids in wine—a review. *American Journal of Enology and Viticulture*, 47(2), 127-133.

- Leiss, K. A., Choi, Y. H., Verpoorte, R., & Klinkhamer, P. G. (2011). An overview of NMR-based metabolomics to identify secondary plant compounds involved in host plant resistance. *Phytochemistry Reviews*, 10, 205-216.
- Lenti, L., Nartea, A., Orhotohwo, O. L., Pacetti, D., & Fiorini, D. (2022). Development and Validation of a New GC-FID Method for the Determination of Short and Medium Chain Free Fatty Acids in Wine. *Molecules*, 27(23), 8195.
- Liang, B., Lehmann, J., Solomon, D., Kinyangi, J., Grossman, J., O'Neill, B., Skjemstad, J. O., Thies, J., Luizão, F. J., Petersen, J., & Neves, E. G. (2006). Black Carbon Increases Cation Exchange Capacity in Soils. *Soil Science Society of America Journal*, 70(5), 1719–1730.
- Llaudy, M. C., Canals, R., Canals, J.-M., Rozés, N., Arola, L., & Zamora, F. (2004). New Method for Evaluating Astringency in Red Wine. *Journal of Agricultural and Food Chemistry*, 52(4), 742–746. <https://doi.org/10.1021/jf034795f>
- Lloyd, N., Johnson, D. L., & Herderich, M. J. (2015). Metabolomics approaches for resolving and harnessing chemical diversity in grapes, yeast and wine. *Australian Journal of Grape and Wine Research*, 21, 723-740.
- López-Rituerto, E., Savorani, F., Avenozza, A., Busto, J. H., Peregrina, J. M., & Engelsen, S. B. (2012). Investigations of La Rioja terroir for wine production using ¹H NMR metabolomics. *Journal of agricultural and food chemistry*, 60(13), 3452-3461.
- Lorrain, B., Chira, K., & Teissedre, P. L. (2011). Phenolic composition of Merlot and Cabernet-Sauvignon grapes from Bordeaux vineyard for the 2009-vintage: Comparison to 2006, 2007 and 2008 vintages. *Food Chemistry*, 126(4), 1991-1999.
- Lund, S. T., & Bohlmann, J. (2006). The molecular basis for wine grape quality-a volatile subject. *Science*, 311(5762), 804-805.
- Mallamace, D., Longo, S., & Corsaro, C. (2018). Proton NMR study of extra virgin olive oil with temperature: Freezing and melting kinetics. *Physica A: Statistical Mechanics and its Applications*, 499, 20-27.

- Martins, C., Brandão, T., Almeida, A., & Rocha, S. M. (2017). Metabolomics strategy for the mapping of volatile exometabolome from *Saccharomyces* spp. widely used in the food industry based on comprehensive two-dimensional gas chromatography. *Journal of separation science*, 40(10), 2228-2237.
- Mascellani, A., Hoca, G., Babisz, M., Krska, P., Kloucek, P., & Havlik, J. (2021). ¹H NMR chemometric models for classification of Czech wine type and variety. *Food Chemistry*, 339, 127852.
- Mateus, N., Marques, S., Gonçalves, A. C., Machado, J. M., & De Freitas, V. (2001). Proanthocyanidin composition of red *Vitis vinifera* varieties from the Douro Valley during ripening: Influence of cultivation altitude. *American Journal of Enology and Viticulture*, 52(2), 115-121.
- Matthews, M. A., & Anderson, M. M. (1988). Fruit Ripening in *Vitis vinifera* L.: Responses to Seasonal Water Deficits. *American Journal of Enology and Viticulture*, 39(4), 313–320. <https://doi.org/10.5344/ajev.1988.39.4.313>
- Mattivi, F., Guzzon, R., Vrhovsek, U., Stefanini, M., & Velasco, R. (2006). Metabolite profiling of grape: flavonols and anthocyanins. *Journal of agricultural and food chemistry*, 54(20), 7692-7702.
- Mattivi, F., Vrhovsek, U., Masuero, D., & Trainotti, D. (2009). Differences in the amount and structure of extractable skin and seed tannins amongst red grape varieties. *Australian Journal of Grape and Wine Research*, 15(1), 27-35.
- Mattivi, F., Zulian, C., Nicolini, G., & Valenti, L. (2002). Wine, biodiversity, technology, and antioxidants. *Annals of the New York academy of sciences*, 957(1), 37-56.
- Mazza, G., Fukumoto, L., Delaquis, P., Girard, B., & Ewert, B. (1999). Anthocyanins, phenolics, and color of Cabernet franc, Merlot, and Pinot noir wines from British Columbia. *Journal of agricultural and food chemistry*, 47(10), 4009-4017.

- Mendes-Pinto, M. M. (2009). Carotenoid breakdown products the—norisoprenoids—in wine aroma. *Archives of Biochemistry and Biophysics*, 483(2), 236-245.
- Monagas, M., Bartolomé, B., & Gómez-Cordovés, C. (2005). Updated knowledge about the presence of phenolic compounds in wine. *Critical reviews in food science and nutrition*, 45(2), 85-118.
- Mulas, G., Galaffu, M. G., Pretti, L., Nieddu, G., Mercenaro, L., Tonelli, R., & Anedda, R. (2011). NMR analysis of seven selections of vermentino grape berry: metabolites composition and development. *Journal of Agricultural and Food Chemistry*, 59(3), 793-802.
- Neina, D. (2019). The role of soil pH in plant nutrition and soil remediation. *Applied and environmental soil science*, 2019, 1-9.
- Nemzer, B., Kalita, D., Yashin, A. Y., & Yashin, Y. I. (2022). Chemical composition and polyphenolic compounds of red wines: their antioxidant activities and effects on human health—a review. *Beverages*, 8(1), 1.
- Nose, A., Hojo, M., Suzuki, M., & Ueda, T. (2004). Solute effects on the interaction between water and ethanol in aged whiskey. *Journal of Agricultural and Food Chemistry*, 52(17), 5359–5365.
- OIV. 2010. Resolution OIV/VITI 333/2010, definition of vitivinicultural “terroir”. <https://www.oiv.int/public/medias/379/viti-2010-1-en.pdf>.
- Ojeda, H., Andary, C., Kraeva, E., Carbonneau, A., & Deloire, A. (2002). Influence of pre-and postveraison water deficit on synthesis and concentration of skin phenolic compounds during berry growth of *Vitis vinifera* cv. Shiraz. *American journal of Enology and Viticulture*, 53(4), 261-267.
- Oliver, S. G., Winson, M. K., Kell, D. B., & Baganz, F. (1998). Systematic functional analysis of the yeast genome. *Trends in biotechnology*, 16(9), 373-378.
- Palmioli, A., Alberici, D., Ciaramelli, C., & Airoidi, C. (2020). Metabolomic profiling of beers: Combining ¹H NMR spectroscopy and chemometric approaches to discriminate craft and industrial products. *Food chemistry*, 327, 127025.

- Pérez Olivero, S. J. P., & Trujillo, J. P. P. (2011). A new method for the determination of short-chain fatty acids from the aliphatic series in wines by headspace solid-phase microextraction–gas chromatography–ion trap mass spectrometry. *Analytica chimica acta*, 696(1-2), 59-66.
- Pérez-Álvarez, E. P., García, R., Barrulas, P., Dias, C., Cabrita, M. J., & Garde-Cerdán, T. (2019). Classification of wines according to several factors by ICP-MS multi-element analysis. *Food chemistry*, 270, 273-280.
- Peyrot des Gachons, C., & Kennedy, J. A. (2003). Direct Method for Determining Seed and Skin Proanthocyanidin Extraction into Red Wine. *Journal of Agricultural and Food Chemistry*, 51(20), 5877–5881. <https://doi.org/10.1021/jf034178r>
- Pinu, F. R. (2018). Grape and wine metabolomics to develop new insights using untargeted and targeted approaches. *Fermentation*, 4(4), 92.
- Pozo-Bayón, M. Á., Hernández, M. T., Martín-Álvarez, P. J., & Polo, M. C. (2003). Study of low molecular weight phenolic compounds during the aging of sparkling wines manufactured with red and white grape varieties. *Journal of Agricultural and Food Chemistry*, 51(7), 2089-2095.
- Rawls, W. J., Pachepsky, Y. A., Ritchie, J. C., Sobecki, T. M., & Bloodworth, H. (2003). Effect of soil organic carbon on soil water retention. *Geoderma*, 116(1–2), 61–76. [https://doi.org/10.1016/S0016-7061\(03\)00094-6](https://doi.org/10.1016/S0016-7061(03)00094-6)
- Ribéreau Gayon, P., & Stonestreet, E. (1965). Le dosage des anthocyanes dans le vin rouge. *Bulletin de la Société Chimique de France*, 9, 2649–2652
- Ribéreau-Gayon, P., & Stonestreet, E. (1966). Dosage des tanins du vin rouge et détermination de leur structure. *Chimie analytique*, 48(4), 188-196.
- Rinaldi, A., Iturmendi, N., Jourdes, M., Teissedre, P. L., & Moio, L. (2015). Transfer of tannin characteristics from grape skins or seeds to wine-like solutions and their impact on potential astringency. *LWT-Food Science and Technology*, 63(1), 667-676.

- Rolle, L., Torchio, F., Giacosa, S., Segade, S. R., Cagnasso, E., & Gerbi, V. (2012). Assessment of physicochemical differences in Nebbiolo grape berries from different production areas and sorted by flotation. *American Journal of Enology and Viticulture*, 63(2), 195-204.
- Saengnil, K., Lueangprasert, K., & Uthaibutra, J. (2011). Sunlight-stimulated phenylalanine ammonia-lyase (PAL) activity and anthocyanin accumulation in exocarp of “Mahajanaka” mango. *Maejo Int. J. Sci. Technol*, 5(03), 365–373.
- Sánchez-Estébanez, C., Ferrero, S., Alvarez, C. M., Villafañe, F., Caballero, I., & Blanco, C. A. (2018). Nuclear magnetic resonance methodology for the analysis of regular and non-alcoholic lager beers. *Food analytical methods*, 11, 11-22.
- Shulaev, V. (2006). Metabolomics technology and bioinformatics. *Briefings in bioinformatics*, 7(2), 128-139.
- Singleton, V. L., Timberlake, C. F., & Lea, A. G. (1978). The phenolic cinnamates of white grapes and wine. *Journal of the Science of Food and Agriculture*, 29(4), 403-410.
- Sirén, H., Siren, K., & Sirén, J. (2015). Evaluation of organic and inorganic compounds levels of red wines processed from Pinot Noir grapes. *Analytical Chemistry Research*, 3, 26-36.
- Soil Survey Staff (2010). *Keys to soil taxonomy*, 11th ed., USDA-Natural Resources Conservation Service, Washington, DC
- Son, H. S., Kim, K. M., Van Den Berg, F., Hwang, G. S., Park, W. M., Lee, C. H., & Hong, Y. S. (2008). ¹H nuclear magnetic resonance-based metabolomic characterization of wines by grape varieties and production areas. *Journal of Agricultural and Food Chemistry*, 56(17), 8007-8016.
- Spayd, S. E., Tarara, J. M., Mee, D. L., & Ferguson, J. C. (2002). Separation of sunlight and temperature effects on the composition of *Vitis vinifera* cv. Merlot berries. *American journal of enology and viticulture*, 53(3), 171-182.
- Spicer, R., Salek, R. M., Moreno, P., Cañueto, D., & Steinbeck, C. (2017). Navigating freely-available software tools for metabolomics analysis. *Metabolomics*, 13, 1-16.

- Squadrito, M., Corona, O., Ansaldi, G., & Di Stefano, R. (2007). Relazioni fra i percorsi biosintetici degli HTCA dei flavonoli e degli antociani nella buccia dell'uva. *Rivista di Viticoltura e di Enologia*, 60(3), 59-70.
- Squadrito, M., Corona, O., Ansaldi, G., & Di Stefano, R. (2010). Evolution of anthocyanin profile from grape to wine. *Oeno One*, 44(3), 167-177.
- Sumner, M. E., & Miller, W. P. (1996). Cation exchange capacity and exchange coefficients. *Methods of soil analysis: Part 3 Chemical methods*, 5, 1201-1229.
- Tabago, M. K. A. G., Calingacion, M. N., & Garcia, J. (2021). Recent advances in NMR-based metabolomics of alcoholic beverages. *Food Chemistry: Molecular Sciences*, 2, 100009.
- Tarara, J. M., Lee, J., Spayd, S. E., & Scagel, C. F. (2008). Berry temperature and solar radiation alter acylation, proportion, and concentration of anthocyanin in Merlot grapes. *American journal of enology and viticulture*, 59(3), 235-247.
- Tejero Rioseras, A., Garcia Gomez, D., Ebert, B. E., Blank, L. M., Ibáñez, A. J., & Sinues, P. M. (2017). Comprehensive real-time analysis of the yeast volatilome. *Scientific reports*, 7(1), 14236.
- Theodoridis, G., Gika, H. G., & Wilson, I. D. (2011). Mass spectrometry-based holistic analytical approaches for metabolite profiling in systems biology studies. *Mass spectrometry reviews*, 30(5), 884-906.
- Torchio, F., Cagnasso, E., Gerbi, V., & Rolle, L. (2010). Mechanical properties, phenolic composition and extractability indices of Barbera grapes of different soluble solids contents from several growing areas. *Analytica Chimica Acta*, 660(1–2), 183–189. <https://doi.org/10.1016/j.aca.2009.10.017>
- Ubalde, J. M., Sort, X., Zayas, A., & Poch, R. M. (2010). Effects of Soil and Climatic Conditions on Grape Ripening and Wine Quality of Cabernet Sauvignon. *Journal of Wine Research*, 21(1), 1–17. <https://doi.org/10.1080/09571264.2010.495851>

- Ulrich, E. L., Akutsu, H., Doreleijers, J. F., Harano, Y., Ioannidis, Y. E., Lin, J., ... & Markley, J. L. (2007). BioMagResBank. *Nucleic acids research*, 36(suppl_1), D402-D408.
- Utpott, M., Rodrigues, E., de Oliveira Rios, A., Mercali, G. D., & Flôres, S. H. (2022). *Metabolomics: An analytical technique for food processing evaluation. Food Chemistry*, 366, 130685.
- Van den Berg, R. A., Hoefsloot, H. C., Westerhuis, J. A., Smilde, A. K., & Van der Werf, M. J. (2006). Centering, scaling, and transformations: improving the biological information content of metabolomics data. *BMC genomics*, 7, 1-15.
- Van Leeuwen, C., Roby, J. P., & De Resseguier, L. (2018). Soil-related terroir factors: A review. *OENO one*, 52(2), 173-188.
- Van Leeuwen, C., Friant, P., Chone, X., Tregogat, O., Koundouras, S., & Dubourdiou, D. (2004). Influence of climate, soil, and cultivar on terroir. *American Journal of Enology and Viticulture*, 55(3), 207-217.
- Versari, A., Du Toit, W., & Parpinello, G. P. (2013). Oenological tannins: A review. *Australian Journal of Grape and Wine Research*, 19(1), 1-10.
- Vilanova, M., Ugliano, M., Varela, C., Siebert, T., Pretorius, I. S., & Henschke, P. A. (2007). Assimilable nitrogen utilisation and production of volatile and non-volatile compounds in chemically defined medium by *Saccharomyces cerevisiae* wine yeasts. *Applied microbiology and biotechnology*, 77, 145-157.
- Vivas, N., Nonier, M. F., de Gaulejac, N. V., Absalon, C., Bertrand, A., & Mirabel, M. (2004). Differentiation of proanthocyanidin tannins from seeds, skins and stems of grapes (*Vitis vinifera*) and heartwood of Quebracho (*Schinopsis balansae*) by matrix-assisted laser desorption/ionization time-of-flight mass spectrometry and thioacidolysis/liquid chromatography/electrospray ionization mass spectrometry. *Analytica Chimica Acta*, 513(1), 247-256.

- Walkley, A., & Black, I. A. (1934). An examination of the Degtjareff method for determining soil organic matter, and a proposed modification of the chromic acid titration method. *Soil science*, 37(1), 29-38.
- Waterhouse, A. L., Sacks, G. L., & Jeffery, D. W. (2016). *Understanding Wine Chemistry* (1a ed.). Wiley. <https://doi.org/10.1002/9781118730720>
- Wishart, D. S. (2008). Metabolomics: applications to food science and nutrition research. *Trends in food science & technology*, 19(9), 482-493.
- Wishart, D. S. (2016). Emerging applications of metabolomics in drug discovery and precision medicine. *Nature reviews Drug discovery*, 15(7), 473-484.
- Wishart, D. S., Sayeeda, Z., Budinski, Z., Guo, A., Lee, B. L., Berjanskii, M., ... & Cort, J. R. (2022). NP-MRD: the natural products magnetic resonance database. *Nucleic Acids Research*, 50(D1), D665-D677.
- Wulf LW, Nagel CW. (1978). High-Pressure Liquid Chromatographic Separation of Anthocyanins of *Vitis Vinifera*. *Am J Enol Vitic.* 29, 42-49
- Xia, J., & Wishart, D. S. (2011). Web-based inference of biological patterns, functions and pathways from metabolomic data using MetaboAnalyst. *Nature protocols*, 6(6), 743-760.
- Yang, C., Wang, Y., Liang, Z., Fan, P., Wu, B., Yang, L., ... & Li, S. (2009). Volatiles of grape berries evaluated at the germplasm level by headspace-SPME with GC-MS. *Food Chemistry*, 114(3), 1106-1114.
- Zhang, P., Fuentes, S., Siebert, T., Krstic, M., Herderich, M., Barlow, E. W. R., & Howell, K. (2016). Terpene evolution during the development of *Vitis vinifera* L. cv. Shiraz grapes. *Food Chemistry*, 204, 463-474.
- Zwingmann, N., Singh, B., Mackinnon, I. D., & Gilkes, R. J. (2009). Zeolite from alkali modified kaolin increases NH₄⁺ retention by sandy soil: Column experiments. *Applied Clay Science*, 46(1), 7-12

AKNOWLEDGEMENTS

A conclusione di questo lavoro di tesi desidero porgere i miei più sentiti ringraziamenti ai miei tutors, prof. Onofrio Corona e prof. Pellegrino Conte, per avermi sempre incoraggiata, spronata e per aver sempre riposto in me tanta fiducia. I loro insegnamenti mi hanno permesso di crescere non solo professionalmente ma anche personalmente. Ringrazio il prof. Luciano Cinquanta che, al pari dei tutors, è sempre stato presente e disponibile durante l'intero percorso di dottorato.

Desidero, inoltre, ringraziare il prof. Giuseppe Lo Papa, il prof. Carmelo Dazzi, il prof. Paolo Lo Meo e la prof.ssa Delia Chillura Martino per aver contribuito, con la loro preziosa conoscenza, alla mia formazione e alla realizzazione del mio progetto di dottorato.

Ma la verità è che, se sono arrivata fin qui, è grazie ai miei genitori. Loro mi hanno cresciuta facendomi credere che sarei potuta diventare chiunque io avessi voluto e - perché no - anche una scienziata! Grazie a loro ho imparato che con l'impegno e la dedizione i sogni, a volte, si avverano.

Infine, grazie ad Alessandro, compagno di vita. Le parole non bastano per descrivere l'importanza della sua presenza in questi anni. Lui crede in me più di quanto non lo faccia io. È il balsamo per la mia anima.

GRAZIE!

Paola.